# Elucidation of the Molecular Mechanisms Responsible for the Central Folate Deficiency Associated with Mitochondrial Disease

Submitted by:

**Sophie-Beth Aylett MPharmacol (Hons)**

*Clinical and Molecular Genetics Unit*

*UCL Institute of Child Health*

*University College London*

***March 2014***

The research documented in this thesis was funded by the Child Health Research Appeal Trust (CHRAT)

This thesis is submitted for the degree of Doctor of Philosophy (Ph.D.) awarded by University College London

# Declaration

I, Sophie-Beth Aylett, confirm that the work presented in this thesis is my own. Where information has been derived from other sources, I confirm that this has been indicated in the thesis.

Signed…… …..Date ……

For my wonderful parents, Donna and Paul Aylett. I would not be where I am today without you.

# Abstract

5-Methyltetrahydrofolate (5-MTHF) is involved in over 100 metabolic reactions. Potentially treatable cerebral folate deficiency (CFD) of 5-MTHF in cerebrospinal fluid (CSF) is associated in mitochondrial disease. The prevalence and significance of CSF 5-MTHF deficiency in mitochondrial disease was initially investigated. Prevalence of CSF 5-MTHF deficiency in skeletal muscle mitochondrial respiratory chain enzyme (RCE) defects was 15% and the minimum population prevalence of mitochondrial disease with CSF 5-MTHF deficiency was at least one in 30,000. This suggests under-diagnosis of the condition. The most common RCE defect in CSF 5-MTHF deficient patients was isolated complex IV deficiency. Severe CSF 5-MTHF deficiencies (<10 nmol/L) were confined to Kearns-Sayre syndrome or *FOLR1* mutations. A novel homozygous missense mutation in *FOLR1* exon 5 was observed. Oral folinic acid supplementation restored CSF 5-MTHF levels to within the age-related reference range in the majority of cases. Measurement of CSF 5-MTHF and, where appropriate, *FOLR1* mutation analysis, in suspected mitochondrial disease patients is recommended. The mechanisms responsible for CFD in mitochondrial disease are unclear. The potential role of oxidative stress as a contributing mechanism was also investigated. CSF conveyed antioxidant properties towards 5-MTHF, which were overcome by hydroxyl radicals. CSF antioxidants may include ascorbic acid (AA). A CSF AA reference range was established and a significant positive correlation between CSF 5-MTHF and AA demonstrated. In SH-SY5Y cells, inhibition of mitochondrial complex I caused increased mitochondrial superoxide generation and significantly increased loss of 5-MTHF from the extracellular medium. Selenium has been reported to be elevated in CFD. The latter observation was also seen following treatment of cells with the selenium compound selenite; selenite has previously been implicated in ROS generation. Addition of AA prevented 5-MTHF degradation. Oxidative stress may be a factor in the development of CFD. Co-supplementation of folinic acid and AA may be of therapeutic benefit.

# Table of Contents

# Table of Figures

# List of Tables

# List of Equations

# Abbreviations

| | |
|---|---|
| •OH | Hydroxyl radical |
| 10-CHO-THF | 10-Formyltetrahydrofolate |
| 5-CHO-THF | 5-Formyltetrahydrofolate |
| 5-HIAA | 5-Hydroxyindoleacetic acid |
| 5-MTHF | 5-Methyltetrahydrofolate |
| A | Alanine |
| AA | Ascorbic acid |
| ABC | ATP-bindind cassette |
| Acetyl coenzyme A | Acetyl CoA |
| AD | Autosomal dominant |
| ADP | Adenosine diphosphate |
| AED | Anti-epileptic drug |
| AICAR | Phosphoribosylaminoimidazole carboxamide ribonucleotide |
| AICARFT | AICAR formyltransferase |
| *AMT* | Gene encoding aminomethyltransferase |
| ANOVA | Analysis of variance |
| ANT | Adenine nucleotide translocase |
| AR | Autosomal recessive |
| Asn | Asparagine |
| ATP | Adenosine triphosphate |
| BBB | Blood brain barrier |
| BG | Basal ganglia |
| BH4 | Tetrahydrobiopterin |
| BHMT | Betaine homocysteine methyltransferase |
| BSA | Bovine serum albumin |
| C | Cysteine |
| c. | Complementary |
| CC | Corpus callosum |
| CFD | Cerebral folate deficiency |
| $CH^+$-THF | 5,10-Methenyltetrahydrofolate |
| $CH_2$-THF | 5,10-Methylenetetrahydrofolate |
| $CH_3$-THF | 5-Methyltetrahydrofolate |
| $Cl^-$ | Chloride |
| CNS | Central nervous system |
| $CO_2$ | Carbon dioxide |
| $CoQ_{10}$ | Coenzyme $Q_{10}$ |
| COX | Cytochrome *c* oxidase |
| CpG | Cytosine phosphodiester bond Guanine |
| CSF | Cerebrospinal fluid |
| CT | Computed tomography |
| Cu/Zn SOD | Copper/Zinc superoxide dismutase |

| | |
|---|---|
| Cys | Cysteine |
| Cyt *c* | Cytochrome *c* |
| D | Aspartic acid |
| d | Days |
| ddATP | 2',3'-Dideoxyadenosine-5'-Triphosphate |
| ddCTP | 2',3'-Dideoxycytidine-5'-Triphosphate |
| ddGTP | 2',3'-Dideoxyguanosine-5'-Triphosphate |
| ddTTP | 2',3'-Dideoxythymidine-5'-Triphosphate |
| DHF | Dihydrofolate |
| DHFR | Dihydrofolate reductase |
| DM | Delayed myelination |
| DMEM/F12 | Dulbecco's modified Eagle's Medium/Ham's F-12 Nutrient mixture |
| DMSO | Dimethyl sulphoxide |
| DNA | Deoxyribonucleic acid |
| DNTB | 5,5'-Dithio-bis (nitrobenzoic acid) |
| dNTPs | Deoxynucleotide triphosphates |
| DTE | 1,4-Dithioerythritol |
| dTMP | Deoxythymidine monophosphate |
| DTT | 1,4-Dithiothreitol |
| dUMP | Deoxyuridine monophosphate |
| E | Glutamic acid |
| $e^-$ | Electron |
| ECD | Electrochemical detection |
| ecSOD | Extracellular superoxide dismutase |
| EDTA | Ethylenediaminetetraacetic acid |
| ExoSAP | Exonuclease I Shrimp Alkaline Phosphatase |
| F | Phenylalanine |
| FACS | Fluorescence activated cell sorting |
| FADH | Flavin adenine dinucleotide (oxidised) |
| $FADH_2$ | Flavin adenine dinucleotide (reduced) |
| FBS | Fetal bovine serum |
| $Fe^{2+}$ | Ferrous (II) iron |
| $Fe^{3+}$ | Ferric (III) iron |
| FMN | Flavin mononucleotide |
| *FOLR1* | Gene encoding FRα |
| FPGS | Folyl-γ-polyglutamate synthase |
| FRα | Folate receptor alpha |
| FRβ | Folate receptor beta |
| FRγ | Folate receptor gamma |
| FRδ | Folate receptor delta |
| FSC | Forward scatter |
| G | Glycine |

| | |
|---|---|
| g. | Genomic |
| GAR | Phosphoribosylglycinamide ribonucleotide |
| GARFT | GAR formyltransferase |
| GCS | Glycine cleavage system |
| *GLDC* | Gene encoding glycine dehydroxylase |
| GLUT | Glucose transporter |
| GNMT | Glycine *N*-methyltransferase |
| GP | Globus pallidus |
| GPI | Glycosylphosphatidylinositol |
| GSH | Glutathione (reduced) |
| GSSG | Glutathione (oxidised) |
| H | Histidine |
| $H^+$ | Hydrogen |
| $H_20$ | Water |
| $H_2O_2$ | Hydrogen peroxide |
| HBSS | Hank's balanced salt solution |
| $HCO_3$ | Carbonate |
| Hcy | Homocysteine |
| HPLC | High performance liquid chromatography |
| HSP | Heavy strand promoter |
| HVA | Homovanillic acid |
| I | Complex I, as indicated |
| I | Isoleucine, as indicated |
| IC | Internal capsule |
| ICP-MS | Inductively coupled plasma mass spectrometry |
| II | Complex II |
| III | Complex III |
| IV | Complex IV |
| K | Lysine |
| k | Rate constant |
| $K^+$ | Potassium |
| $K_2HPO_4$ | Dipotassium hydrogen phosphate |
| KCN | Potassium cyanide |
| $KH_2PO_4$ | Monopotassium dihydrogen phosphate |
| KSS | Kearns-Sayre syndrome |
| L | Leucine |
| LD | Leukodystrophy |
| LHON | Lebers Hereditary Optic Neuropathy |
| LSP | Light strand promoter |
| Lys | Lysine |
| M | Methionine |
| m | Months |

| | |
|---|---|
| *MECP2* | Gene encoding methyl CpG binding protein 2 |
| MELAS | Mitochondrial encephalomyopathy with lactic acidosis and stroke-like episodes |
| MEMSA | Myoclonic epilepsy, myopathy, sensory ataxia |
| MERFF | Myoclonus epilepsy with ragged red fibres |
| MIDD | Maternally inherited diabetes and deafness |
| MILS | Maternally inherited Leigh syndrome |
| min | Minute(s) |
| MNGIE | Mitochondrial neurogastrointestinal encephalopathy |
| MnSOD | Manganese superoxide dismutase |
| MRI | Magnetic resonance imaging |
| MRP | Multidrug-resistance protein |
| MS | Methionine synthase |
| mtDNA | Mitochondrial deoxyribonucleic acid |
| MTHFR | Methylenetetrahydrofolate reductase |
| N | Asparagine |
| $Na^+$ | Sodium |
| $NAD^+$ | Nicotinamide adenine dinucleotide (oxidised) |
| NADH | Nicotinamide adenine dinucleotide (reduced) |
| $NADP^+$ | Nicotinamide adenine dinucleotide phosphate (oxidised) |
| NADPH | Nicotinamide adenine dinucleotide phosphate (reduced) |
| NARP | Neuropathy, ataxia and retinitis pigmentosa |
| nDNA | Nuclear deoxyribonucleic acid |
| NTD | Neural tube defect |
| $O_2$ | Oxygen |
| $O_2^{\bullet-}$ | Superoxide |
| $O_H$ | Origin of replication of the heavy strand |
| $OH^-$ | Hydroxyl anion |
| Ox | Oxidised |
| P | Proline |
| p. | Protein |
| PCFT | Proton coupled folate transporter |
| *PCFT1* | Gene encoding PCFT |
| PCH | Pontocerebellar hypoplasia |
| PCR | Polymerase chain reaction |
| PEO | Progressive external opthalmoplegia |
| Pi | Inorganic phosphate |
| *POLG* | Gene encoding polymerase gamma catalytic subunit |
| Pro | Proline |
| PV | Periventricular |
| PVL | Periventricular leukomalacia |
| Q | Glutamine |
| R | Arginine |

| | |
|---|---|
| rBAT | Related to the $B^0$ amino acid transporter |
| RC | Respiratory chain |
| RCE | Respiratory chain enzyme |
| Red | Reduced |
| RFC | Reduced folate carrier |
| RNA | Ribonucleic acid |
| *RNASEH2A* | Gene encoding ribonuclease H2A |
| *RNASEH2B* | Gene encoding ribonuclease H2B |
| *RNASEH2C* | Gene encoding ribonuclease H2C |
| ROS | Reactive oxygen species |
| RRF | Ragged red fibres |
| rRNA | Ribosomal ribonucleic acid |
| S | Serine |
| SAH | S-adenosylhomocysteine |
| SAM | S-adenosylmethionine |
| *SAMHD1* | Gene encoding SAM domain and HD domain-containing protein 1 |
| SANDO | Sensory ataxia, neuropathy, dysarthria and opthalmoplegia |
| SCL | Selenocysteine-γ lyase |
| SD | Standard deviation |
| SDS | Sodium dodecyl sulphate |
| Se | Selenium or selenite, as indicated |
| Sec | Selenocysteine |
| SEM | Standard error of the mean |
| SePP | Selenoprotein P |
| Ser | Serine |
| SHMT | Serine hydroxymethyltransferase |
| SLC | Solute carrier protein |
| SNHL | Sensorineural hearing loss |
| SOD | Superoxide dismutase |
| SSC | Side scatter |
| SUMO | Small ubiquitin-like modifier |
| SVCT1 | Sodium dependent vitamin C transporter 1 |
| SVCT2 | Sodium dependent vitamin C transporter 2 |
| T | Threonine |
| TBE | Tris-borate-EDTA |
| THF | Tetrahydrofolate |
| *TREX1* | Gene encoding three prime repair exonuclease 1 |
| tRNA | Transfer ribonucleic acid |
| TS | Thymidylate synthase |
| Ubi | Ubiquinone |
| V | Complex V, as indicated |
| V | Valine, as indicated |
| W | Tryptophan |
| WM | White matter |

| | |
|---|---|
| X | Stop |
| Y | Tyrosine |
| y | Years |
| μ | Mean |

# Acknowledgements

Firstly, I would like to thank my primary supervisor, Professor Simon Heales, and my secondary supervisor, Dr Shamima Rahman, who have both been a great inspiration to me. To Simon for his ongoing enthusiasm, guidance and encouragement. To Shamima for her passion, patience and support. I am especially grateful to them both for the breadth of scientific knowledge and numerous opportunities they have provided me with, and the endless hours of time they have given me throughout. Despite their hectic schedules, the door was always open. Thank you both for a valuable and unique scientific experience that I will treasure.

I am indebted to the Child Health Research Appeal Trust (CHRAT), a charity established to support the research of the UCL Institute of Child Health and Great Ormond Street Hospital for Children NHS Trust. Without the funding from CHRAT, this thesis would not be possible and I am extremely grateful.

My many thanks also go to Dr Simon Eaton, whose laboratory I frequented for the majority of my time. His ability to dismantle and fix any piece of equipment in sight, especially the 'Sophie 1' HPLC apparatus, was incredibly impressive and hugely appreciated.

To Viruna Neergheen, Dr Iain Hargreaves, Dr Simon Pope, Marcus Oppenheim, Dr John Land and everyone else in the Neurometabolic Unit at the National Hospital for Neurology and Neurosurgery, London, UK. Thank you for all your help with clinical biochemistry interpretations. I am especially thankful to Viruna for all her teaching at the initial stages of my research.

I would also like to acknowledge the Chemical Pathology department in the Camelia Botnar Laboratories and Dr W. K. Chong in the Radiology Department, at Great Ormond Street Hospital for Children NHS Trust, London, UK, and Jose Saldanha in the Division of Mathematical Biology at the National Institute for Medical Research, Mill Hill, London, UK, for their analysis work of total serum folate, brain MRI/CT imaging interpretation and FRα protein modelling, respectively.

Thank you to Sean Hughes and Dr Kevin Mills at the UCL Institute of Child Health. To Sean, who I shared my PhD journey with from start to finish, it was an absolute

pleasure and a memorable experience. To Dr Kevin Mills, the ‘morale officer’, who was incredibly motivational and always checked in on me to see if everything was okay.

Finally, a heart-felt thank you to my parents, Donna and Paul Aylett, who have supported me in many ways throughout my education and life as a whole. Thank you for your love, kindness and generosity, but ultimately, thank you for the incredible start in life you have given me. For their support and encouragement, I would also like to thank my grandmother, Ivy Campbell, my sister and her husband, Chloe and Graham Brown, and Stephen Dando, whose patience showed no bounds.

# Chapter 1
# Introduction

# 1. Introduction

## 1.1 Mitochondria and the mitochondrial respiratory chain

Mitochondria, originally known as bioblasts, attracted the attention of the scientific community in the late 19$^{th}$ century (Altmann, 1890). Owing to their thread-like appearance throughout spermatogenesis, the term bioblast was replaced by mitochondria (mitos=thread, chondros=granule) (Benda, 1898). Mitochondria are thought to have evolved one to two billion years ago from aerobic α-proteobacteria that colonised primordial eukaryotic cells (Galluzzi et al., 2012; Margulis, 1975; Sagan, 1967), thus forming a symbiotic relationship which facilitated the evolution of eukaryotic cells by more efficient energy production via oxygen metabolism (Gray et al., 1999; Vafai and Mootha, 2012). Mitochondria occupy a substantial proportion of cytoplasmic volume with hundreds to thousands of mitochondria present per cell. They are responsible for countless cellular functions, including calcium homeostasis and apoptosis (Adachi et al., 1997; Borle, 1975; Duchen, 2000; Kluck et al., 1997; Lee and Thévenod, 2006). However, they are mainly renowned for their role in bioenergetic transduction processes whereby metabolic fuels are utilised in order to generate adenosine triphosphate (ATP) (Green and Blondin, 1978; Mitchell and Moyle, 1965; Mitchell, 1961; Sherratt, 1991). For this reason, mitochondria are particularly extensive in high aerobic energy requiring tissues and organs including skeletal muscle, the heart, the liver and the brain.

### 1.1.1 Structure

A mitochondrion consists of a double phospholipid membrane structure, the outer membrane and the inner membrane, which divides the mitochondrion into two aqueous compartments, the intermembrane space and the matrix (Palade, 1956; Sherratt, 1991; Sjostrand, 1955). Both the outer and the inner membranes enclose the intermembrane space, whilst the inner membrane, folded into finger-like protruding cristae, solely encloses the matrix. The outer membrane contains transport porins, which facilitate the movement of solutes <5 kDa to freely enter into the intermembrane space (Ha et al., 1993). With respect to small molecules, the intermembrane space is chemically equivalent to the cytoplasm. In contrast, the inner membrane contains a number of selective transport proteins which only allow specific molecules to pass into the matrix (Mühlenbein et al., 2004). These include

enzymes for metabolic pathways, for example the Krebs cycle, ribosomal RNAs (rRNAs), transfer RNAs (tRNAs) and mitochondrial DNA (mtDNA). In addition, approximately 20% of the inner membrane is composed of cardiolipin, a diphosphatidylglycerol lipid, which provides a barrier against ion influx into the matrix (Chen and Li, 2001; Fleischer et al., 1967; Pope et al., 2008). The mitochondrial respiratory chain (RC), associated with cardiolipin on the inner membrane, is responsible for mediating the production of ATP (Mitchell and Moyle, 1965). The cristae greatly increase the surface area of the inner membrane and are more abundant in high ATP demanding tissues (Forner et al., 2006; Scheffler, 2001; Sherratt, 1991).

### 1.1.2 Oxidative phosphorylation

The mitochondrial RC consists of a series of four multi-subunit complexes (complexes I-IV). The mitochondrial RC, together with complex V (ATP synthetase), produces ATP by the metabolic process, oxidative phosphorylation (Green and Zande, 1982; Nogueira et al., 2001; Smeitink et al., 2001). Substrates supplied to mitochondria, including pyruvate, amino acids and products of β-oxidation of fatty acids, enter the Krebs cycle and maintain the reduced state of nicotinamide adenine dinucleotide ($NADH/NAD^+$) and flavin adenine dinucleotide ($FADH_2$/FAD) couples (Heales et al., 2002; Schapira, 2003). The transport of electrons from these electron donors through the mitochondrial RC is coupled to the pumping of protons from the matrix into the intermembrane space. This creates a chemiosmotic gradient described as a membrane potential estimated at 150-180 mV negative to the cytoplasm (Mitchell, 1961). The proton motive force drives the movement of protons down this gradient, driving the turbines of the $F_0F_1$-ATP synthetase to phosphorylate adenosine diphosphate (ADP) to ATP (Stock et al., 2000; Walker et al., 1995). Upon synthesis, ATP is transported from the mitochondria into the cytoplasm of the cell via the adenine nucleotide translocase (ANT), expressed on the inner mitochondrial membrane (Kholodenko et al., 1987). Each mitochondrial RC enzyme or complex plays a specific role in electron transport (Figure 1).

Complex I (NADH:ubiquinone oxidoreductase) (enzyme commission (EC) 1.6.5.3) consists of 44 subunits and catalyses the transfer of two electrons from NADH via flavin mononucleotide (FMN) and iron-sulphur prosthetic groups in order to reduce

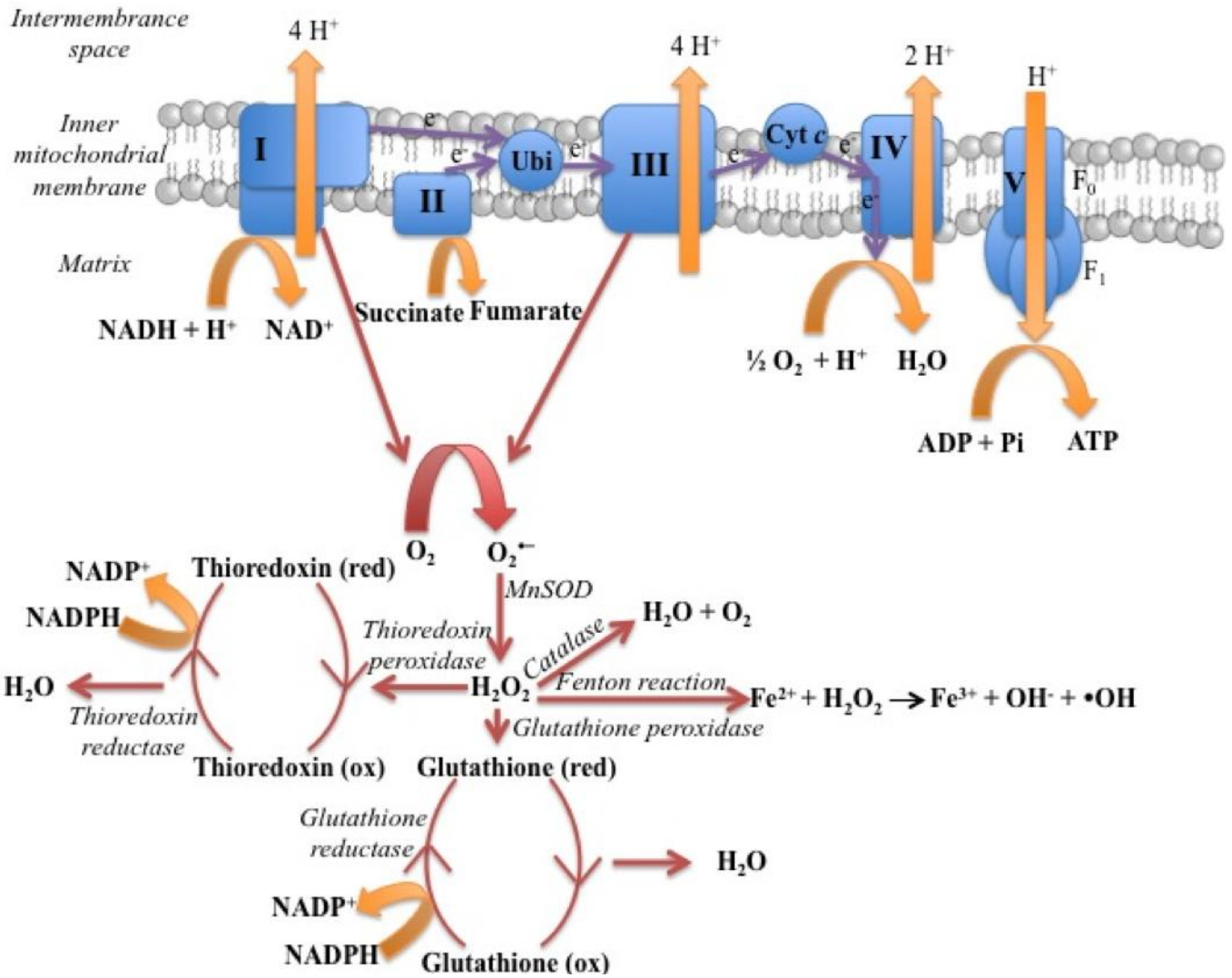


***Figure 1 The mitochondrial respiratory chain and ROS generation***. See sections 1.1.2 and 1.1.3 for detailed explanation. Ubi = ubiquinone; Cyt *c* = cytochrome *c*; red = reduced; ox = oxidised, I = complex I, II = complex II, III = complex III, IV = complex IV, V = complex V (ATP synthase), Mn-SOD = manganese superoxide dismutase, $O_2$ = oxygen, $O_2^{\bullet-}$ = superoxide, $H_2O_2$ = hydrogen peroxide, $Fe^{2+}$ = ferrous (II) iron, $Fe^{3+}$ ferric (III) iron, •OH = hydroxyl radical, $H_2O$ = water, $H^+$ = proton, $OH^-$ = hydroxyl anion, ATP = adenosine triophosphate, ADP = adenosine diphosphate, Pi = inorganic phosphate, NADH/NAD = nicotinamide adenine dinucleotide reduced/oxidised, NADPH/$NADP^+$ = nicotinamide adenine dinucleotide phosphate reduced/oxidised.

ubiquinone to ubiquinol (Balsa et al., 2012; Friedrich and Böttcher, 2004; Hirst, 2010). This electron transfer is coupled to the pumping of four protons across the inner membrane from the matrix into the intermembrane space.

Complex II (succinate:ubiquinone oxidoreductase) (EC 1.3.5.1) comprises 4 subunits and catalyses the oxidation of succinate to fumarate, which takes place in the matrix. This reaction is part of the Krebs cycle. Electrons are transferred first to FAD, generating $FADH_2$. The electrons are then transferred from $FADH_2$ via iron-sulphur clusters to reduce ubiquinone to ubiquinol (Cecchini, 2003; Horsefield et al., 2004).

Complex III (ubiquinol:cytochrome *c* oxidoreductase) (EC 1.10.2.2) comprises 11 subunits and contains three haem centres, cytochrome $b_L$, cytochrome $b_H$ and cytochrome $c_1$. Complex III also contains two ubiquinone binding sites, $Q_0$ and $Q_i$. $Q_0$ binds one molecule of ubiquinol and $Q_i$ binds one molecule of ubiquinone (Crofts, 2004; De Vries et al., 1982). One electron from bound ubiquinol is transferred to cytochrome *c* via an iron-sulphur cluster and cytochrome $c_1$. Cytochrome *c* then freely diffuses away from complex III. The remaining electron from ubiquinol is transferred to the ubiquinone at $Q_i$ via cytochrome $b_L$ and cytochrome $b_H$, thus forming a ubisemiquinone intermediate. This 'Q' cycle is then repeated with a second molecule of ubiquinol bound to $Q_0$, with one electron being transferred to cytochrome *c* and the other electron being transferred to ubisemiquinone at $Q_i$, forming ubiquinol. The reduction of ubiquinone at $Q_i$ utilises two protons from the mitochondrial matrix, with two protons being released into the intermembrane space with each reduction of ubiquinol (De Vries et al., 1982).

Complex IV (cytochrome *c* oxidase) (EC 1.9.3.1) comprises 14 subunits and contains two copper centres, $Cu_A$ and $Cu_B$, and two haem centres, $haem_a$ and $haem_{a3}$ (Balsa et al., 2012; Pitceathly et al., 2013). An electron from one cytochrome *c* is transferred to $Cu_B$ via $Cu_A$ and the two haem centres, reducing $Cu^{2+}$ to $Cu^{+}$. An electron from a second cytochrome *c* is transferred to $haem_{a3}$ via $Cu_A$ and $haem_a$, reducing $Fe^{3+}$ to $Fe^{2+}$. Oxygen binds initially to $haem_{a3}$ and then to $Cu_B$ forming a peroxide bridge between the two centres. A third and fourth electron from two further cytochrome *c* molecules and two protons from the matrix break the peroxide bridge, resulting in the formation of hydroxyl groups at the two centres, $Cu_B$ and $haem_{a3}$ (Brzezinski and Gennis, 2008; Wikström, 2004). Two additional protons

from the matrix result in the formation of $2H_20$ from the hydroxyl groups at these centres. A total of four protons are pumped across the inner membrane from the matrix into the intermembrane space.

Complex V comprises 17 subunits and contains two main domains, $F_0$ and $F_1$. $F_0$ is the transmembrane portion of complex V and $F_1$ is the soluble domain portion of complex V located on the matrix side of the inner membrane (Carbajo et al., 2007, 2005; Collinson et al., 1994; Walker et al., 1995). The binding and subsequent translocation of protons from the intermembrane space via $F_0$, causes the complex structure to rotate. This rotation results in a conformational change in the subunits of the $F_1$ domain, which in turn, alters the binding affinity of adenine nucleotides, thus driving ATP synthesis (Stock et al., 2000, 1999).

### 1.1.3 Generation of reactive oxygen species

More than 90% of oxygen consumed by mitochondria undergoes a four-electron reduction to water via the activity of complex IV of the mitochondrial RC (Equation 1). However, a small amount (0.1-4% of the electrons that flow through the mitochondrial RC) leak, which results in the generation of reactive oxygen species (ROS) (Boveris and Chance, 1973; Boveris et al., 1972; Loschen and Azzi, 1975). ROS are generated as by-products of normal physiological processes and several cellular ROS sources have been identified. However, it is often assumed that among such sources, the mitochondrial RC is the most important quantitatively (Adam-Vizi, 2005; Sipos et al., 2003) (Figure 1).

ROS are molecules derived from oxygen that retain the ability to readily oxidise other molecules. They are key determinants in cell function and whilst they play a key role in redox signalling from the mitochondria to the rest of the cell, their production can also promote mitochondrial and cellular damage (Halliwell and Whiteman, 2004; Musatov and Robinson, 2012). For example, extensive ROS production may cause nuclear and mitochondrial DNA damage, protein modification and lipid peroxidation. ROS are generated in all cells containing mitochondria. However, highly oxidative tissues including the brain, the heart and skeletal muscle tend to produce higher levels as a direct consequence of increased number of mitochondrial RCs embedded into the inner mitochondrial membrane and higher rates of mitochondrial RC activity (Halliwell, 1992; Tsutsui et al., 2001).

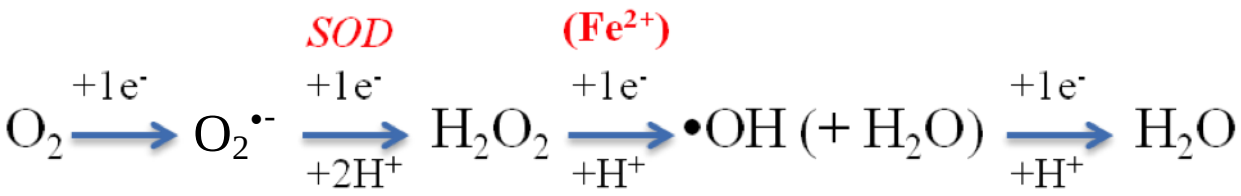


***Equation 1 Four electron reduction of oxygen***. One electron reduction of oxygen generates superoxide. Superoxide plus one electron and two protons generates hydrogen peroxide. This reaction may be catalysed by the activity of superoxide dismustase (SOD). Hydrogen peroxide plus one electron (for example, an electron from ferrous (II) iron) and one proton generates the hydroxyl radical and a molecule of water. A hydroxyl radical plus one electron and one proton generates a molecule of water. $O_2$ = oxgen, $O_2^{\bullet-}$ = superoxide, $H_2O_2$ = hydrogen peroxide, $Fe^{2+}$ = ferrous (II) iron, •OH = hydroxyl radical, $H_2O$ = water $e^-$ = electron $H^+$ = proton.


***Equation 2 Fenton reaction***. Ferrous (II) iron is oxidised by hydrogen peroxide to produce ferric (III) iron, a hydroxyl radical and a hydroxyl anion. $Fe^{2+}$ = ferrous (II) iron, $H_2O_2$ = hydrogen peroxide, $Fe^{3+}$ = ferric (III) iron, $OH^-$ = hydroxyl anion, •OH = hydroxyl radical.

The primary ROS produced by mitochondria is superoxide. Superoxide is generated as a result of the monoelectronic reduction of oxygen (see Equation 1) (Cadenas et al., 1977; Loschen and Azzi, 1975; Weisiger and Fridovich, 1973). Upon generation, superoxide may undergo enzymatic dismutation via the activity of manganese superoxide dismutase (Mn-SOD) present in the mitochondrial matrix, copper/zinc superoxide dismutase (Cu/Zn-SOD) present in the intermembrane space and cytoplasm, or extracellular (Cu/Zn) SOD (ecSOD) present in extracellular fluids, to produce the more stable hydrogen peroxide (see Equation 1) (Boveris et al., 1972; Okado-Matsumoto and Fridovich, 2001; Sturtz et al., 2001; Weisiger and Fridovich, 1973). The importance of the SOD enzymes in the enzymatic dismutation of superoxide is represented by perinatal lethality in knockout animals (Lebovitz et al., 1996; Li et al., 1995; Melov et al., 2001). Unlike superoxide, hydrogen peroxide has a number of fates as a result of its relative stability and membrane permeative nature, as detailed below. Hydrogen peroxide is transported between the mitochondrion, cytoplasm and the extracellular environment via aquaporins present in the mitochondrial and cell membranes (Bienert et al., 2007; Lee and Thévenod, 2006). Transport and diffusion of hydrogen peroxide can either lead to its elimination by intracellular and extracellular antioxidant systems including catalase (present in the heart and liver mitochondria) (Radi et al., 1991; Salvi et al., 2007), glutathione peroxidase, thioredoxin peroxidase and small non-enzymatic antioxidant molecules converting hydrogen peroxide to water (see Equation 1) (Aon et al., 2012; Kowaltowski et al., 2009; Ng et al., 2007). Conservely, hydrogen peroxide can act as a signalling molecule in a variety of biological networks including cell cycle, stress response, energy metabolism and redox balance (Czech et al., 1974; Ray et al., 2012; Toledano et al., 2010).

In the absence of hydrogen peroxide removal, hydrogen peroxide can generate the hydroxyl radical in the presence of transition metal ions including iron and copper (Aust et al., 1985; Halliwell and Gutteridge, 1990). This is illustrated by the Fenton reaction (Equation 2, see also Equation 1) (Fenton, 1894; Thomas et al., 2009). Free iron and copper are mostly bound to proteins, membranes, nucleic acids and ATP. However, in conditions whereby transition metal ions may be released, for example during ischaemia or cellular acidosis, hydroxyl radicals may be consequentially propagated (Rustin et al., 1998; Stankiewicz et al., 2007). The hydroxyl radical is the

most reactive of the ROS. As a result, intracellular and extracellular antioxidant mechanisms are thought to have evolved in order to counteract hydroxyl radical generation (Venditti et al., 2013).

Non-enzymatic small antioxidant molecules confer secondary defence against ROS. These include, α-tocopherol (vitamin E), ascorbic acid (AA, vitamin C) and reduced glutathione (GSH) (Halliwell, 1996; Marquardt et al., 2013; Montecinos et al., 2007). α-Tocopherol is present in cell membranes and plasma lipoproteins, and functions as a chain breaking antioxidant (Gomez-Fernandez et al., 1989; Marquardt et al., 2013). During ROS scavenging, α-tocopherol is oxidised to the tocopherol radical, which in turn is reduced back to α-tocopherol at the membrane surface by AA or GSH (Halpner et al., 1998; Nakagawa et al., 1991). The relatively unreactive AA radical (formed from the one electron oxidation of AA) or dehydroascorbate (formed from the two electron oxidation of AA), or oxidised glutathione (GSSG) are generated as a result (Halliwell, 1996). AA is regenerated from the AA radical or dehydroascorbate by reduction with GSH, whilst the resultant GSSG from this reaction is reduced back to GSH via the NADPH dependent glutathione reductase system (Vethanayagam et al., 1999; Winkler, 1992, 1994). Like α-tocopherol, both AA and GSH can effectively scavenge ROS in their reduced forms (Cuddihy et al., 2008).

As previously discussed, the mitochondrial RC is considered to be the most important source of cellular ROS generation from a quantitative perspective (Adam-Vizi, 2005; Sipos et al., 2003). Electron leakage leading to the univalent reduction of oxygen forming superoxide can be localised to specific complexes. Complex I is a well-documented site for mitochondrial superoxide generation and produces large amounts by two proposed mechanisms (Barja and Herrero, 1998; Barja, 1999; Kushnareva et al., 2002). The first mechanism involves a reaction between reduced FMN with oxygen. The proportion of reduced FMN is thought to be dependent on the $NADH/NAD^+$ ratio. Therefore, under conditions whereby the mitochondrial RC may be inhibited, for example owing to damage, mutation, ischaemia, loss of cytochrome *c* or by the build-up of NADH because of low ATP demand and consequential low respiration rate, the $NADH/NAD^+$ ratio may increase leading to increased superoxide production (Esterházy et al., 2008; Hirst et al., 2008; Kussmaul

and Hirst, 2006). The second mechanism is associated with reverse electron transport. Reverse electron transport may occur in situations whereby electron donation to the ubiquinone pool coupled with a high proton motive force, forces electrons back into complex I (Lambert and Brand, 2004; Murphy, 2009; Treberg et al., 2011). This process would reduce $NAD^+$ to NADH at the FMN site likely resulting in superoxide generation.

In addition to complex I, complex III has also been reported to be a site of superoxide production (Boveris et al., 1976; Cadenas et al., 1977). The proposed mechanism responsible for superoxide production at this complex involves a reaction between oxygen and ubisemiquinone bound to the $Q_0$ site, following supply of complex III with ubiquinol and $Q_i$ site inhibition. Under conditions whereby the stability of ubisemiquinone at the $Q_0$ is compromised, for example due to loss of cytochrome *c*, changes in proton motive force or redox state of ubiquinone pools, superoxide production may be augmented (Cadenas et al., 1977; Turrens, 2003; Turrens et al., 1985). Complex III appears to be responsible for most of the superoxide produced in heart and lung mitochondria (Turrens and Boveris, 1980; Turrens et al., 1982), where complex I appears to be the primary source of superoxide in the brain (Barja and Herrero, 1998; Barja, 1999).

The contribution of complex IV to superoxide production remains controversial. Mechanistic studies on enzyme catalysis mediated by complex IV have shown formation of reactive oxygen intermediates at the metal centres of the enzyme (Adam-Vizi, 2005; Srinivasan and Avadhani, 2012). However, whilst reactive intermediates may be produced within the enzyme, it is highly adapted to efficiently reduce a single oxygen molecule to two water molecules and bind partially reduced intermediates tightly. Therefore, the rapid kinetics of electron transfer of complex IV may prevent the formation of ROS. This decreases the likelihood of reactive intermediates being released from the enzyme. However, indirect mechanisms of ROS production via complex IV have been suggested. Under conditions of decreased flux through complex IV, for example during ischaemia, there may be an accumulation of reduced intermediates upstream of the mitochondrial RC. This accumulation may lead to loss of electrons from the mitochondrial RC leading to superoxide formation (Cooper and Davies, 2000; Dawson et al., 1993). In turn, loss of cardiolipin via ROS mediated lipid peroxidation, may lead to decreased enzyme

activity and cytochrome *c* levels leading to exacerbated upstream superoxide production (Chen and Lesnefsky, 2006; Paradies et al., 2000).

Similarly, complex II can theoretically generate one-electron reductions of oxygen. However, whether significant amounts of superoxide are formed from this enzyme is questionable (Guo and Lemire, 2003; Kowaltowski et al., 2009; Liu et al., 2013b). Recently, it has demonstrated that when complex III is inhibited and rapid re-oxidation of the Q pool is prevented, complex II generates superoxide in both a forward and reverse direction with electrons supplied from succinate and the ubiquinol pool, respectively (Moreno-Sánchez et al., 2013; Quinlan et al., 2012; Selivanov et al., 2011). Fully reduced $FADH_2$ and semi-reduced FADH are thought to be the relevant producers of superoxide, releasing electrons from the mitochondrial RC, when the succinate binding site is not occupied with substrate (Quinlan et al., 2012). Whilst these studies provide a mechanism, the contribution of the superoxide produced at complex II to the overall total oxidant release from the other mitochondrial RC complexes may be relatively insignificant.

### 1.2 Mammalian mitochondrial genetics

Owing to their endosymbiotic origin, mitochondria have their own DNA. In the course of evolution, most genes encoding mitochondrial proteins have transferred to nuclear chromosomes (Smeitink et al., 2001). Therefore, the biosynthesis of mitochondria is under the dual control of both the mitochondrial and nuclear genome. Unlike nuclear DNA (nDNA), mtDNA is densely packed, made up mostly of coding sequence, and lacks histones and repair enzymes. As a consequence of this lack of protective histones and repair enzymes, mtDNA is susceptible to damage, which in turn, has led to a high mutation rate (Enright et al., 1992; Miyazono et al., 2002).

#### 1.2.1 Structure

Mammalian mtDNA is a 16,569 bp circular, double-stranded molecule (Figure 2) (Larsson, 2010). Each mitochondrion contains between two to ten copies and each cell contains approximately $10^3$-$10^4$ identical copies, with the exception of sperm (~$10^2$) and mature oocytes (~$10^5$) (Smeitink et al., 2001). MtDNA represents approximately 0.5-1% of the total DNA in most cells and encodes for 37 proteins

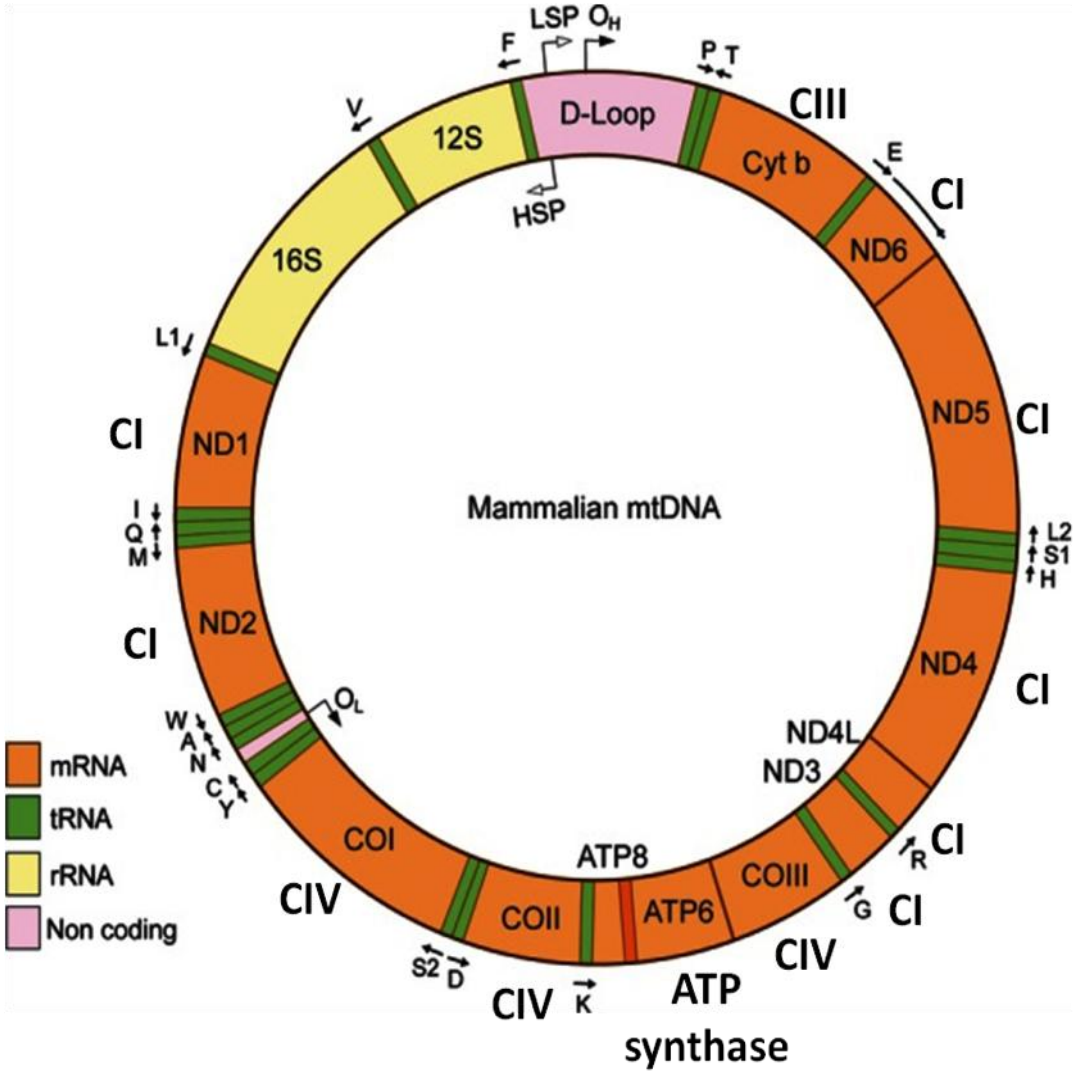


***Figure 2 Organisation of mammalian mtDNA.*** Mammalian mtDNA is a double-stranded, 16,569 bp circular molecule and comprises the heavy (H) and the light (L) strand. The noncoding D-loop region contains the promoters for the H and L strands, heavy strand promoter (HSP) and light strand promoter (LSP), and the origin of replication of the leading heavy strand of mtDNA ($O_H$). Transcription from HSP produces two rRNAs (12S and 16S rRNA), 10 mRNAs (ND1, ND2, ND3, ND5, Cyt b, COI, COII, COIII, ND4/ND4L and ATP6/ATP8) and 14 tRNAs (F = phenylalanine, V = valine, L1 = leucine$^{UUR}$ (R=A or G), I = isoleucine, M = methionone, W = tryptophan, D = aspartic acid, K = lysine, G = glycine, R = arginine, H = histidine, S1 = serine$^{UCN}$, L2 = leucine$^{CUN}$ (N=A or G or U or C) and T = threonine). Transcription from LSP produces one mRNA (ND6) and eight tRNAs (P = proline, E = glutamic acid, S2 = serine$^{AGU/C}$, Y = tyrosine, C = cysteine, N = asparagine, A = alanine and Q = glutamine). ND1, ND2, ND3 ND4, ND4L, ND5 and ND6 encode subunits of complex I (CI), Cytb encodes a subunit of complex III (CIII), COI, COII and COIII encode subunits of complex IV (CIV) and ATP6 andATP8 encodes subunits of ATP synthase. Figure adapted from Larsson (2010).

contributing to the mitochondrial RC, complex V (ATP synthase), tRNAs and rRNAs. Of the approximate 90 proteins encoding the mitochondrial RC, mtDNA encodes for seven subunits of complex I, one subunit of complex III, three subunits of complex IV and two subunits of complex V. In addition, mtDNA also encodes for 22 tRNAs and the 12S and 16S rRNAs that are specific for mitochondrial protein synthesis (Chinnery and Hudson, 2013). All the other proteins involved in the structure and assembly of the oxidative phosphorylation complexes are encoded by the nuclear genome (Leigh-Brown et al., 2010; Shoubridge, 2001). Cytosolically synthesised nuclear encoded proteins are transported into the mitochondria via protein translocators in the mitochondrial membranes and co-assembled with mtDNA-encoded counterparts in the inner membrane (Chacinska et al., 2010; Fox, 2012).

### 1.2.2 Maternal inheritance

The mitochondrion is exclusively maternally inherited. During oogenesis, a small random subset of mitochondria are selected and amplified in a process known as the genetic bottleneck (Cree et al., 2008). Upon fertilisation of the ovum, all the mtDNA is from the maternal line. Therefore, the mode of mtDNA transmission differs from that of Mendelian inheritance patterns (Pasternak, 2005). Point mutations of mtDNA have the potential to be inherited in a matrilineal fashion. Thus a disease expressed in both sexes but with no evidence of paternal transmission is highly suggestive of a mtDNA point mutation (Schon et al., 2012). In comparison, most large-scale mtDNA deletions either may occur sporadically or if multiple, be caused by defects in nDNA encoding mitochondrial proteins (Moslemi et al., 1996; Murphy et al., 2008). Defects in nDNA causing mitochondrial RC defects follow Mendelian rules of inheritance and may be autosomal dominant, recessive or X linked (Mansergh et al., 1999; Moslemi et al., 1996; Shoubridge, 2001).

### 1.2.3 Homoplasmy, heteroplasmy and the threshold effect

There are hundreds to thousands of mtDNA molecules per cell (polyploidy) (Pasternak, 2005). Normally, all mtDNA molecules are identical, a state known as homoplasmy (Figure 3). However, pathogenic mutations in mtDNA may be present in some, but not all the genomes. Therefore, when there are two or more mtDNA genotypes, with cells and tissues containing a mixture of wild-type and mutant

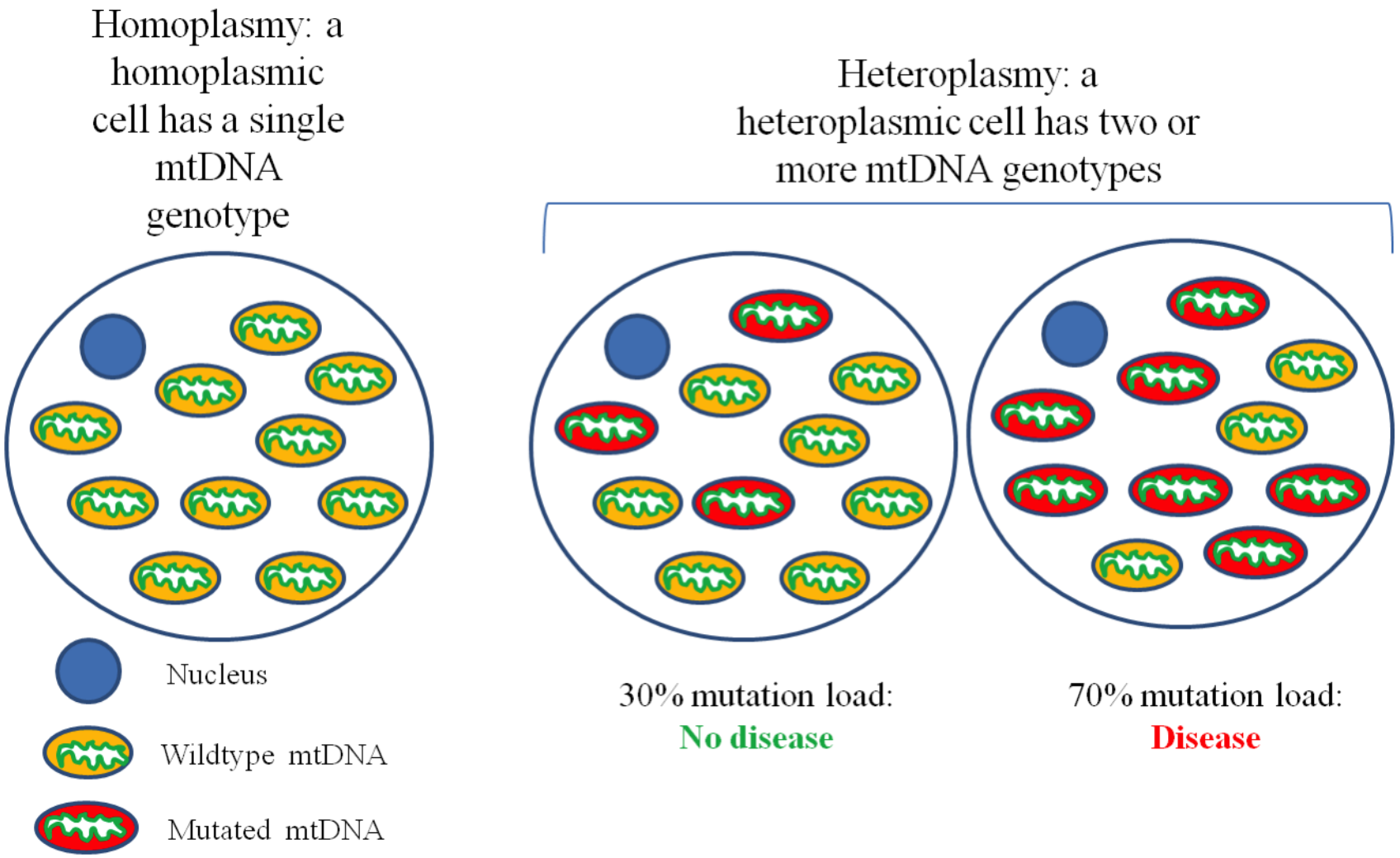


***Figure 3 Homoplasmy, heteroplasmy and the threshold effect***. The term homoplasmy is used when there is a single mtDNA genotype in each cell/tissue i.e. all mtDNA molecules are identical. The term heteroplasmy is used when there are two or more mtDNA genotypes present in cells/tissues i.e. cells and tissues containing a mixture of wild-type and mutant mtDNA. The term threshold effect is associated with heteroplasmy. A threshold level of mutant mtDNA needs to be reached for both the clinical expression of disease and biochemical defects to be observed. The above figure is a representative scenario. Threshold levels vary for different mutations and tissues.

mtDNA, it is known as a state of heteroplasmy (Figure 3) (Dimauro and Davidzon, 2005; Wonnapinij et al., 2008). Whilst some pathogenic mutations are heteroplasmic, others may be homoplasmic, affecting all copies of the mitochondrial genome, including point mutations associated with Leber's Hereditary Optic Neuropathy (LHON) (Gropman et al., 2004; McFarland et al., 2007).

In the presence of heteroplasmy, a threshold level of mutation needs to be reached in order for both the clinical expression of the disease and biochemical defects to be observed (Figure 3) (Rossignol et al., 2003, 1999). Threshold levels vary between different mutations and tissues but are usually in the range of >70%. The threshold level is lower in high energy demanding tissues including the brain, heart, skeletal muscle, retina, renal tubules and endocrine glands (Chinnery et al., 1997; Huang et al., 2002). Not surprisingly, these tissues are especially vulnerable to the effects of pathogenic mtDNA mutations (Rahman and Hanna, 2009).

### 1.2.4 Mitotic segregation

During mitosis of a heteroplasmic cell, the proportion of mutant mtDNA passed on to daughter cells may change. Therefore, the mtDNA genotype may drift towards homoplasmy, be it wild-type or mutant. In addition, if the pathogenic threshold is reached in the tissue, the phenotype may also change. This phenomenon is known as mitotic segregation and is responsible, in part, for the age-related and tissue-related variability in clinical phenotype observed in mtDNA disorders (Kwong and Sohal, 2000; Rossignol et al., 1999). Examples of mitotic segregation may include clearance of mutant mtDNA from the blood in Pearson syndrome (mtDNA deletion) or mitochondrial encephalomyopathy with lactic acidosis and stroke-like episodes (MELAS; point mutation m.3243 A>G) (Huang et al., 1996; Rahman et al., 2001).

## 1.3 Mitochondrial disorders

Mitochondrial disorders constitute of group of metabolic disorders that directly or indirectly affect the mitochondrial RC and can be caused by pathogenic mutations in mtDNA or nDNA (DiMauro and Schon, 2003). Many mitochondrial disorders affect high-energy requiring organ systems. Those affecting skeletal muscle and the brain are also referred to as mitochondrial encephalomyopathies (Khurana et al., 2008; Lim et al., 2009). Mitochondrial disorders have a birth prevalence of one in 5,000 (Thorburn, 2004) and since the first initial mitochondrial disorder was published in

1959 (Ernster et al., 1959), more than 150 distinct genetic causes of mitochondrial disease have been identified (Vafai and Mootha, 2012).

### 1.3.1 Mitochondrial respiratory-chain enzyme disorders; defects in mtDNA and nDNA

Since mitochondria are under dual genetic control from both mtDNA and nDNA, inheritance of these disorders follows both mitochondrial and Mendelian inheritance patterns (DiMauro and Schon, 2003). Approximately 75-90% of mitochondrial disease patients have nuclear encoded genetic defects transmitted in an autosomal recessive or to a lesser extent autosomal dominant or X-linked manner. In contrast, 10-25% of mitochondrial disease patients inherit their disorder via the maternal lineage (Naviaux, 2004). Spontaneous mutations or drug-associated mitochondrial defects, for example chemotherapy treatment for cancer, can also lead to severe mitochondrial disease (Catania et al., 2012; Murphy et al., 2008).

Mitochondrial diseases attributable to mutations in mtDNA can be split into two subgroups, mutations in genes encoding mitochondrial synthesis proteins, for example in tRNA or rRNA, or mutations in mitochondrial RC protein-coding genes (Table 1) (Ding et al., 2013; Horváth et al., 2009; Taylor and Turnbull, 2005). The former include diseases such as MELAS and myoclonus epilepsy with ragged red fibres (MERRF) (Brackmann et al., 2012; Liu et al., 2013a), whilst the latter include LHON and neuropathy, ataxia and retinitis pigmentosa (NARP) (Duno et al., 2012; Gropman et al., 2004). Defects in mtDNA can be further divided into diseases associated with large-scale mtDNA deletions that may occur during oogenesis or early embryogenesis, such as Kearns-Sayre syndrome (KSS), progressive external opthalmoplegia (PEO) and Pearson syndrome (McShane et al., 1991; Moslemi et al., 1996; Oldfors et al., 1990; Zeviani et al., 1988). Mitochondrial diseases attributable to mutations in nDNA following Mendelian inheritance can be caused by mutations in genes encoding protein subunits of the mitochondrial RC, accessory proteins of the mitochondrial RC, proteins needed for maintenance or expression of mtDNA, proteins required for import of solutes or proteins into mitochondria, or proteins for

***Table 1 Examples of mitochondrial disorders caused by mutations in mtDNA***. Table adapted from (Rahman and Hanna, 2009; Taylor and Turnbull, 2005).

| Mitochondrial disorder | Clinical phenotype | mtDNA gene | Defect | Status | Inheritance |
|---|---|---|---|---|---|
| **Kearns-Sayre syndrome** | PEO, pigmentary retinopathy, cardiomyopathy | A single large-scale deletion | Several deleted genes (in most tissues) | Heteroplasmic | Usually sporadic |
| **PEO** | Progressive External Opthalmoplegia | A single large-scale deletion | Several deleted genes (skeletal muscle) | Heteroplasmic | Usually sporadic |
| **Pearson syndrome** | Pancytopaenia, lactic acidosis | A single large-scale deletion | Several deleted genes (mostly in blood) | Heteroplasmic | Usually sporadic |
| **MELAS** | Myopathy, Encephalopathy Lactic Acidosis, Stroke-like episodes | *MTTL1*<br><br>*ND1, ND5* | tRNA (L1)<br><br>Complex I | Heteroplasmic<br><br>Heteroplasmic | Maternal<br><br>Maternal |
| **MERRF** | Myoclonic Epilepsy, Ragged Red Fibres, myopathy | *MTTK* | tRNA (K) | Heteroplasmic | Maternal |
| **NARP** | Neuropathy, Ataxia, Retinitis Pigmentosa | *ATP6* | ATPase 6 | Heteroplasmic | Maternal |
| **MILS** | Progressive brain-stem disorder (Maternally Inherited Leigh Syndrome) | *ATP6* | ATPase 6 | Heteroplasmic | Maternal |
| **MIDD** | Maternally Inherited Diabetes and Deafness | *MTTL1* | tRNA (L1) | Heteroplasmic | Maternal |
| **LHON** | Leber's Hereditary Optic Neuropathy | *ND1*<br><br>*ND4*<br><br>*ND6* | Complex I<br><br>Complex I<br><br>Complex I | Hetero- or homoplasmic<br><br>Hetero- or homoplasmic<br><br>Hetero- or homoplasmic | Maternal<br><br>Maternal<br><br>Maternal |
| **Myopathy with diabetes** | Myopathy, weakness, diabetes mellitus | *MTTE* | tRNA (E) | Hetero- or homoplasmic | Maternal |
| **Sensorineural hearing loss (SNHL)** | Deafness | *RNR1*<br><br>*MTTS1* | 12S rRNA<br><br>tRNA (S1) | Homoplasmic<br><br>Hetero- or homoplasmic | Maternal<br><br>Maternal |
| **Exercise intolerance** | Fatigue, muscle weakness | *CYB* | Cytochrome *b* | Heteroplasmic | Usually sporadic |
| **Leigh syndrome** | Encephalopathy, lactic acidosis | *ND3* | Complex I | Heteroplasmic | Usually sporadic |

***Table 2 Examples of mitochondrial disorders caused by mutations in nDNA***. AD = autosomal dominant, AR = autosomal recessive. Table adapted from (Angelini et al., 2009; Rahman and Hanna, 2009; Rahman, 2012; Zeviani and Di Donato, 2004).

| Mitochondrial disorder | Clinical phenotype | nDNA gene | Defect | Inheritance |
|---|---|---|---|---|
| **Leigh syndrome** | Encephalopathy, lactic acidosis, seizures | *NDUFS4* | Complex I | AR |
| | | *NDUFS8* | Complex I | AR |
| | | *NDUFA1* | Complex I | X-linked |
| | | *SDHA* | Complex II | AR |
| | | *SURF1* | Complex IV (biosynthesis) | AR |
| **MNGIE** | Mitochondrial Neurogastrointestinal Encephalopathy | *TYMP* | Thymidine phosphorylase (mtDNA depetion/deletions) | AR |
| **Alpers syndrome** | Seizures, liver disease, dementia | *POLG* | DNA polymerase- γ (mtDNA depletion/deletions) | AR |
| **MEMSA** | Myoclonic Epilepsy, Myopathy, Sensory Ataxia | *POLG* | DNA polymerase- γ (mtDNA depletion/deletions) | AR |
| **SANDO** | Sensory Ataxia, Neuropathy, Dysarthria and Opthalmoplegia | *POLG* | DNA polymerase- γ (mtDNA depletion/deletions) | AR |
| **PEO** | Progressive External Opthalmoplegia | *ANT1* | Adenine Nucleotide Translocase (mtDNA deletions) | AD |
| **GRACILE** | Growth Retardation, Amino aciduria, Cholestasis, Iron overload, Lactic acidosis, Early death | *BCS1L* | Complex III (biosynthesis) | AR |

maintenance of mitochondrial membrane lipids and dynamics (Table 2) (Angelini et al., 2009). Such nuclear encoded mitochondrial diseases include Leigh syndrome and Alpers syndrome, respectively (Chan et al., 2005; Wedatilake et al., 2013).

### 1.3.2 Clinical presentation

Mitochondrial diseases encompass a wide range of clinical symptoms and presentations (Tables 1 and 2) in which the age of onset is variable (Chi et al., 2010). Owing to the complexity of mitochondrial genetics and biochemistry, the site of the mtDNA or nDNA mutation, or sporadic deletion, does not always have a clear correlation with the clinical phenotype, even when there is a mutation in a single gene (Scaglia et al., 2004). Since mitochondria are ubiquitous cellular organelles, every tissue in the body can be affected, which is why mitochondrial diseases are often multisystematic (Kierdaszuk et al., 2009; Nissenkorn et al., 1999). Characteristically, tissues harbouring a mtDNA defect can be affected to different degrees because of heteroplasmy and the threshold effect. Therefore, carriers of the mutation within a family may have variable symptoms or may fail to present at all (Rossignol et al., 1999). In general, childhood mitochondrial disease may be more severe than adult-onset disease and can include progressive neurological, cardiac and liver dysfunction. Dysfunction of these organ systems can, in turn, lead to lethargy, hypotonia, failure to thrive, seizures, cardiomyopathy, deafness, blindness, movement disorder and/or lactic acidosis. Consequently, a clinician should adopt a high level of suspicion when reviewing a patient with elements of a number of different syndromes, and referral to a tertiary centre for evaluation of a possible mitochondrial disease may be necessary (Chi et al., 2010; Rahman and Hanna, 2009). In contrast, adult-onset mitochondrial diseases may present in more subtle ways. The disease may manifest for the first time in adulthood, or be first recognised in adulthood following a history of symptoms dating back to the patient's childhood. Adult-onset mitochondrial disease may be a progressive multisystem disorder or take quite an indolent disease course (Mattman et al., 2011; Miró et al., 2000).

Lesions in the central nervous system (CNS), peripheral nervous system and neuromuscular system are among the most common manifestations in mitochondrial disease (Chi et al., 2011; Lindner et al., 1997; Scarpelli et al., 2013). Developmental delay or regression, seizures and movement disorders are characteristic of a mitochondrial disorder in the paediatric population, whilst stroke or stroke-like

episodes are more common in adults (Koga et al., 2005; Lee et al., 2011). In addition, peripheral neuropathy is also frequently observed in mitochondrial disease (Stickler et al., 2006). For both the paediatric and adult population, a secondary deficiency of 5-methyltetrahydrofolate (5-MTHF) in cerebrospinal fluid (CSF) known as cerebral folate deficiency (CFD), is increasingly associated and diagnosed in mitochondrial disease patients (Garcia-Cazorla et al., 2008; Mangold et al., 2011; Pérez-Dueñas et al., 2011; Ramaekers et al., 2007c; Serrano et al., 2010). Symptoms related to the neuromuscular system can range from nonspecific exercise intolerance or exercise-induced myalgia, to muscle wasting or weakness in a predominantly proximal distribution (Massie et al., 2010; Schreuder et al., 2010).

Ocular muscles have the highest density of mitochondria per cell of any type of muscle reflecting their high ATP demand. Therefore, opthalmological manifestations of mitochondrial disease are commonly observed (Grönlund et al., 2010). Common eye manifestations include progressive external opthalmoplegia and ptosis. The retinal cells may also be affected by pigmentary retinopathy, and progressive loss of visual acuity by optic atrophy may manifest as a result of lesions in nerve ganglion layer cells (Lindner et al., 1997; Sciacco et al., 2001). In addition, sensorineural deafness attributable to cochlear dysfunction in combination with dysfunction of cranial nerve VIII is associated with sensorineural hearing loss (Mansergh et al., 1999; Mezghani et al., 2013).

Cardiac manifestations related to mitochondrial disease include cardiac conduction block. In more severe cases, patients may present with cardiomyopathy, which can either be hypertrophic or dilated (Obara-Moszynska et al., 2013; van Beynum et al., 2012). In addition, endocrine system and gastrointestinal system lesions including diabetes mellitus, delayed gastric emptying with nausea and vomiting, constipation and diarrhoea are also common hallmarks of mitochondrial disease (Mattman et al., 2011; Mezghani et al., 2013; Rahman, 2013; Schaefer et al., 2013).

### 1.3.3 Diagnosis

As a consequence of the heterogeneous clinical manifestations of mitochondrial disease, a multidisciplinary approach to diagnosis is often required. Assessment of family history is of paramount importance in identifying family members with mitochondrial disease or susceptibility to developing a mitochondrial disorder. In

addition, physical and neurological examination, diagnostic laboratory tests in blood, skeletal muscle and CSF, and neurological imaging, are of diagnostic importance (Rahman and Hanna, 2009).

If a mitochondrial disease is suspected, analysis of mtDNA and/or nDNA mutations in blood samples may be carried out. A positive genetic diagnosis of mitochondrial disease prohibits the need for further invasive investigations (Munnich et al., 1996; Wong, 2004). However, under circumstances whereby a genetic diagnosis has not been achieved, a muscle biopsy may be performed. Histochemical techniques allow for the detection of ragged red fibres (RRF, accumulation of mitochondria in the subsarcolemmal region of the muscle fibre when stained with Gomori trichrome stain) and histoenzymatic reactions allow for the evaluation of enzyme activities such as cytochrome *c* oxidase (COX, complex IV) (DiMauro and Hirano, 1993). The presence of COX-negative fibres and RRF, are highly indicative of a mitochondrial disorder. In addition, specific mitochondrial RC enzyme (RCE) complex assays may also be performed. Deficiencies in a single RCE complex are commonly associated with either a nuclear gene defect or a mtDNA mutation in a mtDNA protein encoding gene. In contrast, multiple mitochondrial RCE complex deficiencies are more commonplace in individuals with a mtDNA or nuclear gene defect affecting intramitochondrial protein synthesis, for example tRNA mutations, large-scale deletions, defects of aminoacyl tRNA synthestases, or translation elongation factors; or a mitochondrial DNA depletion syndrome (Jackson et al., 1995; Taylor et al., 2004). A combined defect in complex II/III in the presence of normal activities of the individual complexes is highly suggestive of a deficiency in coenzyme $Q_{10}$ ($CoQ_{10}$) since the combined complex II/III assay uses endogenous $CoQ_{10}$ to determine enzyme activity (Ogasahara et al., 1989; Rahman et al., 2001). Additional genetic diagnoses may also be performed in muscle in order to search for pathogenic mtDNA mutations, since they are more reliably detected in this tissue as opposed to blood (Rahman and Hanna, 2009). Further diagnostic evaluation may be carried out in CSF following a lumbar puncture, with elevated lactate concentrations being suggestive of mitochondrial disease (Yamada et al., 2012). CSF protein may be elevated in KSS (Serrano et al., 2010). In addition, imaging techniques, such as brain magnetic resonance imaging (MRI) and computed tomography (CT) imaging, which may demonstrate neurological abnormalities such as leukoencephalopathy, basal

ganglia calcification and/or delayed myelination, may also be of diagnostic utility (Chi et al., 2011; Taylor et al., 2004).

### 1.3.4 Treatment

A multidisciplinary approach to the management and treatment of mitochondrial disease patients is required (Schon et al., 2010). Access to specialists within the fields of rehabilitation medicine, physiotherapy, occupational therapy, cardiology, endocrinology/diabetes, ophthalmology, audiology and speech therapy are of paramount importance when treating the associated symptoms. Symptomatic therapy in these clinical areas can improve quality of life and reduce morbidity in mitochondrial disease patients. For example, hearing aids or cochlear implants may maximise hearing function (Scarpelli et al., 2012; Sinnathuray et al., 2003), prosthetic inserts or surgical interventions in patients with ptosis may improve visual acuity (Rahman and Hanna, 2009) and insertion of implantable cardiac defibrillators may be life-saving in those patients with cardiac conduction defects, for example in some patients with KSS or PEO (Hara et al., 2004; Lev et al., 2004). In addition, treatment with low dose insulin in those patients with mitochondrial diabetes or anticonvulsant drugs in those with epilepsy is essential (Guillausseau et al., 2001; Lee et al., 2011). Importantly, managing seizures with sodium valproate should try to be avoided in mitochondrial disease patients, since it has been shown to inhibit mitochondrial oxidative phosphorylation and may cause deterioration, particularly in patients with *POLG* mutations (Rahman, 2012).

Genetic counselling according to the Mendelian rules of inheritance in cases where a nDNA mutation is identified, may be appropriate. However, where a mtDNA mutation is identified, genetic counselling may be more difficult owing to the complexity of mitochondrial genetics and biochemistry (Chinnery and Hudson, 2013; Vento and Pappa, 2013). The only definite way to avoid maternal transmission of a mtDNA mutation leading to the onset of a mitochondrial disease would be to consider ovum donation. Oocyte manipulation to replace maternal mutant mtDNA with donor mtDNA by transferring the pronclei from an oocyte carrying a mtDNA mutation into an enucleated donor egg, may eliminate mitochondrial disease from the progeny (Craven et al., 2010), but it is not yet licensed for clinical use.

Pharmacological techniques including supplementation with $CoQ_{10}$ have been shown to be effective in individuals with a $CoQ_{10}$ deficiency (Montero et al., 2013; Pfeffer et al., 2012). Moreover, metabolite replacement therapy including L-arginine therapy, since strokes may be caused by impaired vasodilation, have had a varying degree of efficacy in MELAS patients (Koga et al., 2005; Moran et al., 2008). In patients with mitochondrial neurogastrointestinal encephalopathy (MNGIE) caused by thymidine phosphorylase deficiency, bone marrow transplantation may be a favoured approach (Filosto et al., 2012; Hussein, 2013). Finally, resistance exercise training aimed at shifting mtDNA genotype and improving oxidative capacity may additionally be beneficial (Murphy et al., 2008; Taivassalo et al., 1999).

One potentially treatable aspect of mitochondrial disease is supplementation with folinic acid in those patients with CFD (Garcia-Cazorla et al., 2008; Hansen and Blau, 2005). This will be discussed in more detail in section 1.5.

### 1.4 Folate

Folate (vitamin $B_9$) is the generic term for a large family of essential, water-soluble coenzymes. Dietary sources include leafy green vegetables and fresh fruit (Jägerstad and Jastrebova, 2013). These coenzymes play an important role in mediating the transfer of one-carbon units that facilitate important cellular processes including nucleic acid synthesis, amino acid metabolism and remethylation of homocysteine to methionine (Bailey, 2010). The biological importance of folate was originally identified in the 1930's when folate-containing yeast extract was used to treat pregnant Indian women with anaemia. Since folate is required for cellular replication, folate deficiency resulting in reduced red blood cell count was implicated as a causative factor of the anaemia observed in these women (Wills, 1991, 1931).

In subsequent years, the requirement for folate in the diet has gained further recognition. For example, it has become widely accepted that adequate maternal consumption of folic acid before pregnancy and during the early weeks of gestation could prevent some, but not all, neural tube defects (NTDs) (Copp and Greene, 2000; Copp et al., 2013; Dunlevy et al., 2007). NTDs are severe congenital malformations that affect an average of one in every 1000 pregnancies (Dunlevy et al., 2007). They encompass varying clinical features and degrees of clinical severity. Open lesions that affect the brain include anencephaly and craniorachischisis, and these types of

lesion are invariably lethal before or at birth. In contrast, open spina bifida is generally compatible with postnatal survival. However, the resulting neurological impairment below the level of the lesion may give rise to a number of clinical symptoms including the inability to walk. Less severe NTDs, including closed spinal lesions such as spina bifida occulta, may be asymptomatic (Copp et al., 2013). The potential importance of dietary folate in the prevention of NTDs was initially noted in the 1970's when Smithells et al. (1976) reported reduced serum concentrations of folic acid, riboflavin and vitamin C in mothers who were pregnant with fetuses with NTDs (Smithells et al., 1976). Several clinical trials evaluating the efficacy of folic acid supplementation in the prevention of NTDs ensued and mandatory folic acid food fortification of cereal and grain products with 140 µg/100 g folic acid (the fully oxidised, metabolically stable, synthetic form of folate) was introduced in North America in 1998 (Daly et al., 1998). Other countries followed suit including Canada and South America. Following this fortification, a decline in the prevalence of children born with NTD's has been documented (Honein et al., 2001).

The mechanisms responsible for NTD prevention and neural tube closure following folic acid supplementation remain relatively unknown and in some cases, controversial. Importantly, NTDs are not considered to be vitamin deficiency disorders, but are in fact associated with a range of genetic and environmental factors (Copp and Greene, 2010; Doudney et al., 2009). The role of folate in cell multiplication may in part account for closure of the neural tube by increasing cell proliferation. In addition, mutations in folate related genes including the 677C>T polymorphism in the 5,10-methylenetetrahydrofolate reductase gene (*MTHFR*), is associated with approximately a 1.8 times higher risk of NTDs (Amorim et al., 2007). Missense mutations in genes encoding enzymes of the glycine cleavage system have also been associated with increased risk of NTDs and include aminomethyltransferase (*AMT*) and glycine dehydroxylase (*GLDC*) (Narisawa et al., 2012). Variants in these genes affect enzyme activity and reduce flux of formate from the mitochondria into the cytoplasm. Formate accounts for roughly 75% of the one-carbon units entering one-carbon metabolism (see section 1.4.4). Treatment of epilepsy with anticonvulsant therapies (Lammer et al., 1987), including carbamezapine (Hernández-Díaz et al., 2001), has been hypothesised to have anti-folate effects. These effects are thought to be associated with inducing teratogenic

mechanisms leading to NTDs. Interestingly, anticonvulsant therapy has also been implicated in causing secondary folate deficiency in other disorders including mitochondrial diseases (Opladen et al., 2010), as discussed in section 1.6.

Taken together, further investigations are required to elucidate the underlying aetiology of NTDs. Specifically, studies to broaden current understanding of the importance of folic acid and folate metabolism in NTD prevention may lead to additional and potentially effective preventative strategies being implemented (Doudney et al., 2009).

### 1.4.1 Structure

Folate coenzymes are structurally and metabolically interconvertable. They comprise a pterin ring structure conjugated to a para-aminobenzoic acid moiety, which is further conjugated to an oligo-γ-glutamyl tail of glutamate residues of varying chain length (Figure 4a). However, the family members differ in the oxidation state of the pyrazine portion of the pterin ring, the character of the one-carbon functional groups at positions N5 and N10, and the number of glutamic acid moieties conjugated to one another via a series of γ-glutamyl links to form the oligo-γ-glutamyl tail.

Of the folate coenzymes, 5-MTHF is the principal bioactive and transport form (Bailey, 2010) (Figure 4b) and is involved in over 100 metabolic reactions (Hyland et al., 1988; Surtees et al., 1994). 5-MTHF is characterised by a reduced pyrazine portion of the pterin ring to give a tetrahydro derivative and a methyl group conjugated at the N5 position. Like other related reduced pterin molecules including tetrahydrobiopterin (Blair and Pearson, 1974; Kirsch et al., 2003), 5-MTHF is susceptible to oxidation in the presence of molecular oxygen and oxidising species. 5-MTHF has been shown to undergo oxidative attack at the C(4a) position with the hydroperoxyl radical implicated as the chain-propagating carrier. This reaction yields two major 5-MTHF degradation products, 4a-hydroxy-5-methyl-4a,5,6,7-tetrahydrofolate and 5-methyl-5,6-dihydrofolate (Blair et al., 1975) (Figure 5).

### 1.4.2 Absorption and transport of folate in the periphery

Food folate is predominantly found in the 5-MTHF form. 5-MTHF can readily oxidise to 5-methyl-5,6-dihydrofolate in food and upon ingestion, 5-methyl-5,6-

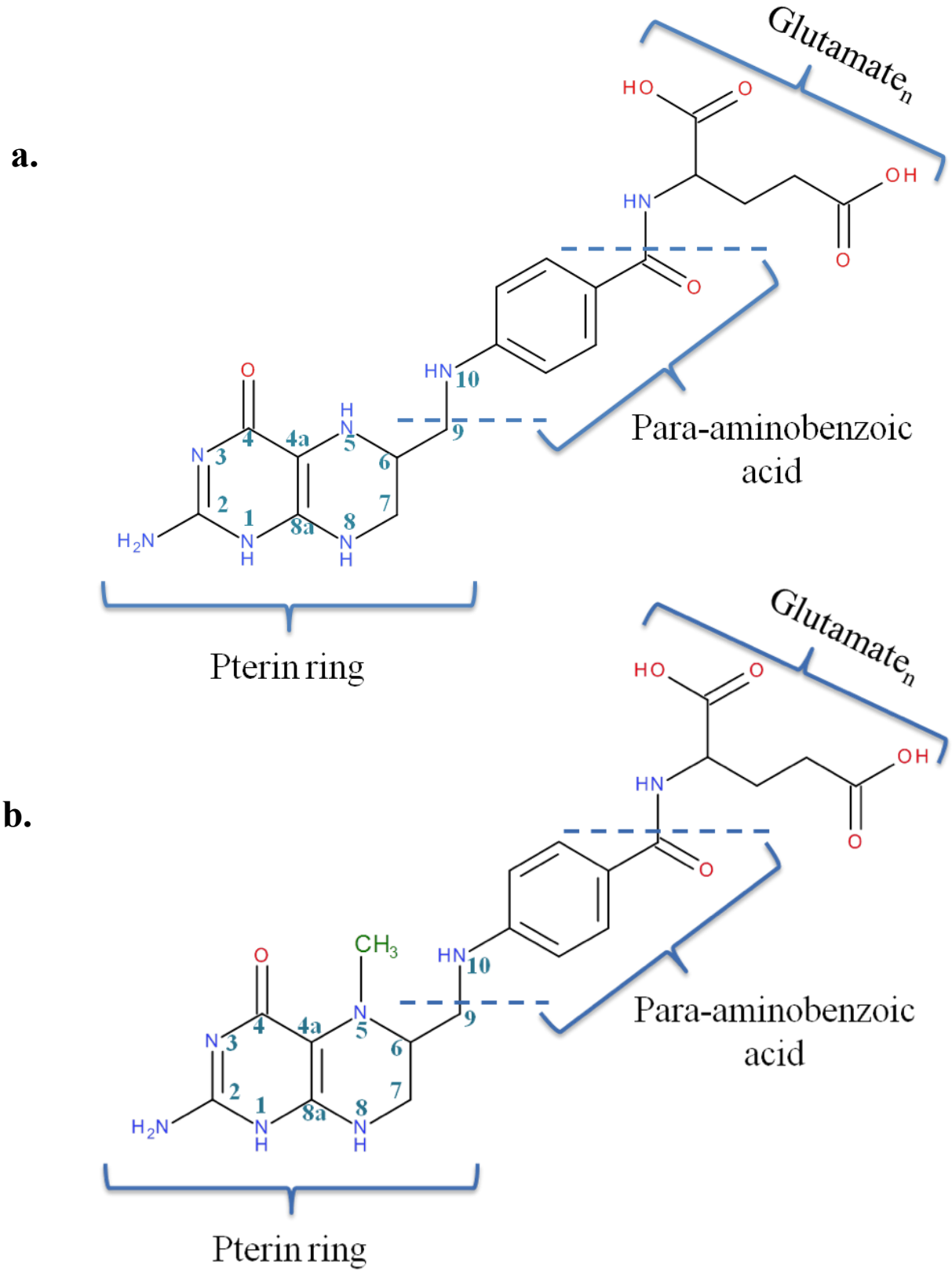


***Figure 4 Folate structure***. a. Tetrahydrofolate and b. 5-MTHF. The folate coenzymes comprise a pterin ring structure conjugated to a para-aminobenzoic acid moiety, which is further conjugated to an oligo-γ-glutamyl tail of glutamate residues of varying chain length. The family differ in the oxidation state of the pyrazine portion of the pterin ring, the character of the one-carbon functional groups at positions N5 and N10, and the number of glutamic acid moieties conjugated to one another via a series of γ-glutamyl links to form the oligo-γ-glutamyl tail.

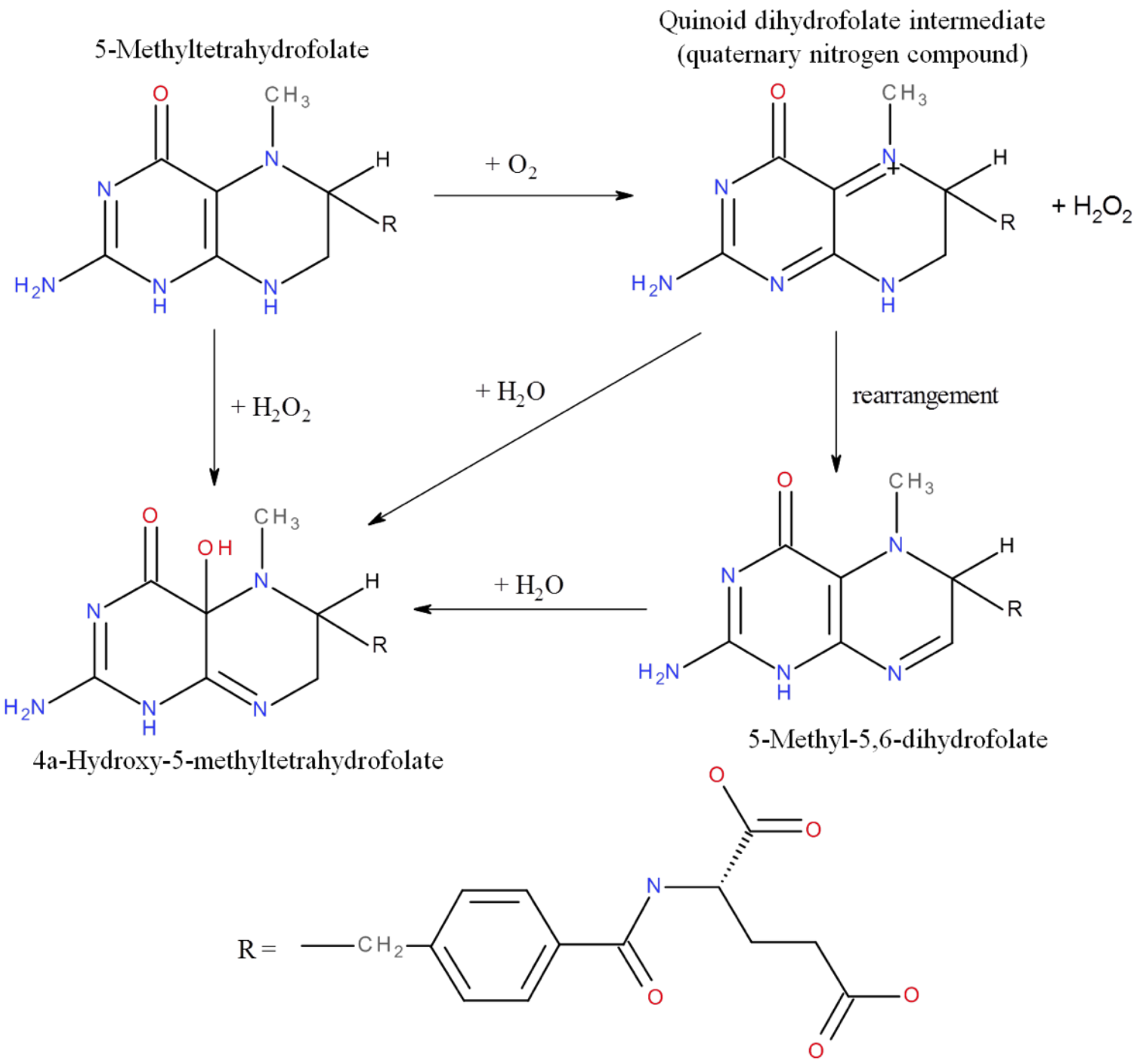


***Figure 5 Degradation of 5-MTHF***. 5-MTHF is susceptible to oxidative catabolism in the presence of molecular oxygen and oxidising species. Figure adapted from Blair et al. (1975).

dihydrofolate can be rapidly degraded in the acidic conditions of the postprandial gastric environment (Lucock et al., 1995). In order to optimise the bioavailability of 5-MTHF in food, AA is actively secreted into the gastric lumen (Verlinde et al., 2008). AA reduces 5-methyl-5,6-dihydrofolate, in a two electron donation reaction, to 5-MTHF which is more stable in acidic environments (Lucock et al., 1995; Wilson and Horne, 1983). In addition, food folate is mostly bound to proteins in a polyglutamate form. Folate cannot be absorbed in the polyglutamate form and prior to absorption, is hydrolysed to the monoglutamate form via the activity of γ-glutamyl hydrolase in the proximal small intestine (Cole et al., 2001; Perry and Chanarin, 1972; Reisenauer et al., 1986).

Ingested folate and folate that is delivered via the bile duct to the duodenum during enterohepatic circulation (Steinberg, 1984; Steinberg et al., 1979), is absorbed in the proximal jejunum primarily by the reduced folate carrier (RFC) and the proton-coupled folate transporter (PCFT) expressed on apical brush border cells (Dudeja et al., 2001; Hinken et al., 2011; Zhao et al., 2009a). The RFC mediates folate transport at neutral pH by a folate/hydroxyl anion exchange mechanism, whilst the PCFT mediates folate transport at low pH via a $H^+$ co-transporter mechanism. However, it is apparent that folate transport occurs primarily via the PCFT carrier since intestinal folate transport is optimal at pH 5.5; the optimal transport conditions for the PCFT (Bailey, 2010; Urquhart et al., 2010; Zhao et al., 2009a). Whilst the RFC does play a role in folate transport within the small intestine, the carrier performs more effective specialised transport in the proximal renal tubules, in the placenta and at the blood brain barrier (Bailey, 2010; Patterson et al., 2008; Solanky et al., 2010). Within the enterocyte, food folate that does not exist as 5-MTHF, is metabolised into the 5-MTHF form mediated by one carbon metabolism (see section 1.4.4) (Stover and Field, 2011). 5-MTHF is exported out of enterocytes into portal circulation by multidrug resistance proteins (MRP), including MRPs 1-5, expressed on the basolateral membrane (Chen et al., 2002; Hooijberg et al., 2003; Matherly and Goldman, 2003; Zhao et al., 2011). These proteins are members of the ATP-binding cassette (ABC) superfamily of transporters, which utilise energy from the hydrolysis of ATP to translocate substrates across membranes. 5-MTHF monoglutamate released into portal circulation can either be directly distributed to extrahepatic tissues or taken up by the liver. In turn, folate delivered to the liver can either be

converted to the polyglutamate form and incorporated into the hepatic folate pool or released into the enterohepatic circulation (Fernández et al., 1998; Steinberg et al., 1979). Enterohepatic circulation is a process whereby folate is discharged into the bile, delivered via the bile duct to the duodenum and reabsorbed by the proximal jejunum before re-entering portal circulation where it can be channelled back to the liver or distributed to extrahepatic tissues. As much as 50% of the circulating folate which reaches the extrahepatic tissues would have undergone enterohepatic recycling in this way (Shin et al., 1995; Steinberg, 1984).

Measurement of total folate may be defined as measuring the pterin ring of the folate skeleton in the tetrahydrofolate form substituted with any functional group at any position. Serum total folate concentrations are age and sex specific and are in the region of 1.1-51.0 nmol/L (0.5-22.7 µg/L), according to the reference ranges used in the Chemical Pathology unit at Great Ormond Street Hospital, UK (Table 3). Approximately 30-40% of the circulating 5-MTHF is bound to low affinity binding proteins including albumin, α2 macroglobulin, transferrin and the high affinity folate binding protein (Markkanen and Peltola, 1971; Markkanen et al., 1973, 1972). Diagnosis of CFD requires additional measurement of serum total folate to exclude a nutritional folate deficiency (Ramaekers et al., 2002). In addition, 5-MTHF and 5-formyltetrahydrofolate in the penta- and hexaglutamate forms are stored in erythrocytes, incorporated into the erythrocyte during erythropoiesis (Clifford et al., 2005; Koury and Ponka, 2004). Whilst erythrocyte folate has no known metabolic role, it is thought that it acts as a storage reservoir and long-term buffer for maintaining peripheral folate homeostasis (Choumenkovitch et al., 2001; Golbahar et al., 2005). Erythrocyte folate is not affected by recent dietary intake, which makes it a good indicator of peripheral folate status. Typical levels of total erythrocyte folate are in the region of 0.3-1.2 µmol/L (119-519 µg/L), according to the reference ranges used in the Chemical Pathology Unit at Great Ormond Street Hospital, UK (Table 4). In senescent erythrocytes, the folate is salvaged via the reticuloendothelial system and transported to the liver. Here, it is recycled and redistributed to extrahepatic tissues via the enterohepatic cycle (Bailey, 2010).

***Table 3 Total serum folate reference ranges***. Total serum folate reference ranges are age- and sex-related. Values are given in nmol/L and µg/L to accommodate how the concentration may be expressed in reporting. These reference ranges are used in in the Chemical Pathology unit at Great Ormond Street Hospital, London, UK.

| **Total serum folate** | | |
|---|---|---|
| **Age (years)** | **Male (nmol/L [µg/L])** | **Female (nmol/L [µg/L])** |
| **0-1** | 16.2 – 50.3 [7.2 -22.4] | 14.2 – 51.0 [6.3 – 22.7] |
| **2-3** | 5.6 – 33.7 [2.5 – 15.0] | 3.8 – 35.3 [1.7 – 15.7] |
| **4-6** | 1.1 – 29.2 [0.5 – 13.0] | 6.1 – 31.7 [2.7 – 14.1] |
| **7-9** | 5.2 – 26.7 [2.3 – 11.9] | 5.4 – 30.1 [2.4 – 13.4] |
| **10-12** | 3.4 – 24.3 [1.5 – 10.8] | 2.2 – 22.9 [1.0 – 10.2] |
| **13-18** | 2.7 – 19.8 [1.2 – 8.8] | 2.7 – 16.2 [1.2 – 7.2] |
| **18+** | 4.5 – 45.3 [2.0 – 20.2] | 4.5 – 45.3 [2.0 – 20.2] |

***Table 4 Total erythrocyte folate reference range***. Values are given in nmol/L and µg/L to accommodate how the concentration may be expressed in reporting. This reference range is used in the Chemical Pathology unit at Great Ormond Street Hospital, London, UK.

| **Total erythrocyte folate** | |
|---|---|
| **All ages/sex (nmol/L [µg/L])** | 0.3 – 1.2 [119 – 519] |

### 1.4.3 5-MTHF transport from the periphery into cerebrospinal fluid

Circulating 5-MTHF from the periphery is transported into CSF across the choroid plexus (Cario et al., 2009; Grapp et al., 2012; Steinfeld et al., 2009). The choroid plexus is the locus of a critical interface between the blood and CSF known as the blood-CSF barrier (Strazielle and Ghersi-Egea, 2000). It is an endothelial-epithelial vascular convolute within the ventricular system of the brain weighing approximately 2 g and is divided into four sections, one in each lateral ventricle, one in the third ventricle and one in the fourth ventricle (Netsky and Shuangshoti, 1975). It consists of fenestrated blood vessels, epithelial cells and stroma, and depending on physiological or pathological conditions, the stroma can contain fibroblasts, mast cells, macrophages or other infiltrates (Dropp, 1976; Matyszak et al., 1992; Serot et al., 1994). The choroid plexus plays an important role in the production of clear and colourless CSF which involves a two-step process involving a number of active transport systems, ion and water channels (Bering, 1955; Milhorat, 1969; Speake et al., 2001). Plasma ions and molecules, including $Na^+$, $Cl^-$, $K^+$, $HCO_3^-$, protein, amino acids, glucose and water, are ultrafiltrated from the fenestrated vasculature of the choroid plexus and are transported from the stroma into choroid plexus epithelial cells (Nilsson et al., 1992). Ion transporters, ion channels and co-transporters mediate the transport of ions and small molecules across the apical and basolateral membranes of the choroid plexus epithelial cells into the ventricles, whilst the transport of larger molecules (vitamins, hormones and peptides) is mediated by transcytosis, endocytosis or specific oligopeptide transporters (Grapp et al., 2013; Roberts et al., 2008; Spector and Johanson, 2010; Tachikawa et al., 2008). The net blood to CSF transport of these ions and molecules results in the formation of CSF (Brodbelt and Stoodley, 2007; Brown et al., 2004; Spector, 2010). Importantly, plasma ultrafiltrate cannot freely pass between the blood and CSF compartments owing to tight junctions adjoining the apical membranes of the choroid plexus epithelial cells. These tight junctions, known as claudins, represent the blood-CSF barrier (Kratzer et al., 2012; Wolburg et al., 2001). Approximately 140 ml of CSF is divided between the ventricular system (35 ml), spinal canal (30-70 ml) and the cranial subarachnoid space (35-75 ml) and the CSF, produced at ~500 ml/day, is consistently replenished (Brodbelt and Stoodley, 2007). CSF circulates rostrocaudally inside the ventricles and in cranial and spinal subarachnoid spaces (Tarnaris et al., 2011). Whilst CSF plays a crucial role in cushioning the brain and

spinal cord, of greater importance is the role of CSF in mediating metabolite, toxin and nutrient exchange between the CNS and the periphery, and facilitating hormonal and signalling mechanisms, chemical buffering and neurodevelopment (Crossgrove et al., 2005; Spector, 2010).

Recently, it has been demonstrated that the transport of 5-MTHF across the choroid plexus is primarily mediated by the high affinity glycosylphosphatidylinositol (GPI)-anchored folate receptor-α (FRα) (Cario et al., 2009; Grapp et al., 2013; Steinfeld et al., 2009; Wollack et al., 2008) (Figure 6). The FRα is localised on the basolateral membrane of the choroid plexus epithelial cells and 5-MTHF uptake occurs via receptor-mediated endocytosis and transcytosis (Grapp et al., 2013). This is an active process requiring energy in the form of ATP. 5-MTHF and FRα are co-transported via an endosomal compartment by a clathrin-independent pathway to form tubular early endocytic compartments. A minor proportion of internalised 5-MTHF is translocated to PCFT-positive vesicles and transported into the cytoplasm (Zhao et al., 2009b). Here, 5-MTHF is converted into the polyglutamate form via the activity of folyl-γ-polyglutamate synthase (FPGS) in order to facilitate cellular retention (Moran and Colman, 1984; Schirch and Strong, 1989). The endosomal compartments are subsequently translocated to multivesicular bodies containing intraluminal vesicles. Multivesicular bodies are known to be sites for intracellular sorting of proteins between recycling, degradation and secretion pathways, and fuse with the apical membrane of the choroid plexus to secrete their intraluminal vesicles into the CSF as exosomes. Approximately 36% of all human CSF exosomes have been shown to contain 5-MTHF-bound FRα. It has also been suggested that fusion of the multivesicular body to the apical membrane may also lead to 5-MTHF release and FRα recycling between the apical membrane and the late endosomal compartment offering a mechanism for 5-MTHF uptake from the CSF. Once present in the CSF, it is thought that these exosomes deliver FRα into the brain parenchyma (Grapp et al., 2013). Other FRα-independent mechanisms of 5-MTHF transport have also been suggested. They include transport mediated by the RFC and ABC transporters (Chen et al., 2002; Leggas et al., 2004; Rao et al., 1999). These mechanisms may be of greater importance when 5-MTHF is present at higher concentrations (>100 nmol/L) (Grapp et al., 2013). Overall, the transport of 5-MTHF

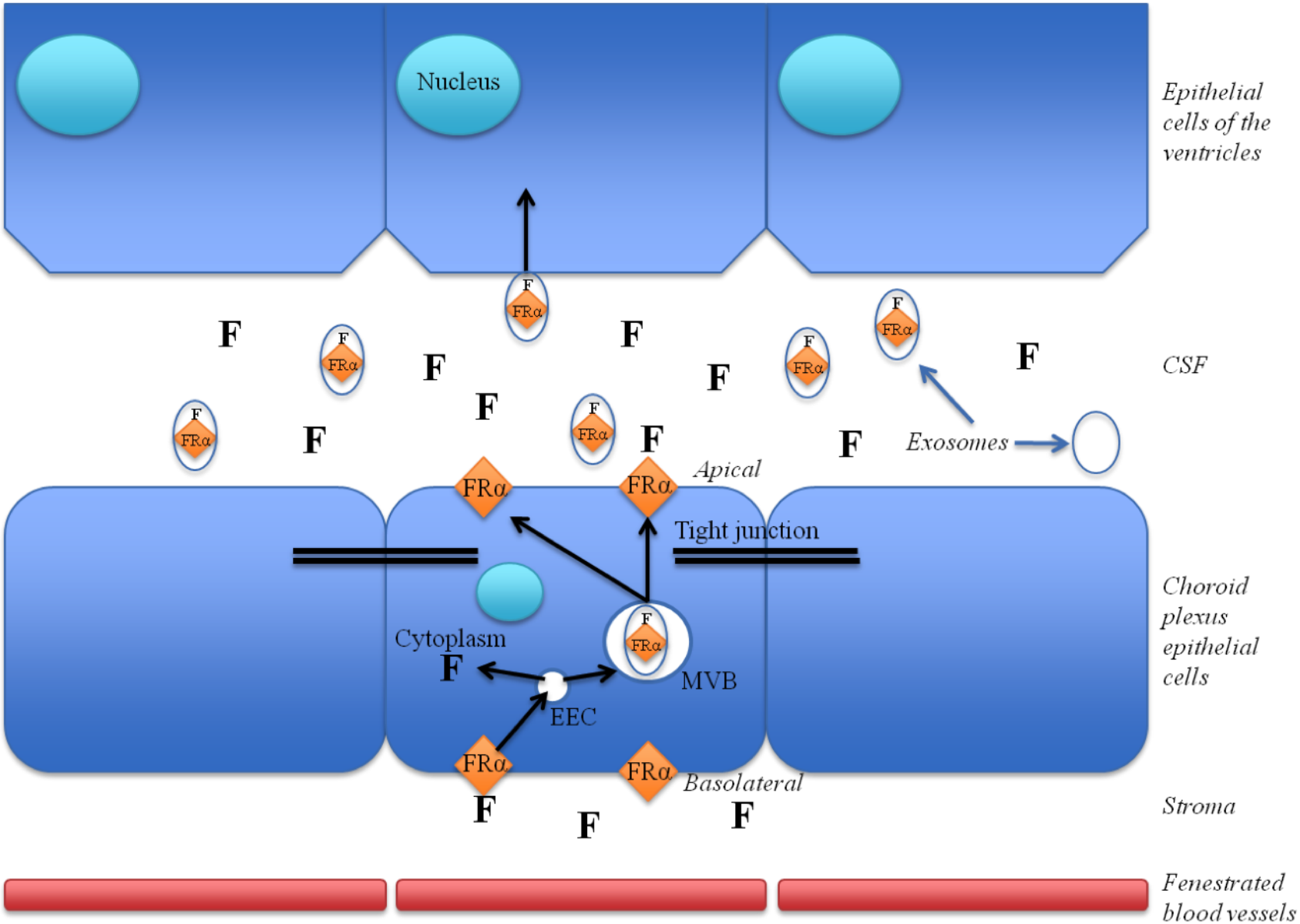


***Figure 6 Transport of 5-MTHF across choroid plexus epithelial cells***. The FRα is localised on the basolateral membrane of the choroid plexus epithelial cells and 5-MTHF uptake occurs via active receptor-mediated endocytosis and transcytosis. 5-MTHF and FRα are co-transported via endosomal compartments, which are subsequently translocated to multivesicular bodies containing intraluminal vesicles. Multivesicular bodies fuse with the apical membrane of the choroid plexus to secrete their intraluminal vesicles into the CSF as exosomes. Fusion of the multivesicular body to the apical membrane may also lead to 5-MTHF release and FRα recycling between the apical membrane and the late endosomal compartment offering a mechanism for 5-MTHF uptake from the CSF. Once present in the CSF, it is thought that these exosomes deliver FRα and 5-MTHF into the brain parenchyma. F = 5-MTHF; EEC = early endosomal compartment; MVB = multivesicular body.

from the periphery into CSF across the choroid plexus results in approximately a 2-4 fold higher 5-MTHF concentration in the CSF compared to plasma (Spector and Lorenzo, 1975). The importance of FRα in mediating 5-MTHF transport across the choroid plexus, is evidenced by the embryonic lethality of FRα -/- knockout mice (Piedrahita et al., 1999; Zhu et al., 2007). In humans, mutations in the *FOLR1* gene encoding the FRα protein do not cause embryonic lethality. Patients with mutations in the *FOLR1* gene present with undetectable CSF 5-MTHF <10 nmol/L at four to six months of age (Cario et al., 2009; Grapp et al., 2012; Steinfeld et al., 2009). This discrepancy between the mouse and human phenotype raises the possibility that an additional transporter, such as the folate receptor β (FRβ), may be responsible for 5-MTHF transport across the choroid plexus during embryonic and fetal development, and expression may be downregulated following birth (Steinfeld et al., 2009). The function of the secreted folate receptor γ (FRγ) and folate receptor δ (FRδ) are not well understood (Grapp et al., 2013). In addition, it has been suggested that high circulating peripheral levels of 5-MTHF at birth may provide the CNS with a degree of protection, which could account for the delay of disease and clinical manifestation onset (Ramaekers and Blau, 2004).

In addition to 5-MTHF transport across the choroid plexus into the CSF, 5-MTHF can also be transported across the blood-brain barrier (BBB) into the brain interstitium. This transport process is facilitated by the RFC (Wu and Pardridge, 1999). However, this transport process alone would not be sufficient in achieving an adequate level of 5-MTHF required in the CNS (Araújo et al., 2010).

CSF 5-MTHF concentration follows a negative age-related trend (Ormazabal et al., 2006). The age-related CSF 5-MTHF reference ranges used in the Neurometabolic Unit at The National Hospital for Neurology and Neurosurgery, London, UK, are given in Table 5.

### 1.4.4 One-carbon metabolism

Upon transportation into the cell, the 5-MTHF monoglutamate is converted by methionine synthase into tetrahydrofolate (THF). Moreover, folate is modified with a covalently bound glutamate polypeptide. This polypeptide consists of between three to eight glutamate residues, with penta- and hexaglutamate being the

***Table 5 CSF 5-MTHF reference ranges***. CSF 5-MTHF follows a negative age-related trend. Therefore, CSF 5-MTHF concentration is age-related and the below reference ranges are used in the Neurometabolic Unit at The National Hospital for Neurology and Neurosurgery, London, UK.

| **CSF 5-MTHF reference ranges** | |
|---|---|
| **Age (years)** | **Concentration (nmol/L)** |
| 0 – 2 | 72 – 305 |
| 2 – 5 | 52 – 178 |
| 5 – 10 | 72 – 172 |
| 10+ | 46 – 160 |

predominant chain lengths (Brody et al., 1982). Polymerisation occurs via the activity of FPGS, which links each glutamate residue with γ-peptide bonds. The importance of the oligo-γ-glutamyl tail is to generate functional coenzymes. It also facilitates the ability of the coenzyme to bind with high affinity to folate-dependent enzymes and binding proteins, and enables cellular and intracellular compartment retention (Moran and Colman, 1984; Schirch and Strong, 1989).

THF polyglutamate molecules carry out their cellular functions by activating and carrying single carbon units at the N5 and/or N10 positions. THF carries activated formate as 5-formyl-THF, 10-formyl-THF or 5,10-methenyl-THF. THF also carries activated formaldehyde as 5,10-methylene-THF and activated methanol as 5-MTHF. THF polyglutamates accept and transfer these one-carbon moieties in a network of biosynthetic and catabolic reactions. This network is known as folate-mediated one-carbon metabolism and the pathways associated with one-carbon metabolism function in three separate compartments, the cytoplasm, the mitochondria and the nucleus (Figure 7) (Tibbetts and Appling, 2010). Each compartment is its own unique entity carrying out its own specialised metabolic function. As such, folate coenzymes do not readily exchange between them. The mitochondrial one-carbon metabolism pathways generate one-carbons in the form of formate through the catabolism of serine, glycine and choline (Pasternack et al., 1994, 1992). The cytoplasmic one-carbon metabolism pathways utilise the mitochondrial-derived formate for nucleotide biosynthesis and for the remethylation of homocysteine to methionine (Lamarre et al., 2012; Stam et al., 2005). Within the nucleus, one-carbon metabolism pathways generate thymidylate during DNA replication and repair (MacFarlane et al., 2011). Whilst each compartment performs its own specialised metabolic function, there is interdependence between the compartments with ongoing shuttling of metabolic intermediates including serine, glycine and formate, and competition for the limiting pool of folate coenzymes (Tibbetts and Appling, 2010).

#### 1.4.4.1 One-carbon metabolism in the cytoplasm

One-carbon metabolism within the cytoplasm includes the biosynthetic pathways leading to the *de novo* synthesis of purines and thymidylate, and the remethylation of

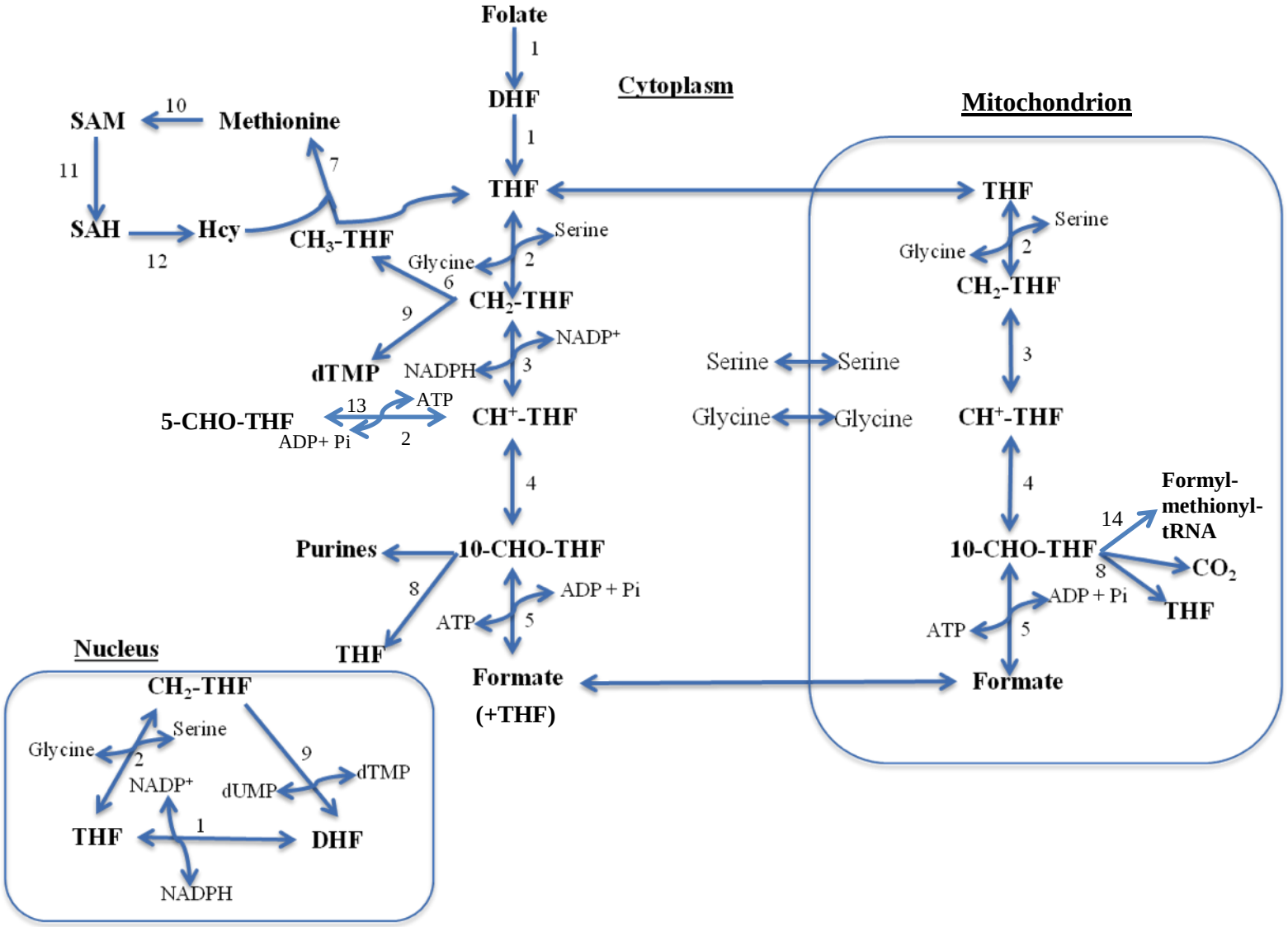


***Figure 7 One-carbon metabolism in the cytoplasm, mitochondrion and nucleus***. DHF=dihydrofolate; THF=tetrahydrofolate; $CH_2$-THF=5,10-methylenetetrahydrofolate; $CH^+$-THF=5,10-methenyltetrahydrofolate; 5-CHO-THF=5-formyltetrahydrofolate; 10-CHO-THF=10-formyltetrahydrofolate; $CH_3$-THF=5-methyltetrahydrofolate; SAM=*S*-adenosylmethionine; SAH=*S*-adenosylhomocysteine; Hcy=homocysteine; dUMP=deoxyuridine monophosphate; dTMP=deoxythymidine monophosphate. 1. Dihydrofolate reductase, 2. Serine hydroxymethyltransferase, 3. 5,10-methylene-THF dehydrogenase, 4. 5,10-methenyl-THF cyclohydrolase, 5. 10-formyl-THF synthetase, 6. 5,10-methylene-THF reductase, 7. methionine synthase, 8. 10-formyl-THF dehydrogenase, 9. thymidylate synthase, 10. *S*-adenosylmethionine synthetase, 11. *S*-adenosylhomocysteine synthase, 12. *S*-adenosylhomocysteine hydrolase, 13. 5,10-methenyl-THF synthetase, 14. Methionyl-$tRNA_F^{MET}$ formyltransferase. For detailed explanation see section 1.4.1.

homocysteine to form methionine (Figure 7) (Fox and Stover, 2008; Girgis et al., 1997). Methionine is an important precursor for the synthesis of *S*-adenosylmethionine (SAM). SAM functions as a cofactor and methyl group donor for numerous methylation reactions (Dixon et al., 1996). These reactions include the methylation of DNA, RNA, neurotransmitters, phospholipids and proteins including histones (Mattson, 2003; Stam et al., 2005). Whilst the mitochondria serve as the main source of one-carbon moieties for these reactions, the cytoplasm can also generate one-carbon entities through the catabolism of histidine, serine and purines (Anguera et al., 2006; Depeint et al., 2006; Fell and Steele, 1982).

Purine nucleotides are precursors for DNA and RNA synthesis and serve as coenzymes and regulatory factors (Bailey, 2010). Purines can be synthesised *de novo* via one carbon metabolism (Berg et al., 2002). The *de novo* pathway consists of a 10-step enzymatic process culminating in the production of inosine monophosphate, the precursor of adenine and guanine nucleotides (Field et al., 2006). 10-Formyl-THF is the cofactor required for this pathway, which is synthesised from THF and mitochondrial-derived formate, in an ATP-dependent reaction catalysed by 10-formyl-THF synthetase. The formyl group of 10-formyl-THF donates a carbon to phosphoribosylaminoimidazole carboxamide ribonucleotide (AICAR) and phosphoribosylglycinamide ribonucleotide (GAR), which ultimately become the C2 and C8 positions of the purine ring (Smith et al., 1980). 10-Formyl-THF that is not used to synthesise purines, is dehydrated and reduced for use in the biosynthesis of thymidylate and methionine. Alternatively, 10-formyl-THF can undergo irreversible, nicotinamide adenine dinucleotide phosphate ($NADP^+$)-dependent oxidation to THF and $CO_2$ via the activity of 10-formyl-THF dehydrogenase (Anguera et al., 2006). THF generated in this reaction can be channelled efficiently to serine hydroxymethyltransferase (SHMT) or 10-formyl-THF synthetase to regenerate an activated one-carbon. Chemotherapeutic anti-folate agents including methotrexate are effective in disrupting purine synthesis via the *de novo* pathway by targeting folate dependent enzymes including GAR formyltransferase (GARFT), AICAR formyltransferase (AICARFT) and dihydrofolate reductase (DHFR) (Allegra et al., 1986; Baggott et al., 1994, 1986).

10-Formyl-THF exists in cytoplasmic equilibrium with 5,10-methenyl-THF. One-carbon units obtained from the catabolism of histidine, adenine and guanine enter the

cytoplasmic one-carbon pool as 5,10-methenyl-THF. During catabolism, the imidazole ring of histidine, adenine and guanine is converted to a formimino goup (Revel and Magasanik, 1958). This formimino group is transferred to THF forming 5-formimino-THF, which is subsequently converted to 5,10-methenyl-THF by the cyclodeaminase activity of the protein (Depeint et al., 2006; Schalinske and Steele, 1996). 5,10-Methenyl-THF is also synthesised from 5-formyl-THF in an ATP-dependent reaction catalysed by 5,10-methenyl-THF synthetase. 5,10-Methenyl-THF synthetase is the only enzyme known to utilise 5-formyl-THF as a substrate and is expressed ubiquitiously. Importantly, 5-formyl-THF is not a coenzyme for one-carbon transfer reactions but a stable storage form of excess formyl folate (Tibbetts and Appling, 2010). The activity of 5,10-methenyl-THF synthetase generating 5,10-methenyl-THF from 5-formyl-THF, and SHMT generating 5-formyl-THF from 5,10-methenyl-THF, constitutes a futile cycle. This cycle regulates the intracellular 5-formyl-THF concentrations (Girgis et al., 1997; Stover and Schirch, 1993).

Thymidylate and dihydrofolate (DHF) are synthesised from 5,10-methylene-THF and deoxyuridine monophosphate in a reaction catalysed by thymidylate synthase (TS) (Schiffer et al., 1995). DHF produced in this reaction is reduced back to THF via the activity of DHFR (Abali et al., 2008). 5,10-Methylene THF pools are derived from the reduction of 10-formyl-THF in sequential reactions catalysed by 5,10-methenyl-THF cyclohydrolase and 5,10-methylene-THF dehydrogenase (Fox and Stover, 2008). This pool is in equilibrium with 5,10-methylene-THF derived from the THF-dependent conversion of serine to glycine catalysed by SHMT (Anderson et al., 2012; MacFarlane et al., 2008). Both pools of 5,10-methylene-THF contribute to the biosynthesis of thymidylate (MacFarlane et al., 2011).

5-MTHF is the required cofactor for the $Zn^{2+}$ and cobalamin (vitamin B12) dependent remethylation of homocysteine to methionine catalysed by methionine synthase (MS) (Dixon et al., 1996; Scott and Weir, 1998). An additional enzyme, betaine homocysteine methyltransferase (BHMT), also remethylates homocysteine to methionine in a folate-independent manner, which makes the metabolic function of MS partially redundant (Teng et al., 2012). However, BHMT expression is limited primarily to the kidney and the liver, whereas MS is ubiquitously expressed (Leclerc et al., 1999; Slow and Garrow, 2006). MS functions to regenerate THF, prevent 5-MTHF accumulation, synthesise methionine and remove cellular homocysteine.

Elevated levels of homocysteine are a risk factor for cardiovascular disease, Alzheimer's disease and NTDs (Minagawa et al., 2010; Rosenquist et al., 1996; Wald et al., 2002). The loss of MS activity, resulting for example from vitamin B12 deficiency, inhibits nucleotide biosynthesis owing to the accumulation of cytoplasmic folate cofactors including 5-MTHF (Banerjee and Matthews, 1990; Yamada et al., 2000). This effect is known as the "5-MTHF trap" and occurs because the 5,10-methylene-THF reductase catalysed reaction is irreversible and MS is a key 5-MTHF utilising enzyme (Fujii et al., 1982; Kaufman, 1991).

5-MTHF is generated from 5,10-methylene-THF in a reduction reaction catalysed by 5,10-methylene-THF reductase. Importantly, 5,10-methylene-THF reductase retains an allosteric binding site for SAM. Under circumstances whereby SAM concentrations are adequate, SAM acts as an allosteric inhibitor to ensure 5,10-methylene-THF is spared for thymidylate biosynthesis (Jencks and Mathews, 1987; Matthews and Daubner, 1982). This feedback inhibition also protects against 'trapping'. Interestingly within the cell, 5-MTHF is bound, but not metabolised, by SHMT and glycine *N*-methyltransferase (GNMT). GNMT functions to catalyse the SAM dependent methylation of glycine to sarcosine, thereby governing transmethylation reactions by regulating and buffering the SAM/*S*-adenosylhomocysteine (SAH) ratio. This is known as the cellular 'methylation potential' (Bailey, 2010; Porter et al., 1985). GNMT is itself allosterically regulated by 5-MTHF (Luka, 2008; Luka et al., 2007). Under conditions whereby SAM inhibits 5,10-methylene-THF reductase, GNMT remains active and metabolises excess SAM. Whereas, under conditions where SAM levels are low, 5-MTHF is produced by 5,10-methylene-THF reductase, thereby inhibiting GNMT activity and conserving methionine supply for essential methylation reactions (Wagner et al., 1989). In addition, 5-MTHF is sequestered by SHMT and may compete with MS for this enzyme. SHMT acting as a 5-MTHF binding protein, conserves and limits the availability of 5-MTHF for homocysteine remethylation (Herbig et al., 2002; MacFarlane et al., 2008).

#### 1.4.4.2 One-carbon metabolism in the mitochondria

One-carbon metabolism in the mitochondria includes the biosynthetic pathways leading to the generation of one-carbon units in the form of formate for one-carbon metabolism in the cytoplasm, the generation of the amino acid glycine and the

synthesis of formyl-methionyl-tRNA, unique for protein synthesis in mitochondria (Figure 7) (Tibbetts and Appling, 2010). In contrast to the cytoplasm, the interconversion of one-carbon substituted folate in the mitochondria is driven in the oxidative direction towards formate production and differs with respect to the source of reducing equivalents (Lamarre et al., 2012; Shane, 1989). Approximately 40% of the total cellular folate is found in the mitochondria (Depeint et al., 2006).

Mitochondrial 5,10-methylene-THF synthesis is initiated via the cleavage of the C3 of serine to glycine, catalysed by the pyridoxal-phosphate dependent SHMT (Pasternack et al., 1994). The C3 of serine is the primary source of folate-activated one-carbon units. The glycine cleavage system (GCS), a multienzyme complex that generates folate-activated one-carbons, catalyses the production of 5,10-methylene-THF, $CO_2$ and ammonia, following the reversible oxidation of glycine (Narisawa et al., 2012; Okamura-Ikeda et al., 2005). GCS accounts for nearly 40% of the overall glycine flux in humans, and the one-carbon produced contributes to the cytoplasmic THF-dependent biosynthesis of purines and thymidylate. Additional glycine production and glycine as a substrate for the GCS, is generated from oxidative choline catabolism (Imbard et al., 2013). This occurs through the sequential conversion of choline to betaine aldehyde to betaine to dimethylglycine to sarcosine to glycine, catalysed by choline dehydrogenase, betaine aldehyde dehydrogenase, betaine homocysteine methyltransferase, dimethylglycine dehydrogenase and sarcosine dehydrogenase, respectively (Bailey, 2010; Wittwer and Wagner, 1980).

The generation of 10-formyl-THF from 5,10-methylene-THF requires the sequential conversion of 5,10-methylene-THF to 5,10-methenyl-THF, followed by the conversion of 5,10-methenyl-THF to 10-formyl-THF (Murta et al., 2009; Pawelek and MacKenzie, 1998). These reactions are catalysed by 5,10-methylene-THF dehydrogenase and 5,10-methenyl-THF cyclohydrolase, respectively (Cheung et al., 1997; MacKenzie, 1997). The final step is the conversion of 10-formyl-THF to formate which requires 10-formyl-THF hydrolysis. Hydrolysis is mediated by the activity of 10-formyl-THF synthetase and a favourable ADP/ATP ratio in mitochondria (Christensen et al., 2013). Additionally, formyl-methionyl-tRNA is synthesised from 10-formyl-THF. Formyl-methionyl-tRNA is required for mitochondrial protein synthesis and is generated via the activity of methionyl-$tRNA_F^{MET}$ formyltransferase (Di Pietro et al., 2002).

#### 1.4.4.3 One-carbon metabolism in the nucleus

In addition to the cytoplasm, *de novo* synthesis of thymidylate also occurs in the nucleus. Approximately 10% of cellular folate resides in the nucleus and TS, SHMT and DHFR have been localised to the nuclear compartment of the cell (Figure 7) (Anderson et al., 2012; MacFarlane et al., 2011; Samsonoff et al., 1997). These enzymes are substrates for UBC9-mediated modification with the small ubiquitin-like modifier (SUMO), which targets proteins for nuclear localisation (Woeller et al., 2007). Thymidylate synthesis in the nucleus is thought to take place directly at the replication fork during the S phase of the cell cycle. This would lead to reduced rates of uracil misincorporation (MacFarlane et al., 2011). The importance of thymidylate for DNA and RNA replication and repair is crucial, since the loss of TS activity due to gene polymorphisms or chemotherapeutic agents, results in decreased rates of DNA synthesis, increased rates of uracil misincorporation into DNA, chromosome damage, fragile site induction and apoptotic cell death (Blount et al., 1997; Hori et al., 1984; Kronenberg et al., 2011).

### 1.5 Cerebral Folate Deficiency

Folate deficiency can occur in both the CNS and periphery, or in the CNS alone (Hyland et al., 2010). Manifestation of folate deficiency may be the consequence of either a primary defect, for example a genetic mutation affecting synthesis, breakdown or transport mechanisms, or a secondary defect, a defect arising as a consequence of the primary cause of disease. Such primary defects that lead to a folate deficiency affecting both the CNS and the periphery may include primary inherited disorders of folate metabolism and transport, for example, mutations in the genes encoding 5,10-methylene tetrahydrofolate reductase, dihydrofolate reductase, and FRα (Banka et al., 2011; Steinfeld et al., 2009; Tsuji et al., 2011). Whereas, disorders such as dietary folate insufficiency, intestinal resection, cancer, use of anti-folate drugs, for example methotrexate, hepatic failure and celiac disease, may lead to a more generalised secondary folate deficiency (Djukic, 2007). Folate deficiency, which occurs solely in the CNS compartment, is called CFD. CFD can be defined as any neurological syndrome associated with a low cerebrospinal fluid (CSF) concentration of 5-methyltetrahydrofolate (5-MTHF) in the presence of normal peripheral folate status (Ramaekers and Blau, 2004). As with the more generalised folate deficiency affecting both the periphery and CNS, manifestation of CFD may

also be the consequence of either a primary defect or secondary defect (see sections 1.5.1 and 1.5.2). CFD can be classified as mild (<30% decrease below the lower reference range limits), moderate (30-60% decrease below the lower reference range limits) and severe (>60% below the lower reference range limits) (Pérez-Dueñas et al., 2011).

### 1.5.1 Primary CFD disorders

Defects in the transport of folate across the choroid plexus from the periphery into the CNS are the main cause of primary CFD. The first report of an isolated CNS folate deficiency was published in 1994 (Wevers et al., 1994). Whilst it was hypothesised that such a deficiency may be the consequence of disturbed transfer of folate across the choroid plexus of the blood-CSF barrier, the exact underlying mechanism(s) was not fully elucidated. Since this time, a number of case reports and cohort studies identifying patients with primary CFD have been documented in the literature and the underlying aetiology of disease examined (Cario et al., 2011; Moretti et al., 2005; Pérez-Dueñas et al., 2011; Ramaekers et al., 2013; Serrano et al., 2012).

Mutations in the *FOLR1* gene encoding the FRα have been associated with inherited primary CFD states. The first reports of mutations in the *FOLR1* gene were published in 2009 (Cario et al., 2009; Steinfeld et al., 2009). Currently, 10 mutations in the coding exons of the *FOLR1* gene have been reported to date, including the unpublished *FOLR1* mutation described in Chapter 3 of this thesis (see Figure 24) (Grapp et al., 2012). In view of the major role of the FRα in mediating transport of 5-MTHF from the periphery into the CSF across the choroid plexus, undetectable concentrations of 5-MTHF (<10 nmol/L) are usually reported in these patients (Ormazábal et al., 2011; Pérez-Dueñas et al., 2011; Serrano et al., 2012). Interestingly, a lack of correlation between clinical severity and residual function of the FRα in patients with *FOLR1* mutations has been demonstrated, suggesting that additional factors and/or mechanisms may contribute to the observed clinical phenotype in CFD (Grapp et al., 2012; Steinfeld et al., 2009).

In addition to *FOLR1* mutations, serum blocking autoantibodies have also been implicated as a cause of primary CFD. In 2005, Ramaekers et al. published a cohort study of 28 patients with CFD (Ramaekers et al., 2005). Interestingly, serum analysis

revealed the presence of FRα blocking autoantibodies in 25 of the 28 patients, and the absence of blocking autoantibodies in none of the 28 matched controls. In addition, serum specimens from 41 subjects with central nervous system disease unrelated to CFD and from five mothers of individual patients, were negative for blocking autoantibodies. In the remaining three CFD patients, the underlying cause of disease was not identified. It was suggested that FRα blocking autoantibodies preferentially bind to the FRα on the epithelial cells on the basolateral membrane of the choroid plexus, preventing effective binding and transport of 5-MTHF from the periphery into the CSF to maintain CSF 5-MTHF concentrations. Ramaekers et al. (2005) further hypothesised that the mechanism responsible for the formation of these autoantibodies could be a consequence of exposure to soluble folate-binding proteins in human or bovine milk or sensitisation by unknown antigens with similar epitopes (Ramaekers et al., 2005). In support of these suggestions is the >90% amino acid sequence homology between the soluble-folate binding proteins in milk and the membrane-bound FRα and FRβ expressed on the human choroid plexus epithelium (Svendsen et al., 1982); FRα and FRβ cross-react with rabbit antibodies against the human-milk folate binding protein. A more recent study published by the same group demonstrated that a bovine milk free diet may downregulate autoantibody titre and be of therapeutic importance in CFD patients where FRα and FRβ blocking autoantibodies have been implicated (Ramaekers et al., 2008).

### 1.5.2 Secondary CFD disorders

Secondary CFD is associated with a wide range of conditions and in the majority of cases the underlying aetiology of disease is not known (Hyland et al., 2010). Specifically, secondary CFD in a subset of patients with mitochondrial disorders is becoming increasingly diagnosed in the clinic (Garcia-Cazorla et al., 2008; Mangold et al., 2011; Ormazábal et al., 2011; Pérez-Dueñas et al., 2011; Serrano et al., 2010). The association between CFD and mitochondrial disease was first described in 1983 in KSS (Macron et al., 1983). In the same year, another case was reported documenting both a CFD and peripheral folate deficiency (Allen et al., 1983). More recently, a severe CFD was reported in a patient with an incomplete form of KSS (Pineda et al., 2006) and in a small cohort study of six patients with KSS published by the same group, five were found to have severe 5-MTHF deficiencies whilst a moderate deficiency was observed in the sixth (Serrano et al., 2010). Moderate CFD

has also been reported in a patient with mitochondrial complex I encephalomyopathy (Ramaekers et al., 2007a) and in a patient with Alpers disease (Hasselmann et al., 2010).

A number of larger cohort studies have also documented CFD in a range of mitochondrial disorders. A study by Garcia-Cazorla et al. (2008) analysed CSF 5-MTHF of 28 patients with mitochondrial disease and 14 of these patients were found to have CFD (Garcia-Cazorla et al., 2008). Severe CFD was reported in four patients with KSS, whilst mild to moderate CFD was described in one patient with KSS, one patient with NARP, two patients with Leigh syndrome and six patients with severe infantile encephalomyopathies and RCE abnormalities. In another study, 36 patients out of 60 with a range of neurological disorders were reported with CFD and 3 of these cases were patients with KSS (Ormazábal et al., 2011). Perez-Duenas et al. (2011) analysed 584 patients with encephalopathies and 71 of these patients had CFD. This group reported two severe CFD in KSS, and moderate CFD in one patient with KSS and four patients with undefined mitochondrial disorders. Similarly, CFD in two patients with undefined mitochondrial disorders were also reported following analysis of a cohort of 103 CFD cases (Mangold et al., 2011).

In addition to mitochondrial disorders, secondary CFD has also been reported in a number of other pathologies. For example, CFD has been described in Rett syndrome, an inherited X-linked neurodevelopmental disease of the grey matter leading to loss of language and motor skills (Weng et al., 2011). Rett syndrome may be caused by mutations in the *MECP2* gene encoding methyl CpG binding protein 2 and studies have suggested that this protein plays an important role in the formation of nerve synapses and gene silencing (Bird, 2008; Nguyen et al., 2012). The association of CFD in Rett syndrome is controversial. Decreased 5-MTHF in CSF was initially observed in four female patients (Ramaekers et al., 2003). Further investigations carried out by other groups indicated that eight out of 16 (Ormazabal et al., 2005), eight out of 25 (Temudo et al., 2009) and 14 out of 33 (Ramaekers et al., 2007b) patients, presented with decreased 5-MTHF in CSF. From the cohort of 33 patients, 14 were found to have blocking autoantibodies against the folate receptors (Ramaekers et al., 2007b). In contrast, a study carried out in North America reported that only two patients with Rett syndrome presented with CFD out of a total of 76. One of these patients also presented with a peripheral folate

deficiency (Neul et al., 2005). The nutritional folate supplementation programme, which is currently in force in North America, may be attributable for the differences observed between these patient cohorts (Hyland et al., 2010). Similarly, the association between CFD and Aicardi-Goutieres syndrome has been debated. Aicardi-Goutieres syndrome is an autoinflammatory disorder mimicking *in utero* viral infection of the brain and may be caused by mutations in the *SAMHD1* gene encoding SAM domain and HD domain-containing protein 1, *TREX1* gene encoding three prime repair exonuclease 1 or ribonuclease H2 encoding genes (*RNASEH2A, RNASEH2B, RNASEH2C*) (Rice et al., 2013). Inheritance of these mutations follows an autosomal recessive pattern. It has been hypothesised that elevated levels of nucleic acid byproducts leads to an inappropriate innate immune system response, since CFD and elevated CSF levels of tetrahydrobiopterin and neopterin have been reported in three patients with the disease (Blau et al., 2003). However, CFD was not observed in nine patients with Aicardi-Gourtiere syndrome in North America, despite elevated CSF levels of tetrahydrobiopterin and neopterin being reported (Hyland et al., 2010). The active nutritional folate supplementation programme in North America may also be accountable for this observation.

Other examples of pathologies where secondary CFD has been indicated include autism and autism-spectrum diseases, and neurodegenerative diseases. Four out of 28 austic patients in one study and seven autistic patients in another study were diagnosed with CFD of varying degrees (Moretti et al., 2008; Ramaekers et al., 2005). More recently, CFD has been reported in 93 patients with autism-spectrum disorder. In these patients a high prevalence (75.3%) of blocking autoantibodies against the folate receptors was reported (Frye et al., 2013). Secondary CFD has also been reported in neurodegenerative disorders including Alzheimer's disease and Parkinson's disease (Banka et al., 2011; dos Santos et al., 2009; Duan et al., 2002; Hinterberger and Fischer, 2013; Serot et al., 2001; Smach et al., 2011). It has been postulated that choroid plexus dysfunction, impeding the transport of 5-MTHF from the blood into the CSF, may be responsible for low CSF folate observed in these patients (Johanson et al., 2004; Rubenstein, 1998). However, a recent study reported CSF data that substantiated the maintenance of choroid plexus transport and homeostatic functions in Alzheimer's disease patients (Spector and Johanson, 2013). In addition to the larger cohort studies, single case reports of patients with secondary

CFD have been published, including in a patient with schizophrenia and catatonia (Ho et al., 2010), and in a patient with severe self-injurious behaviour (Leuzzi et al., 2012). In the former patient, elevated blocking autoantibodies against the folate receptors were reported.

### 1.5.3 Clinical presentation

CFD was first described in five patients with normal neurodevelopmental progress during the first four to six months followed by the onset of a neurological condition (Ramaekers et al., 2002). The initial manifestation of disease may include agitation and insomnia, followed by marked irritability, decelerating head growth, psychomotor retardation, cerebellar ataxia, dyskinesia and pyramidal signs in the lower limbs and seizures (Ramaekers and Blau, 2004). Autistic features may also be present (Frye et al., 2013; Moretti et al., 2005; Ramaekers et al., 2007a). After the age of 6 years, visual disorders may develop (Ramaekers et al., 2002). Despite normal peripheral blood and serum levels, 5-MTHF may show a steady decline. Brain MRI findings may be variable among patients, ranging from normal scans, to fronto-temporal atrophy with signs of periventricular and subcortical demyelination by the age of 18 months (Serrano et al., 2010).

Whilst the described clinical picture for patients with primary CFD could be considered neurologically diverse, those patients presenting with a secondary CFD, specifically mitochondrial disorders, may display even greater clinical heterogeneity (Garcia-Cazorla et al., 2008). In addition, the clinical phenotypes associated with mitochondrial disease and CFD may overlap. Therefore, it is understandable that CFD may go undetected following clinical assessment and may represent an under-recognised condition in patients such as these. For example, short stature, progressive muscle weakness and leukoencephalopathy, as visualised by brain MRI, have been reported in patients with KSS and secondary CFD (Garcia-Cazorla et al., 2008; Ormazábal et al., 2011; Pineda et al., 2006; Serrano et al., 2010). In addition, hypotonia, spastic diplegia and refractory seizures have been described in a patient with mitochondrial complex I encephalopathy and secondary CFD (Ramaekers et al., 2007c). In a patient with Alpers disease and secondary CFD, acute onset of status epilepticus and movement disorder occurred (Hasselmann et al., 2010). Interestingly in this patient, brain MRI at the time of disease onset showed no abnormalities.

However, a second brain MRI performed 3 months after disease onset demonstrated mild cerebral atrophy and an ischaemic lesion in the left thalamus.

In other pathologies where secondary CFD has been implicated, similar overlapping clinical heterogeneity may be observed. For example, patients with Rett syndrome and secondary CFD have been shown to present with small hands and feet, deceleration of head growth, seizures and gastrointestinal disorders (Ormazabal et al., 2005; Ramaekers et al., 2007b; Temudo et al., 2009). In those patients with Aicardi-Goutieres syndrome and secondary CFD, chronic pleocytosis, postnatal microcephaly, developmental delay, spastic quadriplegia and refractory seizures have been described (Blau et al., 2003; Hyland et al., 2010). Severe psychomotor retardation, developmental delay and slowing of head growth were also reported in patients with secondary CFD associated with autism, schizophrenia and catatonia, and self-injurious behaviour (Ho et al., 2010; Leuzzi et al., 2012; Moretti et al., 2008, 2005; Ramaekers et al., 2005).

### 1.5.4 Diagnosis

Once CFD is suspected in patients clinically presenting with the associated symptoms, confirmation of the diagnosis requires biochemical analysis of the CSF in conjunction with assessment of peripheral folate status in serum and red blood cells (Hyland et al., 2010). At the UCL Institute of Child Health and the National Hospital for Neurology and Neurosurgery, London, UK, techniques used for analysis of 5-MTHF in CSF include high performance liquid chromatography (HPLC) with electrochemical detection (Hyland and Surtees, 1992) or fluorescence detection (Ormazabal et al., 2006). Additional laboratory investigations to determine the integrity of one-carbon metabolism (discussed in section 1.4.4) may be carried out and may include evaluation of methionine, homocysteine, serine and glycine (Hyland and Bottiglieri, 1992; Surtees et al., 1991).

In the aforementioned laboratories, strict CSF collection protocols are adhered to. These protocols are consistent with other centres around the world. CSF is obtained from the patient by lumbar puncture, immediately snap frozen at the bedside, stored at -80°C and transported to the diagnostic laboratory on dry ice (Hyland et al., 2010). Patient information including date of birth and collection date should be provided since CSF 5-MTHF concentrations are age-dependent especially in the first year of

life (Ormazabal et al., 2006). Moreover, specific drug treatments can affect CSF 5-MTHF values, including L-dopa and methotrexate. L-dopa is methylated by SAM in a catechol-*O*-methyltransferase dependent reaction whilst methotrexate is a DHFR inhibitor. Therefore, both drugs interfere with 5-MTHF metabolism. Such medication should be identified on the request form to avoid inappropriate diagnosis and treatment. Owing to the rostral-caudal gradient of CSF, 5-MTHF analysis is always performed in the second 0.5 ml aliquot.

Following documentation of CFD, further laboratory investigations may be carried out and could include determination of FRα autoantibody status (although not widely available), evaluation of pterin profiles, mitochondrial RCE analyses and/or genetic testing for diseases associated with CFD, for example Rett syndrome or Aicardi-Goutieres syndrome (Hyland et al., 2010; Ramaekers et al., 2007b, 2005). These additional exploratory investigations may provide further biochemical and/or genetic information, which may facilitate more appropriate treatment regimens.

### 1.5.5 Treatment

Following a positive CFD diagnosis, patients are treated with oral calcium folinate (folinic acid; 5-formyltetrahydrofolate) (Hansen and Blau, 2005; Hyland et al., 2010; Moretti et al., 2005; Ormazabal et al., 2005). Folinic acid is a reduced and metabolically active form of folate that is readily incorporated into one-carbon metabolism. Folinic acid is not susceptible to oxidation owing to the presence of the formyl group at position N5 stabilising the pyrazine ring of the structure (Bailey, 2010). Folic acid is not administered for CFD since it may exacerbate the CFD phenotype (Hyland et al., 2010). Folic acid is the oxidised, metabolically inactive form of folate with a high folate receptor binding affinity. Thus, upon administration, folic acid competes for binding sites on the folate receptors expressed on choroid plexus epithelial cells of the blood-CSF barrier (Frye et al., 2013; Wu and Pardridge, 1999). Folinic acid may be prescribed as Leucovorin, which is a mixture of the active L isomer and the inactive D isomer. Isovorin is a preparation of the biologically active L isomer only and its administration may lead to an improved biochemical outcome (Hyland et al., 2010). Typically, folinic acid is prescribed at 0.5-1.0 mg/kg/day. However, in cases where there is a severe CFD, higher doses of 2.0-3.0 mg/kg/day may be administered. It has been reported that folinic acid treatment could lead to side effects including gastrointestinal complications and

exacerbation of seizures. Therefore, patients should be monitored accordingly (Ramaekers and Blau, 2004).

In general, patients diagnosed with CFD have a positive response to folinic acid treatment and demonstrate an improvement in biochemical and clinical phenotype. For example, administration of folinic acid has been shown to lead to reversal of white matter changes in patients with KSS (Pérez-Dueñas et al., 2011; Pineda et al., 2006) and mitochondrial complex I deficiency (Ramaekers et al., 2007c). In addition, improvements in seizure frequency have been described in three patients with Rett syndrome (Pérez-Dueñas et al., 2011) and in three patients, two of which are related, with mutations in the *FOLR1* gene (Cario et al., 2009; Grapp et al., 2012). Importantly, treatment with folinic acid should commence as soon as a CFD state has been demonstrated, since improvement in neurological function may be more marked in those patients that undergo therapy before six years of age (Ramaekers and Blau, 2004).

## 1.6 Pathogenesis of secondary CFD associated with mitochondrial disorders

### 1.6.1 Pathogenic mechanisms

In the absence of mutations in the *FOLR1* gene or FRα autoimmunity, the mechanism(s) responsible for the secondary CFD associated, in particular with a subset of mitochondrial disease patients, is not known. In the presence of normal peripheral folate levels, a disorder of folate transport across the blood-CSF barrier has been suspected and a number of hypotheses have previously been suggested to explain the defective transport, as discussed below.

1. *ATP depletion*

   Owing to the role of mitochondria in ATP production, perhaps the most widely speculated pathogenic mechanism responsible for secondary CFD in a subset of mitochondrial disorders is an energy deficit impeding the active transport of 5-MTHF across the choroid plexus from the periphery into the CSF (Hyland et al., 2010; Pérez-Dueñas et al., 2011; Ramaekers et al., 2007c). In addition, since the activity of FPGS is ATP-dependent, failure of polyglutamation and intracellular retention of 5-MTHF in choroid plexus cells have also been suggested (Ramaekers et al., 2013a).

*2. Choroid plexus dysfunction*

In patients with KSS presenting with a secondary CFD and perhaps in other mitochondrial disorders, it has been suggested that transport of 5-MTHF across the choroid plexus may be disrupted as a result of oncocytic transformation and accumulation of mutated mtDNA copies in choroid plexus cells (Spector and Johanson, 2010). Neuropathological investigations of the choroid plexus from two patients with KSS revealed enlarged choroid plexus epithelial cells and extensive cytoplasmic eosinophil granule infiltrate, when compared to normal controls (Tanji et al., 2000). These changes to the normal pathology associated with patients with KSS could disrupt the receptor-mediated endocytotic transport of 5-MTHF by FRα and intracellular retention of 5-MTHF owing to a lack of polyglutamation (Grapp et al., 2013; Ramaekers et al., 2013a).

*3. Reactive oxygen species*

Seizures are a common clinical feature of patients with mitochondrial disease and secondary CFD (Lee et al., 2011; Opladen et al., 2010; Rahman, 2012). Treatment with anti-convulsant therapies including sodium valproate, carbamazepine and phenytoin may be prescribed in these patients (Rahman, 2012). However, as previously discussed, sodium valproate should if possible be avoided in mitochondrial disease patients, since it has been shown to inhibit mitochondrial oxidative phosphorylation and may cause clinical worsening (Rahman and Hanna, 2009). Degradation of sodium valproate and carbamazepine by the cytochrome P450 enzyme system is associated with ROS generation (Opladen et al., 2010). Opladen et al. (2010) demonstrated that prior exposure of KB cells (a keratin-forming subline of the HeLa (Henrietta Lacks) tumour cell line cloned from a cervical adenocarcinoma in 1951 (Verlinde et al., 2008)) expressing the FRα, to superoxide and hydrogen peroxide *in vitro*, led to decreased cellular 5-MTHF uptake. In addition, previous studies have also suggested that phenytoin may inhibit the formation of polyglutamyl folates in rat liver (Carl et al., 1997). Therefore, anti-convulsant therapy in mitochondrial disease patients with secondary CFD may increase ROS generation causing an inhibitory effect on cellular folate incorporation across the blood-CSF barrier and/or prevent polyglutamylation and subsequent cellular retention. These

proposed mechanisms could also account for the secondary CFD associated with other disorders where anti-convulsant therapy for seizure control may be required and where the underlying aetiology of secondary CFD is not known, for example Rett syndrome (Ramaekers and Blau, 2004; Ramaekers et al., 2003).

Whilst these speculated mechanisms responsible for the secondary CFD associated with mitochondrial disease may be biologically plausible and have a contributory role in disease pathogenesis, there is a lack of supportive evidence for each. For example, there does not appear to be a relationship between the severity of RCE defect measured in skeletal muscle and the degree of CFD measured in CSF (Hyland et al., 2010). It is important to consider, however, that RCE activity measurements in skeletal muscle are used to represent RCE activity in the brain, since performing a brain biopsy is surgically more complex and involves greater risk. In addition, variable degrees of secondary CFD have been reported in patients with KSS. In two large cohort studies, there has been no difference in the concentrations of folate in serum and CSF when comparing children with and without anti-convulsant therapy (Mangold et al., 2011; Pérez-Dueñas et al., 2011). Therefore, this suggests that other pathogenic mechanisms may be involved, and prompts the need for further hypothesis-led investigations to be carried out to more extensively decipher the underlying aetiology of CFD associated with mitochondrial disease.

### 1.6.2 Oxidative stress

As discussed in section 1.1.3, mitochondria are considered to be the most important quantitative source of ROS, which are generated as by-products of oxidative phosphorylation at the level of the mitochondrial RC (Figure 1) (Adam-Vizi, 2005; Sipos et al., 2003). Mitochondrial dysfunction and impaired mitochondrial RC activity is associated with an increase in ROS production. Previous studies have demonstrated that partial inhibition of the mitochondrial RC, to a degree insufficient to perturb oxidative phosphorylation, can lead to an increase in ROS generation (Jacobson et al., 2005; Sipos et al., 2003). Under these conditions, oxidative stress may ensue, which represents an imbalance between ROS generation and antioxidant availability. Increased ROS production and oxidative stress can lead to significant cellular destruction including nuclear and mitochondrial DNA damage, protein modification and lipid peroxidation (Halliwell and Whiteman, 2004; Musatov and

Robinson, 2012). This, in turn, may initiate a vicious cycle leading exponentially to more ROS production and mitochondrial damage (Ma et al., 2009; Wang et al., 2013). Since mitochondria are particularly numerous in the brain, owing to the high-energy demand, the CNS may be more susceptible to oxidative stress when mitochondrial RC activity is compromised. In addition, the brain has a relatively high iron and, to a lesser extent, copper content, for example mitochondrial iron-sulphur clusters, copper centres and haem, and a low free iron binding capacity in CSF (Bleijenberg et al., 1971; Bradbury, 1997; Harrison et al., 1968). Therefore, the production of the hydroxyl radical via the Fenton reaction may be more likely.

Oxidative stress and increased generation of ROS have been associated with conditions where CFD has been implicated, including mitochondrial disease (Opladen et al., 2010; Pérez-Dueñas et al., 2011; Serrano et al., 2010). Oxidative stress has previously been proposed to contribute to CFD by causing modification of the FRα leading to impaired transport (Opladen et al., 2010). However, 5-MTHF, together with other reduced pterin molecules, is susceptible to autoxidation in the presence of molecular oxygen and direct oxidative attack by oxidising species, which leads to increased catabolism (Blair et al., 1975; Heales et al., 1988; Lam and Heales, 2007). Consequently, in conditions where ROS formation is increased, accelerated catabolism of 5-MTHF may ensue, thereby further contributing to a CFD state. Since increased ROS generation is associated with impaired mitochondrial RC activity and loss of mitochondrial function (Jacobson et al., 2005; Sipos et al., 2003), oxidative stress could provide a mechanistic link between mitochondrial disorders and CFD.

In addition to impaired mitochondrial RC activity and loss of mitochondrial function, other factors may play a contributory role in inducing oxidative stress in mitochondrial disorders, including selenium and AA. These factors are discussed in the following sections 1.6.2.1 and 1.6.2.2, respectively.

#### 1.6.2.1 Selenium

The trace element selenium is an essential micronutrient required for the biosynthesis of selenocysteine-containing selenoproteins. Selenium exists in both inorganic (selenite and selenate) and organic (selenomethionine, selenocysteine, and Se-methylselenocysteine) (Figure 8) forms and is predominant in foods such as

bread, cereals, brazil nuts and dairy products (Fairweather-Tait et al., 2011; Lu et al., 2009). Plant foods are also a major dietary source of selenium and the selenium content of these foods is dependent on the selenium availability in the soil in which they are grown. In countries such as Russia and China, there are low amounts of selenium in soil, which may predispose to selenium deficiency. Such a deficiency may lead to the onset of Keshan disease or Kashin-Beck disease. Regarding the former, onset of this disease is dependent on exposure to the mutated strain of Coxsackievirus and is characterised by a potentially fatal severe cardiomyopathy (Li et al., 2012). Regarding the latter, disease onset is dependent on a concomitant iodine deficiency and is characterised by atrophy, degeneration and necrosis of cartilage tissue (Ning et al., 2013).

The mechanisms responsible for intestinal absorption of dietary selenium and the identity of the transporter proteins required remain uncertain. Studies have suggested that selenomethionine, selenocysteine and Se-methylselenocysteine may be transported by certain amino acid transporters, specifically the $B^0$ and $b^{0+}$rBAT systems; high-affinity, sodium-independent transporters of cysteine and amino acids (Nickel et al., 2009). In addition, the SLC26 multifunctional anion exchanger family are good candidates for intestinal selenate transport since inhibition of these exchangers reduces selenate uptake (Shennan, 1988; Wolffram et al., 1985). Similarly, the mechanisms responsible for the transport of selenium between the periphery and the CNS have yet to be fully elucidated. However, both the apolipoprotein E receptor 2 and the megalin receptor have been implicated in mediating selenium transport across BBB endothelial cells (Alvira-Botero et al., 2010; Burk et al., 2007), and a hypothetical transport model has been proposed (Richardson, 2005) (Figure 9). This model suggests that selenium-containing selenoprotein P (SePP), which is synthesised in the liver from dietary selenium sources and is the most abundant selenoprotein in plasma, binds to a SePP receptor expressed on the BBB endothelial cell basolateral membrane. Upon binding, it is postulated that the complex is internalised by endocytosis and selenium cleaved via the activity of selenocysteine γ-lyase (SCL). Whether the SePP receptor is recycled or degraded is not known. The cleaved selenium may then either enter into the

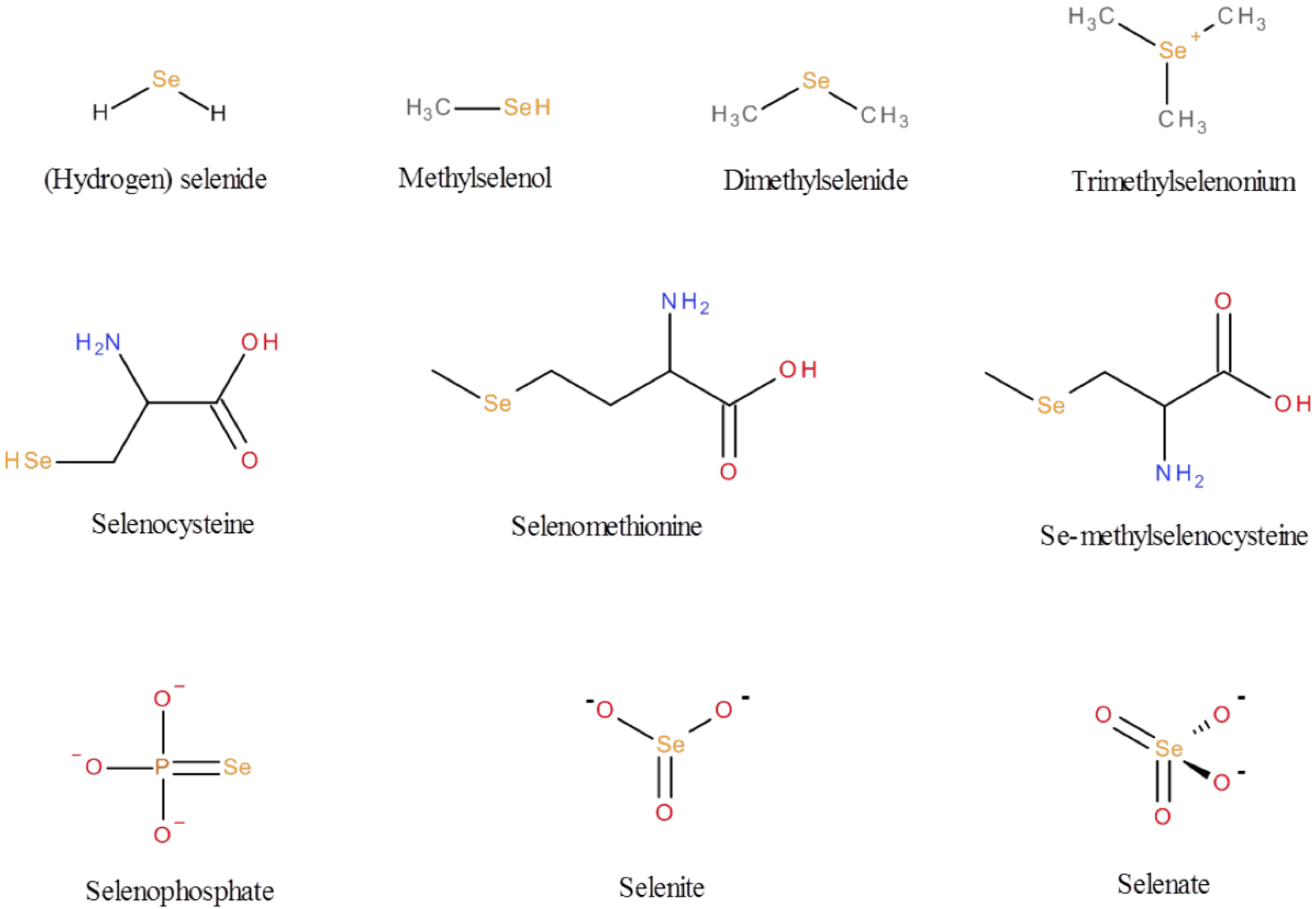


***Figure 8 Chemical structures of the selenium compounds***. Structures were sourced from the National Center for Biotechnology Information (www.ncbi.nlm.nih.gov).

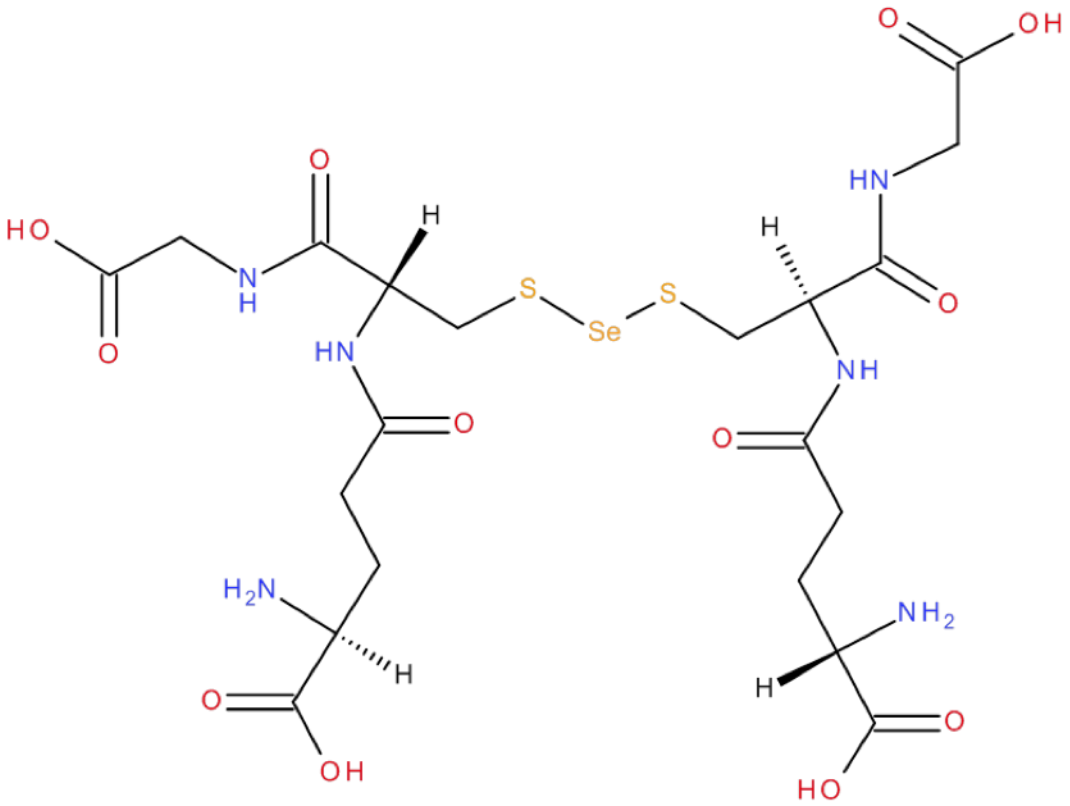


Selenodiglutathione

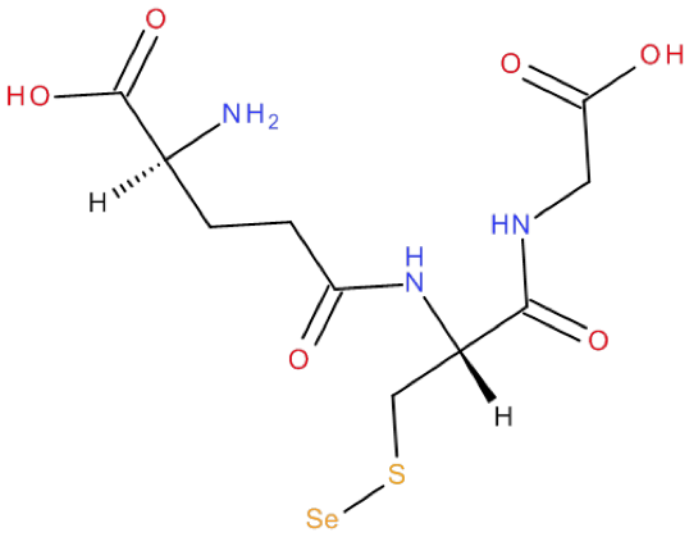


Glutathioselenol

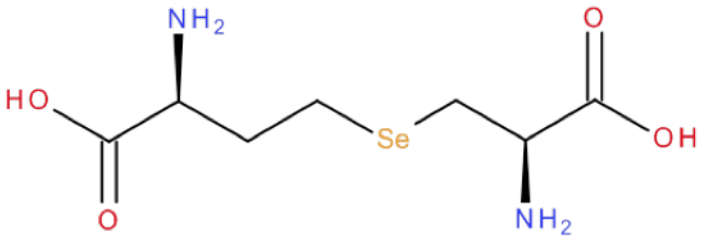


Selenocystathionine

***Figure 8 (continued) Chemical structures of the selenium compounds.*** Structures were sourced from the National Center for Biotechnology Information (www.ncbi.nlm.nih.gov).

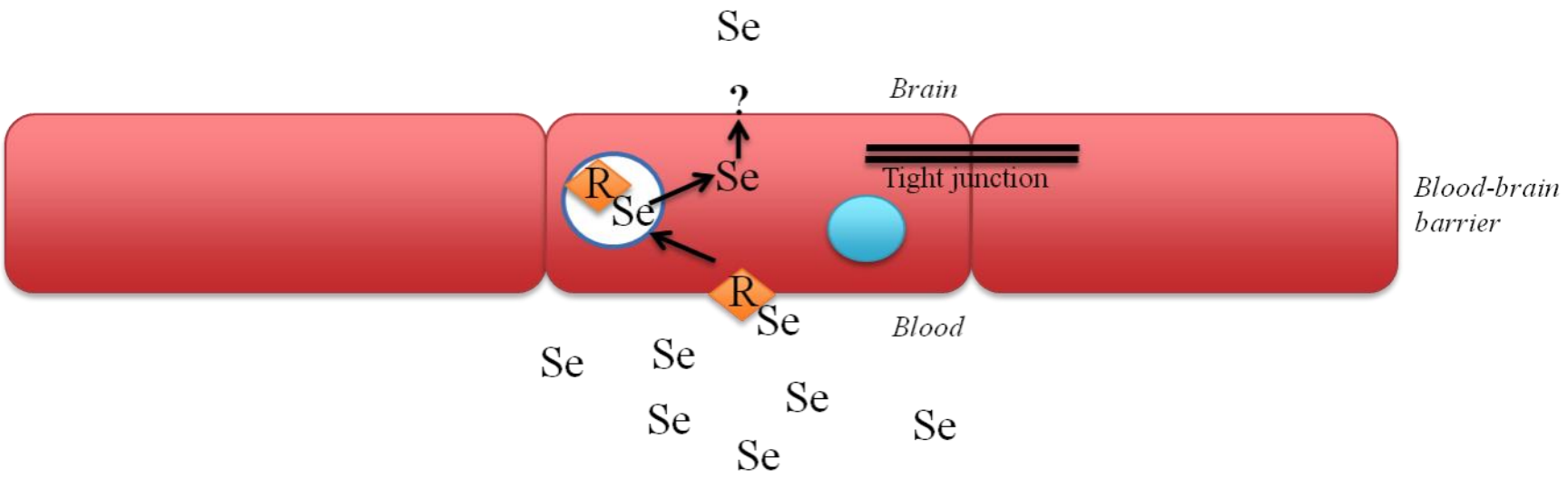


***Figure 9 Proposed mechanism of transport of selenium across the blood-brain barrier***. Selenoprotein P (Se), binds to a selenoprotein P receptor (R) (hypothesised to be apolipoprotein E receptor 2 or the megalin receptor) expressed on the blood-brain barrier endothelial cell basolateral membrane. Upon binding, the complex is internalised by endocytosis and selenium cleaved via the activity of selenocysteine γ-lyase (SCL). The cleaved selenium may then either enter into the metabolic cycle of the cell facilitating selenoprotein synthesis or be re-incorporated into *de novo* synthesis of selenoprotein P and released from the apical membrane, by an unknown mechanism, into the interstitial space of the brain, represented by the "?" in the figure. Selenium concentration is 30-fold lower in CSF than in plasma, which suggests that efflux from the CNS to the blood would occur in an energy-dependent manner.

metabolic cycle of the cell facilitating selenoprotein synthesis or be re-incorporated into *de novo* synthesis of SePP and released from the apical membrane, by an unknown mechanism, into the interstitial space of the brain. The subsequent uptake of SePP by brain cells and the activity of intracellular SCL could provide the cell with selenium for cellular metabolism and selenoprotein synthesis (Richardson, 2005). Selenium concentration is 30-fold lower in CSF than in plasma, which suggests that efflux from the CNS to the blood would occur in an energy-dependent manner (Tondo et al., 2011, 2010). Moroever, it has been postulated that the choroid plexus may play a pivotal role in selenium transport from the blood to the CSF (Tondo et al., 2011), which is further supported by the proposed mechanism of Richardson (2005). CSF selenium concentration follows a negative age-related trend. Tondo et al. (2010) reported CSF selenium reference ranges as shown in Table 6.

The assimilation of dietary selenium into selenoproteins occurs through a series of metabolic interconversions with selenide being the central metabolic intermediate of both the inorganic and organic selenium compounds (Figure 10) (Lu et al., 2009). Dietary selenomethionine and selenomethionine released from proteins is initially converted to selenocysteine via the activity of cystathionine-β-synthase and cystathionine γ-lyase through a selenocystathionine intermediate. In turn, selenocysteine is converted to selenide in a reaction catalysed by selenocysteine β-lyase (Ohta and Suzuki, 2008). Dietary Se-methylselenocysteine can be converted to methylselenol in a cystathionine γ-lyase reaction, which can in turn be demethylated to produce selenide (Gabel-Jensen et al., 2010). Thioredoxin reductase and thioredoxin can directly reduce selenite to selenide. Alternatively, selenite can react with glutathione to form selenodiglutathione (Lu et al., 2009). Selenodiglutathione is a substrate for reduction to glutathioselenol by glutathione reductase. A reaction between glutathioselenol and glutathione yields selenide (Cui et al., 2008). Selenate is assimilated into proteins following reduction to selenide via the same thioredoxin reductase and thioredoxin/glutathione pathways (Björnstedt et al., 1997). However, the mechanism responsible for the conversion of selenate to selenite remains unclear but may involve the activity of thioredoxin reductase in the presence of thioredoxin and/or glutathione. The assimilation of selenide into selenoproteins involves the generation of the highly reactive selenium donor, selenophosphate, synthesized via

***Table 6 CSF selenium reference ranges according to Tondo et al. (2010)***. CSF selenium concentration is age-related. Values are given in nmol/L and µg/L to accommodate how the concentration may be expressed in reporting.

| **CSF selenium reference ranges** | |
|---|---|
| **Age (days (d), months (m), years (y))** | **Concentration (nmol/L [µg/L])** |
| 1 – 30 d | 22.8 – 59.5 [1.8 – 4.7] |
| 1 m – 3y | 8.6 – 38.0 [0.68 – 3.0] |
| 4 – 18 y | 9.2 – 27.0 [0.73 – 2.13] |

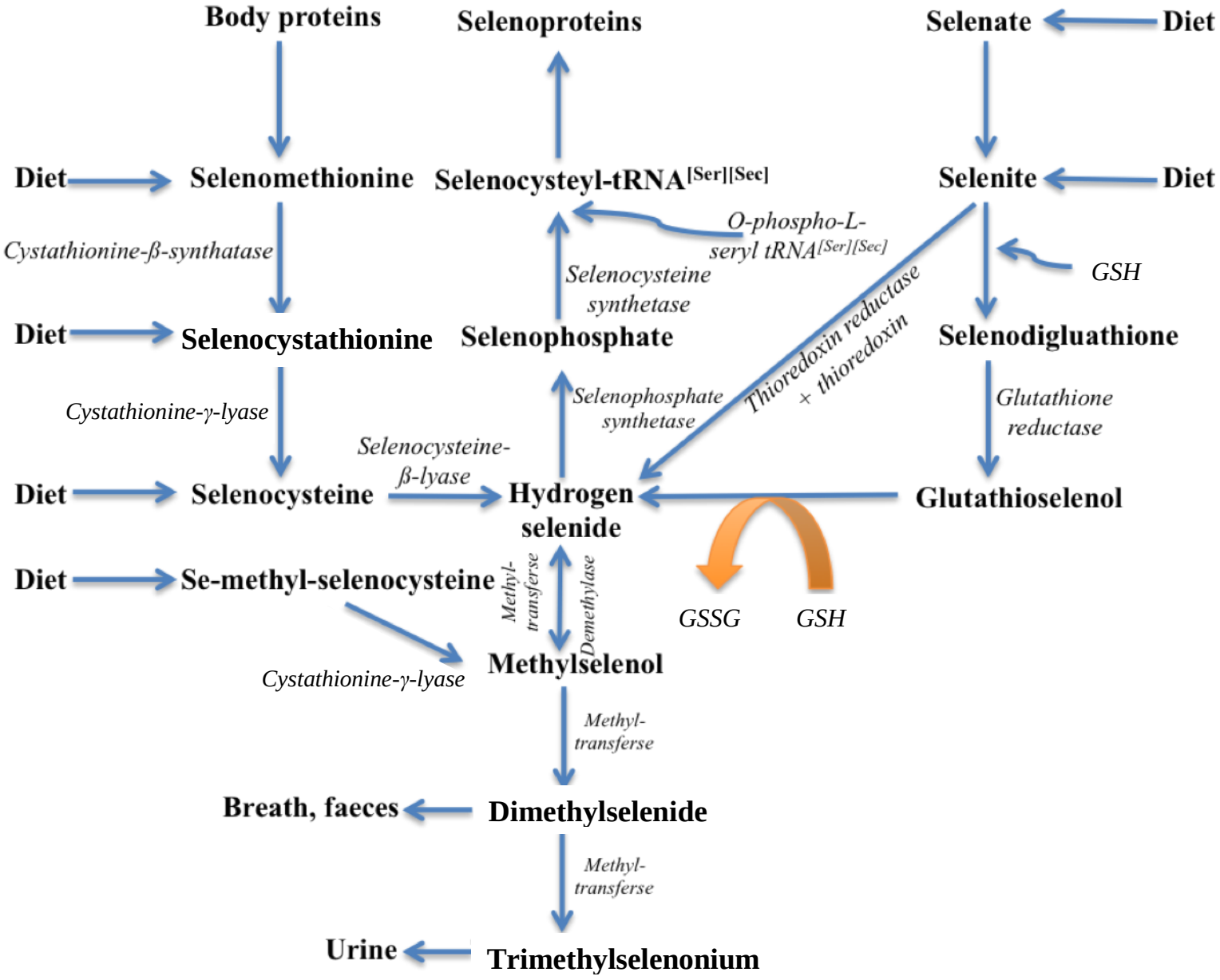


***Figure 10 Selenium metabolism***. The assimilation of selenium into selenoproteins. GSH = reduced glutathione, GSSG = oxidised glutathione. See section 1.6.2.1 for detailed explanation.

the activity of selenophosphate synthetase. Selenocysteyl-tRNA$^{[Ser][Sec]}$, which is incorporated into selenoproteins, is generated from selenophosphate and *O*-phospho-L-seryl-tRNA$^{[Ser][Sec]}$ in a reaction catalysed by selenocysteine synthetase (Ganichkin et al., 2008). Whilst selenide is the key intermediate for selenoprotein synthesis, selenide is also the key intermediate for selenium excretion. Methyltransferases sequentially add methyl groups to selenide to generate methylselenol, dimethylselenide and trimethylselenonium (Fernandes et al., 2012). Dimethylselenide is excreted in the breath and faeces, whilst trimethylselenonium is excreted in the urine (Ohta and Suzuki, 2008).

The main biological function of selenoproteins is antioxidant defence (Moghadaszadeh and Beggs, 2006; Tinggi, 2008). Specifically, the antioxidant enzymes, glutathione peroxidase and thioredoxin reductase, are well-characterised selenoenzymes (Das and Das, 2000; Steinbrenner et al., 2006). For example, these selenoenzymes catalyse the reduction of hydrogen peroxide and hydroperoxides, and are particularly important in reducing ROS generated in mitochondria, during viral infections and during thyroid hormone synthesis (Fairweather-Tait et al., 2011). Regarding the latter, previous studies have demonstrated that selenium availability and maintenance are tightly regulated in the thyroid gland (Arthur et al., 1999; Schomburg and Köhrle, 2008). Whilst selenium plays an important biological function in antioxidant defence, selenium is also a CNS-sensitive toxic trace element when present at high physiological concentrations and patients with selenium toxicity in the CNS may present with a range of clinical symptoms including ataxia, irritability and lethargy (Tondo et al., 2011; Wilber, 1980).

The sensitivity of the CNS to toxic levels of selenium may be a consequence of increased ROS production. Selenide is an auto-oxidisable molecule and may undergo thiol-mediated redox cycling, including with thioredoxin and glutathione systems which are present in CSF, leading to a rapid non-stoichiometric increase in ROS production (Chen et al., 2007a; Tarze et al., 2007; Wallenberg et al., 2010; Yan and Spallholz, 1993). In turn, NADPH may be depleted owing to continued reduction of thiols (Lu et al., 2009). Theoretically, high physiological selenium concentrations in the CNS would initiate selenide redox cycling and toxicity via increased ROS production, and oxidative stress would ensue. The threat of inducing such a redox

cycle may explain why there is no free pool of selenide in cells (Lu and Holmgren, 2009; Lu et al., 2009).

Interestingly, elevated CSF selenium concentrations were reported in six patients with KSS and secondary CFD. All patients (mean (SD) [range] age, 16 (9.4) [7 – 34] years) presented with CSF 5-MTHF concentrations ranging from 0.6 – 24.0 nmol/L (reference range 42 -81 nmol/L for patients older than 4 years) and CSF selenium concentrations ranging from 2.4 – 7.3 µg/L (reference range 0.73 – 2.13 µg/L for patients older than 4 years) (Tondo et al., 2011). The group hypothesised that owing to choroid plexus dysfunction in KSS, impaired transport processes may account for the elevated CSF selenium concentrations in these patients. However, selenium was not implicated as a factor responsible for CFD in these patients and the data were not correlated to 5-MTHF availability. In view of the potential association of selenium toxicity with ROS generation and the susceptibility of 5-MTHF to oxidative catabolism, oxidative stress in these patients may ensue leading to accelerated breakdown of 5-MTHF.

#### 1.6.2.2 Ascorbic acid

Ascorbic acid (AA) is an essential, water-soluble vitamin (vitamin C) (Mandl et al., 2009). Plants and most animals are able to synthesise AA from glucose. However, humans, guinea-pigs and a number of species of fruit-eating bats cannot synthesise AA owing to a lack of functional L-gulonolactone oxidase activity; the enzyme required for the last step in AA synthesis (Nishikimi et al., 1994). Therefore, it is a requirement in these species that an adequate supply of AA is taken in with the diet and dietary sources include many citrus fruits and leafy green vegetables. However, failure to consume enough AA may predispose to AA deficiency. Such a deficiency in humans may lead to the onset of scurvy. Scurvy is a disease that affects collagen stability (Barnes, 1947; Carpenter, 2012; van Robertson, 1952). AA is a required cofactor for a number of enzymes, including prolyl-3-hydroxylase, prolyl-4-hydroxylase and lysyl-hydroxylase, which are important in the hydroxylation of proline and lysine residues of collagen (Murad et al., 1983; Tryggvason et al., 1979). In the absence of AA, there is a reduction in hydroxylation of these residues resulting in unstable collagen fibres. As a consequence, scurvy leads to brown spots on the skin, spongy gums and bleeding from mucous membranes and the patient may

be partially immobilised and suffer from fatigue (DelVecchio and Dancea, 2011; Olmedo et al., 2006).

Intestinal absorption of dietary AA is mediated via the sodium-dependent vitamin C transporter 1 (SVCT1) expressed on the brush border surface of enterocytes, which transports sodium and AA in a 2:1 stoichiometry (Liang et al., 2001; Padayatty et al., 2004; Tsukaguchi et al., 1999; Verlinde et al., 2008). Upon binding, the SVCT1 undergoes a conformational change, releasing both sodium and AA into the cell (Nualart et al., 2013). Similarly, the SVCT1 mediates absorption and re-absorption of AA in the kidneys and is expressed on renal tubular cells. However, the efflux of AA from enterocytes is not fully characterised (Padayatty et al., 2004). Proposed mechanisms regarding the efflux of AA from enterocytes include anion channels and gap-junctions (Corti et al., 2010; Khatami et al., 1986; Wilson, 2002). Once in circulation, the transport of AA across the choroid plexus from the blood into the CSF is mediated by the SVCT2 isoform expressed on the basolateral membrane (Harrison and May, 2009; Verlinde et al., 2008) (Figure 11). Similarly to SVCT1, the SVCT2 transports sodium and AA in a 2:1 stoichiometry and upon sodium and AA binding, undergoes a conformation change causing intracellular release (Tsukaguchi et al., 1999). As with intestinal AA efflux mechanisms, efflux of AA from choroid plexus cells into the CSF is not known (Liang et al., 2001; Padayatty et al., 2004). However, there is a 2-4 times higher concentration of AA in CSF compared to plasma suggesting that AA release into the CSF may be energy dependent (Spector and Johanson, 2010). Within the brain, the SVCT2 is ubiquitously expressed and facilitates AA uptake into cells (Caprile et al., 2009; Mun et al., 2006). A glutamate-AA heteroexchange system has been proposed for AA efflux from cells. The oxidised form of AA, dehydroascorbic acid (DHA), is transported across cellular membranes via the facilitative glucose transporters, including glucose transporter (GLUT) 1 and 3 (Figure 12) (Hosoya et al., 2008; Tsukaguchi et al., 1999). These transporters are ubiquitously expressed throughout the body and are present on both the apical and basolateral membranes of BBB cells, facilitating transport of DHA from the periphery into the CNS (Du et al., 2012; Farrell et al., 1992). Upon entry into brain parenchyma, DHA may either be reduced to AA by intracellular glutathione or be released in its oxidised form for reduction at a later stage (Lloyd et al., 1972; Washko et al., 1993).

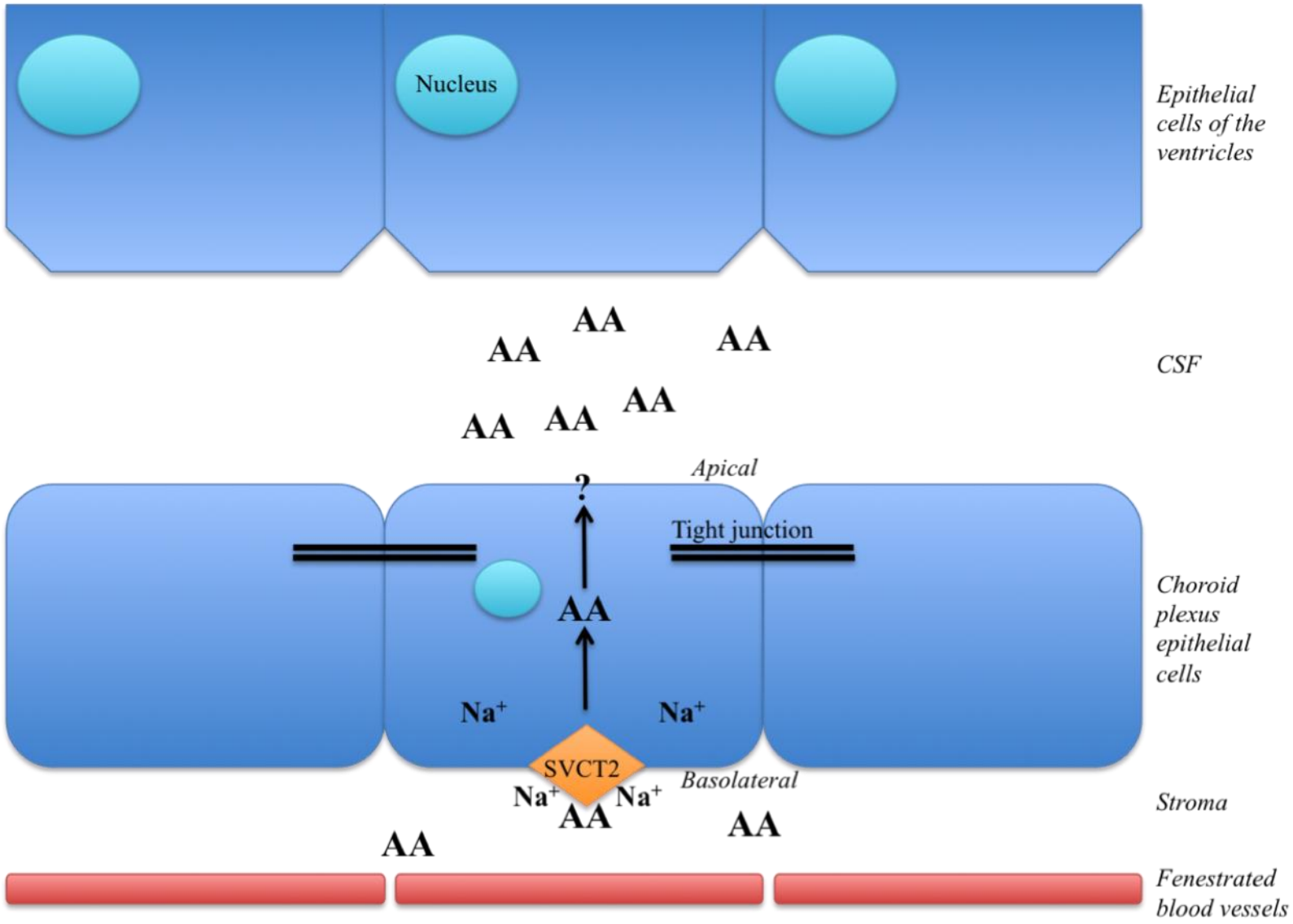


***Figure 11 Transport of AA across choroid plexus epithelial cells***. The SVCT2 transports sodium and AA across the choroid plexus epithelial cell in a 2:1 stoichiometry and upon sodium and AA binding, undergoes a conformation change causing intracellular release. The mechanism(s) responsible for efflux of AA from choroid plexus cells into the CSF is not known. However, there is a 2-4 times higher concentration of AA in CSF compared to plasma suggesting that AA release into the CSF may be energy dependent. Within the brain, the SVCT2 is ubiquitously expressed and facilitates AA uptake into cells. In contrast, a glutamate-AA heteroexchange system has been proposed for AA efflux. SVCT2 = sodium dependent vitamin C transporter 2; AA = ascorbic acid, $Na^+$ = sodium.

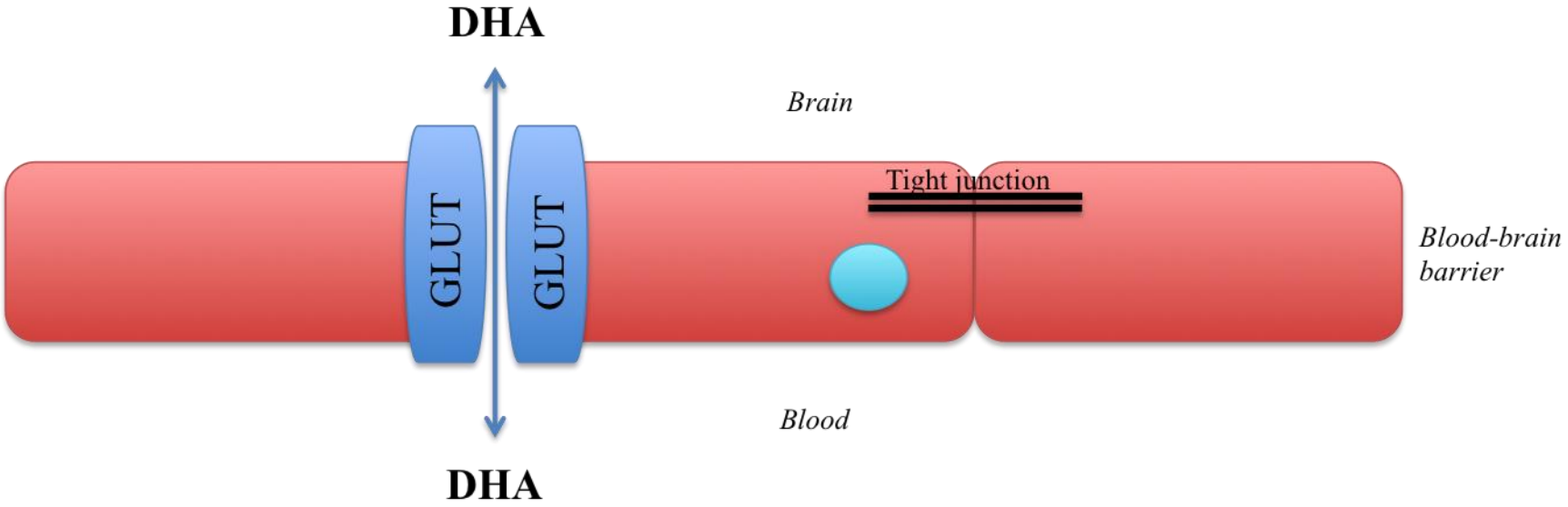


***Figure 12 Transport of DHA across the blood brain barrier***. DHA is transported across cellular membranes via the facilitative glucose transporters, including GLUT1 and 3. These transporters are expressed on both the apical and basolateral membranes of blood brain barrier cells, facilitating transport of DHA from the periphery into the CNS. GLUT = glucose transporter; DHA = dehydroascorbic acid.

AA, present in the monoanion form at physiological pH, is a ketolactone with two ionisable hydroxyl groups (Du et al., 2012). AA acts as a reducing agent and can readily undergo two consecutive, one-electron oxidations to form the AA radical and DHA (Figure 13) (May et al., 2003). The AA radical is relatively unreactive owing to resonance stabilisation of the unpaired electron and can readily oxidise to form DHA. However, recycling of AA by reduction of the AA free radical and DHA can occur (Arrigoni and De Tullio, 2002). Reduction of the AA free radical can be mediated by NADH-cytochrome $b_5$ reductase, which is localised to the outer mitochondrial membrane, endoplasmic reticulum and plasma membrane (Ito et al., 1981). NADH-cytochrome $b_5$ reductase donates one electron to the AA radical, which in turn, draws an electron from NADH. The transmembrane AA radical reductase in erythrocytes can also use electrons from NADH or intracellular AA to regenerate extracellular AA from the AA radical generated in blood, or the AA radical generated by the reduction of α-tocoperoxyl radical during lipid oxidation (May, 1998; May et al., 2001a). Additionally, the thioredoxin reductase system can function as a cytosolic mechanism for AA recycling, however, thioredoxin reductase can also catalyse the NADPH-dependent reduction of DHA (Du et al., 2012; May et al., 1997; Mendiratta et al., 1998). DHA is mostly recycled by glutathione directly or by glutaredoxin in the cytoplasm (May et al., 2001b).

AA has numerous biological functions. As described above, AA is an essential enzyme cofactor for a number of hydroxylase enzymes. These enzymes include prolyl-3-hydroxylase, prolyl-4-hydroxylase and lysyl-hydroxylase, required for collagen synthesis (Murad et al., 1983; Tryggvason et al., 1979), dopamine β-hydroxylase, required for the synthesis of noradrenaline from dopamine and trimethyllysine dioxygenase and butyrobetaine dioxygenase, required for carnitine synthesis (Menniti et al., 1986; Rebouche, 1991). In addition, AA is also one of the most abundant, low molecular weight antioxidants, particularly in the CNS. Typical concentrations of AA in the plasma of healthy individuals are 40-60 µmol/L, where concentrations range from 100-400 µmol/L in CSF and 2-10 mmol/L in neurons (Harrison and May, 2009). AA can readily donate one electron to damaging ROS including hydroxyl radicals, alkoxyl radicals, peroxyl radicals, thiol radicals and tocopheroxyl radicals (Regoli and Winston, 1999; Winston et al., 1998). These one

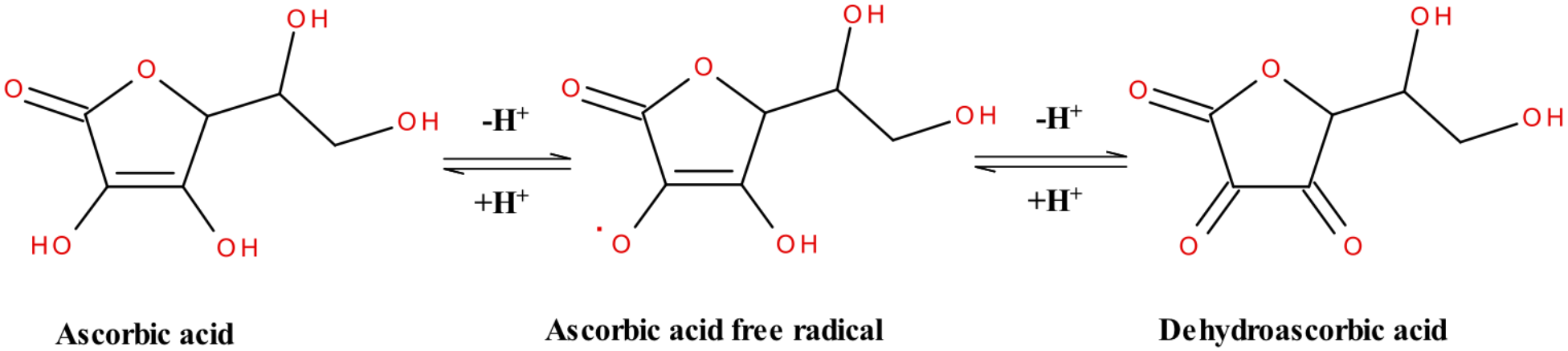


***Figure 13 Ascorbic acid metabolism***. AA can readily undergo two consecutive, one-electron oxidations to form the AA radical and DHA. AA=ascorbic acid. DHA=dehydroascorbic acid.

electron donations may result in the formation of the AA radical or DHA, which in turn, may be recycled back to AA by the mechanisms described above. Whilst AA can act as an antioxidant, AA may also have pro-oxidant effects when present at low concentrations (Buettner and Jurkiewicz, 2010; Fisher and Naughton, 2003; Mandl et al., 2009) and in the presence of catalytic metals, including iron and copper. For example, ferric iron ($Fe^{3+}$) may be reduced to ferrous iron ($Fe^{2+}$) by AA, which in turn, may react with AA to produce hydrogen peroxide in a system termed the Weissberger system (Weissberger et al. 1943). As a result, subsequent cycles of the Fenton reaction may ensue resulting in the generation of the hydroxyl radical (Hamilton et al., 1964). Importantly, the pro-oxidant effects of AA are dependent on the availability of catalytic metals *in vivo*. Whilst iron is sequestered by iron binding proteins such as transferrin and ferritin, biological reductants such as thiols and AA, may release iron from these proteins for cytochrome and iron-containing enzyme synthesis (Boyer and McCleary, 1987; Somjai et al., 1974). Moreover, the high iron, and, to a lesser extent, copper content in the brain, and the low free iron binding capacity in CSF, as previously described in this section, may increase transition metal availability (Bleijenberg et al., 1971; Bradbury, 1997; Harrison et al., 1968). Under these conditions and in the presence of low AA concentration, the formation of the hydroxyl radical may be more likely, which in turn, may induce oxidative stress.

Interestingly, in patients with KSS and secondary CFD, it has been predicted that CSF AA concentrations may be low (Spector and Johanson, 2010). This suggestion is supported by the combination of prominent anatomical changes, which may be present in the choroid plexus of patients with KSS (Tanji et al., 2000), and an energy deficit impeding the proposed active transport mechanism of molecules across the apical membrane of the choroid plexus cells (Garcia-Cazorla et al., 2008; Hasselmann et al., 2010; Hyland et al., 2010), such as AA. Given the biological function of AA as a pro-oxidant when present at low concentrations, a decrease in antioxidant capacity and a potential increase in hydroxyl radical generation could lead to exacerbation of oxidative stress and promote oxidative catabolism of 5-MTHF. In addition, AA availability could be a factor in governing 5-MTHF stability.

### 1.7 Hypotheses

1. CFD is an under-recognised condition in patients with mitochondrial disease.
2. 5-MTHF is vulnerable to oxidative catabolism in the presence of ROS.
3. AA protects against oxidative catabolism of 5-MTHF in the CNS.
4. Reduced mitochondrial RCE activity and/or high selenium levels in mitochondrial disease induces oxidative stress which is responsible for secondary CFD.

### 1.8 Aims

1. To determine the prevalence and significance of CFD in mitochondrial RCE deficiencies.
2. To examine the stability of 5-MTHF in CSF in the presence and absence of hydroxyl radicals or selenite.
3. To examine the ability of AA to confer 5-MTHF stability.
4. To investigate (i) mitochondrial RCE inhibition and (ii) selenite treatment on the stability of extracellular 5-MTHF in a cellular system.

# Chapter 2
# Materials and Methods

# 2. Materials and Methods

## 2.1 Materials

*The following were purchased from Sigma Aldrich (Poole, UK):*

Ethylenediaminetetraacetic acid (EDTA); 1,4-dithiothreitol (DTT); 1,4-dithioerythritol (DTE); sodium octyl sulphate; L-glutathione reduced (GSH); pall nanosep® centrifugal device with omega membrane (10 kDa); 5-methyltetrahydrofolate (5-MTHF) sodium salt; L-ascorbic acid (AA); sodium selenite; metaphosphoric acid; dehydroascorbic acid; sodium bicarbonate; sodium chloride; calcium chloride; magnesium sulphate; D-glucose; sodium phosphate monobasic; magnesium chloride; tris base; tris-HCl; sterile modified Hank's balanced salt solution with sodium bicarbonate without phenol red, calcium chloride or magnesium sulphate (HBSS); sodium dodecyl sulphate (SDS); triton-X 100; sterile 4 ml/L trypan blue; β-nicotinamide adenine dinucleotide reduced (β-NADH); potassium cyanide (KCN); ubiquinone; cytochrome *c*; rotenone; ferricyanide; acetyl coenzyme-A (acetyl CoA); 5,5'-dithio-bis (nitrobenzoic acid) (DNTB); oxaloacetate; Folin-Ciocalteu phenol reagent; copper sulphate pentahydrate; tartrate; sodium carbonate; bovine serum albumin (BSA); ethidium bromide; iron (III) sulphate; hydrogen peroxide.

*The following were purchased from VWR International Ltd (Lutterworth, UK):*

Methanol HiPerSolv for HPLC; ethanol HiPerSov for HPLC; disodium hydrogen orthophosphate; potassium dihydrogen orthophosphate; sodium hydroxide; orthophosphoric acid HPLC electrochemical grade; hydrochloric acid; potassium dihydrogen phosphate; dipotassium hydrogen phosphate; dimethyl sulphoxide (DMSO); betaine hydrochloride; agarose; tris-borate-EDTA (TBE) buffer x10 concentrate; Exonuclease I Shrimp Alkaline Phosphatase (ExoSAP) for PCR clean-up.

*The following were purchased from Invitrogen Ltd (Paisley, UK):*

Dulbecco's modified Eagle's Medium/Ham's F-12 Nutrient mixture (DMEM/F-12) (1:1); L-glutamine; fetal bovine serum (FBS) heat inactivated; 2.5 g/L trypsin-EDTA; MitoSOX$^{TM}$ Red.

*The following were purchased from Bioline Reagents Ltd (London, UK):*

BIOTAQ DNA polymerase; x10 $NH_4$ (ammonium) buffer; deoxynucleotide triphosphates (dNTPs; 2.5 mmol/L); magnesium chloride (50 mmol/L); crystal x5 DNA loading buffer (bromophenol) blue.

*The following were purchased from Chromacol (Welwyn Garden City, UK):*

HPLC crimp top tapered vials (200 µl); HPLC aluminium crimp caps (rubber/PTFE).

*The following were purchased from Anachem Ltd (Luton, UK):*

PCR tube Ind At Dom Cap 0.2 ml vial.

*All other materials and reagents were analytical grade and purchased from Sigma Aldrich or VWR International, except where stated.*

## 2.2 Patient samples

All patient samples were obtained as part of diagnostic investigations requested by the patient's clinician and after informed consent.

### 2.2.1 Cerebrospinal fluid

CSF samples were taken following lumbar puncture, immediately frozen in liquid nitrogen at the bedside according to standard written instructions and stored at -80°C until analysis. A proforma for clinical information and drug history was completed by the clinician at the time of sampling and returned with the CSF sample. Redundant CSF samples remaining after diagnostic investigations had been performed in the Neurometabolic Unit at the National Hospital for Neurology and Neurosurgery, London, UK, were anonymised and used throughout this thesis. Disease control CSF was defined as being sourced from patients with no evidence of conditions relating to an inborn error of 5-MTHF metabolism or a leukodystrophy. CSF samples underwent a maximum of two freeze-thaw cycles and blood-stained samples were excluded.

### 2.2.2 Skeletal muscle

Open skeletal muscle biopsies (50-100 mg) were taken, immediately frozen in liquid nitrogen at the bedside according to standard written instructions and stored at -80°C

until analysis. A proforma for clinical information and drug history was completed by the clinician at the time of sampling and returned with the skeletal muscle sample. Diagnostic investigations were performed in the Neurometabolic Unit at the National Hospital for Neurology and Neurosurgery, London, UK.

## 2.3 Measurement of 5-MTHF by high performance liquid chromatography

CSF 5-MTHF reference ranges used in the Neurometabolic Unit at the National Hospital for Neurology and Neurosurgery, London, UK, are given in Table 5.

### 2.3.1 Function

5-MTHF was quantified using reverse-phase HPLC with fluorescence detection. Reverse-phase HPLC utilises a non-polar stationary phase and an aqueous mobile phase to separate analytes. Non-polar molecules tend to adsorb to the stationary phase and are retained on the HPLC column longer than polar molecules. Fluorescence detection uses different excitation and emission wavelengths of light, specific for the analyte of interest. At the excitation wavelength, the analyte adsorbs light and is excited, transitioning from a ground state level to a higher electronic state. Once the analyte has reached its highest electronic state, the analyte begins to lose energy. As the analyte decays to ground state levels, the analyte fluoresces and emits light at a longer wavelength. The emission wavelength is detected and is directly proportional to the quantity of analyte in the sample. The signal is amplified and recorded using data acquisition software (Lough and Wainer, 1996).

### 2.3.2 Equipment

PU-1580 Intelligent HPLC pump (Jasco UK Ltd., Great Dunmow, UK); AS-1555 intelligent autosampler (Jasco); FP-920 intelligent fluorescence detector (Jasco); CO-1560 column oven (Jasco). The mobile phase was degassed using a DG-1580-53 3 line degasser (Jasco). The fluorescence detector was connected to a computer and data was recorded using EZChrom Elite data capture and analysis software (Agilent Technologies UK Limited, Stockport, UK). The equipment was assembled as shown in Figure 14.

### 2.3.3 Analytical procedure

The method was based on the diagnostic method routinely used to quantify 5-MTHF in CSF in the Neurometabolic Unit at the National Hospital for Neurology and

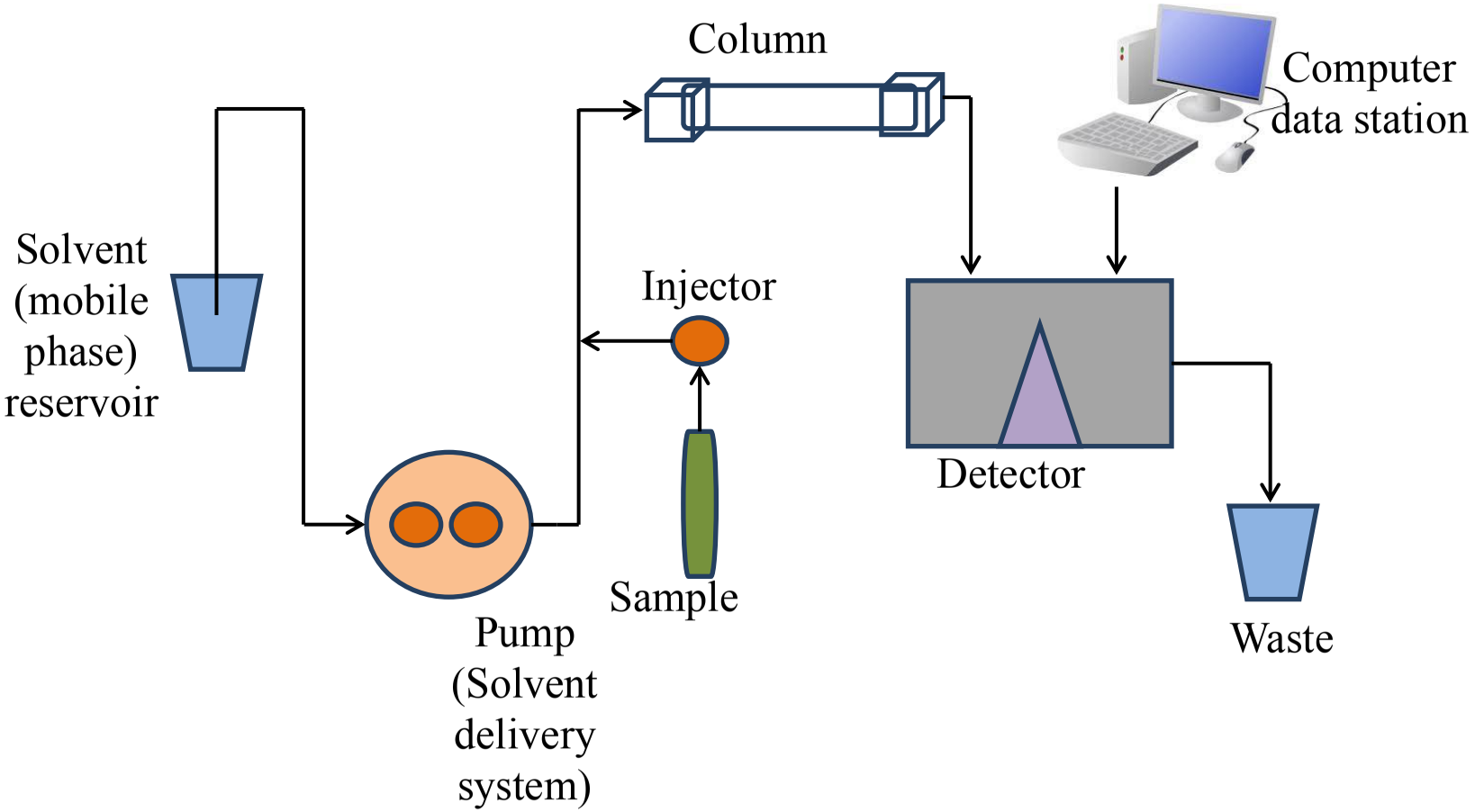


***Figure 14 Flow diagram of the HPLC system***. Reverse-phase HPLC with fluorescence detection was used for 5-MTHF quantification.

Neurosurgery, London, UK, adapted from the published method of (Ormazabal et al., 2006). Analysis of 5-MTHF in CSF was performed in the second 0.5 ml CSF sample. Samples underwent a maximum of two freeze-thaw cycles. Blood-stained samples were excluded from analysis owing to the risk of contamination by erythrocyte derived 5-MTHF contamination and iron release, which could propagate the hydroxyl radical via the Fenton reaction (Fenton, 1894; Heales et al., 1988). This would lead to oxidative catabolism of 5-MTHF and subsequent anomaolous results. The mobile phase consisted of 0.05 mol/L monopotassium phosphate, 54 µmol/L EDTA and 14% v/v HPLC grade methanol in ultrapure water, adjusted to pH 4.77 with sodium hydroxide. The flow rate was set at 1.3 ml/min. Samples were thawed, transferred to vials and loaded into the autosampler. Each sample (50 µL) was injected into the flow and separated on a reverse phase 250 x 4.6 mm i.d. HiQSil C18W column (KYA Tech. Corp. Tokyo, Japan), maintained at 35°C. 5-MTHF was detected by fluorescence detection. The excitation wavelength and the emission wavelength were set at 290 nm and 358 nm, respectively. Samples were quantified against an external standard of 100 nmol/L 5-MTHF prepared in a 0.1 mg/ml DTE solution. A quality control was prepared by pooling CSF from previous patients with no evidence of an inborn error of 5-MTHF metabolism or leukodystrophy. Results of the internal quality control were recorded. Data obtained from samples were kept within ±2 standard deviations of the measured values of the current quality control. A calibration curve was performed to determine the linearity between the fluorescence spectra and standard concentration (Figure 15). Linearity was demonstrated between 0-100 nmol/L. Example chromatograms of a 5-MTHF 100 nmol/L standard and 5-MTHF in CSF are presented in Figure 16.

### 2.3.4 Data analysis

5-MTHF data were visualised and quantified using EZChrom Elite data capture and analysis software (Agilent Technologies) using the following equation:

Concentration (nmol/L) =

(sample peak area/external standard peak area) x calibration standard concentration (nmol/L)

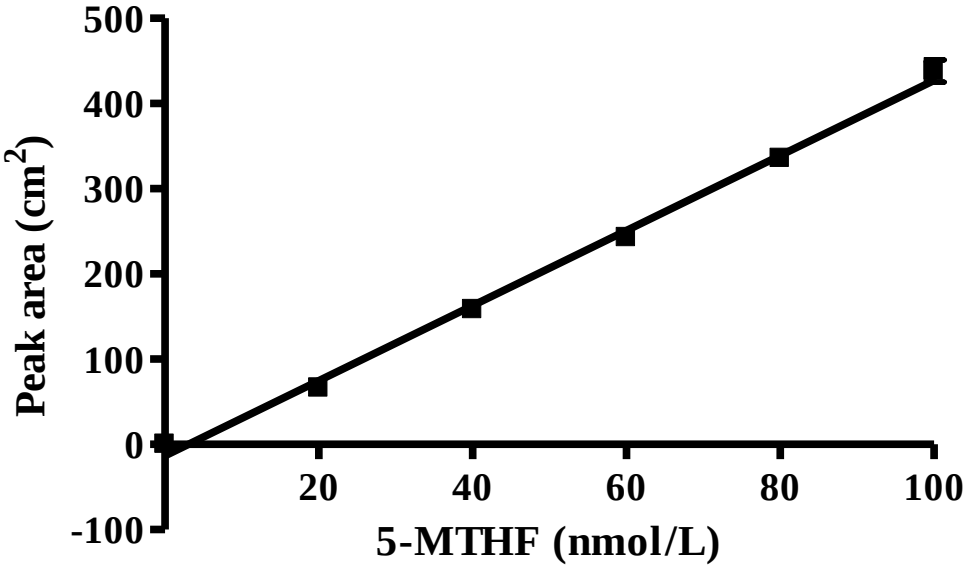


***Figure 15 5-MTHF calibration curve.*** The linearity of 5-MTHF concentration was demonstrated between 0–100 nmol/L. Samples were prepared in air saturated conditions at ambient temperature. Samples were analysed by reverse-phase HPLC with fluorescence detection as described in section 2.3. All values are mean ± SEM of 4 independent experiments, $r^2$=0.99.

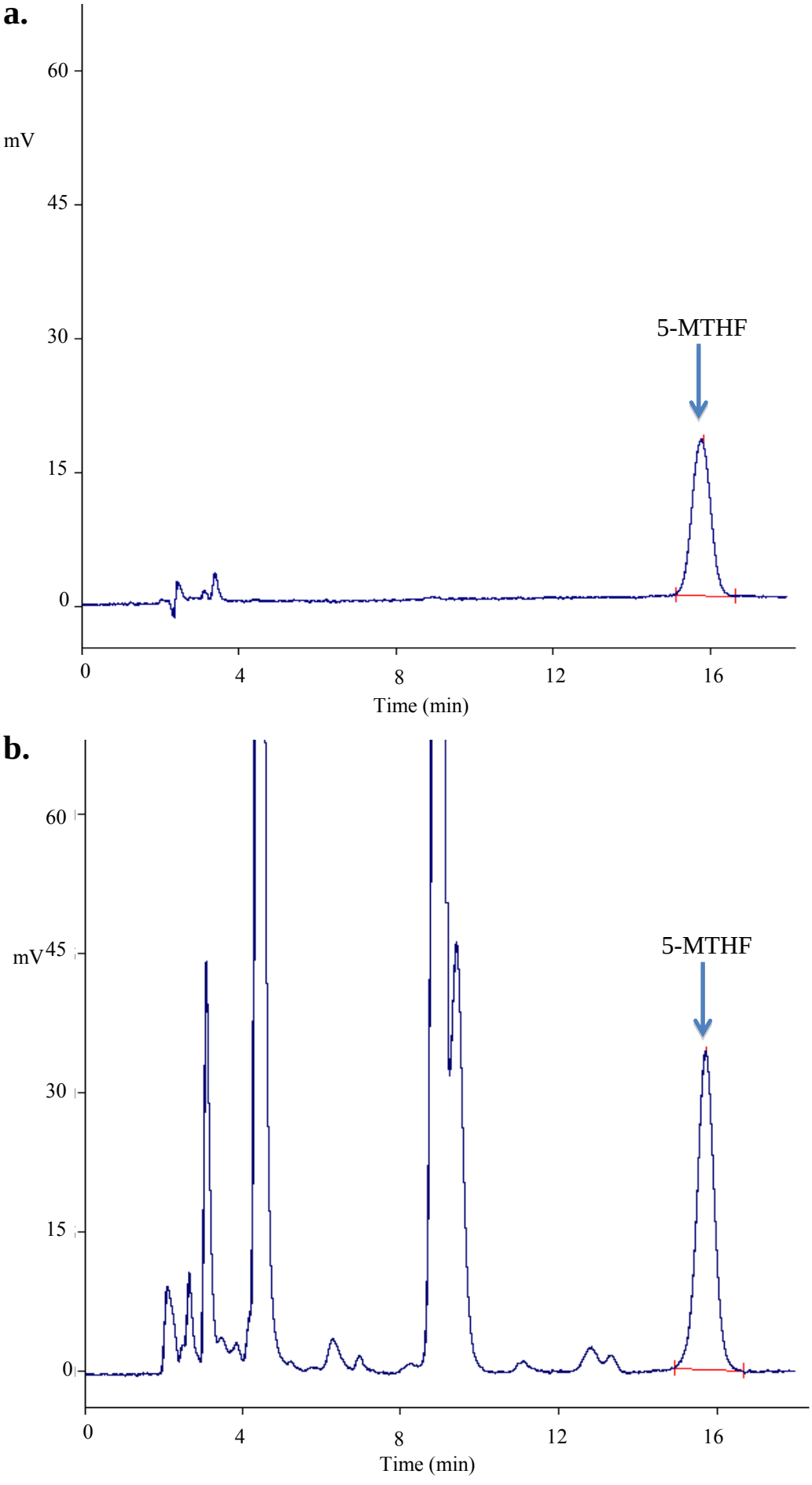


***Figure 16 Sample chromatograms of 5-MTHF.*** **a.** 5-MTHF peak in a 100 nmol/L standard solution and **b.** 5-MTHF peak in CSF. 5-MTHF retention time ~16 min.

## 2.4 SH-SY5Y cell culture

### 2.4.1 SH-SY5Y cell line

The SK-N-SH cell line was originally established in 1973 from a bone-marrow biopsy of a four-year-old female patient with a neuroblastoma of the chest (Biedler et al., 1973). The cell line contained two distinct cell types, a neuroblast- like cell and an epithelial-like cell. The neuroblast-like cell types were subcloned sequentially to SH-SY, then to SH-SY5 and finally to SH-SY5Y. The SH-SY5Y cells have neuroblast-like morphology and retain neurite-like processes (Figure 17). The cells are robust and are capable of proliferating exponentially for long periods of time without contamination.

The SH-SY5Y cell line has been extensively utilised as a model for neurological research, including studies exploring the underlying pathophysiology of Parkinson's disease and Alzheimer's disease (Cheung et al., 2009; Presgraves et al., 2004).

### 2.4.2 Cell storage

SH-SY5Y cells were obtained from the European Collection of Cell Cultures (Health Protection Agency, Salisbury, UK) and cultured in accordance with the supplier's instructions. Cells were seeded at 1 x $10^4$ cells/$cm^2$ in a 75 $cm^2$ tissue culture flask in DMEM/F-12 supplemented with 100 ml/L fetal bovine serum (FBS) and 5 mmol/L L-glutamine. Cells were grown at +37°C in 5% $CO_2$. Cell culture medium was replaced the day after seeding and every 48 hours thereafter. Cells were passaged at 80-90% confluence approximately every 6 days. For cell passage, medium was removed from the flask and cells were washed once with 10 ml Hank's balance salt solution (HBSS) at +37°C. Cells were lifted from each flask with 6 ml 2.5 g/L trypsin, 0.38 g/L EDTA in HBSS (trypsin-EDTA) incubated at +37°C for 3 minutes. Trypsin-EDTA bathed cells were diluted with 8 ml DMEM/F-12, harvested and centrifuged at 500x *g* for 5 minutes at +20°C. Supernatant was removed and cells resuspended in DMEM/F-12 + 100 ml/L FBS + 5 mmol/L L-glutamine. An aliquot of cell suspension, 10 µl, was mixed 1:1 with 4 g/L trypan blue and counted using a Countess Automated Cell Counter (Invitrogen Ltd). Cells of passage number 17 to 19 were stored at a density of 1 x $10^6$ cells/ml in 300 ml/L FBS, 100 ml/L

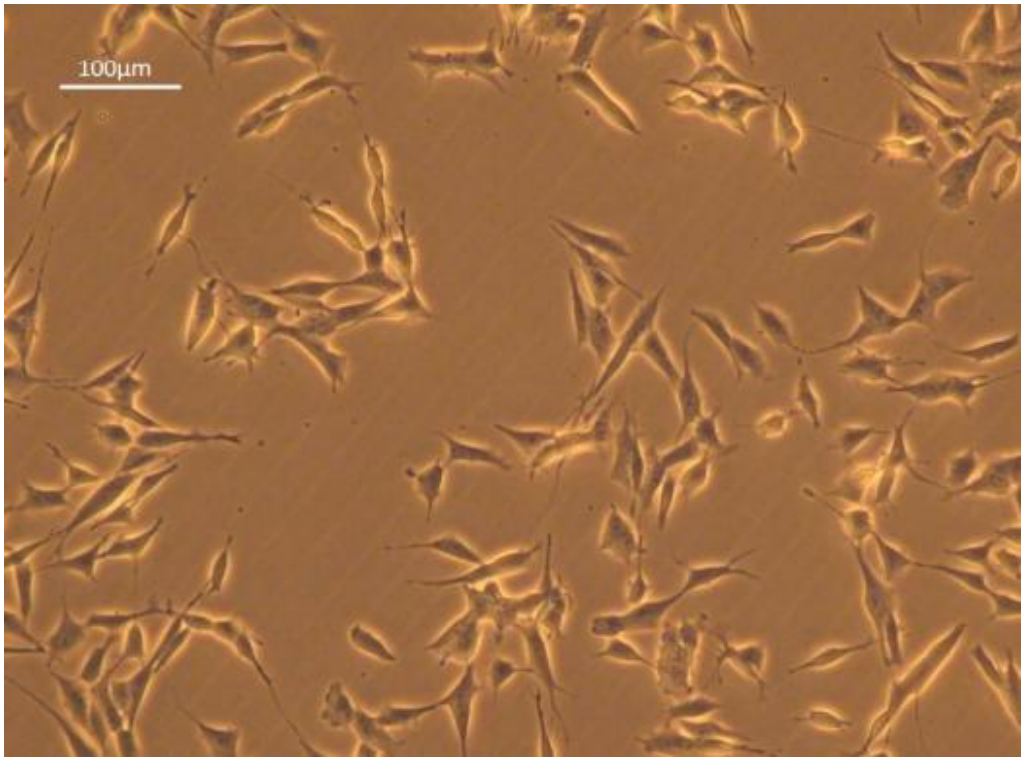


***Figure 17 SH-SY5Y cells.*** An image of SH-SY5Y cells under a light microscope. The cells have neuroblast-like morphology and retain neurite-like processes.

DMSO and 700 ml/L DMEM/F-12 as 1 ml aliquots. Cells were frozen to -80°C using an isopropanol freezing vessel for 24 hours and then transferred to liquid nitrogen for storage.

### 2.4.3 Cell recovery and passage

Cells were recovered from the liquid nitrogen and seeded at a density of 1 x $10^4$ cells/$cm^2$ in 75 $cm^2$ flasks. Cells were grown in DMEM/F-12 + 100 ml/L FBS + 5 mmol/L L-glutamine at +37°C in 5% $CO_2$. Cell culture medium was replaced the day after seeding and every 48 hours thereafter. Cells were passaged at 80-90% confluence. For cell passage, medium was removed from the flask and cells were washed once with 10 ml HBSS at +37°C. Cells were lifted from each flask with 6 ml trypsin-EDTA incubated at +37°C for 3 minutes. Trypsin-EDTA bathed cells were diluted with 8 ml DMEM/F-12, harvested and centrifuged at 500x *g* for 5 minutes at +20°C. Supernatant was removed and cells resuspended in DMEM/F-12 + 100 ml/L FBS + 5 mmol/L L-glutamine. An aliquot of cell suspension, 10 µl, was mixed 1:1 with 4 g/L trypan blue and counted using a Countess Automated Cell Counter (Invitrogen Ltd). Cells were seeded at 1 x $10^4$ cells/$cm^2$ in a 75 $cm^2$ tissue culture flask in DMEM/F-12 + 100 ml/L FBS + 5 mmol/L L-glutamine. Cells were grown at +37°C in 5% $CO_2$. Cell culture medium was replaced the day after seeding and every 48 hours thereafter. Cells were passaged as above at 80-90% confluence approximately every 6 days. In order to maintain experimental consistency, cells of passage number 19 to 24 were used throughout.

### 2.4.4 Cell seeding for experiments

For experiments, cells were seeded in 75 $cm^2$ flasks at a density of 5.3 x $10^4$ cells/$cm^2$. Cells were incubated in DMEM/F-12 + 100 ml/L FBS + 5 mmol/L L-glutamine at +37˚C in 5% $CO_2$ and left to stabilise and attach for 24 hours prior to each experiment.

### 2.4.5 Minimal medium harvesting for 5-MTHF quantification by HPLC

Minimal medium consisted of 44 mmol/L sodium bicarbonate, 110 mmol/L sodium chloride, 1.8 mmol/L calcium chloride, 5.4 mmol/L magnesium sulphate, 0.92 mmol/L sodium phosphate monobasic and 5 mmol/L D-glucose prepared in sterile cell culture grade water adjusted to pH 7.4 with $CO_2$. Following incubation with cells, minimal medium aliquots of 120 µl were removed and immediately snap

frozen in liquid nitrogen. Samples were stored at -80°C until analysis by HPLC as described in section 2.3.

### 2.4.6 SH-SY5Y cell harvesting for mitochondrial respiratory chain complex assays

Following treatment, cells were washed once with 10 ml HBSS and lifted with 6 ml trypsin-EDTA at +37°C for 3 minutes. Trypsin-EDTA bathed cells were diluted with 8 ml DMEM/F-12 + 100 ml/L FBS + 5 mmol/L L-glutamine, harvested and centrifuged at 500x *g* for 5 minutes at +4°C. The supernatant was removed and the cells were washed by resuspension in 10 ml HBSS at +4°C. Samples were centrifuged at 500x *g* for 5 minutes at +4°C. The supernatant was removed and the cells were resuspended in isolation buffer (600 µl) consisting of 10 mmol/L tris (pH 7.4), 1 mmol/L EDTA, 320 mmol/L sucrose in HPLC grade water. Each cell sample (200 µl) was stored at -80°C in three aliquots, one for the complex of interest, one for citrate synthase and one for total protein. Immediately prior to analysis, each aliquot was thawed at +37°C and immediately snap frozen in liquid nitrogen three times in order to lyse the cells. Samples were analysed as described in section 2.5 and 2.6.

### 2.4.7 SH-SY5Y cell harvesting for mitochondrial superoxide estimation by flow cytometry

Following treatment, cells were washed once with 10 ml HBSS and lifted with 6 ml trypsin-EDTA incubated at +37°C for 3 minutes. Trypsin-EDTA bathed cells were diluted with 8 ml DMEM/F-12 + 100 ml/L FBS + 5 mmol/L L-glutamine, harvested and centrifuged at 500x *g* for 5 minutes at +4°C. The supernatant was removed and the cells were washed by resuspension in 10 ml HBSS at +4°C. Samples were centrifuged at 500x *g* for 5 minutes at +4°C. The supernatant was removed and the cells were resuspended in 600 uL HBSS. Samples were analysed immediately by flow cytometric analysis as described in section 2.7.

## 2.5 Mitochondrial respiratory chain enzyme assays

Mitochondrial RCE activity reference ranges in skeletal muscle used in the Neurometabolic Unit at The National Hospital for Neurology and Neurosurgery, London, UK, are given in Table 7.

***Table 7 Mitochondrial RCE activity (ratio to citrate synthase activity) reference ranges in skeletal muscle.*** These reference ranges are used in the Neurometabolic Unit at The National Hospital for Neurology and Neurosurgery, London, UK.

| **Mitochondrial RCE activity reference ranges** | |
|---|---|
| **Mitochondrial RCE** | **Activity (ratio to citrate synthase)** |
| Complex I | 0.104-0.268 |
| Complex II/III | 0.040-0.204 |
| Complex IV | 0.014-0.034 |

### 2.5.1 Function

A spectrophotometer is an instrument which measures the amount of light absorbed by a medium at a specified wavelength. According to the Beer-Lambert law, the amount of light absorbed by a medium is proportional to the concentration of the solute present. Light from a source is passed through a monochromator in order to produce the analytical spectrum, which in turn is passed through a wavelength selector. At a specific wavelength the beam passes through the sample and is detected on a photocell detector. The signal from the detector is amplified and digitally represented (Williams, 1995).

### 2.5.2 Equipment

Analysis of samples was carried out using a Uvikon XL spectrophotometer (Secomam, Ales, France).

### 2.5.3 Procedure

All complex and citrate synthase assays were carried out at a total protein concentration of 2 mg/ml (see section 2.6).

#### 2.5.3.1 Complex I (NADH:ubiquinone oxidoreductase) (EC 1.6.5.3)

The complex I assay was based on the method by (Ragan et al., 1987). The method measures the oxidation of NADH as a decrease in absorbance at a starting wavelength of 340 nm, during the reduction of ubiquinone to ubiquinol by complex I. The proportion of NADH oxidation, which is independent of complex I, is determined using the specific complex I inhibitor rotenone. Sample (50 µl) was added to a 1 ml cuvette containing a final concentration of 2.5 mg/ml BSA, 0.15 mmol/L β-NADH, 1 mmol/L KCN in 20 mmol/L potassium phosphate buffer (pH 7.2) and 8 mmol/L magnesium chloride in HPLC grade water.

The reaction was started following the addition of 10 µl 5 mmol/L ubiquinone to the sample cuvette. The final concentration of ubiquinone in the cuvette was 50 µM and the final volume in the cuvette was 1 ml. The reaction was measured at 340 nm at 30-second intervals for 5 minutes at +30°C. Rotenone (1 mmol/L; 20 µl) was added to the sample cuvette. The final concentration of rotenone in the cuvette was 20 µM. Measurement was continued for a further 5 minutes. Each sample cuvette was run against a reference cuvette. The reference cuvette contained all the components of

the sample cuvette except ubiquinone. A specific value for complex I was calculated by subtracting the change in absorbance at 340 nm following rotenone addition from the change in absorbance at 340 nm before rotenone inhibition. Absorbance was converted to molar concentration using the NADH extinction coefficient, 6.81 x $10^3$ $M^{-1}$ $cm^{-1}$ (path length 1 cm, volume 1 ml), taking account of ubiquinone, using a re-arrangement of the Beer-Lambert law:

$$\frac{\Delta A}{\varepsilon} = c$$

Where $\Delta A$ is the specific change in absorbance; $\varepsilon$ = extinction coefficient; and c = mole/min/ml. Results are expressed as nmol/min/mg of protein or as a ratio to citrate synthase activity. A calibration curve was performed to determine the linearity between complex I activity and protein concentration. Linearity was demonstrated between a protein concentration range of 0-2.5 mg/ml (Figure 18).

#### 2.5.3.2 Complex II/III (Succinate:ubiquinone oxidoreductase, ubiquinol:cytochrome *c* oxidoreductase) (EC 1.3.5.1 + EC 1.10.2.2)

Complex II/III activity was measured by Dr Iain Hargreaves in the Neurometabolic Unit laboratory at the National Hospital for Neurology and Neurosurgery, London, UK and patient results were analysed retrospectively, as indicated.

The complex II/III assay was based on the method of (King, 1967). During the oxidation of succinate to fumarate, complex II reduces ubiquinone to ubiquinol. Ubiquinol is an electron donor and reduces cytochrome *c*. This reaction is catalysed by complex III. The complex II/III assay measures the succinate dependent reduction of cytochrome *c* by measuring the increase in absorbance at 550 nm. The complex III inhibitor, antimycin A, is used to determine the proportion of cytochrome *c* reduction which is independent of complex II/III activity. A complex II/III activity value is generated by subtracting the change in absorbance at 550 nm following the addition of antimycin A from the change in absorbance at 550 nm before antimycin A addition. Absorbance was converted to molar concentration using Beer-Lambert law (see section 2.5.3.1) and the cytochrome *c* extinction coefficient, 19.2 x $10^3$ $M^{-1}$ $cm^{-1}$. Results are expressed as a ratio to citrate synthase activity.

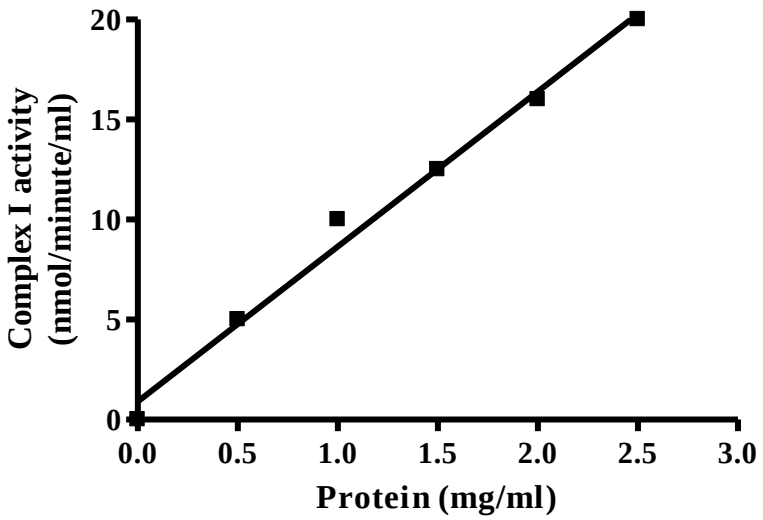


***Figure 18 Complex I calibration curve.*** The linearity of complex I activity was demonstrated between a protein concentration range of 0–2.5 mg/ml. Samples were prepared in air saturated conditions at ambient temperature. Samples were analysed as described in section 2.5.3.1. All values are mean ± SEM of 3 independent experiments, $r^2$=0.99.

#### 2.5.3.3 Complex IV (Cytochrome *c* oxidase) (EC 1.9.3.1)

The complex IV assay was based on the method of (Wharton and Tzagoloff, 1967). The method measures the oxidation of cytochrome *c* catalysed by complex IV. To obtain reduced cytochrome *c*, a few ascorbic acid crystals are added to 0.8 mol/L oxidised cytochrome c in HPLC grade water. A PD10 desalting column equilibrated with 50 ml of 10 mmol/L potassium phosphate buffer (pH 7.0) in HPLC grade water was used to remove the ascorbic acid from the reduced cytochrome *c*. Reduced cytochrome *c* (50 µl) was added to 950 µl of HPLC grade water in a reference and sample cuvette. The sample cuvette was blanked against the reference cuvette at 550 nm. Cytochrome *c* in the reference cuvette was oxidised using 10 µl of 100 mmol/L ferricyanide. The final concentration of ferricyanide in the cuvette was 1 mmol/L. The absorbance was recorded after 1 minute and used to determine the concentration of reduced cytochrome *c*. The concentration of cytochrome *c* was calculated using the Beer-Lambert law (see section 2.5.3.1). The extinction coefficient used for cytochrome *c* was 19.2 x $10^3$ $M^{-1}$ $cm^{-1}$ (path length 1 cm, volume 1 ml). Reduced cytochrome *c* prepared at a final concentration of 50 µmol/L was added to a sample and reference cuvette containing potassium phosphate buffer (pH 7.0) at a final concentration of 10 mmol/L in HPLC grade water. The sample cuvette was blanked against the reference cuvette at 550 nm. Ferricyanide (100 mmol/L; 10 µl) was added to the reference cuvette to oxidise cytochrome *c*. The final concentration of ferricyanide in the cuvette was 1 mmol/L. The reaction was started following the addition of 40 µl of sample to the sample cuvette. The change in absorbance at 550 nm was measured over a 3 minutes at +30°C. The reaction of complex IV with cytochrome *c* follows first-order kinetics since it is dependent on the concentration of cytochrome *c*. Therefore, activity is expressed as a first order rate constant (k). The rate constant (k) is calculated by plotting the natural log of absorbance against time and determining the slope. Results are expressed as k/min/mg of protein or k/mol when expressed as ratio to citrate synthase activity. A calibration curve was performed to determine the linearity between complex IV activity and protein concentration. Linearity was demonstrated between a protein concentration range of 0-2.5 mg/ml (Figure 19).

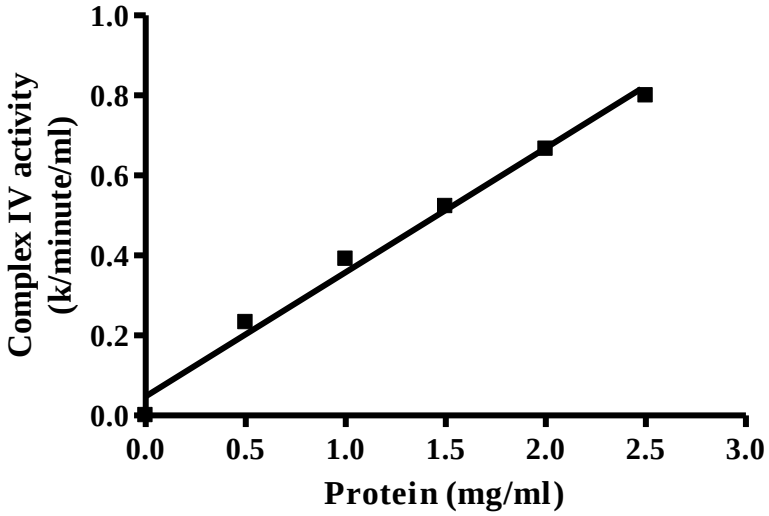


***Figure 19 Complex IV calibration curve.*** The linearity of complex IV activity was demonstrated between a protein concentration range of 0–2.5 mg/ml. Samples were prepared in air saturated conditions at ambient temperature. Samples were analysed as described in section 2.5.3.3. All values are mean ± SEM of 3 independent experiments, $r^2$=0.99.

#### 2.5.3.4 Citrate synthase (EC 2.3.3.1)

Citrate synthase catalyses the condensation of oxaloacetate and acetyl-coenzyme A to form citric acid and coenzyme A in the first step of the Krebs cycle, which takes place in the mitochondrial matrix. Citrate synthase activity is commonly used as a measure of mitochondrial enrichment (Almeida and Medina, 1998; Hargreaves et al., 1999). The citrate synthase assay was based on the method of (Shepherd and Garland, 1969). The assay measures the production of coenzyme A as a result of a reaction between free coenzyme A with DTNB. Sample (10 µl) was added to a cuvette containing a final concentration of 0.1 mmol/L acetyl-coenzyme A, 0.2 mmol/L DTNB in 100 mmol/L tris (pH 8.0), 1 g/L triton X-100 in HPLC grade water. The reaction was started following the addition of 10 µl of 20 mmol/L oxaloacetate. The final concentration of oxaloacetate in the cuvette was 0.2 mmol/L. The reaction was measured at 412 nm for 5 minutes at 30 second intervals at +30°C. The absorbance was converted to molar concentration using the Beer-Lambert law (see section 2.5.3.1). The extinction coefficient used for DTNB was $13.6 \times 10^3$ $M^{-1}$ $cm^{-1}$ (path length 1 cm, volume 1 ml). Results are expressed as nmol/min/mg of protein. A calibration curve was performed to determine the linearity between citrate synthase activity and protein concentration. Linearity was demonstrated between a protein concentration range of 0-2.5 mg/ml (Figure 20).

### 2.5.4 Data analysis

All data were captured and analysed using Lab Power Junior (Secomam).

## 2.6 Total protein assay

### 2.6.1 Function

See section 2.5.1.

### 2.6.2 Equipment

Analysis of samples was carried out using a Uvikon XL spectrophotometer (Secomam, Ales, France).

### 2.6.3 Procedure

Total protein was measured using the Lowry-Peterson protein assay method (Lowry et al., 1951; Peterson, 1977). All samples were diluted in HPLC grade water and prepared in 4.5 ml cuvettes. A 5-point standard curve was prepared for each assay to

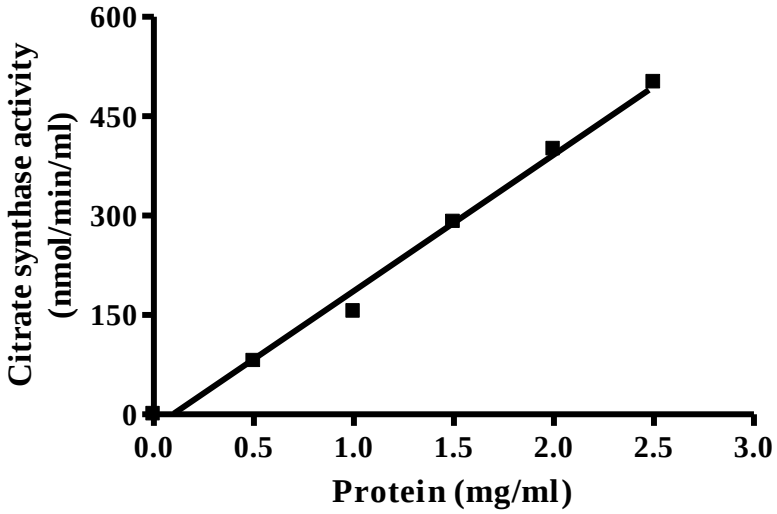


***Figure 20 Citrate synthase calibration curve.*** The linearity of citrate synthase activity was demonstrated between a protein concentration range of 0–2.5 mg/ml. Samples were prepared in air saturated conditions at ambient temperature. Samples were analysed as described in section 2.5.3.4. All values are mean ± SEM of 3 independent experiments, $r^2$=0.99.

determine the linearity between absorbance and protein concentration. Linearity was demonstrated between a BSA concentration range of 0-40 µg/ml, using a 200 µg/ml BSA stock (Figure 21). Total protein in the BSA standards ranged from 0-40 µg. Sample (10 µl) and HPLC grade water (990 µl) was added to each sample cuvette. A solution of copper-tartrate-carbonate (CTC) was prepared by adding 0.2% copper sulphate pentahydrate, 0.4% tartrate and 20% sodium carbonate to HPLC grade water. A 1:1:1:1 ratio of CTC, 10% sodium dodecyl sulphate (SDS), 0.8 mol/L sodium hydroxide and HPLC grade water was prepared. This was called reagent A. A 5:1 ratio of HPLC grade water to Folin-Ciocalteu phenol reagent was also prepared. This was called reagent B. Reagent A (1 ml) was added to each cuvette and left to incubate at room temperature for 10 minutes. Reagent B (0.5 ml) was then added to every cuvette and left to incubate at room temperature for 30 minutes. After incubation, absorbance was measured at a fixed wavelength of 750 nm.

### 2.6.4 Data analysis

All data were captured and analysed using Lab Power Junior (Secomam). Total protein in the unknown samples was determined from linear regression of the unknown sample absorbance units against the BSA standard line.

## 2.7 Flow cytometry for mitochondrial superoxide estimation

### 2.7.1 Function

Flow cytometry is a technique most commonly used for cell counting and sorting. Flow cytometry relies on the movement of cells in suspension past a detector which can measure cell size, granularity and fluorescence, if fluorescent markers have been utilised in the experiment. Specifically, measurement of fluorescent cells is termed fluorescence activated cell sorting (FACS). The prepared cell sample is taken up from the FACS tube under pressure and transported into the flow cell. In the flow cell, the cell sample combines with the sheath fluid. At high pressure, the sheath fluid containing the cell sample is passed through a narrow chamber allowing the cells to pass through the light source for sensing in single file. As the cells pass through the light source, they scatter light. Scattered light is collected by the forward and side collection lenses, which provides the forward scatter (FSC) and side scatter data (SSC). These refer to cell size and granularity respectively and provide

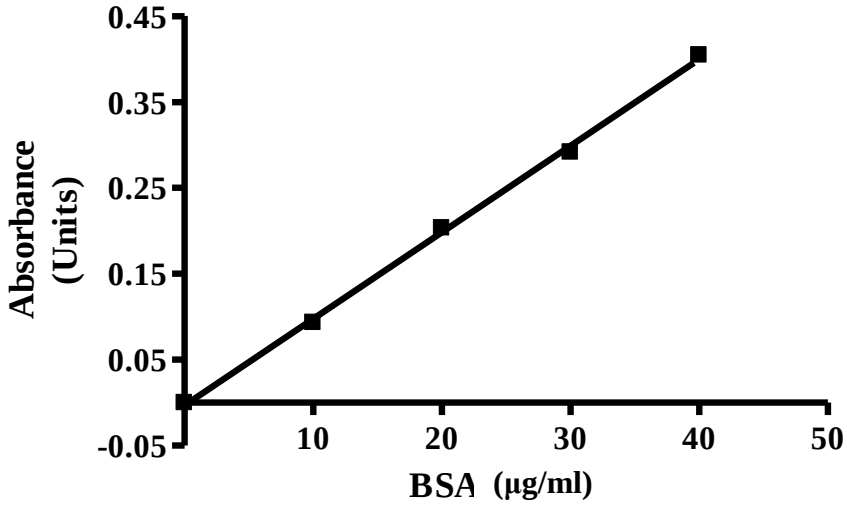


***Figure 21 BSA calibration curve.*** The linearity of BSA was demonstrated between a BSA concentration range of 0–40 ug/ml. Samples were prepared in air saturated conditions at ambient temperature. Samples were analysed as described in section 2.6.3. All values are mean ± SEM of 3 independent experiments, $r^2$=0.99.

information on cell morphology and viability. The FSC and SSC is passed on to the light detector which generates an electrical pulse. If cells are tagged with a fluorescent marker, cells emit fluorescence as they pass through the light source. The emitted fluorescence passes through filters depending on the excitation and emission wavelengths of the fluorophore and is detected by fluorescent detectors. Similarly, the fluorescent detector generates an electrical pulse. When the electrical pulse exceeds the threshold limit, the signal is amplified, recorded by the data acquisition software on a computer and an "event" is counted. Once a certain number of events have been counted, the data can be analysed (Ormerod, 2000).

### 2.7.2 Equipment

Analysis of samples was carried out using a Beckton Dickenson LSR II flow cytometer (BD Biosciences).

### 2.7.3 Procedure

Cells were harvested as described in section 2.4.7. Reactive oxygen species (ROS) were estimated using MitoSOX$^{TM}$ Red (see section 6.5). MitoSOX$^{TM}$ Red indicator is a derivative of dihydroethidium. The cationic triphenylphosphonium substituent of the indicator is responsible for the electrophoretically driven uptake of the probe in actively respiring mitochondria. Oxidation of MitoSOX$^{TM}$ Red indicator by superoxide results in hydroxylation of the molecule, producing a 2-hydroxyethidium MitoSOX$^{TM}$ Red derivative. This molecule exhibits a fluorescence excitation peak at ~400 nm. No products of ethidium oxidation mediated by other ROS are excited within this spectrum. For MitoSOX$^{TM}$ Red fluorescence, the argon laser (L1) was utilised and the excitation and emission wavelengths of the FL3 Red channel (PE-Texas Red®), 488 nm and 615 nm respectively, were set. For each sample, cells were acquired by the flow cytometer and 10,000 events were counted.

### 2.7.4 Data analysis

Data were analysed using FACSDiva software (BD Biosciences). Mean fluorescence intensity was generated for each sample and recorded.

## 2.8 Molecular biology

### 2.8.1 Polymerase chain reaction

#### 2.8.1.1 Function

Polymerase chain reaction (PCR) was used to exponentially amplify specific regions of genomic DNA. Generally, PCR amplifies fragments of genomic DNA between 0.1-10 kilobase pairs in size. PCR primers, complementary to the 5' end of the coding strand and 3' end of the non-coding strand, were designed specifically to the gene of interest. PCR consists of a series of temperature controlled cycles. Each cycle consists of a number of steps. 1. An initialisation step which activates the DNA polymerase. 2. A denaturation step which disrupts the hydrogen bonds between complementary bases yielding two single-stranded DNA molecules. 3. An annealing step which allows annealing of the PCR primers to the single-stranded DNA template. 4. An extension/elongation step where DNA polymerase synthesises a new DNA strand complementary to the DNA template strand by adding dNTPs to complementary bases. 5. After the last PCR cycle, a final elongation step may be performed to ensure any remaining single-stranded DNA is fully extended in the reaction tube. 6. To allow for short term storage of the PCR product, a final hold step may be performed where the reaction tube is kept at 15°C for a period of time (Mullis et al., 1986; Strachan et al., 2011).

#### 2.8.1.2 Equipment

Genomic DNA concentrations were measured using a Nanodrop 1000 Spectrophotometer (Thermo Scientific, North Carolina, USA). PCR was carried out using a Veriti 96-well Thermal Cycler (Applied Biosystems, Paisley, UK).

#### 2.8.1.3 Procedure

Genomic DNA concentration was measured and adjusted to a concentration of 50-200 ng/PCR reaction. Each PCR sample was prepared in a 0.2 ml PCR tube containing x10 $NH_4$ buffer, DMSO, 125 mmol/L betaine, 50-200 ng DNA, 125 µmol/L dNTP mix, 0.1 µl BIOTAQ, 2.5 mmol/L $MgCl_2$, 5 µmol/L forward (5') primer, 5 µmol/L reverse (3') primer, made up to 20 µl in ultra-pure double distilled water. In place of patient DNA, negative control samples were prepared using surplus genomic DNA from a different patient found not to have DNA mutations in the gene of interest (wild-type). In a similar fashion, negative control samples were

prepared using ultra-pure double distilled water. In order to ensure uniformity of conditions in each reaction tube, a master mix containing the necessary reagents was prepared prior to the addition of DNA or ultra-pure double distilled water. A reference DNA sequence for *FOLR1* was obtained from the open source bioinformatics genome browser database Ensembl (http://www.ensembl.org) and the primers for the gene were designed using the open source bioinformatics programme Primer3Plus (http://www.primer3plus.com). The primers used to amplify the *FOLR1* gene encoding the FRα were as follows:

| | |
|---|---|
| Exon 1: | Non-coding sequence |
| Exon 2: | Non-coding sequence |
| Exon 3: | Non-coding sequence |
| Exon 4: | 5'-AAGGCATTGTGGACCTATGG-3' |
| | 3'-CAGGATGGGTCACTCCAACT-5' |
| Exon 5: | 5'-TACAAGTCCCCATCCGTCTC-3' |
| | 3'-TCATGGCTGCAGCATAGAAC-5' |
| Exon 6 + 7: | 5'-CAGTTCTATTCGGGGCTGAGT-3' |
| | 3'-TCCTGGGCTTGGCTCTAGATTG-5' |

The PCR conditions were one cycle of initial denaturation at +95°C for 2 minutes, followed by 36 cycles of denaturation at +95°C for 30 seconds, annealing at +57°C for 30 seconds and elongation at +72°C for 1 minute, followed by one cycle of final elongation at +72°C for 3 minutes and final hold/cooling down at +15°C for 5 minutes. The PCR products were then immediately resolved by 1% agarose gel electrophoresis.

### 2.8.2 Resolution of PCR products

#### 2.8.2.1 Function

Agarose gel electrophoresis was used to separate the PCR products. Gel electrophoresis separates protein fragments based on their size and charge.

Application of an electric field moves the negatively charged molecules through the agarose matrix. Smaller molecules move faster and migrate further than larger molecules (Lee et al., 2012; Sanger and Coulson, 1978).

#### 2.8.2.2 Equipment

Gel electrophoresis was carried out in a gel electrophoresis tank (BIO-RAD, Hertfordshire, UK) connected to a power pack (BIO-RAD).

#### 2.8.2.3 Procedure

PCR products were resolved and confirmed using a 1% agarose gel. Agarose (1.6 g) was added to 160 ml of x1 TBE buffer and dissolved by heating on high power for 2.5 minutes in a microwave oven. Once cooled, 7 µl of ethidium bromide (10 mg/ml) was added. The gel was poured into a mould, a well divider comb positioned and left to set. The well divider comb was removed once the gel had set. The gel was placed in a gel electrophoresis tank and submerged in x1 TBE buffer. PCR product (5 µl) was mixed with 5 µl of x5 loading buffer and 5 µl of this mix was loaded into the appropriate well. The tank was connected to a power pack set at 100 V and allowed to run for 45 minutes.

#### 2.8.2.4 Analysis

After 45 minutes of gel electrophoresis had elapsed, the power pack was disconnected and the gel was removed from the tank. The PCR products were visualised under a GeneSmart and GeneView UV transilluminator (VWR) and digital images were captured.

### 2.8.3 DNA sequencing

#### 2.8.3.1 Function

Sanger sequencing is a method used to elucidate the sequence of nucleotides in a length of DNA. Sanger sequencing can also be referred to as dideoxy sequencing or chain termination. The method is based on the addition of fluorescently labelled dideoxynucleotides to the nucleotides in DNA. Each dideoxynucleotide, ddATP, ddTTP, ddCTP and ddGTP is labelled with a specific fluorescent dye. Dideoxynucleotides differ in comparison to nucleotides by the presence of a hydrogen group on the 3’ carbon instead of a hydroxyl group. When integrated into the DNA sequence, the dideoxynucleotides prevent the addition of further

nucleotides. This occurs because a phosphodiester bond cannot form between the dideoxynucleotide and the next incoming nucleotide. Thus, the incorporation of the didoxynucleotide terminates DNA chain elongation. The products of the sequencing reaction can be resolved by gel electrophoresis. Since the four dideoxynucleotides fluoresce at different wavelengths, the sequence of nucleotides can be determined.

#### 2.8.3.2 Procedure

Excess primers from the PCR products were removed following the addition of 3 µl ExoSAP/20 µl PCR product. The removal was carried out using the Veriti 96-well Thermal Cycler (Applied Biosystems). The conditions were one cycle of activation at +37°C for 15 minutes and inactivation at +80°C for 15 mintues. PCR products and primers for sequencing were prepared according to the instructions provided by Source Bioscience (Nottingham, UK) and sent off to Source Bioscience for overnight Sanger sequencing analysis.

#### 2.8.3.3 Data analysis

Data was analysed using Sequencher 4.9 (Gene Codes, Michigan, USA). The sequences were compared to that of the reference sequence obtained from the Ensembl database (http://www.ensembl.org).

### 2.9 General data analysis

All results are expressed as mean ± standard error of the mean (SEM) or standard deviation (SD). Visual inspection and cluster analysis of the data was performed. Obvious outliers were excluded from the overall analysis.

#### 2.9.1 Statistics

All statistical analyses were carried out using Graphpad Prism 4 software (Graphpad Software Inc. San Diego, CA, USA) unless otherwise indicated. The Kolmogorov-Smirnov test was used to determine whether data were normally distributed and Pearson correlation coefficient (r) was used for correlative analyses. Multivariate regression analyses were performed to investigate correlations where an age-dependency was associated with the data (IBM SPSS Statistics, Armonk, NY, USA). Individual comparison of means was performed using Student's t-test and multiple comparisons were made using one-way analysis of variance (one-way ANOVA). Independent variables found to be significant by one-way ANOVA were further

analysed by performing a Bonferroni multiple comparison *post-hoc* test. In all cases $p<0.05$ was considered significant.

### 2.9.2 Calculation of first order rate constants

For studies monitoring the decay of 5-MTHF, specifically in CSF and potassium phosphate buffer, the first order rate constant (k) was determined from the slope of a natural log (ln) of 5-MTHF concentration versus incubation time (min) plot. The gradient of the slope was determined by performing linear regression analysis of the data (Graphpad Software Inc).

# Chapter 3
# CFD in mitochondrial respiratory chain enzyme deficiencies: a retrospective cohort study.

# 3. CFD in mitochondrial respiratory chain enzyme deficiencies: a retrospective cohort study.

## 3.1 Introduction

The essential water-soluble B vitamin, 5-MTHF, is the principle transport and bioactive form of the folate species that is involved in over 100 metabolic reactions (Hyland et al., 1988; Surtees et al., 1994). CFD, characterised by a low CSF concentration of 5-MTHF in the presence of normal peripheral folate status, is increasingly diagnosed in a range of neurological conditions (Garcia-Cazorla et al., 2008; Hyland et al., 2010; Moretti et al., 2005; Pérez-Dueñas et al., 2011; Serrano et al., 2012). A distinct clinical phenotype for CFD has previously been described which is characterised by normal development until 4-6 months of age and evolving agitation, insomnia, psychomotor retardation, deceleration of head growth, ataxia, hypotonia, spasticity, dyskinesia and epilepsy (Ramaekers et al., 2002). The underlying aetiology of CFD may be inherited or acquired. For example, mutations in the *FOLR1* gene encoding the FRα receptor, the protein transporter responsible for ATP-dependent transport of 5-MTHF from the periphery into the CSF across the choroid plexus cells of the blood-CSF barrier, have been reported to cause brain-specific 5-MTHF (<10 nmol/L) deficiency leading to neurodegeneration in early childhood (Cario et al., 2009; Steinfeld et al., 2009). Conversely, CFD diagnosed in patients with neurological disorders, such as mitochondrial diseases, is not well understood, as discussed in sections 1.5 and 1.6.

Mitochondrial diseases are a common group of metabolic disorders affecting mitochondrial RCE activity, with a combined prevalence of one in 5000 (Thorburn, 2004). These disorders encompass a wide range of clinical symptoms and presentations, in which the age of onset is variable. The clinical features vary from single to multiple affected organs, with high-energy requiring tissues, including the brain and skeletal muscle, most notably impaired (Barkovich et al., 1993; Chi et al., 2011; Jackson et al., 1995). For further discussion, see section 1.3.

In view of the overlapping clinical heterogeneity of CFD and mitochondrial disease phenotypes, CFD may represent an under-recognised condition in patients with mitochondrial disease. As a consequence, since CFD is a potentially treatable aspect

of mitochondrial disease (Garcia-Cazorla et al., 2008; Hansen and Blau, 2005), patients may also be excluded from receiving effective treatment.

From the available literature and current knowledge, no large-scale systematic analysis of CFD in mitochondrial diseases has been performed. Therefore, the prevalence and significance of CFD diagnosed in mitochondrial diseases remains unknown. Consequently, data from a large cohort of children with suspected mitochondrial disease, as described in section 3.4.1, were analysed retrospectively.

## 3.2 Aims

1. To analyse biochemical data from a large cohort of paediatric patients with a suspected mitochondrial disease in whom a skeletal muscle biopsy for biochemical mitochondrial RCE activity measurement and a lumbar puncture for CSF 5-MTHF measurement were performed.

2. To perform *FOLR1* mutation analysis in patients with CSF 5-MTHF <10 nmol/L in the absence of a peripheral folate deficiency.

3. To examine the potential relationship between individual mitochondrial RCE complex deficiencies and CSF 5-MTHF.

4. To evaluate the biochemical benefit of folinic acid supplementation therapy in patients with severe CSF 5-MTHF deficiencies.

## 3.3 Acknowledgement

All data collection and analysis work, and molecular genetic analysis of the *FOLR1* gene throughout this Chapter was my own. Whilst this was not a clinical study, interpretation of clinical data and brain MRI/CT imaging results was facilitated by Dr. Shamima Rahman, Consultant Metabolic Paediatrician and Dr. W. K. Chong, Consultant Paediatric Neuroradiologist, at Great Ormond Street Hospital, London UK. CSF 5-MTHF analysis and mitochondrial respiratory chain enzyme activities were performed by Viruna Neergheen and Marcus Oppenheim, and Dr. Iain Hargreaves, respectively, in the Neurometabolic Unit at the National Hospital for Neurology and Neurosurgery, London, UK. Total serum folate analysis was performed by the Chemical Pathology Department at Great Ormond Street Hospital,

London, UK. Protein modelling was performed by Jose Saldanha in the Division of Mathematical Biology at the National Institute for Medical Research, Mill Hill, London, UK.

## 3.4 Methods

### 3.4.1 Patients

Paediatric patients with suspected mitochondrial disease investigated at Great Ormond Street Hospital, London, UK from July 2006 to November 2012 inclusive in whom both a skeletal muscle biopsy for biochemical mitochondrial RCE activity analysis and a lumbar puncture for CSF 5-MTHF analysis were performed, were collated from the central pathology database.

A total of 260 paediatric patients (mean ± SD [range] age: 6.1 ± 5.2 [0.2-16.7] years; 141M:119F) were identified and subdivided into groups as shown in Figure 22. Fifty-one of the 260 patients only had mitochondrial RCE activity measured. These patients were retrieved from the database because they had CSF neurotransmitter and pterin analyses performed. However, CSF 5-MTHF had not been measured in these cases, so they were excluded from further analyses. CSF neurotransmitter, pterin and 5-MTHF analyses are reported together under the same diagnostic test heading within the central pathology database, explaining the retrieval of these cases which did not fit the inclusion criteria for the study. Additionally, 22 patients only had CSF 5-MTHF measured. These patients were retrieved from the database for a number of reasons, including: patients who had a skeletal muscle biopsy but the sample was too small (<50 mg) for biochemical analysis; patients with a confirmed genetic diagnosis of mitochondrial disease from blood investigations, which superseded the requirement for skeletal muscle biopsy; and suspected mitochondrial disease patients who did not have a skeletal muscle biopsy for various reasons, including parental refusal and being considered too unwell for general anaesthesia.

One hundred and eighty seven patients had both biochemical mitochondrial RCE activity and CSF 5-MTHF measured. These patients, together with those who had CSF 5-MTHF measured only, were further subdivided into groups (Figure 22).

### 3.4.2 Patient samples

All patient samples were tested as part of diagnostic investigations requested by the patient's clinician and after informed parental consent.

#### 3.4.2.1 CSF

Patient CSF samples were taken as described in section 2.2.1.

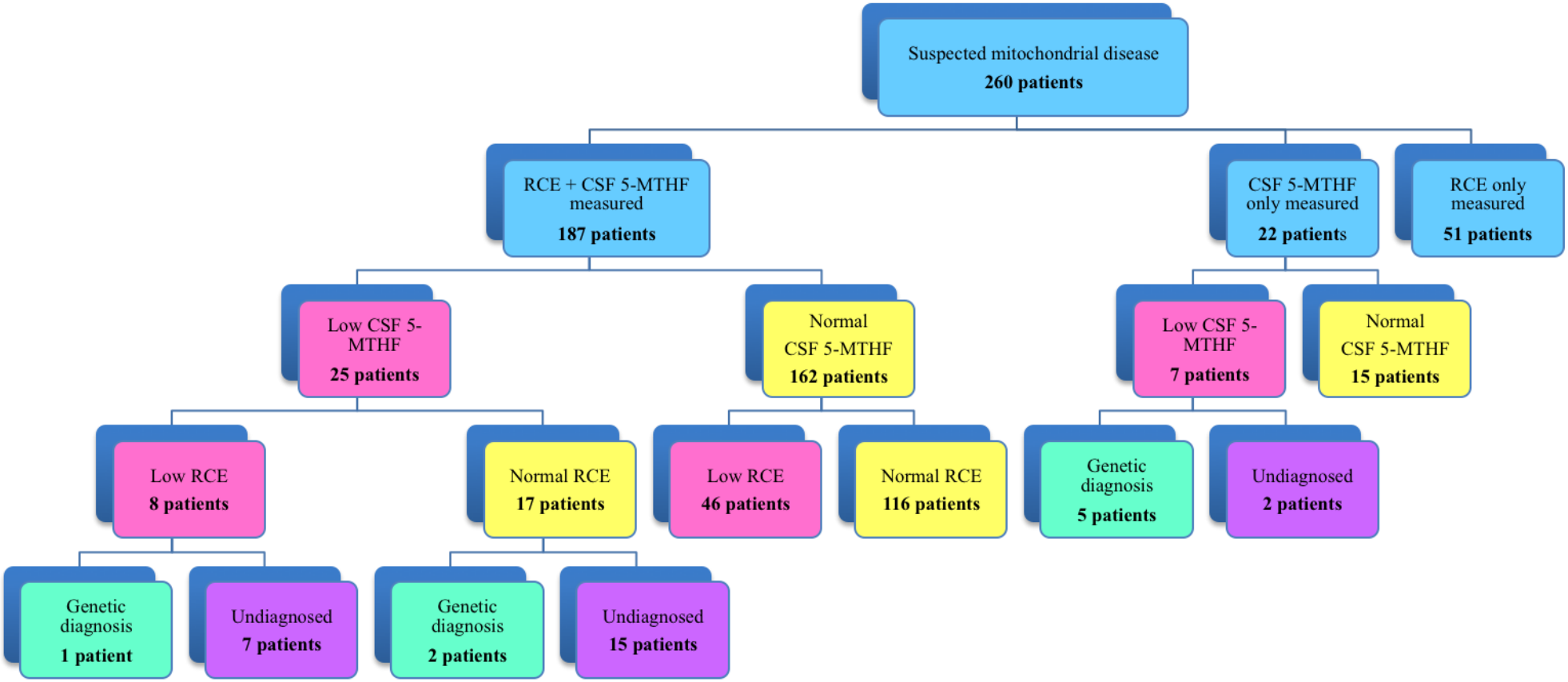


***Figure 22 Decision tree for the distribution of patients in the cohort.*** The patient cohort was split into 3 subgroups (blue). Patients with low 5-MTHF and RCE activity are represented in pink and patients with normal 5-MTHF and RCE activity in yellow. Genetically diagnosed patients are represented in green and undiagnosed patients in purple. RCE = respiratory chain enzyme, CSF = cerebrospinal fluid.

#### 3.4.2.2 Skeletal muscle

Patient skeletal muscle biopsies were taken as described in section 2.2.2

### 3.4.3 Measurement of CSF 5-MTHF

CSF 5-MTHF was measured by HPLC as described in section 2.3. CSF 5-MTHF data were analysed retrospectively. The age-related CSF 5-MTHF reference ranges are shown in Table 5. CFD was classified as mild (<30% below lower reference range limit), moderate (30-60% below lower reference range limit) and severe (>60% below lower reference range limit) (Pérez-Dueñas et al., 2011).

### 3.4.4 Measurement of mitochondrial respiratory chain enzyme activity in skeletal muscle

Mitochondrial RCE activities were measured as described in section 2.5. The mitochondrial RCE activity data were analysed retrospectively. Mitochondrial RCE activities were calculated as a ratio to citrate synthase, a mitochondrial marker enzyme, to compensate for mitochondrial enrichment of the muscle samples. Mitochondrial RCE activity (ratio to citrate synthase activity) reference ranges in skeletal muscle are shown in Table 7.

### 3.4.5 Genetic analysis

In patients with very low CSF 5-MTHF levels (<10 nmol/L) who did not already have a confirmed genetic diagnosis, Sanger sequence analysis of the *FOLR1* gene was performed in genomic DNA isolated from blood samples. All 4 coding exons and exon-intron boundaries of the *FOLR1* gene were amplified by polymerase chain reaction and sequenced using standard methods as described in section 2.8.

### 3.4.6 FRα protein modelling

A protein structure model of the novel *FOLR1* homozygous missense mutation (c.335A>T; p.N112I) described in this Chapter (see section 3.5.1.2) and the known mutations in the FRα, was created based on the known crystal structure of FRα in complex with folic acid; protein data bank code 4LRH (Chen et al., 2013). Models were built using the MOE 2012.10 (2) incorporating the Amber12EHT forcefield running on a Linux workstation. The same program was used to visualise, analyse and generate images.

### 3.4.7 Additional data

In those patients with low CSF 5-MTHF, clinical features, diagnoses (where available), brain MRI/CT imaging and total serum folate data were collated and analysed retrospectively. The genetic diagnoses of two patients with normal mitochondrial RCE acitivity and low CSF 5-MTHF were also identified.

#### 3.4.7.1 Brain MRI/CT imaging analysis

Brain MRI/CT scans were retrospectively reviewed and findings were recorded qualitatively. Specific note was made of the appearances of white matter myelination, volume, the presence of any focal lesions or evidence of leukodystrophy. Quantitative MRI analysis was not performed.

#### 3.4.7.2 Measurement of total serum folate

Total serum folate was measured by competitive immunoassay and analysed using an IMMUNLITE 2000 immunoassay system analyser, according to the manufacturer's instructions (Siemens Healthcare, Surrey, UK). In patients with low CSF 5-MTHF (n=32), results of total serum folate concentrations were obtained, where available, to verify the absence of a peripheral nutritional folate deficiency and confirm CFD. Total serum folate data were analysed retrospectively. Owing to the retrospective nature of this study, the dataset for this parameter was incomplete, since total serum folate values were only available for patients in whom concurrent blood sampling had been performed at the time of lumbar puncture. The age and sex-related total serum folate reference ranges are shown in Table 3.

### 3.4.8 Data analysis

Data analysis was carried out as described in section 2.9.

## 3.5 Results

### 3.5.1 Patients with both biochemical mitochondrial RCE activity and CSF 5-MTHF measured, and patients with CSF 5-MTHF measured only

#### 3.5.1.1 Skeletal muscle mitochondrial RCE activity and CSF 5-MTHF data analysis

Both skeletal muscle mitochondrial RCE activities and CSF 5-MTHF levels had been determined in 187 of 260 patients with suspected paediatric mitochondrial disease (Figure 22). CSF 5-MTHF analysis was performed in a further 22 patients who did not have skeletal muscle biopsies. From these two groups of patients, a total of 32 patients with suspected mitochondrial disease (mean ± SD [range] age, sex ratio: 5.2 ± 4.2 [0.6-15.4] years; 19M:13F) had decreased CSF 5-MTHF (mean ± SD [range] value, 39 ± 21 [<10-71] nmol/L), a prevalence of 15% (Table 8).

Of the subgroup of 25 CFD patients who had both skeletal muscle mitochondrial RCE activity and CSF 5-MTHF analysis, 8 patients (mean ± SD [range] age, sex ratio: 6.1 ± 4.7 [0.6-12.5] years; 3M:5F) with low CSF 5-MTHF concentrations also had low skeletal muscle mitochondrial RCE activity, a prevalence of 32% (Figure 23). All 8 patients had isolated complex IV deficiency (mean ± SD [range] value, 0.006 ± 0.002 [0.004-0.010] ratio to citrate synthase) (Table 8 and Figure 23). Patient 28 had isolated complex IV deficiency (activity [reference range]: 0.007 [0.014-0.034]) and undetectable (<10 nmol/L) CSF 5-MTHF, fulfilling the criteria for *FOLR1* mutation analysis and a genetic diagnosis was established (see section 3.5.1.2). A genetic diagnosis was not established in the other 7 patients with both low skeletal muscle mitochondrial RCE activity and CFD. Genetic diagnoses were established for two of the remaining 17 patients in this subgroup, Patient 13 and Patient 25, who had normal skeletal muscle mitochondrial RCE activities (see section 3.5.1.2).

Of the 187 patients who had both skeletal muscle mitochondrial RCE activity and CSF 5-MTHF analysis, 162 had CSF 5-MTHF concentrations within the age-related reference range, including 46 patients with low skeletal muscle mitochondrial RCE activity (mean ± SD [range] age, sex ratio: 6.7 ± 4.5 [0.9 to 16.1] years; 25M:21F). One hundred and sixteen patients had normal skeletal muscle mitochondrial RCE

***Table 8 Patient demographics, clinical features, brain MRI/CT imaging findings and biochemical data of patients with low CSF 5-MTHF.*** Total serum folate and CSF 5-MTHF age-related reference ranges are shown in Table 3 and Table 5, respectively. MRI = magnetic resonance imaging, y = years, CT = computed tomography, BG = basal ganglia, CC = corpus callosum, DM = delayed myelination, GP = globus pallidus, IC = internal capsule, LD = leukodystrophy, PCH = pontocerebellar hypoplasia, PV = periventricular, PVL = periventricular leukomalacia, WM = white matter.

| **Patient** | **Age at CSF sampling (years)** | **Sex** | **Major clinical features** | **Brain MRI/CT imaging findings** | **CSF 5-MTHF nmol/L (ref. range)/ Total serum folate nmol/L (ref. range)** | **RCE activity (ratio to citrate synthase)** | | |
|---|---|---|---|---|---|---|---|---|
| | | | | | | **CI (0.104-0.268)** | **CII/III (0.040-0.204)** | **CIV (0.014-0.034)** |
| **1** | 6.7 | M | Severe motor and cognitive delay<br>Seizure disorder<br>Upper airway obstruction<br>Feeding difficulties | CT normal at 4y | 52 (72-172)/ - | 0.160 | 0.190 | 0.022 |
| **2** | 5.3 | M | Epilepsy (phenytoin treatment)<br>Four limb motor disorder with hypotonia,<br>No speech<br>Minimal interaction | MRI at 5.3y: mild generalised reduction in WM bulk | 59 (72-172)/<br>21.7 (1.1 – 29.2) | 0.257 | 0.113 | 0.029 |
| **3** | 2.4 | F | Motor skills and speech regression<br>Mild low frequency hearing impairment in the right ear | MRI at 2.3y: hypomyelination | 57 (72-305)/ - | 0.117 | 0.119 | 0.024 |
| **4** | 6.8 | F | Intractable epilepsy (levetiracetam treatment)<br>Movement disorder<br>Developmental regression and delay<br>Mild nephrocalcinosis | MRI at 2.7y: symmetrical subcortical and deep WM signal abnormalities;<br>CT at 4y: symmetrical BG calcification, frontal atrophy and WM density change;<br>MRI + CT at 6.9y: progressive LD with extensive frontal WM disease, progressive cerebellar atrophy and symmetrical BG calcification | <10 (72-172)/<br>54.4 (6.1 – 31.7) | - | - | - |
| **5** | 2.3 | M | Perimembranous ventricular septal defect with signs of pulmonary congestion and volume overload. | MRI at 1.9y: symmetrical LD | 50 (52-178)/- | 0.200 | 0.04 | 0.016 |

| | | | | | | | | |
|---|---|---|---|---|---|---|---|---|
| **6** | 5.5 | M | Leigh syndrome<br>Developmental delay<br>Gastro-oesophageal reflux disease | MRI 5.5y: bilateral symmetrical abnormal signal within WM of cerebellar hemispheres, medulla, pontomedullary junction, superior cerebellar peduncles.<br>MRI at 10.3y: as before with new bilateral lesions in caudate nuclei heads and progressive cerebellar atrophy | 44 (72-172)/<br>54.4 (1.1 – 29.2) | 0.141 | 0.079 | 0.004 |
| **7** | 1.8 | F | Hypotonia right upper limb, lower limbs and trunk<br>Developmental regression | MRI at 1.8y: mild DM and two WM lesions (right posterior frontal subcortical WM and right frontal corona radiata)<br>MRI at 2y: partial resolution of frontal WM lesions<br>MRI at 3.2y: new small posterolateral temporal WM lesion with progressive cerebral atrophy | 52 (72-305)/<br>54.4 (14.2 – 51.0) | 0.126 | 0.049 | 0.005 |
| **8** | 5.5 | F | Epilepsy (phenytoin treatment)<br>Global developmental delay | MRI at 10m: generalised lack of WM bulk and DM | 62 (72-172)/ - | 0.119 | 0.068 | 0.01 |
| **9** | 6.5 | F | KSS | CT at 4.8y and MRI at 4.9y both normal<br>MRI at 6.5y: bilateral symmetrical signal abnormalities of cerebellar WM, dorsal brainstem, GP and thalamus<br>MRI at 7.6y slight progression of disease especially in midbrain and cerebellum | <10 (72-172)/<br>54.4 (6.1 – 31.7) | - | - | - |
| **10** | 1.6 | M | Severe intestinal failure<br>Impaired renal function<br>Cardiomegaly but good cardiac function<br>Hypothyroidism | MRI at 9m: DM and lack of WM bulk<br>MRI at 1.7y: bilateral symmetrical cortical injury with atrophy and gliosis, bilateral subcortical WM lesions and symmetrical cerebellar lesions | 35 (72-305)/ - | 0.123 | 0.06 | 0.023 |
| **11** | 14.3 | M | KSS | MRI normal at 13.2y | 54 (72-172)/<br>16.3 (2.7 – 19.8) | - | - | - |
| **12** | 0.6 | F | Epilepsy (sodium valproate treatment)<br>Global developmental delay | MRI at 5.5m: mild lack of WM bulk MRI at 11m: new restricted diffusion in GP, thalami, brainstem and dentate nuclei | 57 (72-305)/<br>45.5 (14.2 – 51.0) | 0.240 | 0.079 | 0.005 |

| | | | | | | | | |
|---|---|---|---|---|---|---|---|---|
| **13** | 15.4 | F | MEMSA | MRI at 13.8y: bilateral symmetrical signal change within both occipital poles around calcarine sulci and in dentate nuclei, and right hippocampal sclerosis | 29 (46-160)/ - | 0.126 | 0.156 | 0.026 |
| **14** | 1.7 | F | Status epilepticus<br>Progressive neurological deterioration | MRI at 1.7y: bilateral abnormal signal in deep WM of both cerebral hemispheres and in cerebellar WM and focal abnormality of right caudate; marked progression 2 weeks later with diffuse cerebral and cerebellar swelling and diffuse cortical and WM lesions, and diffuse leptomeningeal nodular process affecting cerebellum and brainstem | 67 (72-305)/ - | 0.211 | 0.079 | 0.018 |
| **15** | 9.5 | M | Dystonic spasms | MRI normal at 9.5y | 29 (72-172)/<br>54.4 (5.2 – 26.7) | 0.334 | 0.085 | 0.024 |
| **16** | 2.3 | F | Developmental delay<br>Nystagmus<br>Hypotonia | MRI at 1.4y: DM and decreased WM bulk | 13 (52-178)/ - | - | - | - |
| **17** | 12.5 | M | Renal failure | MRI at 12.4y: generalised sulcal and ventricular prominence and prominence of cerebellar fissures | 40 (46-160)/<br>54.4 (3.4 – 24.3) | 0.134 | 0.041 | 0.01 |
| **18** | 1.6 | F | Global developmental delay<br>Movement disorder | MRI at 11m: generalised lack of WM bulk | 70 (72-305)/ - | 0.225 | 0.068 | 0.004 |
| **19** | 2.4 | M | Seizures (sodium valproate treatment)<br>Developmental arrest<br>Sensorineural deafness<br>Poor visual attentions<br>Hypothyroidism | MRI at 3.4y: extensive reduction of cerebral WM bulk, with less marked reduction of brainstem and cerebellar bulk | 24 (52-178)/<br>54.4 (5.6 – 33.7) | 0.183 | 0.159 | 0.023 |
| **20** | 0.9 | M | Developmental regression<br>Seizures (phenytoin treatment)<br>Bilateral deafness | MRI at 9m: DM | 16 (72-172)/ - | 0.204 | 0.148 | 0.021 |

| | | | | | | | | |
|---|---|---|---|---|---|---|---|---|
| **21** | 5.3 | M | Motor and speech regression<br>Movement disorder | MRI normal at 5.2y | 58 (72-172)/ - | 0.187 | 0.167 | 0.030 |
| **22** | 9.6 | F | Optic atrophy<br>Ataxia | MRI at 3.3y: immature signal in posterior limb of IC and GP | 46 (72-172)/<br>51.4 (5.4 – 30.1) | 0.180 | 0.126 | 0.029 |
| **23** | 1.4 | M | Global developmental delay<br>Epilepsy (sodium valproate treatment)<br>Four limb dyskinetic movement disorder | CT at 13m: bilateral BG calcification with PV and deep WM LD and cerebellar hypoplasia<br>MRI at 2.6y: PCH and generalised lack of cerebral volume and myelination, with bilateral symmetrical mature haemorrhagic infarction of BG and symmetrical PV and deep WM change of frontal lobes | <10 (72-305)/ - | - | - | - |
| **24** | 1.4 | M | Developmental delay<br>Learning difficulties<br>Epilepsy (sodium valproate treatment) | MRI normal at 10m<br>MRI at 2.6y: DM and lack of WM bulk<br>MRI at 4.2y: normal appearances with myelination now appropriate for age<br>MRI normal at 5.2y and 8.2y | <10 (52-178)/<br>0.2 (at diagnosis)<br>(16.2 – 50.3) | - | - | - |
| **25** | 6.1 | M | KSS<br>Renal tubulopathy<br>Short stature<br>Left sided ptosis | MRI at 5.7y: bilateral symmetrical signal abnormality within GP, subthalamic nuclei and dorsal brainstem, with mild cerebellar hypoplasia<br>MRI at 8.7y extensive signal abnormality bilaterally within GP and rest of BG, anterior thalami, midbrain, pons and medulla as well as diffuse symmetrical signal abnormality within deep and subcortical WM of cerebral hemispheres, mild volume loss of cerebrum and cerebellum<br>MRI at 10.1y striking and extensive WM signal abnormality in addition to symmetrical lesions within thalami, BG, midbrain and dorsal pons | <10 (72-305)/<br>54.4 (1.1 – 29.2) | 0.203 | 0.142 | 0.017 |
| **26** | 2.8 | F | Premature infant 31 weeks gestation with severe failure to thrive, hypotonia and global developmental delay | MRI at 3y: marked lack of WM bulk, thin CC, PVL | 28 (52-178)/<br>54.4 (3.8 – 35.3) | 0.219 | 0.091 | 0.022 |

| | | | | | | | | |
|---|---|---|---|---|---|---|---|---|
| **27** | 5.1 | M | Ophthalmoplegia<br>Ataxia | MRI at 4.8y: mild lack of WM bulk | 66 (72-172)/ - | 0.161 | 0.101 | 0.026 |
| **28** | 12.1 | M | Intractable epilepsy (sodium valproate treatment)<br>Profound learning difficulties | MRI at 5.6y: thin CC, otherwise normal<br>MRI at 11.2y global atrophy affecting cerebellum more severely than cerebellar hemispheres<br>CT at 12y: small cerebellum and punctate BG calcification | <10 (46-160)/<br>54.4 (3.4 – 24.3) | 0.248 | 0.181 | 0.007 |
| **29** | 1.5 | M | Intractable epilepsy (sodium valproate treatment)<br>Severe developmental delay | MRI at 2y: progressive cortical atrophy, thin CC | 71 (72-305)/<br>54.4 (16.2 – 50.3) | 0.114 | 0.073 | 0.017 |
| **30** | 2.4 | M | Global developmental regression<br>Epilepsy (carbamezapine treatment) | MRI normal at 6m<br>MRI at 2y: new bilateral occipito-temporal WM and cortical signal abnormality | 31 (52-178)/<br>22.4 (5.6 – 33.7) | 0.201 | 0.122 | 0.028 |
| **31** | 9.4 | F | Epilepsy (sodium valproate treatment)<br>Motor and speech regression | MRI normal at 7.7y | 52 (72-172)/<br>54.4 (5.4 – 30.1) | 0.224 | 0.217 | 0.005 |
| **32** | 6.5 | M | KSS | MRI normal at 2.4y | <10 (72-172)/<br>48.3 (1.1 – 29.2) | - | - | - |

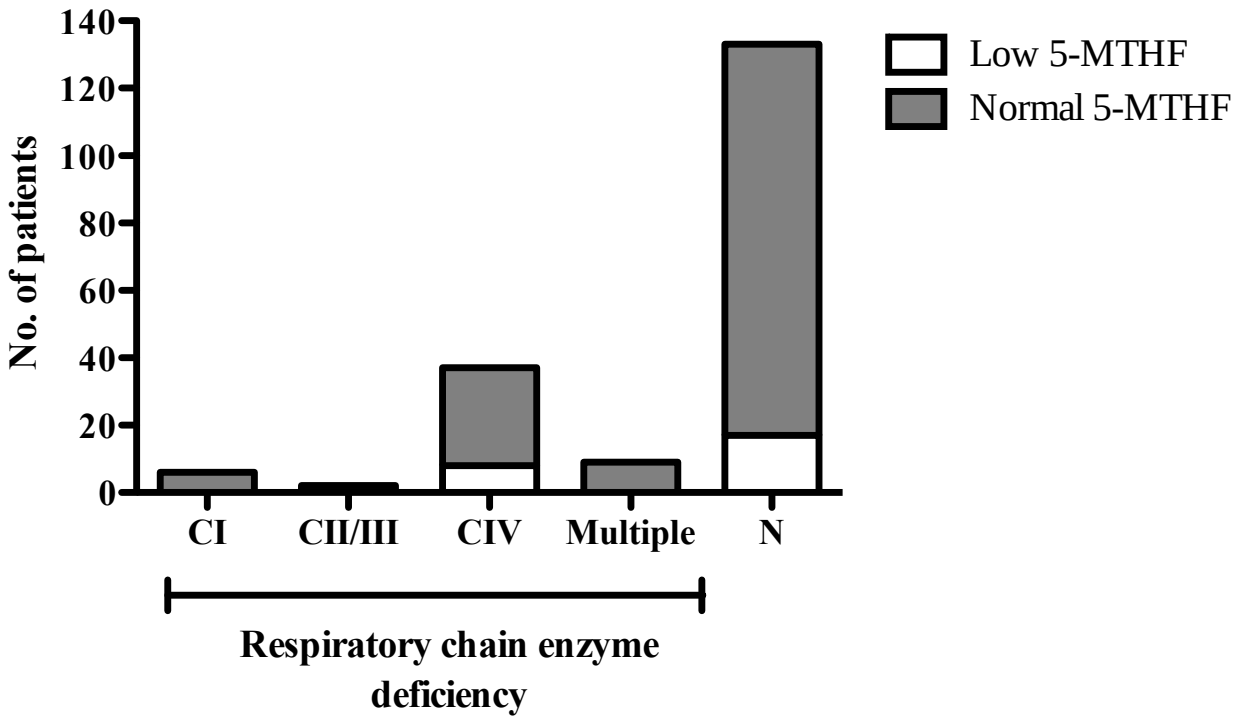


***Figure 23 Proportion of patients with low/normal CSF 5-MTHF concentration and low/normal mitochondrial RCE activity.*** CI=Complex I (n=6), CII/III=Complex II/III (n=2), CIV=Complex IV (n=29, 8), Multiple=multiple respiratory chain defects (Complex I and Complex IV) (n=9), N=normal (n=116, 17).

activities (Figure 23). Combining the 46 patients who had low skeletal muscle mitochondrial RCE activity and normal CSF 5-MTHF concentrations with the 8 patients who had low skeletal muscle mitochondrial RCE activity and low CSF 5-MTHF concentrations, the prevalence of CFD in biochemically confirmed skeletal muscle mitochondrial RCE defects was calculated to be 15%.

Of the subgroup of 22 patients who only had CSF 5-MTHF measured, seven patients had decreased CSF 5-MTHF (mean ± SD [range] age, sex ratio: 7.3 ± 4.6 [1.2-15.4] years; 4M:3F), whilst the remaining 15 patients in this subgroup had CSF 5-MTHF concentrations within the normal age-related reference ranges. Genetic diagnoses were established in five of the seven patients who had low CSF 5-MTHF levels but did not have skeletal muscle biopsies (Patients 4, 9, 11, 24 and 32) (see section 3.5.1.2). The remaining two patients did not have genetic diagnoses.

#### 3.5.1.2 Genetic diagnoses

Of the subgroup of eight patients with low CSF 5-MTHF and complex IV deficiency, one patient (Patient 28) had CSF 5-MTHF <10 nmol/L. *FOLR1* mutation analysis was performed and a genetic diagnosis was established. Patient 28 had a homozygous nonsense mutation in exon 7 of *FOLR1* (c.610C>T; p.R204X) and his consanguineous parents were both heterozygous for the mutation (Figure 24 and Figure 25). The arginine at position 204 (R204) is highly conserved across species (Figure 26a).

Of the subgroup of 17 patients with low CSF 5-MTHF and normal RCE activities, genetic diagnoses were established for two patients (Patients 13 and 25). Patient 13 had MEMSA (Myoclonic Epilepsy, Myopathy, Sensory Ataxia) associated with a homozygous p.A467T *POLG* mutation, whilst Patient 25 had KSS caused by a single large-scale mtDNA deletion.

Of the subgroup of seven patients with low CSF 5-MTHF but did not have muscle biopsies, five were found to have genetic diagnoses. Patient 4, had severe CFD (<10 nmol/L) and *FOLR1* mutation analysis in this patient revealed a novel homozygous missense mutation (c.335A>T; p.N112I) (Figure 24 and Figure 27). The consanguineous parents were both heterozygous for the mutation and the asparagine at position 112 is highly conserved across species (Figure 26b). Patients 9, 11, and

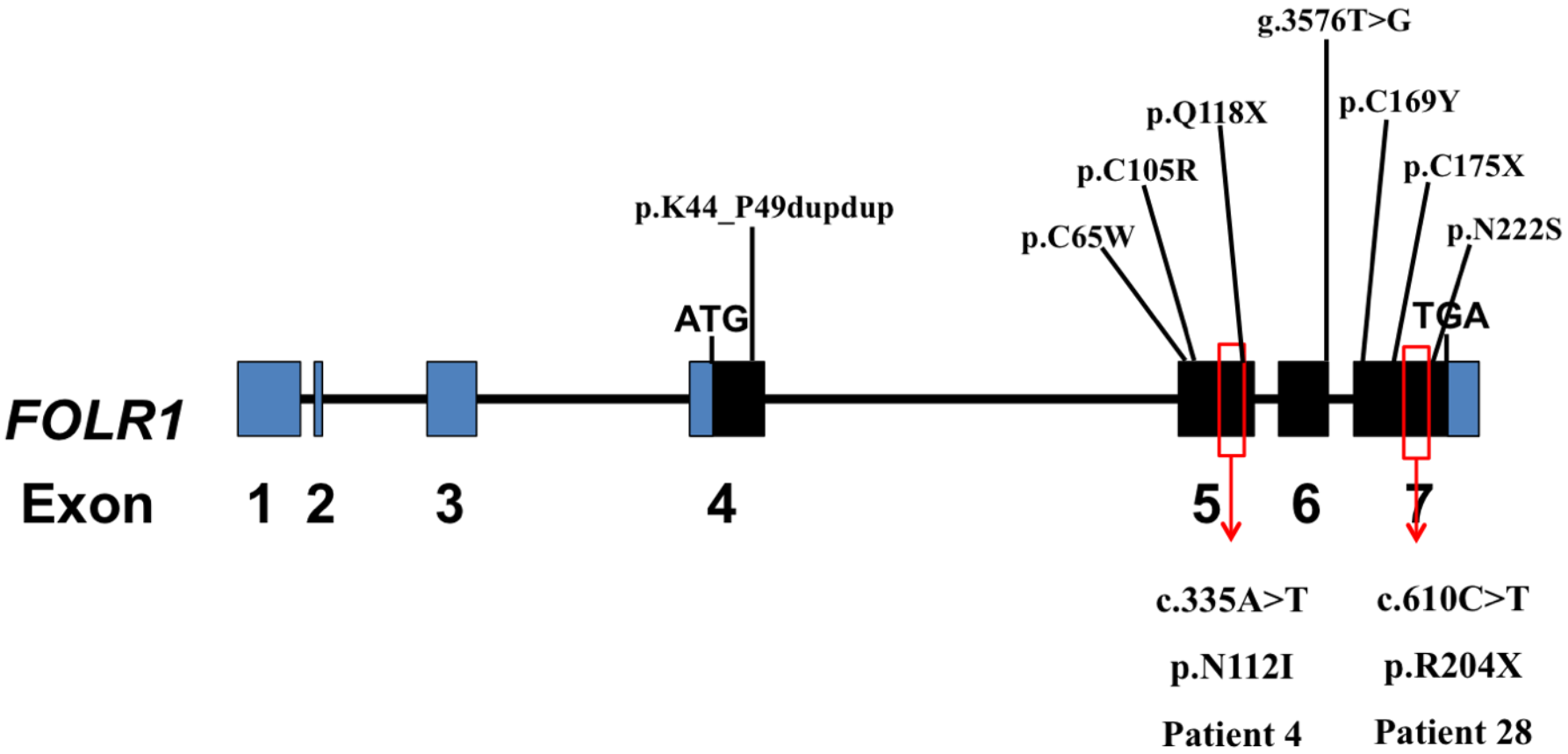


***Figure 24 Genetic organisation of the FOLR1 gene.*** The *FOLR1* gene contains 7 exons in total. Coding exons are represented in black. Mutation analysis of exon and exon-intron boundaries revealed mutations in Patient 4 and Patient 28, as indicated. Mutations represented above the figure have been previously reported (Grapp et al. 2012). Types of mutation, p.K44_P49dup = duplication, p.C65W = missense, p.C105R = missense, p.Q118X = nonsense, g.3576T>G = splice site, p.C169Y = missense, p.C175X = nonsense, p.N222S = missense. Amino acid abbreviations, K = lysine, P = proline, C = cysteine, W = tryptophan, R = arginine, Q = glutamine, X = stop, Y = tyrosine, N = asparagine, S = serine, I = isoleucine. Nucleotide bases abbreviations, A = adenine, T = thymine, C = cytosine, G = guanine, p = protein, g = genomic, c. = complementary.

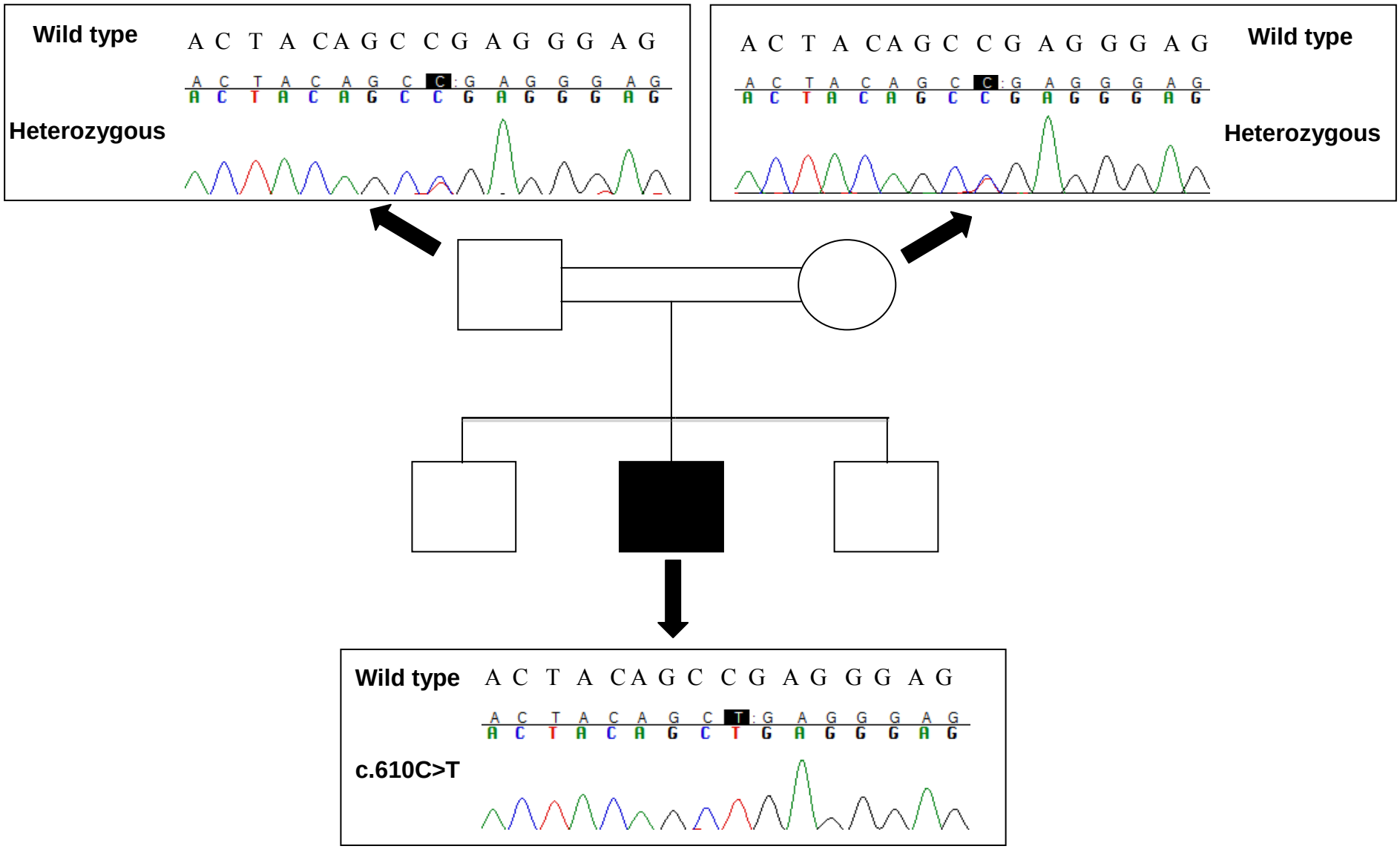


***Figure 25 Family pedigree of Patient 28 and electropherograms showing sequencing results of FOLR1 exon 7.*** The c.610C>T is homozygous in Patient 28 (black square). The consanguineous parents are heterozygous for the mutation (square = father, circle = mother).

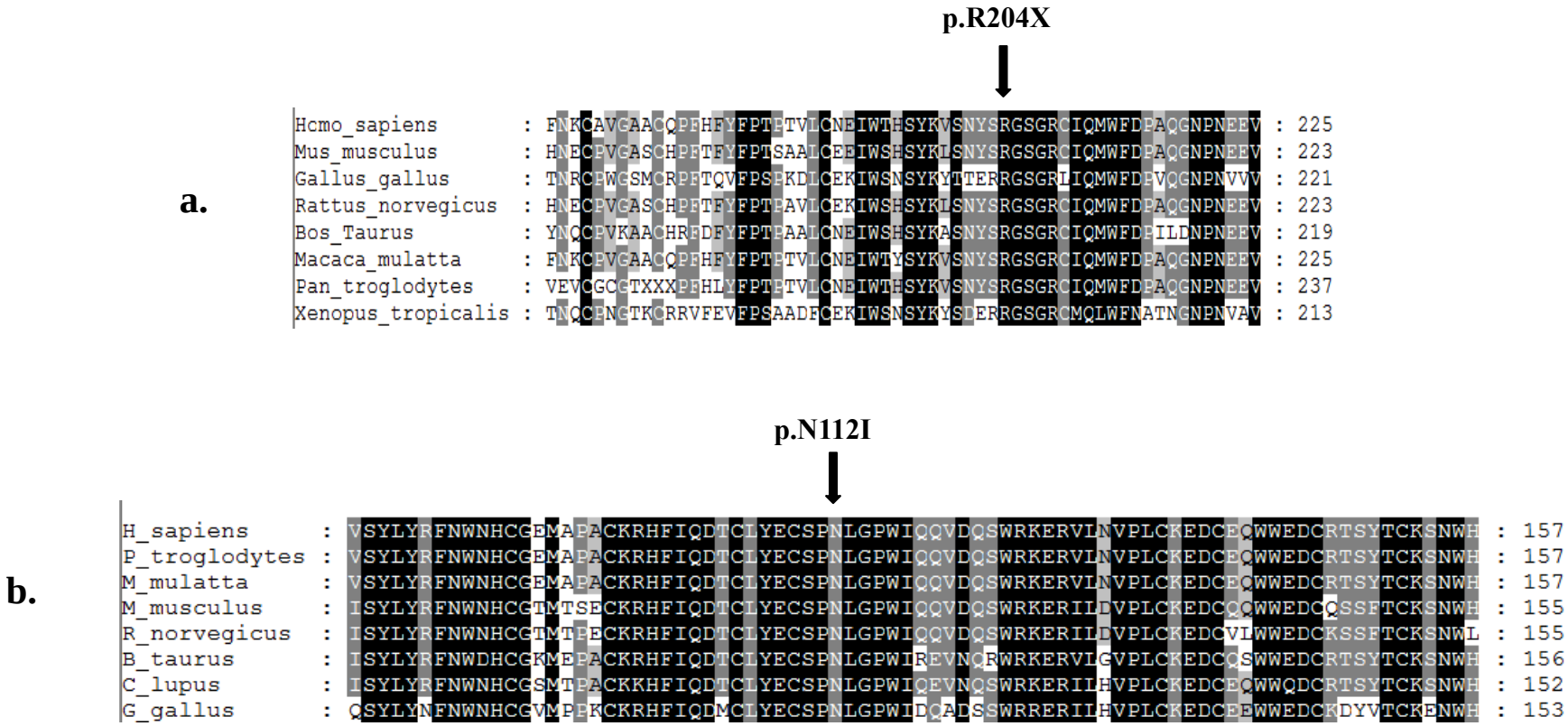


***Figure 26 FOLR1 evolutionary conservation.*** The R204 (a.) and N112 (b.) residues in exons 7 and 5, respectively, are highly conserved across species. This suggests that the R204X stop mutation and the N112I amino acid change are likely to be pathogenic and have significant functional impacts.

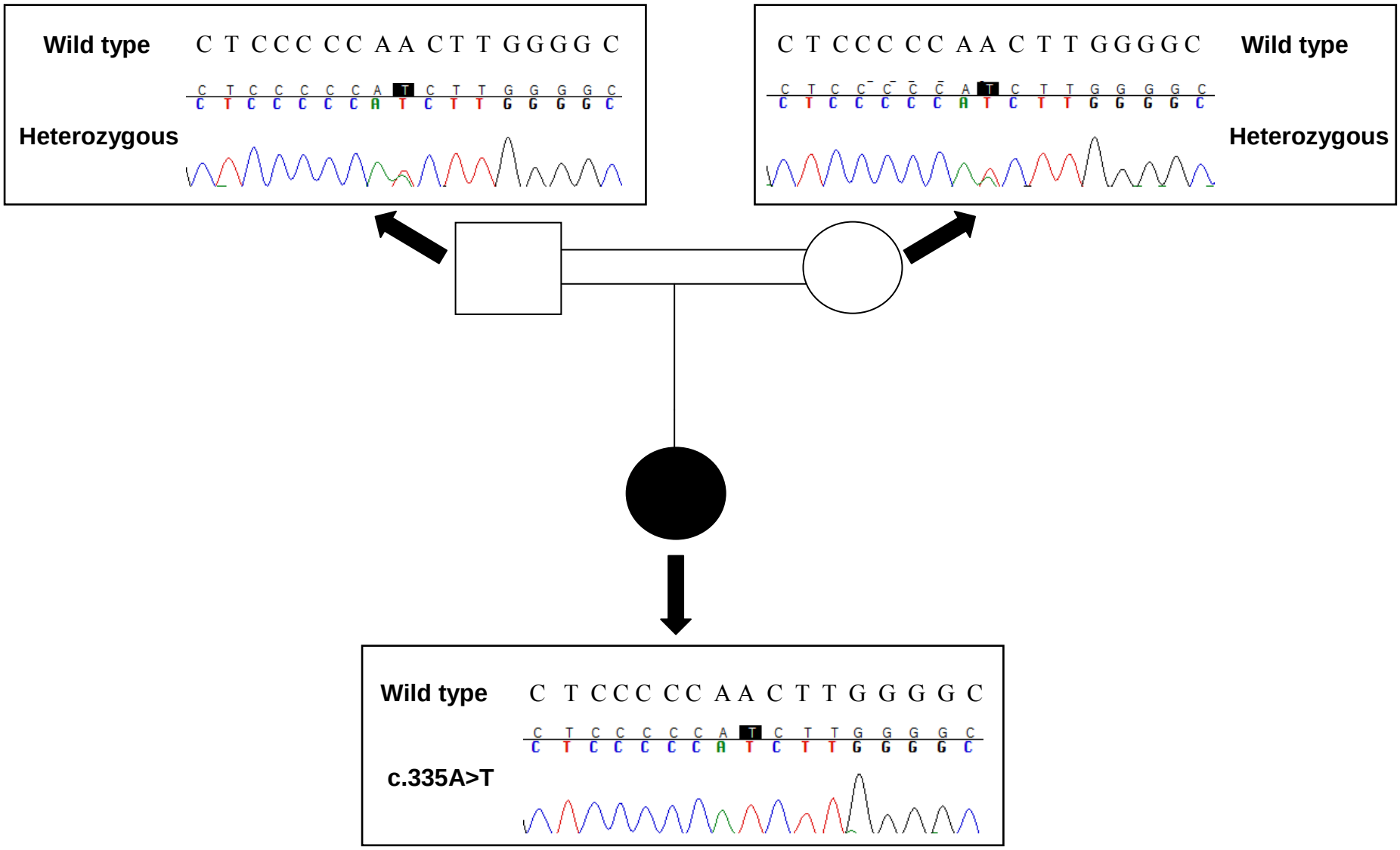


***Figure 27 Family pedigree of Patient 4 and electropherograms showing sequencing results of FOLR1 exon 5.*** The c.335A>T is homozygous in Patient 4 (black circle). The consanguineous parents are heterozygous for the mutation (square = father, circle = mother).

32 had KSS, Patient 24 had previously reported *PCFT* mutations (Paul et al., 2011). Taken together, the most profound CSF 5-MTHF deficiencies were observed in patients with KSS (n=4) and in those harbouring *FOLR1* mutations (n=2) or *PCFT* mutations (n=1). CFD was milder (29 nmol/L) in the patient with *POLG* mutations.

#### 3.5.1.3 FRα protein modelling of the novel *FOLR1* homozygous missense mutation (c.335A>T; p.N112I) documented in this Chapter and the known mutations in the FRα

The novel *FOLR1* homozygous missense mutation (c.335A>T; p.N112I) documented in this Chapter (see section 3.5.1.2), as well as the known missense mutation resulting in an amino acid change from asparagine to serine at position 222 (p.N222S), were shown to be located in a region of the FR-α near the membrane (Figure 28). The remaining known mutations were shown to be located near the binding pocket of the FR-α (Figure 28). Nonsense mutations are not shown since these mutations do not result in protein expression. The g.3576T>G mutation is not shown since this mutation is located in an intron (Grapp et al. 2012).

#### 3.5.1.4 Clinical features and brain MRI/CT imaging

All patients with low CSF 5-MTHF shared a heterogeneous clinical phenotype, with no single patient exhibiting all the symptoms considered distinctive for CFD (Ramaekers et al., 2002). Seizure disorder, movement disorder and developmental delay and/or regression were the most common clinical features in these patients (Table 8). Brain MRI/CT imaging showed no clear correlations with CFD. For specific diagnoses such as KSS, where there were brain MRI/CT imaging findings, these were consistent with those previously described in the literature for mitochondrial disease (Serrano et al., 2010). In other situations, the findings were either normal or non-specific.

#### 3.5.1.5 Total serum folate data

Total serum folate concentrations were obtained for 19 of the 32 patients with decreased CSF 5-MTHF (Table 8). Patients 2, 11, 12 and 30 had total serum folate concentrations within the age and sex-specific reference ranges, whilst Patient 24 had a total serum folate concentration below the age and sex-specific reference range. The remaining patients had concentrations above the respective reference ranges. In some of these cases, total serum folate concentrations were recorded at the upper limit of detection for the assay.

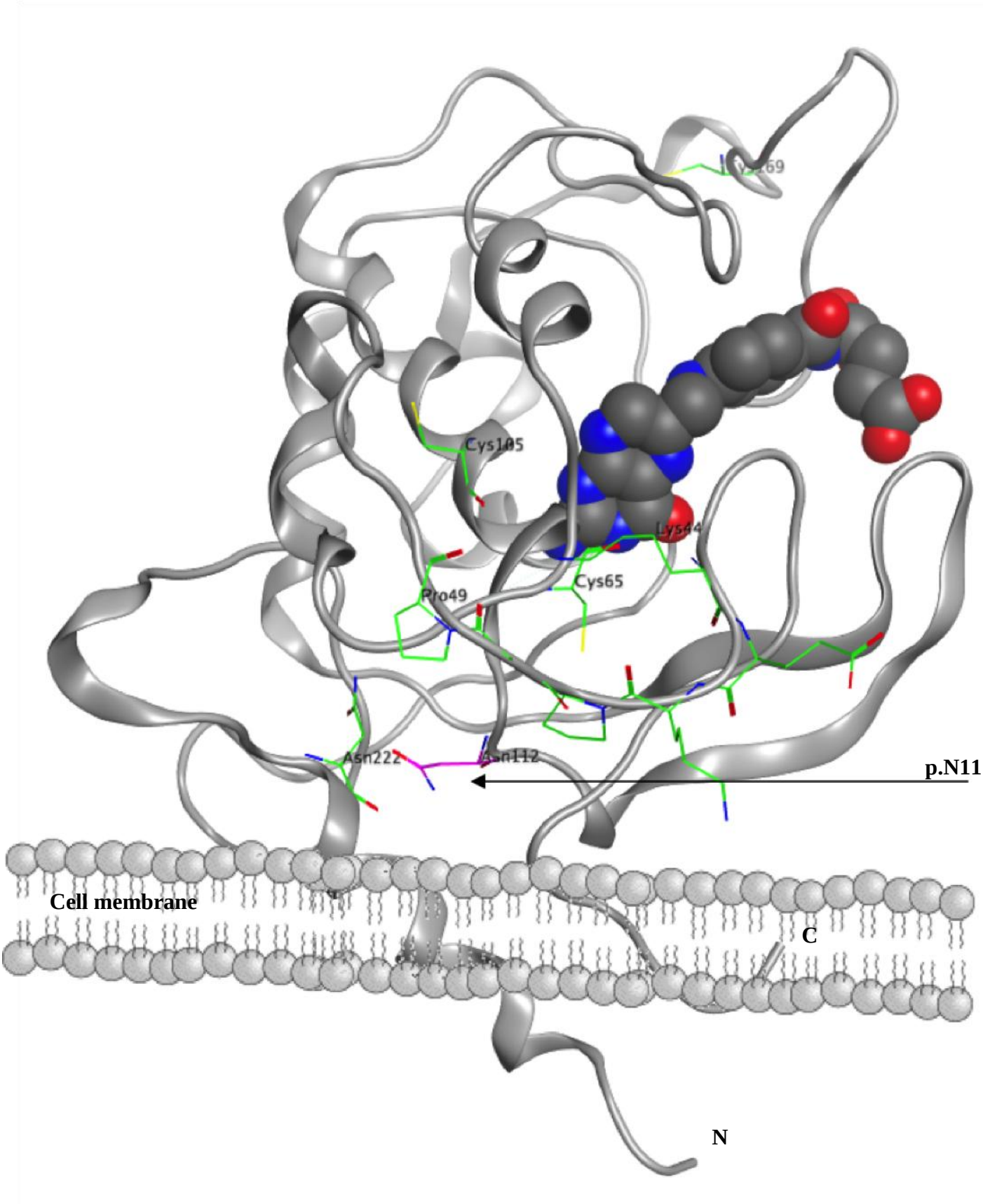


***Figure 28 Three dimensional model of the FRα protein based on the known crystal structure in complex with folic acid showing the novel FOLR1 homozygous missense mutation (c.335A>T; p.N112I) documented in this Chapter and the known mutations in the FRα.*** The novel mutation is represented in pink (arrow), whilst the known mutations are represented in green. Folic acid is in the binding pocket (spacefill). Grey represents carbon, blue represents nitrogen, red represents oxygen and yellow represent sulphur. N terminus = amine (-$NH_2$) terminus, C terminus = carboxyl (-COOH) terminus, Asn/N = asparagine, Pro = proline, Lys = lysine, Cys = cysteine.

#### 3.5.1.6 Effect of anti-epileptic drugs on the levels of CSF 5-MTHF in children receiving treatment

Antiepileptic drugs (AEDs), notably sodium valproate, carbamezapine and phenytoin, have been reported to impair the active transport of 5-MTHF across the blood-CSF barrier from the periphery into the CSF (Opladen et al., 2010). From the group of 32 patients with suspected mitochondrial disease who had low CSF 5-MTHF concentration, 12 had received AEDs. However, there was no difference in CSF 5-MTHF levels between the 12 patients treated with AEDs and the 20 patients not on AEDs (Figure 29). The impact of specific AEDs on CSF 5-MTHF availability was not determined owing to small sample size for individual AEDs.

### 3.5.2 No correlation between CSF 5-MTHF and mitochondrial RCE activity in skeletal muscle

To study the relationship between skeletal muscle mitochondrial RCE activity and CSF 5-MTHF concentration, a potential correlation between skeletal muscle mitochondrial RCE activity and corresponding CSF 5-MTHF concentrations in patients with an isolated RCE defect, was tested. No correlation was observed between isolated complex I deficiency (n=6) or isolated complex IV deficiency (n=37) and CSF 5-MTHF concentration (Figure 30a and Figure 30b). Sample size was too small (n=2) to test for correlation between isolated complex II/III deficiency and CSF 5-MTHF concentration.

### 3.5.3 Biochemical response to folinic acid supplementation in patients with low CSF 5-MTHF

Serial lumbar puncture and CSF 5-MTHF analysis was performed in four patients who were treated with folinic acid supplementation (Patients 4, 9, 25 and 28). Patients 9, 25 and 28 demonstrated a good biochemical response to treatment with increase of CSF 5-MTHF to within the respective age-related reference range (Figure 31a). However, after 11.6 months of therapy, CSF 5-MTHF was not yet restored to within the age-related reference range in Patient 4 (Figure 31a). Disease progression was observed in Patient 32. This patient presented with Pearson syndrome (transfusion dependent sideroblastic anaemia and neutropaenia) at 2.4 years. Initial lumbar puncture at 2.4 years demonstrated a normal CSF 5-MTHF concentration of 142 nmol/L (52-178). The patient's clinical phenotype progressed from Pearson syndrome to KSS and repeat lumbar puncture at 6.5 years revealed a CSF 5-MTHF concentration of <10 nmol/L (72-172) (Figure 31b).

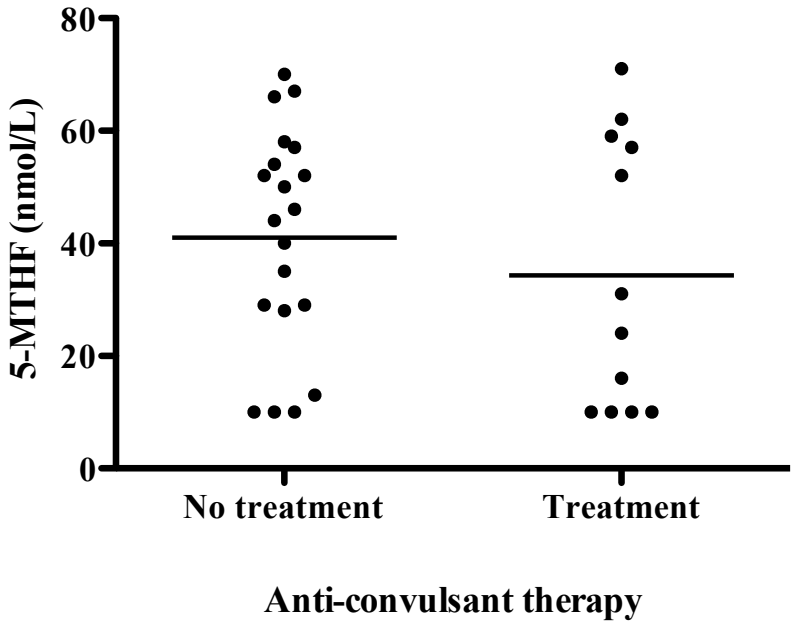


***Figure 29 Individual comparison of mean CSF 5-MTHF concentrations between patients not receiving/receiving anti-convulsant therapy.*** No significant difference between the two groups was observed, determined by Student's t-test.

**a.**

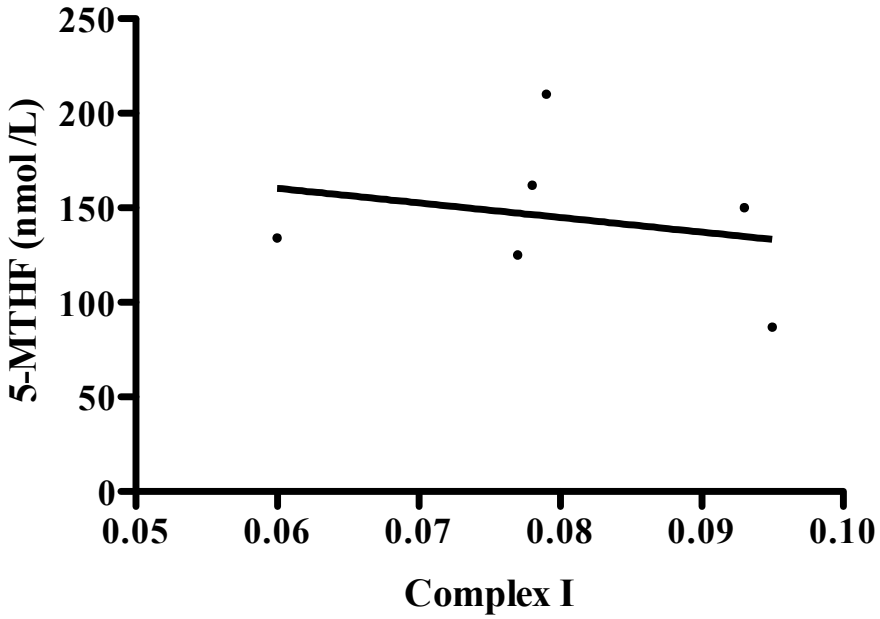


**b.**

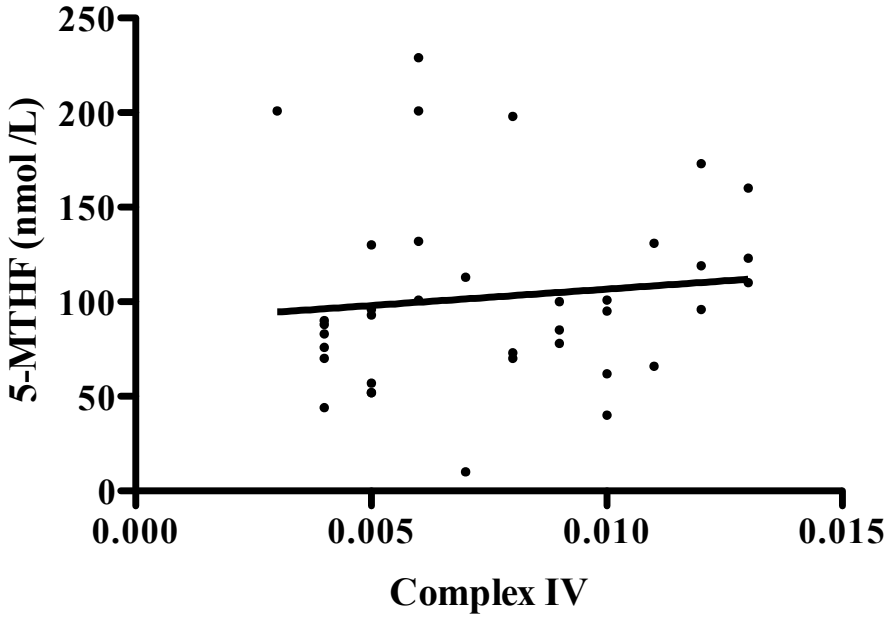


***Figure 30 No correlation between CSF 5-MTHF and skeletal muscle RCE activity.*** A correlation could not be demonstrated for **a.** Complex I deficient patients (r=-0.24; p=0.65; n=6), or **b.** complex IV deficient patients (r=-0.03; p=0.89; n=29).

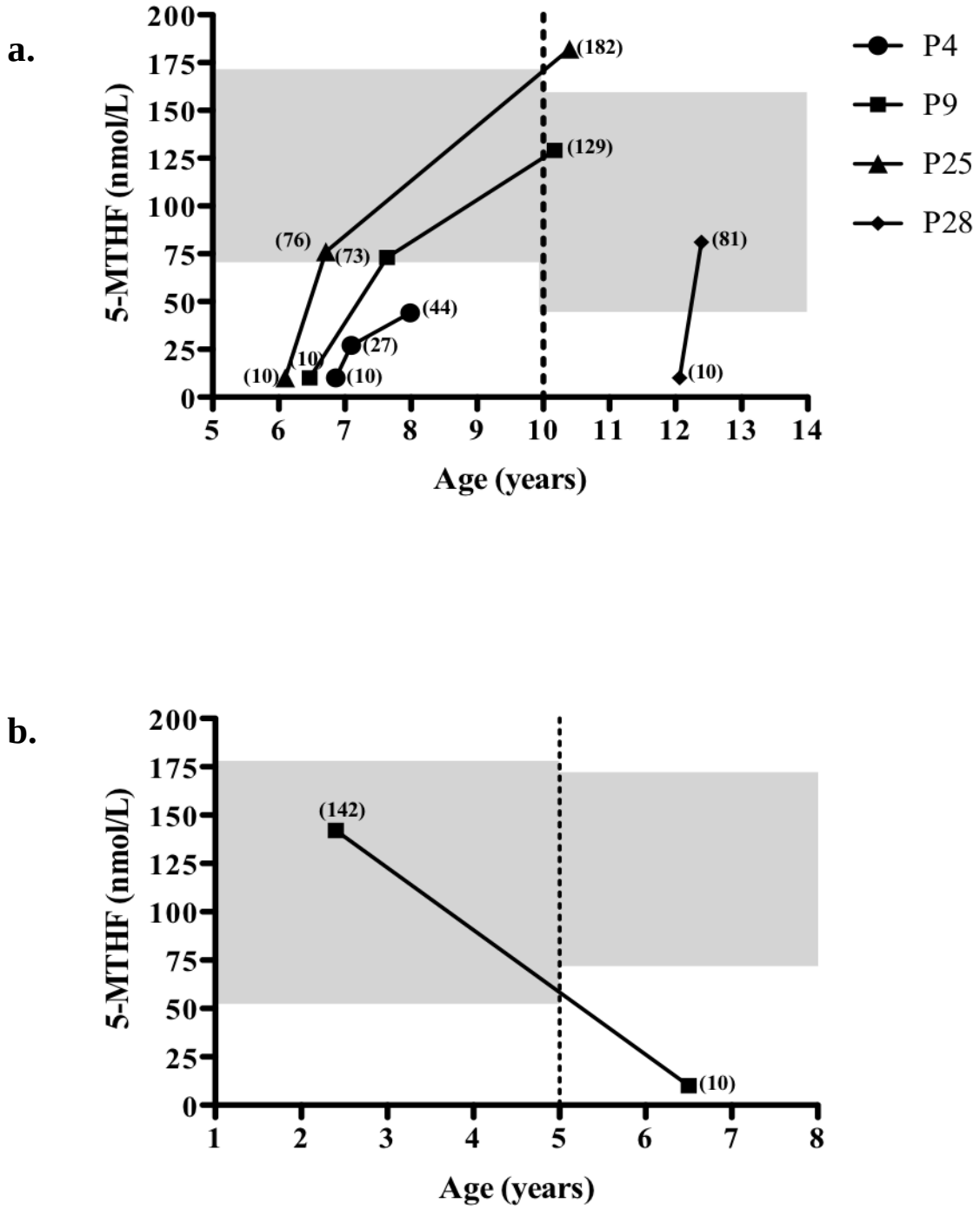


***Figure 31 Biochemical responses of patients with low CSF 5-MTHF on folinic acid supplementation who had serial lumbar punctures.*** **a.** The shaded areas represent the age related reference range for 5-MTHF at the time of sampling; 72-172 nmol/L (5-10 years), 46- 160 nmol/L (10 years-adult). Individual 5-MTHF values (nmol/L) are in brackets. Oral folinic acid supplementation dose (mg/kg/day) at each subsequent CSF 5-MTHF measurement; Patient 4 = 1.2, 5.0 + 6.25 (intravenously); Patient 9 = 0.9, 1.4; Patient 25 = 1.1, 1.5; Patient 28 = 1.7. **b.** Decrease in CSF 5-MTHF concentration in Patient 32 who initially presented with Pearson syndrome and whose disease progressed to KSS. The shaded areas represent the age-related reference range for 5-MTHF at the time of sampling; 52-178 nmol/L (2-5 years), 72-172 nmol/L (5-10 years). Individual 5-MTHF values (nmol/L) are in brackets. Patient 32 is now receiving folinic acid supplementation at a dose of 1.0 mg/kg/day.

## 3.6 Discussion

In this Chapter, data from a large cohort of paediatric patients with a suspected mitochondrial disease, in whom both a skeletal muscle biopsy for mitochondrial RCE analysis and CSF 5-MTHF analysis was performed, were collated from the central pathology database at Great Ormond Street Hospital, London, UK. Although CFD was first noted in a patient with KSS in 1983 (Allen et al., 1983), from the available literature and current knowledge, this is the first study to systematically document prevalence of CSF 5-MTHF deficiency in a large cohort of patients with suspected or proven mitochondrial disease investigated in a single centre. In this cohort, the prevalence of CSF 5-MTHF deficiency in suspected mitochondrial disease patients was 15%. In addition, the prevalence of CSF 5-MTHF deficiency was also 15% in those patients who had biochemically confirmed skeletal muscle mitochondrial RCE deficiency. From this data it can be extrapolated that, based on a birth prevalence for mitochondrial disease of one in 5000 (Thorburn, 2004), the minimum population prevalence of mitochondrial disease with CSF 5-MTHF deficiency is approximately one in 30,000, suggesting that CSF 5-MTHF deficiency in mitochondrial disease is not as rare as initially anticipated.

Severity of CSF 5-MTHF deficiency was variable in the cohort, but the most profound CSF 5-MTHF deficiencies were seen in patients with KSS caused by single large-scale mtDNA deletions (Patients 9, 11, 25 and 32), those with mutations in the *FOLR1* gene encoding FRα (Patients 4 and 28), and in Patient 24 who had a mutation in the *PCFT* gene. KSS manifests as external ophthalmoplegia, pigmentary retinopathy, ataxia and aberrant cardiac conduction (Oldfors et al., 1990; Rahman and Hanna, 2009; Zeviani et al., 1988). Oncocytic transformation, comprising cellular enlargement and granular eosinophilic cytoplasm, of choroid plexus cells has been observed in KSS, possibly because of accumulation of mutated mtDNA in these cells leading to decreased ATP production (Spector and Johanson, 2010; Tanji et al., 2000). Choroid plexus cells are involved in the production of CSF at the blood-CSF barrier (Bering, 1955; Milhorat, 1969; Speake et al., 2001). Therefore, choroid plexus dysfunction may explain the severe CFD observed in KSS patients. Similarly, impaired folate transport across choroid plexus cells may also represent the cause of the severe CFD observed with *FOLR1* mutations (Cario et al., 2009; Steinfeld et al., 2009), since FRα is responsible for active transport of 5-MTHF across choroid plexus cells from the peripheral circulation into CSF (Grapp et al.,

2013). In this cohort, two patients with severe CSF 5-MTHF deficiency (<10 nmol/L) had *FOLR1* mutations: a novel homozygous missense mutation in exon 5 (c.335A>T; p.N112I), and a homozygous nonsense mutation in exon 7 (c.610C>T; p.R204X), which was previously reported to be pathogenic (Dill et al., 2011; Grapp et al., 2012). Both sets of healthy consanguineous parents were found to be carriers for the respective mutations. Regarding the former novel *FOLR1* mutation, the asparagine at position 112 was found to be conserved throughout evolution and both consanguineous parents were heterozygous for the mutation, suggesting that this missense mutation is pathogenic and responsible for the severe CSF 5-MTHF deficiency observed in this patient. The clinical heterogeneity of patients with CFD and the lack of aetiological diagnosis in the majority of cases, suggests that *FOLR1* sequence analysis should be performed in all patients with CSF 5-MTHF values <10 nmol/L in the absence of peripheral folate deficiency.

Patient 24 has previously been reported in the literature to have compound heterozygous mutations in the *PCFT1* gene (Paul et al., 2011). Briefly, a mutation in exon 2 (c.1004C>A; p.A335D) was inherited from the heterozygous father whilst the heterozygous mother contributed an allele with deletion of two nucleotides in exon 1 that caused a frameshift starting at position N68 with early termination of translation (c.204-205delCC). PCFT is responsible for intestinal absorption of 5-MTHF from the diet and transport of 5-MTHF from the blood into the CSF (Urquhart et al., 2010; Zhao et al., 2009a). Therefore, mutations in the *PCFT1* gene cause hereditary folate malabsorption leading to global 5-MTHF deficiency (Shin et al., 2011). These patients present with CSF 5-MTHF concentrations <10 nmol/L and low peripheral folate levels, as demonstrated in Patient 24. Global 5-MTHF deficiency should be considered as an indicator of a potential mutation in the *PCFT1* gene and *PCFT1* mutation analysis should be carried out in patients with similar biochemical presentations. In view of the global 5-MTHF deficiency and according to the definition (Ramaekers and Blau, 2004), patients with mutations in this gene are not wholly considered to have CFD.

Deficiency of complex IV was the most common mitochondrial RCE defect in patients with CSF 5-MTHF deficiency in the cohort. This is in contrast to the findings of other groups who have reported abnormalities in other mitochondrial RCE complexes in CFD patients (Garcia-Cazorla et al., 2008; Pineda et al., 2006; Ramaekers et al., 2007c). This could partly be explained by a CFD diagnosis

superseding the need for a skeletal muscle biopsy and subsequent biochemical mitochondrial RCE analysis. Seven out of the eight patients with complex IV deficiency had mild-moderate CSF 5-MTHF deficiency, suggesting the deficiency is secondary to the complex IV defect, with the exception of patient 28 who had severe CSF 5-MTHF deficiency and a homozygous *FOLR1* mutation. From the available literature and current knowledge, this is the first time mitochondrial RCE activity has been measured and isolated complex IV deficiency documented in a patient with a confirmed *FOLR1* gene mutation. It is unclear whether the complex IV deficiency is secondary to the *FOLR1* mutations in this patient, or whether he may have a second recessive disorder, since the coexistence of two recessive disorders is not uncommon in consanguineous pedigrees (Bittles et al., 1991; Hamamy, 2012). Taken together, mitochondrial RCE defects in patients with CFD cannot be predicted from CSF 5-MTHF data and vice versa, highlighting the importance of performing both a skeletal muscle biopsy and lumbar puncture in patients with suspected mitochondrial disease. This may be especially appropriate in patients with CSF 5-MTHF <10 nmol/L who have suspected or confirmed *FOLR1* mutations. These suggestions are supported by the lack of correlation between CSF 5-MTHF values and the degree of mitochondrial RCE deficiency measured in skeletal muscle, although relatively low n numbers were used for analysis. Nevertheless, in view of this lack of correlation, other mechanisms arising from loss of mitochondrial function need to be considered, for example oxidative stress leading to increased 5-MTHF catabolism, which is investigated in the following Chapters (Aylett et al., 2013).

In two patients, genetically confirmed mitochondrial disease was associated with CSF 5-MTHF deficiency but normal mitochondrial RCE activity. In one case (Patient 25), this could be explained by the mtDNA deletion being heteroplasmic and therefore, the patient had enough wild type mtDNA to compensate. The other case (Patient 13), had *POLG* mutations with a predominantly CNS phenotype and very low levels of multiple mtDNA deletions in skeletal muscle.

FRα protein modelling of the novel *FOLR1* homozygous missense mutation (c.335A>T; p.N112I) documented in this Chapter and the known mutation resulting in an amino acid change from asparagine to serine at position 222 (Grapp et al., 2012), showed that these changes were located in two separate regions of the FRα near to the membrane. This could suggest that the interaction between the receptor

and the membrane may be affected. For example, the receptor may not be anchored to the membrane sufficiently or receptor-mediated endocytosis (see section 1.4.3) may not function properly. The remaining known mutations were shown to be located near to the binding pocket of the FRα. This could suggest that folate binding to the receptor could be affected. For example, folate may not bind to the binding pocket at all (loss of the formation of a ligand/receptor complex) or folate may bind weakly within the binding pocket but not sufficiently enough to activate the receptor.

The clinical heterogeneity associated with CSF 5-MTHF deficiency, including that associated with proven mitochondrial diseases (Garcia-Cazorla et al., 2008; Hasselmann et al., 2010; Pineda et al., 2006; Serrano et al., 2010), is demonstrated in Table 8. Seizure disorder, movement disorder and developmental delay and/or regression were the most common clinical features. However, no patient exhibited all the symptoms considered distinctive for CFD (Ramaekers et al., 2002), suggesting that it is important to measure CSF 5-MTHF in all patients at risk of CFD, rather than relying on clinical manifestations. With regard to the neuroimaging data, an apparent association between the degree of CSF 5-MTHF and the severity of lesions was observed. Patients who presented with normal scans had CSF 5-MTHF deficiencies within the mild-moderate range, whereas, patients with severe CSF 5-MTHF deficiencies were typically more affected than others. In general, the majority of patients presented with delayed myelination and/or leukodystrophy, which were more evident at different stages of disease progression.

Total serum folate was documented for 19 out of 32 patients with decreased CSF 5-MTHF concentrations (Table 8). CFD could be could be confirmed in four patients who had total serum folate concentrations within the age and sex-specific reference ranges, indicating the absence of a periphery nutritional folate deficiency (Ramaekers and Blau, 2004; Ramaekers et al., 2002). However, a peripheral nutritional folate deficiency was noted in Patient 24 who had *PCFT* mutations, which confirmed global folate deficiency characteristic of patients with *PCFT* mutations (Paul et al., 2011; Shin et al., 2011). Total serum folate concentrations in the remaining patients were above the age and sex-specific reference ranges and, in some cases, at the upper limit of detection for the assay. Whilst CFD could also be confirmed in these patients, possible explanations for these high peripheral folate levels could include: parental administration of vitamin supplements, or empirical treatment with folinic acid treatment by a clinician owing to the patient's potential

risk of developing CFD and/or the patient's clinical presentation. It is critically important for concurrent blood samples and lumbar punctures to be taken and subsequent analysis of 5-MTHF in these samples, in order to diagnostically confirm CFD. In those patients where a total serum folate measurement was absent, only a CSF 5-MTHF deficiency may be inferred.

Seizures are a common clinical feature in patients with CFD and mitochondrial disease (Lee et al., 2011; Rahman, 2012). Treatment with AEDs including sodium valproate, carbamazepine and phenytoin has been reported to reduce *FOLR1*-mediated uptake of 5-MTHF from the periphery into CSF in cell model systems (Opladen et al., 2010). In this cohort, 38% of patients were treated with AEDs. However, no difference in CSF 5-MTHF concentration was observed between patients not receiving and receiving AEDs, indicating that these findings do not necessarily support the work of Opladen et al. (2010). However, this could be accounted for by the lack of data regarding the impact of specific AEDs on CSF 5-MTHF availability since the sample size for individual AEDs was too small. It also cannot be ruled out that anticonvulsant treatment may have contributed to the decreased CSF 5-MTHF concentrations in this group of patients.

Recognition and prompt diagnosis of CFD is of paramount importance since CFD is treatable in patients with a primary deficiency (Cario et al., 2009; Grapp et al., 2012; Steinfeld et al., 2009) and is one potentially treatable aspect of disease in patients with mitochondrial disorders (Garcia-Cazorla et al., 2008; Grapp et al., 2012; Moretti et al., 2005; Pérez-Dueñas et al., 2011). Positive clinical response to folinic acid treatment has previously been reported in the literature (Hasselmann et al., 2010; Pérez-Dueñas et al., 2010; Pineda et al., 2006; Serrano et al., 2012). However, from the available literature and current knowledge, this is the first report of serial CSF 5-MTHF measurements demonstrating biochemical improvement in CSF 5-MTHF status in multiple patients with KSS or *FOLR1* gene mutations receiving folinic acid supplementation. Therapeutic benefit of folinic acid and restoration of CSF 5-MTHF values to within the age-related reference range was demonstrated in both KSS (n=2) and in one patient with a *FOLR1* mutation (n=1). Specifically for KSS, empirical treatment with folinic acid to all paediatric patients with single large mtDNA deletions may be beneficial. This recommendation is supported by the observation that the onset of CFD may be associated with disease progression from Pearson syndrome to KSS as demonstrated by the serial CSF 5-MTHF

concentrations in Patient 32. From the available literature and current knowledge, this is the first report documenting progressive loss of CSF 5-MTHF. CSF 5-MTHF levels have not yet been restored to within the age-related reference range in Patient 4 despite ongoing folinic acid supplementation. The folinic acid dosing regimen in this patient is currently being escalated. Biochemical improvement in patients with a CSF 5-MTHF deficiency following folinic acid supplementation further illustrates the importance of performing lumbar punctures and measuring CSF 5-MTHF. Whilst it is essential to explore all therapeutic options for patients on an individualised basis, it is critically important to identify those patients with a treatable element to their disease.

### 3.7 Conclusion

In conclusion, from the cohort described here, a minimum population prevalence of mitochondrial disease with CSF 5-MTHF deficiency is approximately one in 30,000, suggesting that CSF 5-MTHF deficiency may be more common in patients with RCE defects than was initially appreciated. A lack of aetiological diagnosis was observed in the majority of cases. Profound CSF 5-MTHF deficiencies may be associated with defects in 5-MTHF transport across the blood-CSF barrier, including KSS and in patients with a *FOLR1* mutation or *PCFT1* mutation. Concerning patients with a *FOLR1* mutation, the data suggests that *FOLR1* mutation analysis should be a priority in patients with CSF 5-MTHF <10 nmol/L in the absence of peripheral folate deficiency. Importantly, in patients with mitochondrial RCE abnormalities, the degree of CSF 5-MTHF deficiency cannot be predicted and vice versa. This emphasises the importance of performing a skeletal muscle biopsy and lumbar puncture, and carrying out the appropriate analyses in those patients suspected of having a mitochondrial disease. Patients with decreased CSF 5-MTHF concentrations had heterogeneous clinical presentation, including brain MRI/CT imaging, suggesting that CSF 5-MTHF analysis may be of critical importance as opposed to relying on clinical manifestations. To confirm CFD, it is critically important to take a concurrent blood sample for total serum folate analysis at the time of lumbar puncture. In this cohort, anti-convulsant therapy was not associated with severity of CSF 5-MTHF deficiency. The biochemical improvement of CSF 5-MTHF deficient patients receiving folinic acid supplementation further highlights the importance of identifying these patients and commencing a treatment regimen as early as possible.

# Chapter 4
# The effect of hydroxyl radicals or selenite on 5-MTHF stability in CSF and the ability of AA to confer protection of 5-MTHF.

# 4. The effect of hydroxyl radicals or selenite on 5-MTHF stability in CSF and the ability of AA to confer protection of 5-MTHF.

## 4.1 Introduction

The study described in Chapter 3 suggests that CSF 5-MTHF deficiency may represent an under-recognised, potentially treatable condition in patients with mitochondrial disease. A lack of aetiological diagnosis was observed in the majority of cases and mitochondrial RCE defects in patients with decreased CSF 5-MTHF could not be predicted from the CSF 5-MTHF data. This work highlights the importance of elucidating the molecular mechanisms responsible for CFD associated with mitochondrial disease in order to gain an understanding of disease pathogenesis. As discussed in section 1.6, the mechanisms responsible for secondary CFD associated with a subset of patients with mitochondrial disease, are not known. Several groups have postulated that CFD in mitochondrial disease may be explained by defective transport of 5-MTHF across the epithelial cells of the choroid plexus from the periphery into CSF (Hyland et al., 2010; Opladen et al., 2010; Pérez-Dueñas et al., 2011; Tanji et al., 2000). However, there is a lack of sufficient evidence supporting these mechanisms, suggesting that other mechanisms may be accountable.

5-MTHF is susceptible to oxidative catabolism in the presence of oxidising species (see section 1.4.1) (Blair et al., 1975; Heales et al., 1988; Lam and Heales, 2007). Consequently, in situations where ROS formation is increased, accelerated catabolism of 5-MTHF may ensue, thereby contributing to a CFD state. The mitochondrial RC is considered to be the most important quantitative source of cellular ROS (Boveris and Chance, 1973; Boveris et al., 1972; Loschen and Azzi, 1975) and dysfunction of the mitochondrial RC is associated with an increase in ROS production (see sections 1.1.3 and 1.6.2) (Jacobson et al., 2005; Sipos et al., 2003). Thus, induction of oxidative stress, represented by an imbalance between ROS generation and antioxidant availability, could provide a mechanistic link between mitochondrial disorders and CFD.

In addition to dysfunction of the mitochondrial RC, abnormal biochemical parameters may also lead to increased ROS generation. Specifically, in six KSS patients with secondary CFD, elevated CSF selenium concentrations were reported (Tondo et al., 2011). However, selenium was not implicated as a factor responsible

for CFD in these patients and the data were not correlated to 5-MTHF availability in this study. Selenium toxicity has previously been associated with increased ROS generation, as a consequence of redox-cycling of selenide with reduced thiols, for example GSH (see section 1.6.2.1) (Chen et al., 2007b; Tarze et al., 2007; Yan and Spallholz, 1993). Therefore, elevated CSF selenium concentrations could promote ROS production and accelerate breakdown of 5-MTHF.

As well as the generation of ROS, antioxidant availability is an additional factor governing induction of oxidative stress. In a paper by Spector and Johanson (2010), AA was predicted to be low in concentration in the CSF of patients with CFD. In the context of CFD, it is of interest to note that AA is also actively transported from the periphery into CSF across the choroid plexus (Harrison and May, 2009; Verlinde et al., 2008) and is prone to oxidation due to its antioxidant properties (see section 1.6.2.2) (Regoli and Winston, 1999; Winston et al., 1998). However, regarding the latter, at low concentrations, AA may function in a pro-oxidant manner (see section 1.6.2.2) (Buettner and Jurkiewicz, 2010; Fisher and Naughton, 2003). Therefore, a decrease in AA availability and a potential increase in ROS generation could exacerbate oxidative stress and promote oxidative catabolism of 5-MTHF. Thus, AA may represent a factor governing 5-MTHF stability.

In the absence of a peripheral folate deficiency, diagnosis of CFD relies on the measurement of 5-MTHF in the CSF compartment of the CNS (Ormazabal et al., 2006; Ramaekers and Blau, 2004). Therefore, building upon what is currently known from the literature, the susceptibility of 5-MTHF to oxidative catabolism in disease control CSF was examined in this Chapter. In addition, the antioxidant capacity of AA to confer protection of 5-MTHF was assessed.

## 4.2 Aims

1. To determine the stability of endogenous 5-MTHF in disease control CSF in the absence and presence of hydroxyl radicals propagated by the Fenton reaction.

2. To determine the effect of sodium selenite, in the absence and presence of GSH, on endogenous 5-MTHF stability in disease control CSF.

3. To examine the ability of AA to confer protection of 5-MTHF.

### 4.3 Acknowledgement

Part of the work presented in this Chapter has been published (Aylett et al., 2013). I can confirm that all of the work documented was my own.

## 4.4 Materials and Methods

### 4.4.1 Materials

Purchasing details of all materials used throughout this Chapter are described in section 2.1, unless otherwise stated.

### 4.4.2 Patient CSF samples

Patient CSF samples were collected as described in section 2.2.

### 4.4.3 Treatment and buffer solutions

*Hydroxyl radical generating system*

Hydroxyl radicals were propagated by the Fenton reaction as previously described (Heales et al., 1988). Stock solutions of 1 mmol/L EDTA, 1 mmol/L iron (II) sulphate and 5 mmol/L hydrogen peroxide, were prepared fresh for each experiment in either potassium phosphate buffer (pH 7.4) or HPLC grade water as indicated in section 4.5. Hydroxyl radicals were used to study CSF 5-MTHF stability because the brain has a relatively high iron and, to a lesser extent, copper content, for example mitochondrial iron-sulphur clusters, copper centres and haem, and a low free iron binding capacity in CSF (Bleijenberg et al., 1971; Bradbury, 1997; Harrison et al., 1968). Therefore, the production of the hydroxyl radical via the Fenton reaction may be more likely.

*Sodium selenite*

Selenite stock solutions as indicated in section 4.5 were prepared fresh for each experiment in HPLC grade water. Selenite was the selenium compound of choice since selenite is routinely used throughout the literature to study thiol-mediated redox cycling of selenium (Selenius et al., 2008; Wallenberg et al., 2010) and is the most commonly used dietary form (Kim et al., 2007).

*GSH*

GSH stock solutions as indicated in section 4.5 were prepared fresh for each experiment in HPLC grade water.

*5-MTHF*

5-MTHF stock solutions as indicated in section 4.5 were prepared fresh for each experiment in potassium phosphate buffer (pH 7.4).

*AA*

An AA stock solution as indicated in section 4.5 was prepared fresh for each experiment in potassium phosphate buffer (pH 7.4).

*Potassium phosphate buffer*

Potassium phosphate buffer (0.1 M) was prepared by dissolving monopotassium dihydrogen phosphate ($KH_2PO_4$) and dipotassium hydrogen phosphate ($K_2HPO_4$) in HPLC grade water. One part $KH_2PO_4$ was added to two parts $K_2HPO_4$. The solution was mixed and incubated at 30°C for one hour and adjusted to pH 7.4 with either $KH_2PO_4$ or $K_2HPO_4$.

### 4.4.4 Measurement of 5-MTHF

5-MTHF was measured by HPLC as described in section 2.3.

### 4.4.5 Data analysis

Data analyses were carried out as described in section 2.9. Figure 32 is an example of a plot from which the first order rate constant (k) was calculated from the gradient of the slope. The gradient of the slope was determined by performing linear regression analysis of the data (Graphpad Software Inc). Natural log (ln) of 5-MTHF concentration (nmol/L) versus incubation time (min) plots were constructed for each experiment where k was calculated.

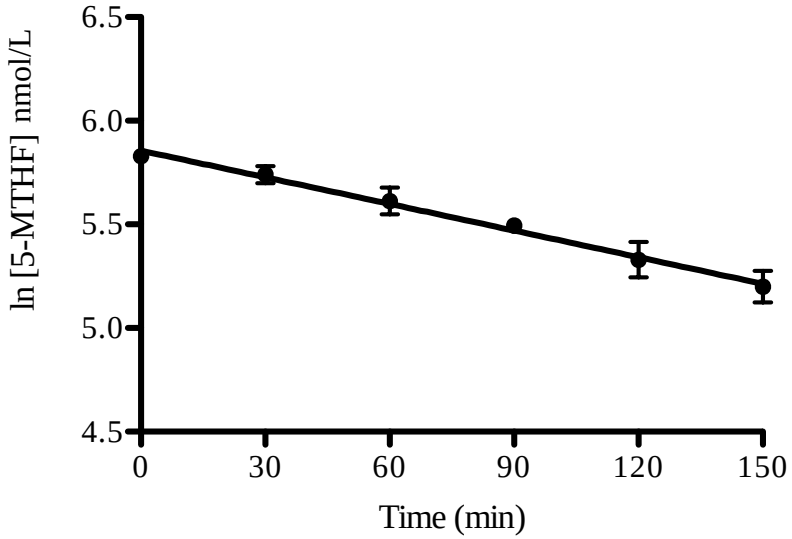


***Figure 32 An example plot from which the rate constant (k) was calculated from the gradient of the slope***. The gradient of the slope was calculated by performing linear regression analysis of the data (Graphpad Softward Inc.).

### 4.5 Experimental protocol

#### 4.5.1 5-MTHF stability in CSF

Pooled disease control patient CSF (n=8) was incubated at +37°C for 30 minute timed intervals, from 0-150 minutes. At each 30 minute time interval, samples (120 µL) were immediately snap frozen in liquid nitrogen and stored at -80°C until analysis of 5-MTHF by HPLC as described in section 2.3. For comparison, the stability of 5-MTHF in potassium phosphate buffer was determined. Samples were prepared by adding 500 uL of 1 µmol/L 5-MTHF (final concentration: 500 nmol/L) or 150 µL of 1 µmol/L 5-MTHF (final concentration: 150 nmol/L) made up in 0.1 M potassium phosphate buffer (pH 7.4), to 500 µL or 850 µL of 0.1 M potassium phosphate buffer, respectively. Samples were mixed and incubated at +37°C for 30 minute timed intervals, from 0-150 minutes. At each 30 minute time interval, samples (120 µL) were immediately snap frozen in liquid nitrogen and stored at -80°C until analysis of 5-MTHF by HPLC as described in section 2.3.

#### 4.5.2 5-MTHF stability in CSF in the presence of a hydroxyl radical generating system

Hydroxyl radicals were propagated by the Fenton reaction (Equation 3). The reaction differs from the original Fenton reaction (see Equation 2) (Fenton, 1894), in that EDTA is also added to the reaction mix. EDTA increases the amount of iron in solution by preventing the formation of $Fe(OH)_3$ and iron oxide precipitates (Pogozelski et al., 1995).

Equation 3: $Fe^{2+}$ (ferrous) + $H_2O_2$ + EDTA → $Fe^{3+}$ (ferric) + $OH^-$ + •OH

Samples were prepared by adding 50 µL of 1 mM EDTA (final concentration in reaction 50 µmol/L) and 50 µL of 1 mM iron (II) sulphate (final concentration in reaction 50 µmol/L) made up in ultrapure water, to 10 µL of 5 mmol/L hydrogen peroxide (final concentration in reaction 50 µmol/L) and 890 µL pooled disease control patient CSF (n=8). Samples were mixed and incubated at +37 °C for 30 minute timed intervals, from 0-150 minutes. At each 30 minute time interval, samples (120 µL) were immediately snap frozen in liquid nitrogen and stored at -80°C until analysis of 5-MTHF by HPLC as described in section 2.3. For

comparison, the stability of 5-MTHF in potassium phosphate buffer in the presence of hydroxyl radicals was determined. Samples were prepared by adding 500 µL of 1 µmol/L 5-MTHF (final concentration: 500 nmol/L) or 150 µL of 1 µmol/L 5-MTHF (final concentration: 150 nmol/L), 50 µL of 1 mmol/L EDTA (final concentration in reaction 50 µmol/L) and 50 µL of 1 mmol/L iron (II) sulphate (final concentration in reaction 50 µmol/L) made up in 0.1 M of potassium phosphate buffer (pH 7.4), to 10 uL of 5 mmol/L hydrogen peroxide (final concentration in reaction 50 µmol/L) and 390 µL or 740 µL of 0.1 M potassium phosphate buffer, respectively. Samples were mixed and incubated at +37 °C for 30 minute timed intervals, from 0-150 minutes. At each 30 minute time interval, samples (120 µL) were immediately snap frozen in liquid nitrogen and stored at -80°C until analysis of 5-MTHF by HPLC as described in section 2.3.

### 4.5.3 5-MTHF stability in CSF in the presence of selenite

Samples were prepared by adding 10 µL of 24 µg/L selenite (final concentration: 2 µg/L) or 10 µL of 240 µg/L selenite (final concentration: 20 µg/L) made up in ultrapure water, to 110 µL of pooled disease control patient CSF (n=8). Control samples were prepared in the absence of selenite. Samples were mixed, incubated at +37°C for 150 minutes (the conditions 5-MTHF is known to be stable for in CSF as determined by experiment 4.5.1), immediately snap frozen in liquid nitrogen and stored at -80°C until analysis of 5-MTHF by HPLC as described in section 2.3.

### 4.5.4 5-MTHF stability in CSF in the presence of GSH and selenite

Samples were prepared by adding 5 µL of 48 µg/L selenite (final concentration: 2 µg/L), 5 µL of 120 µg/L selenite (final concentration: 5 µg/L), 5 µL of 240 µg/L selenite (final concentration: 10 µg/L), 5 µL of 360 µg/L selenite (final concentration: 15 µg/L) or 5 µL of 480 µg/L selenite (final concentration: 20 µg/L) made up in ultrapure water, to 5 µL of 7.2 µM GSH (final concentration 300 nmol/L) made up in ultrapure water and 110 µL of pooled control patient CSF. Control samples were prepared in the absence of GSH and selenite. Samples were mixed, incubated at +37°C for 150 minutes (the conditions 5-MTHF is known to be stable for in CSF as determined by experiment 4.5.1), immediately snap frozen in liquid nitrogen and stored at -80°C until analysis of 5-MTHF by HPLC as described in section 2.3.

### 4.5.5 5-MTHF stability in CSF in the presence of GSH and selenite (40:1)

Samples were prepared by adding 5 μL of 24.0 μmol/L GSH (final concentration: 1.0 μmol/L) and 5 μL of 48 μg/L selenite (final concentration: 2 μg/L) or 5 μL of 62.4 μmol/L GSH (final concentration: 2.6 μmol/L) and 5 μL of 120 μg/L selenite (final concentration: 5 μg/L) or 5 μL of 122.4 μmol/L GSH (final concentration: 5.1 μmol/L) and 5 μL of 240 μg/L selenite (final concentration: 10 μg/L), made up in ultrapure water, to 110 μL of pooled disease control CSF. Control samples were prepared in the absence of GSH and selenite. Samples were mixed, incubated at +37°C for 150 minutes (the conditions 5-MTHF is known to be stable for in CSF as determined by experiment 4.5.1), immediately snap frozen in liquid nitrogen and stored at -80°C until analysis of 5-MTHF by HPLC as described in section 2.3.

### 4.5.6 5-MTHF stability in (i) filtered CSF and (ii) filtered CSF in the presence of GSH and selenite (40:1)

(i) Pooled control patient CSF (n=12) was aliquoted into 10 kDa pore size filter centrifugal eppendorf tubes. Molecules >10 kDa in size would be filtered out of the CSF. Control samples remained unfiltered. Samples were centrifuged for 10 minutes at 14000 rpm. Samples were pooled and incubated at +37°C for 30 minute timed intervals, from 0-150 minutes. At each 30 minute time interval, samples (120 μL) were immediately snap frozen in liquid nitrogen and stored at -80°C until analysis of 5-MTHF by HPLC as described in section 2.3.

(ii) Pooled disease control patient CSF (n=12) was aliquoted into 10 kDa pore size filter centrifugal eppendorf tubes, centrifuged for 10 min at 14000 rpm and pooled. Samples where then prepared and analysed as described in section 4.5.5.

### 4.5.7 5-MTHF stability in potassium phosphate buffer and AA

Samples were prepared by adding 150 μL of 1 μmol/L 5-MTHF (final concentration: 150 nmol/L) and 150 μL of 1 mmol/L AA (final concentration: 150 μmol/L) made up in 0.1 M potassium phosphate buffer (pH 7.4), to 700 μL of 0.1 M potassium phosphate buffer. Control samples were prepared in the absence of AA. Samples were mixed and incubated at +37°C for 30 minute timed intervals, from 0-150 minutes. At each 30 minute time interval, samples (120 μL) were immediately snap

frozen in liquid nitrogen and stored at -80°C until analysis of 5-MTHF by HPLC as described in section 2.3.

### 4.5.8 5-MTHF stability in potassium phosphate buffer in the presence of a hydroxyl radical generating system and AA

Hydroxyl radicals were propagated by the Fenton reaction (Equation 3). Samples were prepared by adding 150 µL of 1 µmol/L 5-MTHF (final concentration: 150 nmol/L), 150 µL of 1 mmol/L AA (final concentration: 150 µmol/L), 50 µL of 1 mmol/L EDTA (final concentration in reaction 50 µmol/L) and 50 µL of 1 mmol/L iron (II) sulphate (final concentration in reaction 50 µmol/L) made up in 0.1 M of potassium phosphate buffer (pH 7.4), to 10 uL of 5 mmol/L hydrogen peroxide (final concentration in reaction 50 µmol/L) and 590 µL of 0.1 M potassium phosphate buffer, respectively. Samples were mixed and incubated at +37 °C for 30 minute timed intervals, from 0-150 minutes. At each 30 minute time interval, samples (120 µL) were immediately snap frozen in liquid nitrogen and stored at -80°C until analysis of 5-MTHF by HPLC as described in section 2.3.

## 4.6 Results

### 4.6.1 5-MTHF is stable in CSF

Reduced pterin molecules, including 5-MTHF, are labile molecules and are susceptible to autoxidation and oxidative attack in the presence of molecular oxygen and oxidising species, respectively (Blair et al., 1975; Heales et al., 1988). In order to determine whether 5-MTHF exhibits similar molecular properties in physiological fluids, the stability of 5-MTHF in CSF was initially determined in pooled disease control patient CSF samples. An endogenous 5-MTHF concentration of 94.4 ± 7.5 nmol/L was recorded at 0 minute. Over the 150 minute incubation period, no significant loss of 5-MTHF was observed compared to 0 minute and 5-MTHF remained relatively stable (Figure 33; Table 9). In contrast, 5-MTHF degraded in potassium phosphate buffer over time. Stability was first determined at an initial 5-MTHF concentration of 500 nmol/L, a concentration within the linearity of the 5-MTHF assay as shown in section 2.3 and comparable to concentrations used in previous studies (Opladen et al., 2006; Ormazabal et al., 2006). A 5-MTHF concentration of 340.1 ± 10.0 nmol/L was recorded at 0 minute. Over time, 5-MTHF progressively decreased in concentration (Figure 34a). An overall significant loss of 46% was observed at 150 minutes, compared to 0 minute ($p<0.01$). In a parallel experiment, the stability of 5-MTHF in potassium phosphate buffer at a more physiological CSF concentration of 150 nmol/L was assessed. This 5-MTHF concentration is within the CSF reference range across all ages (72-305 nmol/L [0-2 years], 52-178 nmol/L [2-5 years], 72-172 nmol/L [5-10 years], 46-160 nmol/L [10 years-adult]). A 5-MTHF concentration of 121.8 ± 3.8 nmol/L was recorded at 0 minute. Over time, 5-MTHF progressively decreased in concentration (Figure 34b). At 150 minutes, an overall significant loss of 25% was observed, compared to 0 minute ($p<0.05$). The decay of 5-MTHF in buffer was found to obey first order kinetics over the 150 minute time period analysed (Table 9).

### 4.6.2 5-MTHF rapidly degrades in CSF in the presence of a hydroxyl radical generating system

In view of the relative stability of 5-MTHF in CSF (as determined in section 4.6.1), the stability of CSF 5-MTHF in the presence of hydroxyl radicals

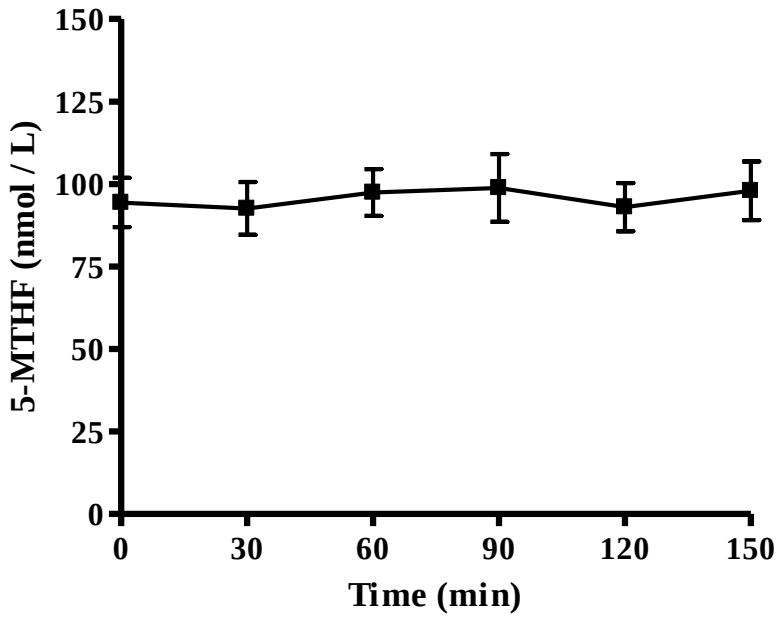


***Figure 33 5-MTHF stability in CSF***. Samples were incubated in air saturated conditions at 37°C. All values are mean ± SEM of 6 independent experiments.

***Table 9 Calculated first or pseudo first (*) order rate constant for 5-MTHF degradation in CSF only, potassium phosphate buffer only, CSF or potassium phosphate buffer and hydroxyl radicals, potassium phosphate buffer and AA (150 µmol/L) and potassium phosphate buffer and hydroxyl radicals and AA (150 µmol/L).*** All values are mean ± SEM of 6 independent experiments. •OH = hydroxyl radicals, ND = not detectable.

| Conditions | Rate constant (k/min) |
|---|---|
| **CSF** | ND |
| **Potassium phosphate buffer (5-MTHF 500 nmol/L)** | 0.004 ± 0.0006 |
| **Potassium phosphate buffer (5-MTHF 150 nmol/L)** | 0.001 ± 0.0002 |
| **CSF + •OH *** | 0.02 ± 0.002 |
| **Potassium phosphate buffer + •OH (5-MTHF 500 nmol/L) *** | 0.04 ± 0.005 |
| **Potassium phosphate buffer + •OH (5-MTHF 150 nmol/L) *** | 0.07 ± 0.005 |
| **Potassium phosphate buffer + AA (5-MTHF 150 nmol/L)** | ND |
| **Potassium phosphate buffer + •OH + AA (5-MTHF 150 nmol/L) *** | 0.05 ± 0.005 |

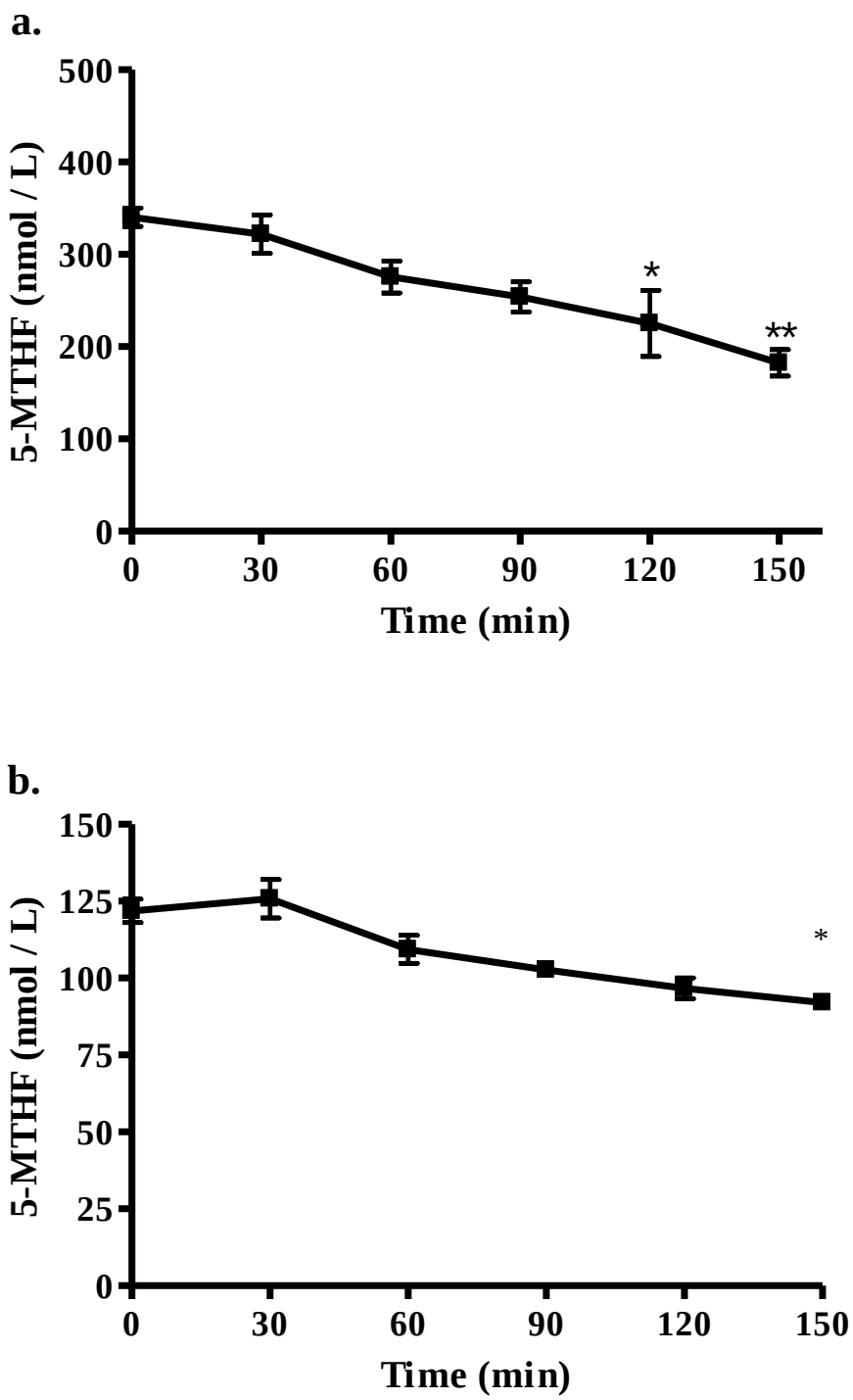


***Figure 34 5-MTHF stability in potassium phosphate buffer.*** **a.** 5-MTHF stability at an initial concentration of 500 nmol/L and **b.** at an initial concentration of 150 nmol/L. Samples were incubated in air saturated conditions at 37°C. All values are mean ± SEM of 6 independent experiments. * $p<0.05$, ** $p<0.01$ difference in comparison to 0 min by one-way ANOVA followed by Bonferroni's multiple comparison test.

propagated by the Fenton reaction (Equation 3) was evaluated. A 5-MTHF concentration of 117.7 ± 2.2 nmol/L was recorded at 0 minute. 5-MTHF was shown to rapidly decay (Figure 35). An overall significant loss of 98% was observed at 150 minutes, compared to 0 minutes ($p<0.001$). 5-MTHF in CSF in the presence of hydroxyl radicals, decayed at a faster rate compared to CSF alone (Table 9). Similarly, 5-MTHF rapidly decayed in potassium phosphate buffer following the introduction of a hydroxyl radical generating system. Stability was first determined at an initial 5-MTHF concentration of 500 nmol/L. A 5-MTHF concentration of 301.4 ± 7.0 nmol/L was recorded at 0 minute. Over time, 5-MTHF rapidly decayed (Figure 36a). An overall significant loss of 100% was observed at 120 minutes, compared to 0 minute ($p<0.001$). In a parallel experiment, the stability of 5-MTHF in potassium phosphate buffer at a more physiological CSF concentration of 150 nmol/L in the presence of hydroxyl radicals was assessed. A 5-MTHF concentration of 137.7 ± 5.0 nmol/L was recorded at 0 minute. Similarly, 5-MTHF rapidly decayed over time (Figure 36b). A significant 100% loss of 5-MTHF was observed at 90 minutes, compared to 0 minutes ($p<0.001$). 5-MTHF, in the presence of hydroxyl radicals in CSF and in potassium phosphate buffer, decayed according to pseudo first order kinetics at a faster rate compared to potassium phosphate buffer alone (Table 9).

### 4.6.3 5-MTHF is stable in CSF in the presence of selenite

The effect of selenite on the stability of 5-MTHF in CSF was further determined. A 5-MTHF concentration in pooled disease control CSF of 90.3 ± 1.1 nmol/L was recorded at 0 minute. In the presence of 2 µg/L selenite [a concentration within the CSF selenium reference range across all ages (1.8-4.7 µg/L (1–30 days), 0.68-3.00 µg/L (1 month – 3 years) 0.73-2.13 µg/L (4 – 18 years) (Tondo et al., 2010)] and 20 µg/L selenite [a selenium concentration associated with induction of ROS production (Maraldi et al., 2011)] no significant loss of 5-MTHF was observed after 150 minutes incubation, compared to control (Figure 37).

### 4.6.4 5-MTHF is stable in CSF in the presence of GSH and selenite

In view of the relative stability of 5-MTHF in CSF in section 4.6.3, the stability of 5-MTHF in the presence of selenite at various concentrations and GSH at a

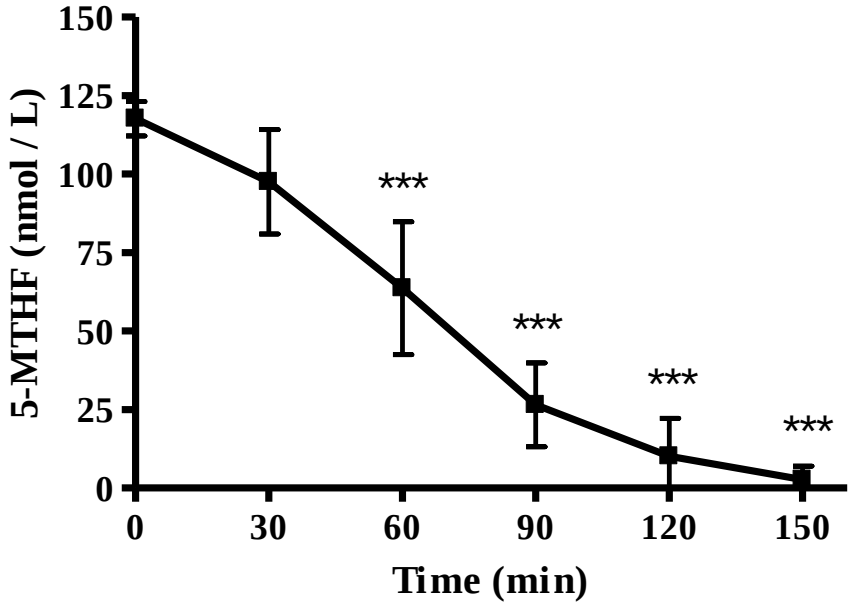


***Figure 35 5-MTHF stability in CSF in the presence of a hydroxyl radical generating system.*** Samples were incubated in air saturated conditions at 37°C. All values are mean ± SEM of 6 independent experiments. *** $p<0.001$ difference in comparison to 0 min by one-way ANOVA followed by Bonferroni's multiple comparison test.

**a.**

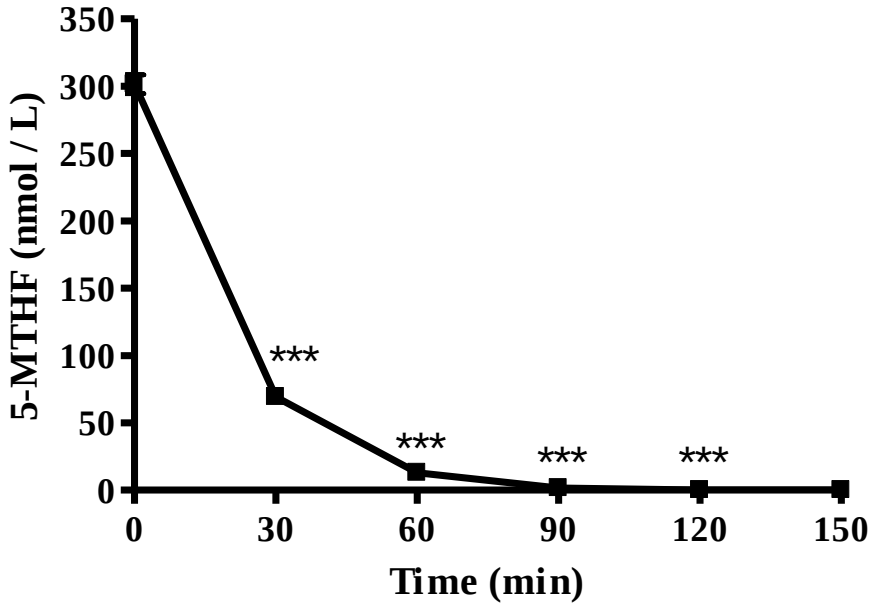


**b.**

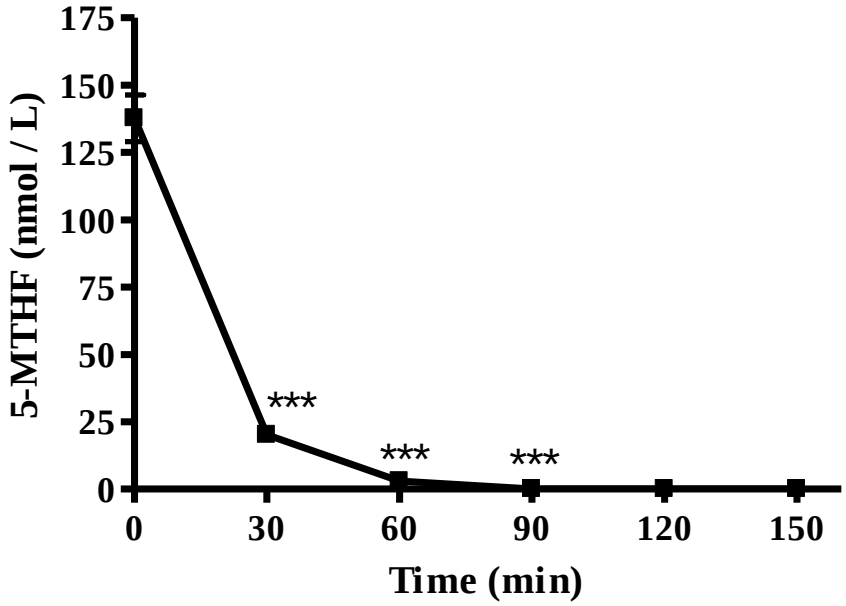


***Figure 36 5-MTHF stability in potassium phosphate buffer in the presence of a hydroxyl radical generating system.*** **a.** Stability of 5-MTHF at an initial concentration of 500 nmol/L and **b.** at an initial concentration of 150 nmol/L. Samples were incubated in air saturated conditions at 37°C. All values are mean ± SEM of 6 independent experiments. *** $p<0.001$ difference in comparison to 0 min by one-way ANOVA followed by Bonferroni's multiple comparison test.

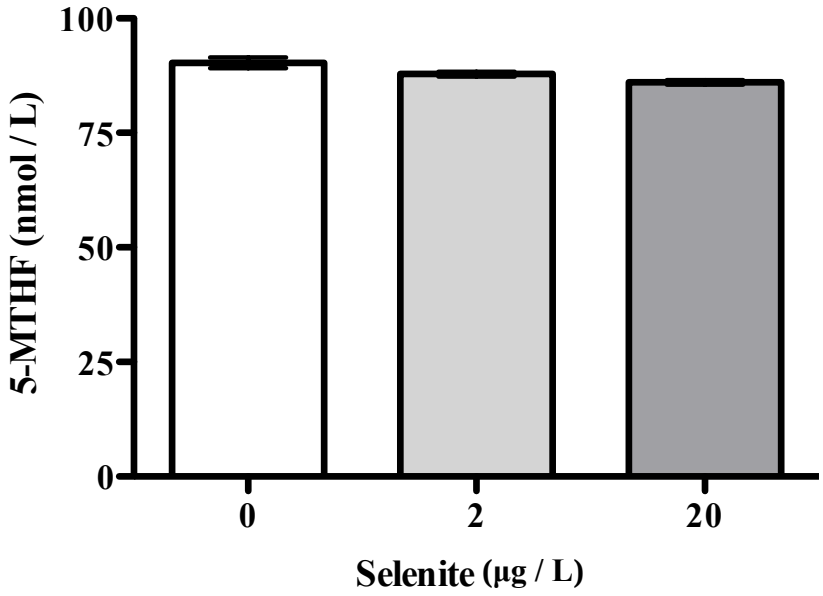


***Figure 37 Concentration of CSF 5-MTHF remaining following incubation with selenite for 150 minutes.*** Samples were incubated in air saturated conditions at 37°C. All values are mean ± SEM of 4 independent experiments.

physiological CSF concentration of 300 nmol/L (Samuelsson et al., 2011), was determined. A 5-MTHF concentration in CSF of 101.1 ± 5.4 nmol/L was recorded at 0 minute. In the presence of GSH and selenite (2, 5, 10, 15 and 20 µg/L), concentrations within the CSF selenium reference range across all ages (1.8-4.7 µg/L (1–30 days), 0.68-3.00 µg/L (1 month – 3 years) 0.73-2.13 µg/L (4 – 18 years) (Tondo et al., 2010) and associated with induction of ROS production (Maraldi et al., 2011), no significant loss of 5-MTHF after 150 minutes incubation was observed, compared to control (Figure 38).

### 4.6.5 5-MTHF is stable in CSF in the presence of GSH and selenite (40:1)

Redox cycling of selenite with reduced GSH resulting in ROS production has been shown to be optimal at a GSH to selenite ratio of 40:1 (Yan and Spallholz, 1993). Since 5-MTHF in CSF remained relatively stable in section 4.6.4, the stability of 5-MTHF in the presence of a GSH to selenite ratio of 40:1 was examined. A 5-MTHF concentration of 76.4 ± 4.0 nmol/L was recorded at 0 minute. No significant loss of 5-MTHF was observed after 150 minutes incubation in the presence of GSH to sodium selenite ratios of 40:1; 1.0 µmol/L: 2 µg/L (25.6 nmol/L), 2.6 µmol/L: 5 µg/L (64.1 nmol/L) and 5.1 µmol/L: 10 µg/L (128.2 nmol/L) (Figure 39). The selenite concentrations used were either within the CSF selenium reference range, 2 µg/L (see section 4.6.3) (Tondo et al., 2010) or concentrations associated with induction of ROS production, 5 µg/L and 10 µg/L (Maraldi et al., 2011).

### 4.6.6 5-MTHF is stable in filtered CSF and in filtered CSF in the presence of GSH and selenite (40:1)

The relative stability of 5-MTHF in CSF observed in sections 4.6.3, 4.6.4 and 4.6.5, could be due to the presence of endogenous enzymatic antioxidant mechanisms reducing ROS to unreactive products, for example extracellular SOD (ecSOD). EcSOD catalyses the production of the more stable intermediate hydrogen peroxide from superoxide (Stewart et al., 2002; Weisiger and Fridovich, 1973). EcSOD is a 32.5 kDa protein. Therefore, prior to each experiment, CSF was filtered through 10 kDa pore size filters in order to eliminate endogenous molecules >10 kDa in size, including ecSOD.

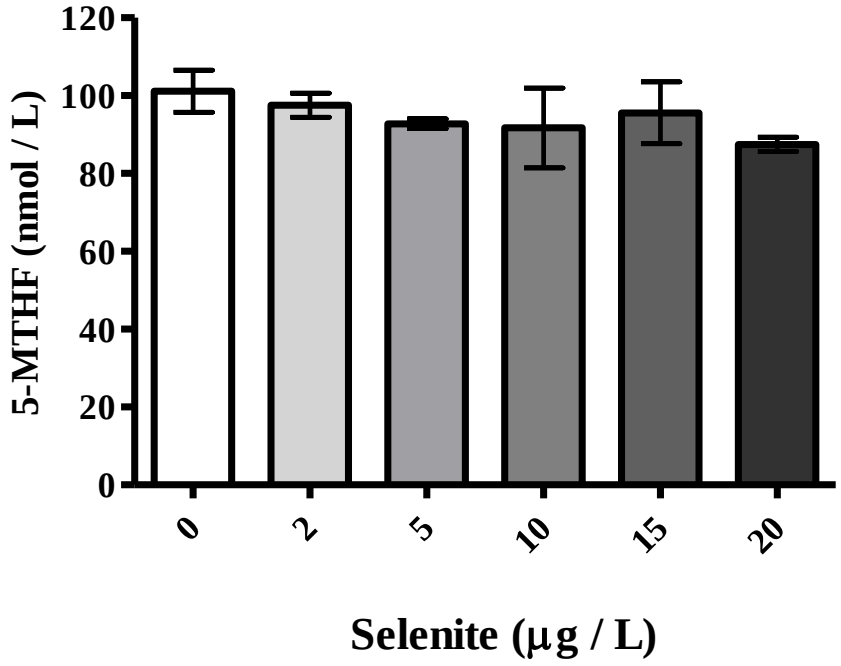


***Figure 38 Concentration of CSF 5-MTHF remaining following incubation with selenite and GSH (300 nmol/L) for 150 minutes.*** Samples were incubated in air saturated conditions at 37°C. All values are mean ± SEM of 4 independent experiments.

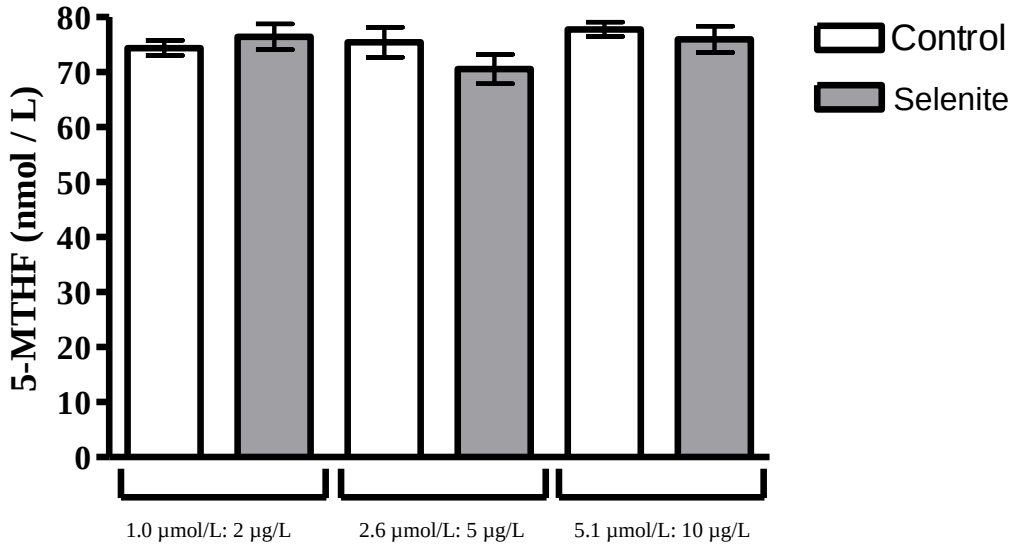


***Figure 39 Concentration of CSF 5-MTHF remaining following incubation with GSH and selenite at a ratio of 40:1, as indicated, for 150 minutes.*** Samples were incubated in air saturated conditions at 37°C. All values are mean ± SEM of 4 independent experiments. Se – selenite.

Initially, the stability of 5-MTHF in filtered CSF was determined. A 5-MTHF concentration of 98.5 ± 15.8 nmol/L was recorded at 0 minute. Over time, 5-MTHF remained relatively stable and no significant loss of 5-MTHF was observed, compared to 0 minute (Figure 40a).

In view of the relative stability of 5-MTHF in filtered CSF, the stability of 5-MTHF in filtered CSF in the presence of a GSH to selenite ratio of 40:1 was examined. A 5-MTHF concentration of 74.4 ± 1.4 nmol/L was recorded at 0 minute. No significant loss of 5-MTHF after 150 minutes incubation was observed compared to control in the presence of GSH to selenite ratios of 40:1; 1.0 µmol/L: 2 µg/L (25.6 nmol/L), 2.6 µmol/L: 5 µg/L (64.1 nmol/L) and 5.1 µmol/L: 10 µg/L (128.2 nmol/L) (Figure 40b).

### 4.6.7 AA confers protection of 5-MTHF in potassium phosphate buffer

The ability of AA at a physiological CSF concentration of 150 µmol/L (Brau et al., 1984) to confer protection of 5-MTHF at an initial concentration of 150 nmol/L in potassium phosphate buffer, was further determined. A 5-MTHF concentration of 116.6 ± 7.9 nmol/L was recorded at 0 minute. Over time, 5-MTHF remained relatively stable in buffer and was no significant loss of 5-MTHF was observed, compared to 0 minute (Figure 41; Table 9).

### 4.6.8 5-MTHF rapidly degrades in potassium phosphate buffer in the presence of a hydroxyl radical generating system and AA

In view of the protective effect of AA on 5-MTHF stability in section 4.6.7, the effect of AA (150 µmol/L) on 5-MTHF stability at an initial concentration of 150 nmol/L in the presence of hydroxyl radicals in potassium phosphate buffer, was assessed. A 5-MTHF concentration of 144.9 ± 4.3 nmol/L was recorded at 0 minute. Over time, 5-MTHF rapidly decayed (Figure 42). An overall significant loss of 100% was observed at 90 minutes, compared to 0 minute ($p<0.001$). 5-MTHF, in the presence of hydroxyl radicals and AA in potassium phosphate buffer, decayed at a faster rate compared to potassium phosphate buffer alone (Table 9).

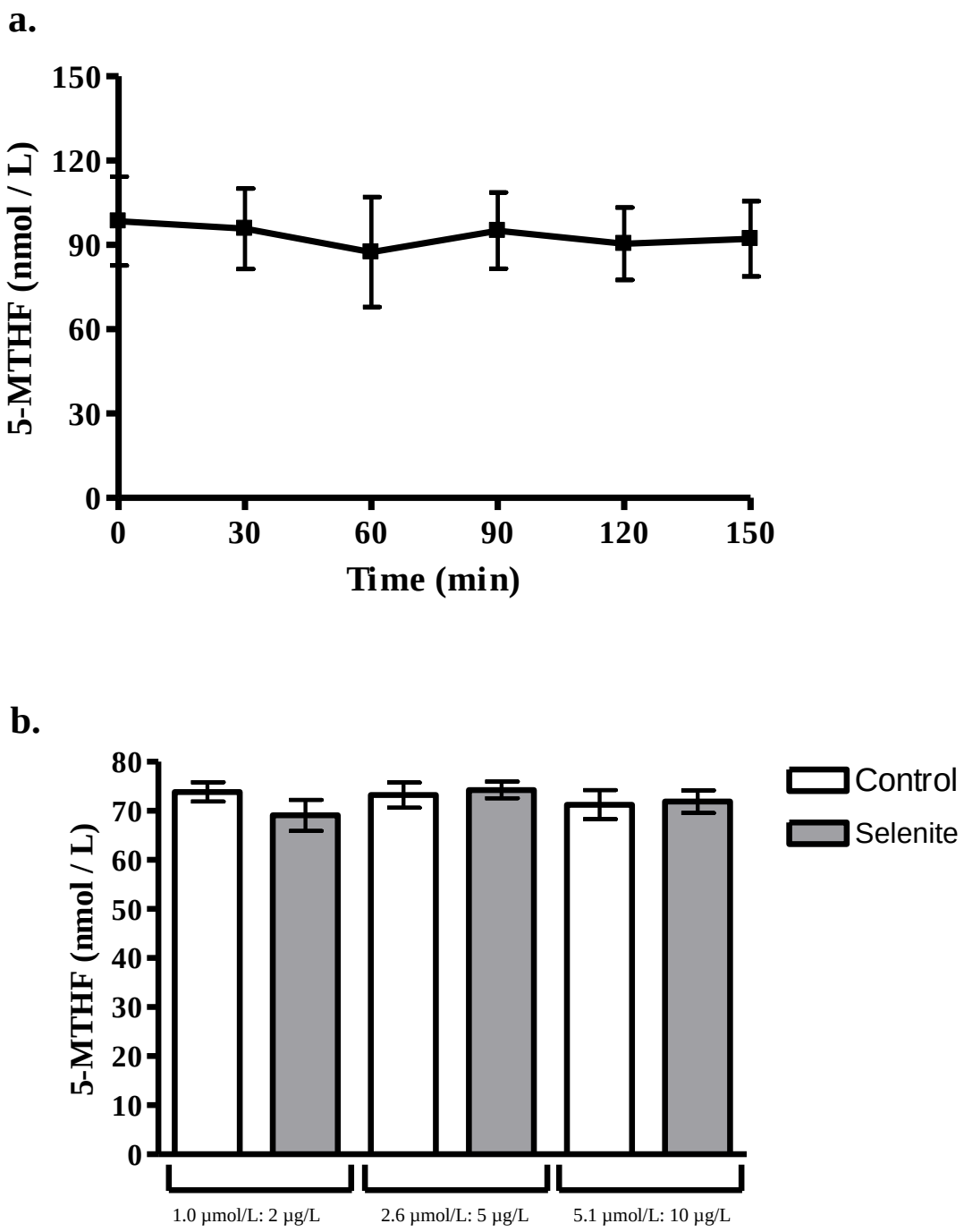


***Figure 40 5-MTHF stability in filtered CSF (a) and concentration of 5-MTHF remaining in filtered CSF following incubation with GSH and selenite at a ratio of 40:1, as indicated (b), for 150 minutes.*** Samples were incubated in air saturated conditions at 37°C. All values are mean ± SEM of 4 independent experiments. Se – selenite.

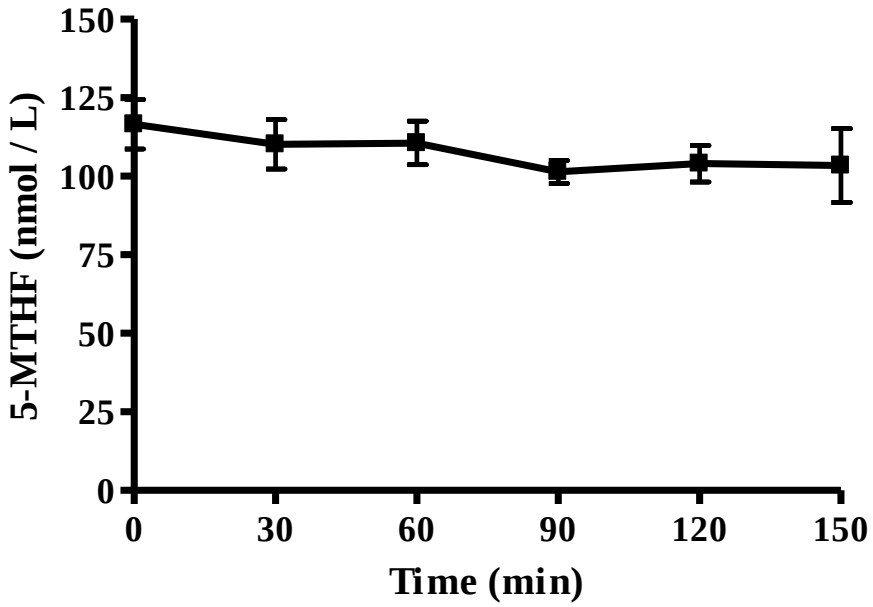


***Figure 41 5-MTHF stability at an initial concentration of 150 nmol/L in potassium phosphate buffer in the presence of AA (150 µmol/L).*** Samples were incubated in air saturated conditions at 37°C. All values are mean ± SEM of 6 independent experiments.

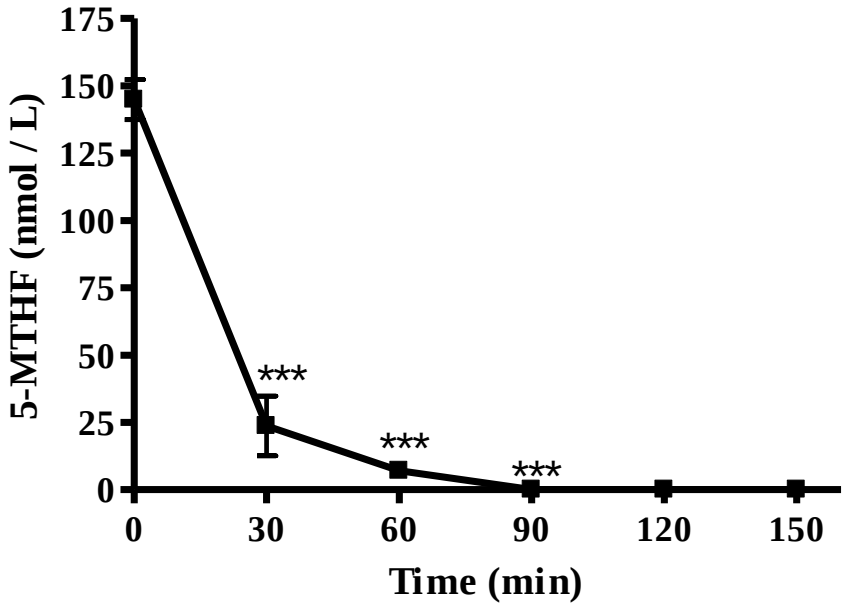


***Figure 42 5-MTHF stability at an initial concentration of 150 nmol/L in potassium phosphate buffer in the presence of a hydroxyl radical generating system and AA (150 µmol/L).*** Samples were incubated in air saturated conditions at 37°C. All values are mean ± SEM of 6 independent experiments. *** $p<0.001$ difference in comparison to 0 min by one-way ANOVA followed by Bonferroni's Multiple comparison test.

### 4.7 Discussion

An initial loss of 5-MTHF was observed between sample preparation and 0 minute for all studies carried out in potassium phosphate buffer owing to the susceptibility of 5-MTHF to autoxidation in the presence of molecular oxygen (Blair et al., 1975) and lack of antioxidants present. Since 5-MTHF is prone to oxidation (Blair et al., 1975), for diagnostic work, 5-MTHF calibrants are made up in the presence of an antioxidant, such as DTE, in order to prevent degradation. This is in accordance with the standard operating procedure used in the Clinical Pathology Accredited Neurometabolic Unit at the National Hospital for Neurology and Neurosurgery, London, UK, as detailed in section 2.3. For the studies reported here relating to the evaluation of 5-MTHF stability in the presence of oxidants, no such antioxidant was initially present. Consequently, a degree of loss of 5-MTHF would be expected to occur prior to quantification of 5-MTHF at the initial time point. The degree of loss appears to be comparable between experiments and so the effect of oxidants and/or antioxidants is being tested against a relatively consistent background. The data also reinforce the requirement for the immediate addition of antioxidants when preparing calibrants for quantitative analysis.

Initially, the stability of endogenous 5-MTHF in CSF was assessed. In contrast to 5-MTHF in potassium phosphate buffer at both initial concentrations of 500 nmol/L and 150 nmol/L, endogenous 5-MTHF in CSF was relatively stable. This apparent stability suggests the presence of protective factors, including non-enzymatic and enzymatic antioxidants (Alho et al., 1998; Boveris et al., 1972; Ng et al., 2007), counteracting 5-MTHF decay. However, introduction of a hydroxyl radical generating system to CSF resulted in loss of 5-MTHF. This finding implies that any protective factors present in CSF may be overwhelmed by ROS generation leading to loss of 5-MTHF from CSF. Similarly, 5-MTHF (500 nmol/L and 150 nmol/L) degradation in the presence of hydroxyl radicals was also observed in potassium phosphate buffer.

The rate constants were also calculated for these experiments. A large k value (Connors, 1990) indicates that the reaction is fast in the forward direction, whereas, a small k value indicates that the reaction is slow in the forward direction . Owing to the observed stability of 5-MTHF in CSF as a consequence of the presence of putative protective factors counteracting 5-MTHF decay, an undetectable rate of decay was recorded. However, in agreement with previous observations (Blair et al.,

1975), 5-MTHF was found to decay according to first order kinetics in buffer; the rate of reaction was proportional to the concentration of reactant i.e. 5-MTHF. This definition of first order kinetics can be applied to the difference in rate constant values observed between 5-MTHF decay in buffer at an initial concentration of 500 nmol/L and 150 nmol/L. The rate is approximately four times faster in the 500 nmol/L decay experiment compared to the 150 nmol/L decay experiment, which is associated with an approximate four times increase in concentration of 5-MTHF in the system. In experiments where hydroxyl radicals were propagated, the reaction is pseudo first order. When there are two reactants in a system, the reaction follows second order kinetics (Connors, 1990). However, owing to hydroxyl radicals being present in large excess within the system (Equation 4), it is not a 'true' reactant. The hydroxyl radicals 'flood' the system and the concentration of hydroxyl radicals is absorbed by the rate constant. Consequently, the observed reaction rate depends on the concentration of 5-MTHF only. This is called a pseudo first order reaction (Connors 1990).

Equation 4: [5-MTHF] + [•OH (excess)] → [Product]

An expected slower rate of CSF 5-MTHF decay in the presence of hydroxyl radicals was observed in comparison to that of 5-MTHF in buffer at both concentrations assessed, owing to the presence of endogenous protective antioxidant molecules and enzyme systems in CSF (Alho et al., 1998; Kolmakova et al., 2010). However, in contrast to the rates of decay observed for 5-MTHF in buffer alone, 5-MTHF at an initial concentration of 150 nmol/L decayed at a faster rate in the presence of hydroxyl radicals compared to 5-MTHF at an initial concentration of 500 nmol/L. This reversal can be explained by the large excess of hydroxyl radicals present in the system leading to an increased rate of 5-MTHF decay.

Elevated selenium concentrations have been reported in CSF of patients with KSS (Tondo et al., 2011) and high physiological selenium concentrations have been shown to undergo redox cycling with reduced thiols, including GSH which is also present in CSF, to propagate ROS (Chen et al., 2007b; Lu et al., 2009; Tarze et al., 2007; Yan and Spallholz, 1993). This reaction has been shown to be optimal at a GSH to selenite ratio of 40:1 (Yan and Spallholz, 1993). In view of the susceptibility of 5-MTHF in CSF to oxidative catabolism by ROS, the effect of selenite in the absence of GSH (due to endogenous GSH in CSF) (Samuelsson et al., 2011) and

presence of GSH was determined. Interestingly, CSF 5-MTHF stability was unaffected following the addition of selenite only, GSH plus selenite and GSH plus selenite at a ratio of 40:1. It was postulated that owing to the physiological nature of CSF, the observed 5-MTHF stability may be attributable to the activity of endogenous non-enzymatic and enzymatic antioxidant mechanisms including ecSOD (Adachi et al., 2001; Stewart et al., 2002). However, upon CSF filtration through a 10 kDa pore size filter to remove 32.5 kDa ecSOD and addition of GSH and selenite at a ratio of 40:1, 5-MTHF remained stable. It is important to note that other large antioxidant proteins with a molecular mass >10 kDa, may also be filtered out of the CSF. These proteins may include catalase (59.8 kDa), glutathione peroxidase (GPx3 (extracellular), 25.6 kDa), thioredoxin (Trx1 (secreted cytosolic form), 12.0 kDa) and thioredoxin peroxidase (Prx4 (secreted endoplasmic reticulum form), 30.5 kDa) (Bendich and Deckelbaum, 2010; Moriarty-Craige and Jones, 2004; Rubartelli et al., 1992) (http://www.uniprot.org/). However, other small molecule antioxidants with a molecular mass <10 kDa may pass through the 10 kDa size filter pores and remain in the CSF. These proteins may include AA (176 Da), GSH (307 Da), α-tocopherol (431 Da), uric acid (168 Da), ubiquinol (865 Da) and melatonin (232 Da) (Alho et al., 1998; Kolmakova et al., 2010; Marquardt et al., 2013; Montecinos et al., 2007) (http://www.uniprot.org/). Therefore, the presence of these small molecular weight (<10 kDa) antioxidant molecules may explain the observed 5-MTHF stability in this system.

Alternatively, other possible explanations may also be possible. For example, it has been documented that the reaction between selenite and GSH occurs favourably in acidic conditions to generate hydrogen selenide. In the presence of molecular oxygen, hydrogen selenide is susceptible to autoxidation and ROS are generated as a by-product. However, at a more neutral pH, the reaction yields elemental selenium (Lu et al., 2009). Since the pH of CSF is 7.33 (Widmaier and Raff, 2006), this environment would favour the production of elemental selenium, not hydrogen selenide and the associated generation of ROS, which could be an additional factor responsible for the observed stability of 5-MTHF in the aforementioned experimental systems. Interestingly, oxidation of GSH catalysed by selenite and subsequent ROS propagation has previously been demonstrated in the presence HTB123/DU4475 cells, a human mammary tumour cell line (Yan and Spallholz, 1993). The presence of a cellular environment may facilitate the formation of

selenium metabolites, following the addition of selenite, that more easily oxidise with GSH to produce ROS. Therefore, use of a cellular system may be of importance when studying the stability of 5-MTHF in the presence of high physiological concentrations of selenium. In order to explore this, the stability of extracellular 5-MTHF in the presence of selenite treated SH-SY5Y cells will be examined in Chapter 6.

AA is a major antioxidant in the CNS that is prone to oxidation owing to its antioxidant capabilities (Barabás et al., 1995; Rice, 1999; Winston et al., 1998). It has been predicted that AA is low in concentration in the CSF of patients with CFD (Spector and Johanson, 2010). Therefore, the ability of AA to confer protection of 5-MTHF was evaluated. The potential importance of AA to confer protection of 5-MTHF was illustrated by the marked reduction in 5-MTHF catabolism observed in potassium phosphate buffer incubations performed in the presence of an AA concentration comparable to that observed in CSF (Brau et al., 1984). Similarly to 5-MTHF in CSF, an undetectable rate of decay was recorded. AA is one of a number of antioxidants present in CSF and, among an array of other protective factors some of which are listed above (Alho et al., 1998; Kolmakova et al., 2010), its presence could explain the apparent stability of 5-MTHF observed in CSF and in the selenite, and GSH plus selenite, CSF systems. However, the ability of AA to confer protection towards 5-MTHF in potassium phosphate buffer was overwhelmed following the addition of a hydroxyl radical generating system. Since hydroxyl radicals are present in excess in the system, this finding suggests that either a higher concentration of AA or lower concentration of hydroxyl radicals is required to achieve redox homeostasis and subsequent 5-MTHF stability.

AA is considered to be a double-edged sword. Whilst AA is an antioxidant, at low physiological CSF concentrations (~ <100 µmol/L) (Brau et al., 1984), AA has pro-oxidant capabilities (Buettner and Jurkiewicz, 2010; Fisher and Naughton, 2003). Therefore, AA may exacerbate ROS generation in the system. Specifically, $Fe^{3+}$ generated in the Fenton reaction can be reduced to $Fe^{2+}$ by AA and/or directly react with AA to produce hydrogen peroxide in the Weissberger system (Weissberger et al., 1943). This system dictates that the generation of $Fe^{2+}$ and/or hydrogen peroxide may facilitate further generation of hydroxyl radicals by subsequent Fenton cycles, leading to accelerated 5-MTHF degradation (Fisher and Naughton, 2003; Hamilton et al., 1964). However, the rate of 5-MTHF degradation in the hydroxyl radicals and

AA system was marginally slower than that of hydroxyl radicals alone, suggesting that ROS generation is not exacerbated in the presence of AA via the mechanisms described above. Instead, the slower rate of 5-MTHF degradation in the hydroxyl radicals and AA system compared to hydroxyl radicals alone, may be attributable to the presence of AA in the system eliciting antioxidant protection. This study also indicates that AA at a physiological CSF concentration of 150 µmol/L has antioxidant capabilities.

### 4.8 Conclusion

In conclusion, the stability of 5-MTHF in CSF is dependent on the availability of antioxidants to counteract oxidative catabolism mediated by ROS. Whilst protective antioxidant molecules, including AA, are present in CSF, introduction of a hydroxyl radical generating system overwhelms such protective mechanisms. The rapid deleterious effect of hydroxyl radicals on 5-MTHF stability in CSF is reflected by an increase in rate of 5-MTHF decay. For comparative purposes, 5-MTHF stability studies were also carried out in potassium phosphate buffer and similar observations were documented. It is important to note that whilst these studies clearly demonstrate the susceptibility of 5-MTHF to oxidative attack by hydroxyl radicals in CSF, they were carried out in a non-cellular environment, *ex vivo*. In addition, whilst there is a high iron content in the brain and CSF has a low free iron binding capacity, the contribution of Fenton chemistry in promoting neurotoxicity *in vivo* remains unclear (Bleijenberg et al., 1971; Bradbury, 1997; Harrison et al., 1968; Stankiewicz et al., 2007). The deleterious effect of ROS generated as a consequence of selenite metabolism has yet to be documented. This may be attributed to a number of factors including the presence of antioxidant mechanisms that exist in CSF, the neutral pH of CSF and the lack of an appropriate cellular system to facilitate selenium metabolism. Moreover, in view of AA, which is present in CSF, conferring stability of 5-MTHF, AA may be a biologically relevant endogenous protective factor, *in vivo*.

# Chapter 5
# Development and utilisation of a method to quantify CSF AA and the potential relationship between AA and 5-MTHF in CSF

# 5. Development and utilisation of a method to quantify CSF AA and the potential relationship between AA and 5-MTHF in CSF

## 5.1 Introduction

As determined in Chapter 4, 5-MTHF is relatively stable in CSF. This apparent stability suggests that protective factors present in CSF may counteract decay of 5-MTHF. However, introduction of a hydroxyl radical generating system led to a significant loss of 5-MTHF from CSF, indicating that any protective mechanisms present may be overwhelmed.

As discussed in section 4.7, CSF is known to contain an array of non-enzymatic and enzymatic antioxidant molecules (Alho et al., 1998; Kolmakova et al., 2010), which may confer protection of 5-MTHF. Such molecules in CSF include the essential water-soluble antioxidant, ascorbic acid (AA) (Barabás et al., 1995; Caprile et al., 2009; Rice, 1999). Like 5-MTHF, AA is actively transported from the periphery into CSF, is prone to oxidation owing to its antioxidant capabilities and has been predicted to be low in concentration in CSF of patients with CFD (Harrison and May, 2009; Spector and Johanson, 2010; Weissberger et al., 1943). The biological role, transport and biochemistry of AA are discussed in detail in section 1.6.2.2. In Chapter 4, AA was demonstrated to counteract decay of 5-MTHF in potassium phosphate buffer at a concentration comparable to that observed in CSF. This observation suggests that AA, among other antioxidant molecules, may be an endogenous protective factor governing 5-MTHF availability and may be of biological relevance in CFD states.

In order to evaluate the importance of AA on 5-MTHF availability in CSF, a method to measure AA in CSF was developed and the potential relationship between CSF AA and 5-MTHF was examined in this Chapter.

The work presented in this Chapter was extended to examine the potential relationships between AA or 5-MTHF and the CSF neurotransmitter metabolites, homovanillic acid (HVA) or 5-hydroxyindoleacetic acid (5-HIAA). This extension was carried out because HVA and 5-HIAA had previously been measured in the CSF samples used in this Chapter for diagnostic purposes and previous studies have demonstrated relationships between 5-MTHF and HVA or 5-HIAA in CSF (Ormazabal et al., 2006; Surtees et al., 1994; Verbeek et al., 2008). Additionally, AA

is a cofactor for dopamine-β-hydroxylase, the enzyme which catalyses the production of noradrenaline from dopamine (Menniti et al., 1986) and has been implicated in influencing tyrosine hydroxylase and tryptophan hydroxylase activities (Stone and Townsley, 1973).

### 5.2 Aims

1. To develop and utilise a method for AA measurement in CSF.

2. To develop an in-house reference range for assessment of AA in disease control CSF samples.

3. To determine whether a potential relationship may exist between AA and 5-MTHF in CSF.

4. To determine whether potential relationships may exist between AA or 5-MTHF and HVA or 5-HIAA in CSF.

5. To examine AA concentration in CSF from patients with a documented CSF 5-MTHF deficiency.

### 5.3 Acknowledgement

Part of the work presented in this Chapter has been published (Aylett et al., 2013). I can confirm that all of the work documented was my own with the exception of CSF 5-MTHF measurements and CSF neurotransmitter metabolite measurements, HVA and 5-HIAA, which were performed by Viruna Neergheen and Marcus Oppenheim, and Dr. Simon Pope, respectively, in the Neurometabolic Unit at the National Hospital for Neurology and Neurosurgery, London, UK.

## 5.4 Materials and Methods

### 5.4.1 Materials

Purchasing details of all materials used throughout this Chapter are described in section 2.1, unless otherwise stated.

### 5.4.2 Patient CSF samples

Patient CSF samples were collected as described in section 2.2.

### 5.4.3 Development of a HPLC with electrochemical detection method to quantify AA in CSF

In order to fulfil the aims of this Chapter, a method to detect and quantify AA in CSF was required. Methods used to measure AA in CSF have previously included colorimetric determination (Hashmi et al., 1973) and spectrophotometric ultraviolet scanning (Cupello et al., 2002). However, the most common direct method for AA quantification in CSF, as well as in other biological samples including plasma, is reverse-phase HPLC coupled with electrochemical detection (ECD) (Khan et al., 2011; Li and Franke, 2009; Nagy and Degrell, 1989). This technique offers sufficient sensitivity and high throughput, and is also used to measure other redox active molecules in biological fluids, including the CSF neurotransmitter metabolites, homovanillic acid (HVA, dopamine metabolite) and 5-hydroxyindoleacetic acid (5-HIAA, serotonin metabolite) (Hyland, 1993; Hyland et al., 1993). The reverse-phase HPLC-ECD method of Nagy and Degrell (1989) was developed and utilised for measurement of AA in CSF in this Chapter.

#### 5.4.3.1 Function

Reverse-phase HPLC utilises a non-polar stationary phase and an aqueous mobile phase to separate analytes. Non-polar molecules tend to adsorb to the stationary phase and are retained on the HPLC column longer than polar molecules. Coulometric ECD is used for the detection of electroactive species in sample eluent, separated by the HPLC system. The HPLC eluent flows sequentially through two porous graphite working electrodes. The first electrode (E1) is the screening electrode, which screens out easily oxidisable compounds in order to reduce noise and produce a cleaner chromatogram. The second electrode (E2) is the detector electrode, which is set to give the maximum oxidation for the compound of interest. Coulometric ECD allows for 100% of the species of interest to be oxidised. As a

result, the observed current signal is directly proportional to the concentration of the analyte of interest in the sample (Flanagan et al., 2005).

#### 5.4.3.2 Equipment

PU-1580 intelligent HPLC pump (Jasco); AS-1555 intelligent autosampler (Jasco); Coulochem II electrochemical detector module (model 5200A) and 5010 analytical cell (ESA Analytical Ltd, Aylesbury, UK). The mobile phase was degassed using a DG-1580-53 3-line degasser (Jasco). The electrochemical detector module was connected to a computer and data recorded using Jasco Borwin data capture and analysis software (Jasco). The equipment was set up as shown in Figure 14.

#### 5.4.3.3 External AA standard sample preparation

AA is susceptible to autoxidation (Weissberger et al., 1943) and is unstable in aqueous solutions containing transition metal ions, including copper (II) and iron (III) ions. However, in aqueous solutions containing metaphosphoric acid and EDTA, AA stabilises. This is because metaphosphoric acid and EDTA lower the pH of the solution and chelate metal ions in order to inhibit the copper (II)/iron (III)-catalysed oxidation of AA (Lyman et al., 1937; Wechtersbach and Cigić, 2007). Therefore, to prevent AA oxidation and anomalous data, all external AA standard samples were prepared in an acidic solution of 0.2 mmol/L metaphosphoric acid and 5 mmol/L EDTA made up in HPLC grade water (Nagy and Degrell, 1989).

#### 5.4.3.4 Analytical procedure

The mobile phase consisted of 0.1 mmol/L disodium hydrogenphosphate, 0.07 mmol/L EDTA, 0.15 mmol/L sodium octyl sulphate and 50 ml/L methanol made up in ultrapure water, adjusted to pH 3.1 using orthophosphoric acid. The flow rate was 0.5 ml/min. Samples were transferred to vials and loaded into the autosampler. Each sample (50 µL) was injected into the flow and separated on a C18 reverse phase Spherisorb ODS-2, 5 µm, 250 x 4.6 mm column (Waters, Elstree, UK), maintained at 28°C. E1 was set to +50 mV to oxidise analytes of low oxidation potential. The optimum voltage E2 was determined by voltammogram by measuring the peak area of 150 µmol/L AA at varying E2 potentials from +50 mV to +800 mV (Figure 43). An E2 potential of +650 mV, where the voltammogram plateaued indicating optimal

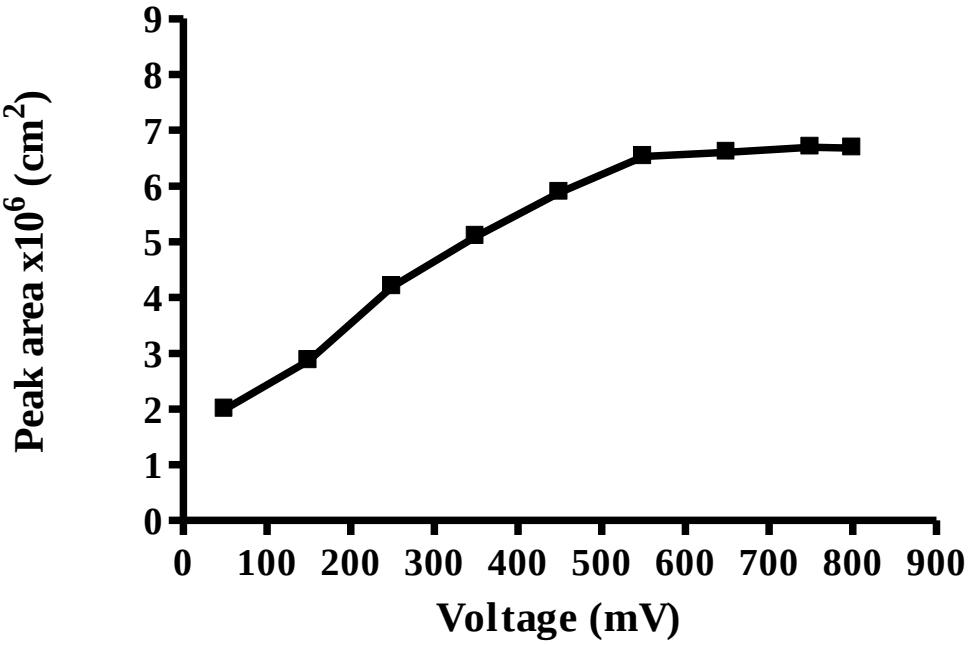


***Figure 43 AA voltammogram.*** AA standards (150 µmol/L) were prepared in an aqueous solution of 0.2 mmol/L metaphosphoric acid and 5 mmol/L EDTA in air saturated conditions at ambient temperature. Samples were analysed at increasing E2 voltage by HPLC-ECD as described in section 5.4.3.

AA quantification, was chosen for determination of AA. External AA standard samples were prepared at a concentration of 150 µmol/L, a concentration comparable to that of AA in CSF. An example chromatogram of an AA 150 µmol/L standard is shown in Figure 44. A quality control was prepared by pooling disease control CSF. Results of the internal quality control were recorded. Data obtained from samples were kept within ±2 standard deviations of the measured values of the current quality control. A calibration curve was performed to determine the linearity between current amplitude and standard concentration. Linearity was demonstrated for AA between 0–80 µmol/L (Figure 45).

#### 5.4.3.5 Measurement of AA in CSF

Analysis of AA in CSF was performed in the first 0.5 ml CSF sample, since there is a sufficient volume of CSF remaining after diagnostic neurotransmitter analysis in the vial. Samples underwent a maximum of two freeze-thaw cycles. Blood-stained samples were excluded from analysis owing to the risk of AA oxidation in the presence of erythrocyte derived iron release, which could propagate the hydroxyl radical via the Fenton reaction (see Equation 2) (Fenton, 1894; Heales et al., 1988). According to the method of Nagy and Degrell (1989), CSF for AA measurement required very little prior sample preparation. Therefore, neat CSF was injected into the HPLC mobile phase flow. AA in CSF was measured using the analytical procedure outlined in section 5.4.3.4. An example chromatogram of AA in CSF is shown in Figure 46.

#### 5.4.3.6 Data analysis

AA chromatograms were visualised and quantified using Jasco Borwin data capture and analysis software (Jasco) using the following equation:

$$\text{Concentration (µmol/L)} = \text{(sample peak area/external standard peak area) x calibration standard concentration (µmol/L)}$$

#### 5.4.3.7 Recovery of AA performed in CSF

Recovery experiments were performed to assess the performance of the method by spiking pooled disease control CSF (100 µl) with 10 µl 550 µmol/L AA (final concentration 50 µmol/L) and measuring the concentration of AA recovered. A mean recovery of 96 ± 2.3% was achieved for AA.

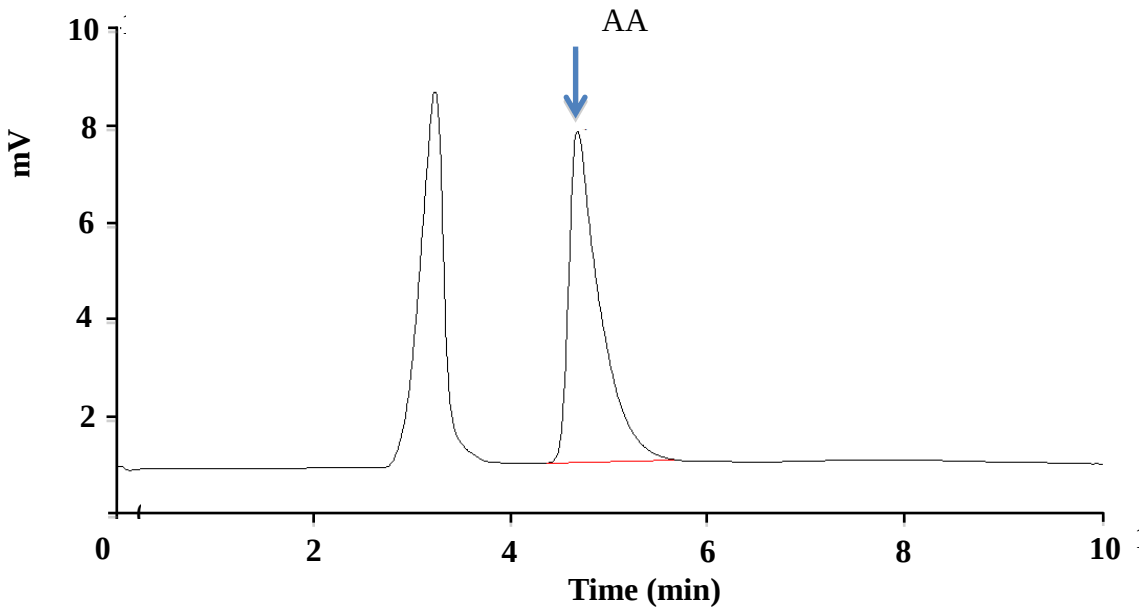


***Figure 44 Sample chromatogram of an external AA standard.*** External AA standard sample peak in a 150 μmol/L standard. AA retention time ~5 min.

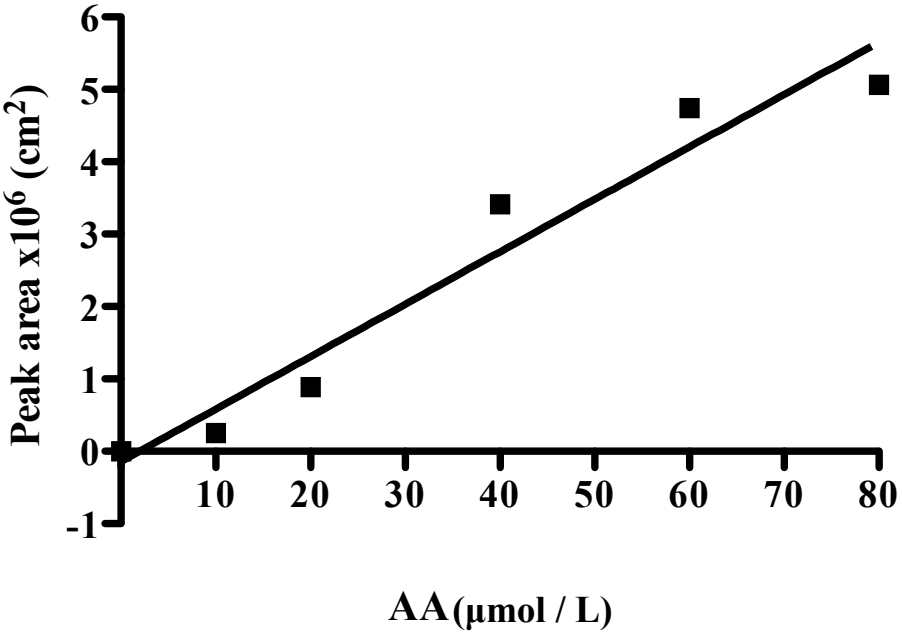


***Figure 45 AA calibration curve.*** The linearity of AA concentration was demonstrated between 0–80 µmol/L. Samples were prepared in an aqueous solution of 0.2 mmol/L metaphosphoric acid and 5 mmol/L EDTA in air saturated conditions at ambient temperature. Samples were analysed by HPLC as described in section 5.4.3. All values are mean ± SEM of 4 independent experiments. $r^2 = 0.94$.

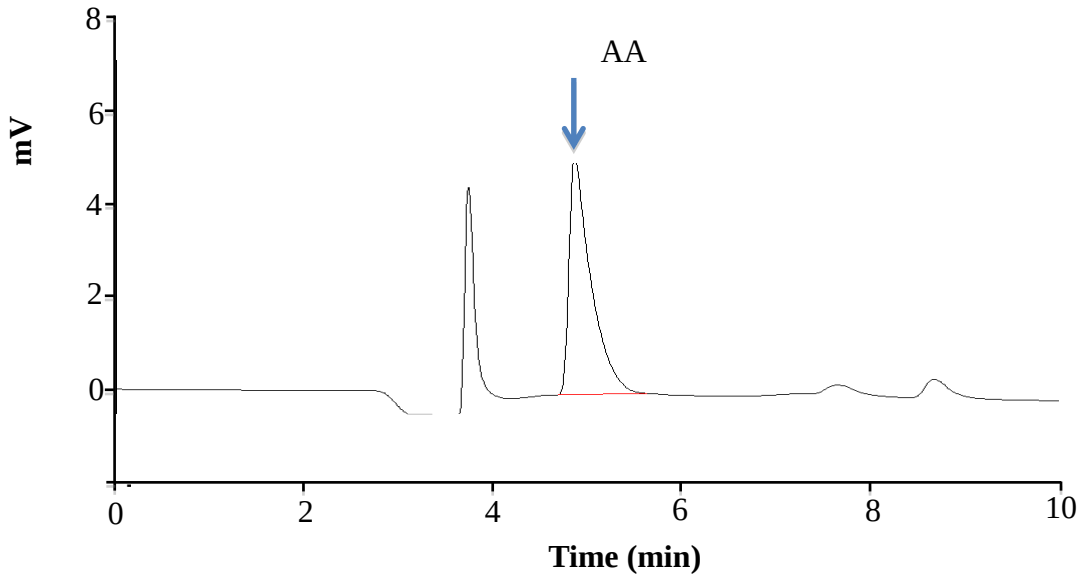


***Figure 46 Sample chromatogram of AA in CSF.*** AA peak in CSF. AA retention time ~5 min.

#### 5.4.3.8 AA stability in CSF

AA stability in CSF was determined in pooled disease control CSF samples. Pooled disease control patient CSF (n=12) was incubated at 37°C for 30 minute time intervals, from 0-150 minutes. AA was analysed in CSF samples (120 µL) by HPLC as described in section 5.4.3.4. Over the period of time studied, no significant loss of AA was observed. AA concentrations at 0 min and 150 min were 233.5 ± 22.4 µmol/L and 214 ± 18.4 µmol/L, respectively ($p>0.05$) (Figure 47).

#### 5.4.3.9 AA availability in filtered CSF

Pooled control patient CSF (n=12) was aliquoted into 10 kDa pore size filter centrifugal eppendorf tubes. Molecules greater than 10 kDa in size would be filtered out of the CSF. Control samples remained unfiltered. Samples were centrifuged for 10 minutes at 14000 rpm. Samples were pooled and incubated at +37°C for 150 minutes (the length of time 5-MTHF is stable for in CSF as determined by experiment 4.5.1). AA was analysed in CSF samples (120 µL) by HPLC as described in section 5.4.3.4. At 150 minutes, no significant loss of AA was observed in either filtered or unfiltered CSF samples. An AA concentration in filtered CSF of 120.9 ± 7.1 µmol/L was recorded at 150 minutes, whilst a CSF AA concentration of 121.1 ± 5.9 µmol/L was recorded at 150 minutes in unfiltered CSF (Figure 48).

#### 5.4.3.10 Reproducibility of the assay

Data from standard samples were analysed to calculate the intra- and inter-assay variation of the method. The intra-batch accuracy had a coefficient of variance of 1.0% and the inter-day accuracy had a coefficient of variance of 12.6%.

### 5.4.4 Measurement of CSF 5-MTHF

CSF 5-MTHF was measured by HPLC as described in section 2.3. CSF 5-MTHF data were analysed retrospectively. The age-related CSF 5-MTHF reference ranges are shown in Table 5.

### 5.4.5 Measurement of CSF HVA and 5-HIAA

CSF HVA and 5-HIAA were measured by HPLC as described below. CSF HVA and 5-HIAA data were analysed retrospectively. The age-related CSF HVA and 5-HIAA reference ranges are shown in Table 10.

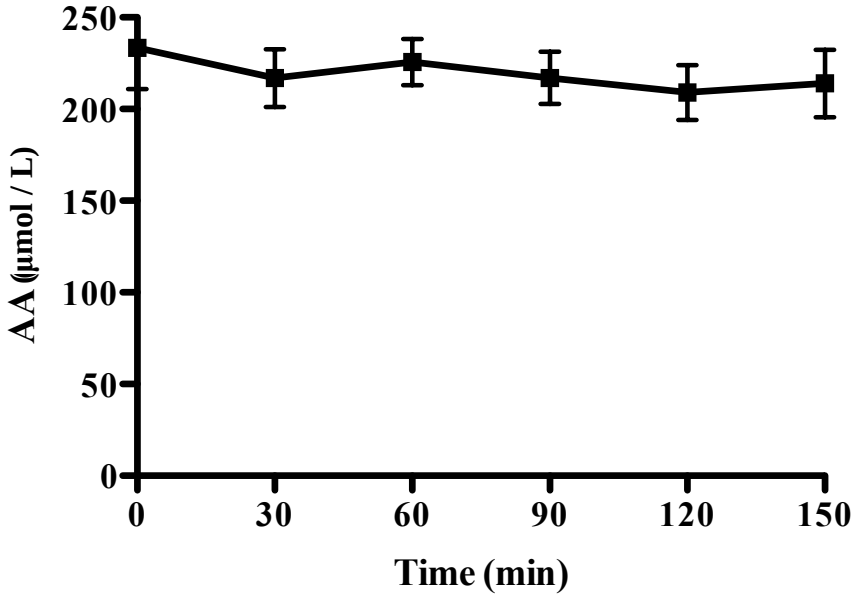


***Figure 47 AA stability in CSF.*** Samples were incubated in air saturated conditions at 37°C. All values are mean ± SEM of 4 independent experiments.

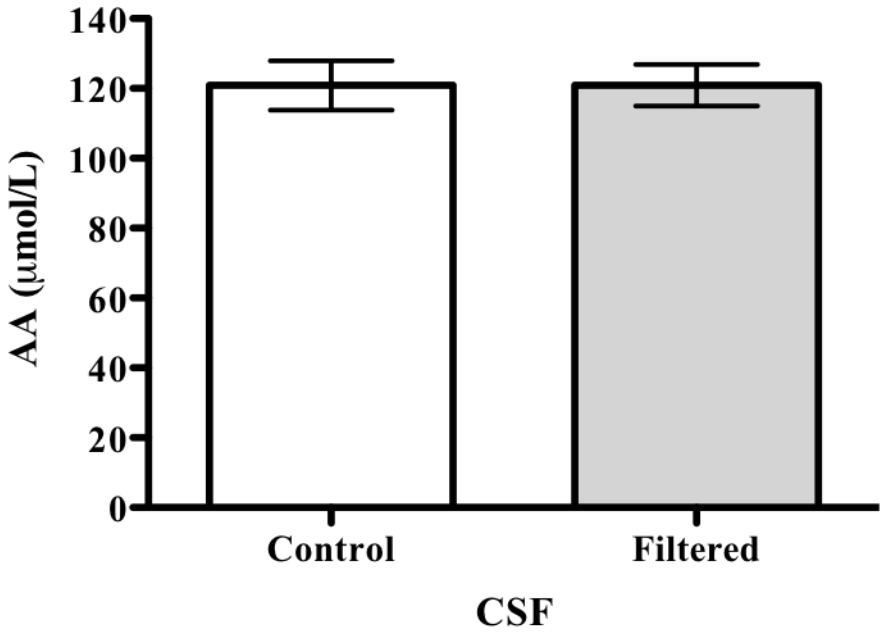


***Figure 48 AA availability in filtered CSF following 150 minute incubation.*** Samples were incubated in air saturated conditions at 37°C for 150 minutes. All values are mean ± SEM of 4 independent experiments.

***Table 10 CSF HVA and 5-HIAA reference ranges.*** CSF HVA and 5-HIAA follow negative age-related trends. Therefore, CSF HVA and 5-HIAA concentrations are age-related and the below reference ranges are used in the Neurometabolic Unit at The National Hospital for Neurology and Neurosurgery, London, UK.

| **CSF HVA and 5-HIAA reference ranges** | | |
|---|---|---|
| **Age (years)** | **Concentration (nmol/L)** | |
| | **HVA** | **5-HIAA** |
| 0 – 0.33 | 324 – 1098 | 199 – 608 |
| 0.34 – 0.66 | 362 – 955 | 63 – 503 |
| 0.67 – 1.0 | 176 – 851 | 68 – 451 |
| 1.1 – 5.0 | 154 – 867 | 89 – 367 |
| 5.1 – adult | 71 – 565 | 58 – 220 |

#### 5.4.5.1 Function

HPLC-ECD function is described in detail in section 5.4.3.1.

#### 5.4.5.2 Equipment

The HPLC-ECD equipment used is described in section 5.4.3.2. The ECD detector was connected to a computer and data was recorded using Azur version 4.6 chromatography data capture and analysis software (Datalys, St Martin D-Heres, France). The equipment was assembled as shown in Figure 14.

#### 5.4.5.3 Analytical procedure

The method was based on the diagnostic method routinely used to quantify HVA and 5-HIAA in CSF in the Neurometabolic Unit at the National Hospital for Neurology and Neurosurgery, London, UK, adapted from previously published methods (Hyland, 1993; Hyland et al., 1993). Analysis of HVA and 5-HIAA in CSF was performed in the first 0.5 ml CSF sample. Samples underwent a maximum of two freeze-thaw cycles. Blood-stained samples were excluded from analysis owing to the risk of contamination by erythrocyte derived iron release which could degrade HVA and 5-HIAA (Fenton, 1894; Heales et al., 1988). This would lead to oxidative catabolism of HVA and 5-HIAA, and subsequent anomaolous results. The mobile phase consisted of 0.05 mol/L monopotassium phosphate, 1 mol/L 1-octanesulphonic acid, 0.05 mol/L EDTA and 18% v/v HPLC grade methanol in ultrapure water, adjusted to pH 2.74 with hydrochloric acid. The flow rate was set at 1.3 ml/min. Samples were thawed, transferred to vials and loaded into the autosampler. Each sample (50 µL) was injected into the flow and separated on a reverse phase 250 x 4.6 mm i.d. HiQSil C18W column (KYA Tech. Corp.), maintained at 35°C. HVA and 5-HIAA were detected by electrochemical detection. The screening electrode (E1) was set to +50 mV to oxidise analytes of low oxidation potential. The detector electrode (E2) was set at +450 mV in order to maximally oxidise HVA and 5-HIAA for quantification in the sample. Samples were quantified against an external standard of 500 nmol/L HVA or 5-HIAA prepared in HPLC grade water with two drops of 12.2 mol/L hydrochloric acid. A quality control was prepared by pooling CSF from previous patients with no evidence of an inborn error of monoamine metabolism. Results of the internal quality control were recorded. Data obtained from samples were kept within ±2 standard deviations of the measured values of the current quality control.

#### 5.4.5.4 Data analysis

HVA or 5-HIAA data were visualised and quantified using Azur version 4.6 chromatography data capture and analysis software (Datalys), using the following equation:

$$\text{Concentration (nmol/L)} = \frac{\text{(sample peak area/external standard peak area)} \times \text{calibration standard concentration (nmol/L)}}{}$$

### 5.4.6 CSF samples for in-house AA reference range and to test for correlations between AA, 5-MTHF, HVA and 5-HIAA in CSF

AA values were established for a total of 105 patients (mean ± SD [range] age, sex ratio: 5.7 ± 8.0 [1 day-19.7 years] years; 68M:37F) whose CSF was investigated in the Neurometabolic Unit laboratory at the National Hospital for Neurology and Neurosurgery, London, UK, from September to November 2012, inclusive.

### 5.4.7 CSF samples from patients with CSF 5-MTHF deficiency

AA values were established for a total of 21 patients (mean ± SD [range] age, sex ratio: 12.6 ± 8.8 [0.7 – 53.8] years; 12M:8F) with low CSF 5-MTHF, whose CSF was investigated in the Neurometabolic Unit at the National Hospital for Neurology and Neurosurgery, London, UK, from November 2012 to January 2013, inclusive. Minimal clinical features and diagnoses (where available) were collated for these patients.

### 5.4.8 Data analysis

Data analyses were carried out as described in section 2.9.

## 5.5 Results

### 5.5.1 In-house AA reference range in CSF

AA is an abundant antioxidant in the CNS with a CSF concentration within the µmol/L range (Rice, 1999). An in-house reference range for AA in CSF was determined by measuring AA in disease control CSF samples (*n*=105). The data was shown to follow a normal distribution (Figure 49). The mean and SD were calculated. Data points greater than mean ± 2 SD were defined as outliers and excluded from overall statistical analyses (*n*=6). Reference ranges are calculated as ±2 SD either side of the mean (Marshall and Bangert, 2008). An AA reference range in CSF was calculated to be 103–303 µmol/L (*n*=99) (Table 11). This range encompasses individual CSF AA concentrations reported in the literature (Brau et al., 1984; Rice, 1999; Spector, 1981).

### 5.5.2 Age has no effect on the AA reference range in CSF

Since age-dependency can have a significant impact on the upper and lower reference range limits, especially in the first year of life, the effect of age on the AA reference range in CSF was determined (Ormazabal et al., 2006). No significant effect of age upon AA concentration could be demonstrated and a non-significant correlation was observed between CSF AA concentration and age (r=-0.043, p=0.67, *n*=99) (Figure 50). Therefore, the reference range for AA in CSF was considered age independent.

### 5.5.3 Correlation between AA and 5-MTHF in CSF, but not with AA and HVA or 5-HIAA

5-MTHF, HVA and 5-HIAA concentrations were determined in the same CSF samples utilised to determine the reference range for AA in CSF (*n*=105). The data were analysed and outliers for both parameters tested (*n*=9, *n*=8, *n*=7, for 5-MTHF, HVA and 5-HIAA correlations with AA, respectively) were excluded. The reference ranges for 5-MTHF, HVA and 5-HIAA in CSF are age dependent. However, since AA concentration in CSF is not dependent on age, the age dependency of 5-MTHF, HVA and 5-HIAA in CSF does not affect the overall analysis and the Pearson correlation test was performed (see section 2.9). A significant positive correlation was observed between AA and 5-MTHF (r=0.284, p=0.002, *n*=96) (Figure 51a). However, non-significant correlations were observed between AA and HVA

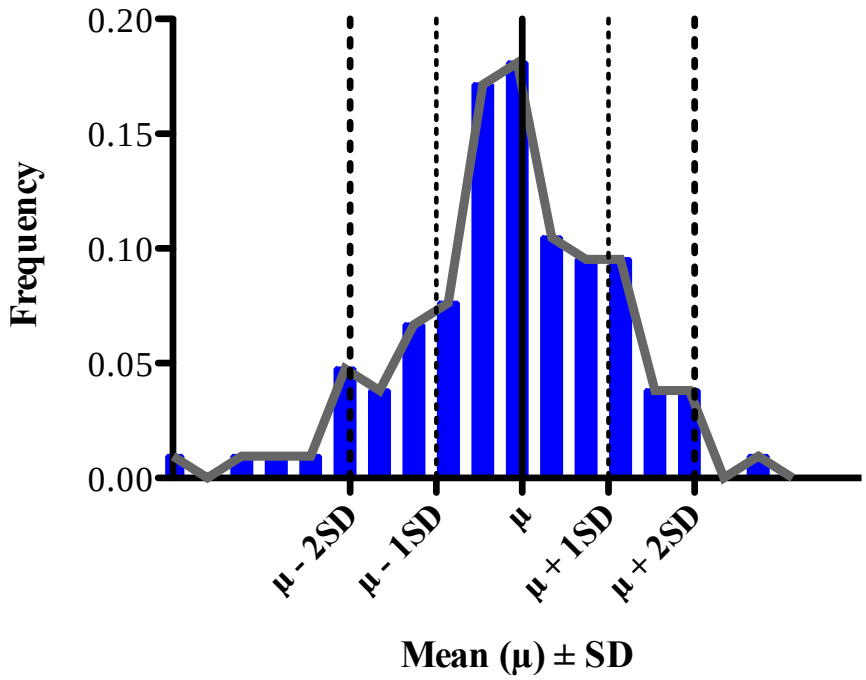


***Figure 49 Normal distribution plot of CSF AA concentration from a reference population.*** Data was shown to follow a normal distribution ($p<0.05$, $n=105$). Samples were prepared in air saturated conditions at ambient temperature. μ=mean, SD=standard deviation.

***Table 11 AA reference range in CSF.*** Data relating to the determination of a reference range for AA in CSF. For determination of the CSF AA reference range, the data were analysed and obvious outliers (n=6) were excluded.

| AA reference range in CSF | |
|---|---|
| ***n* number** | 99 |
| **AA concentration (µmol/L)** | |
| **Minimum value (mean – 2 SD)** | 103 |
| **Median** | 196 |
| **Maximum value (mean + 2 SD)** | 303 |
| **Mean ± SD** | 203 ± 50 |

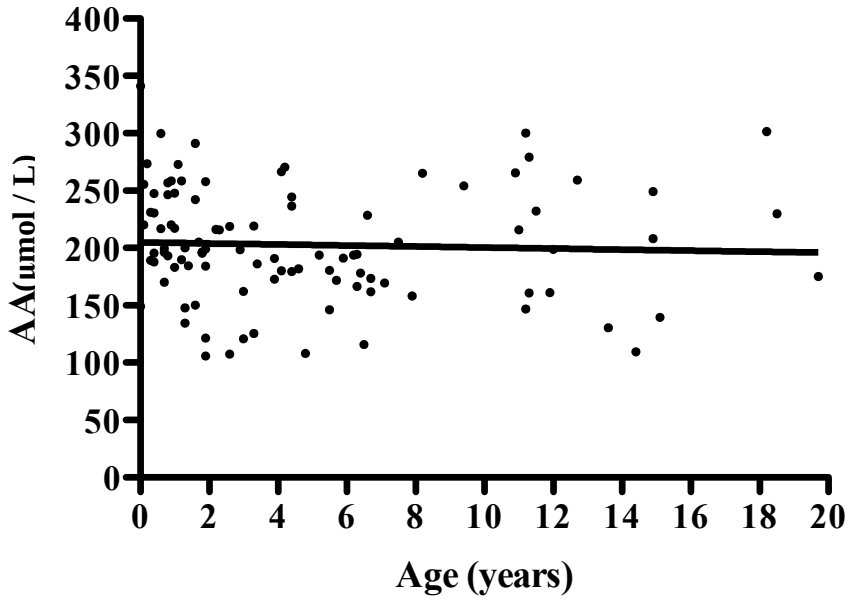


***Figure 50 Effect of age on AA concentration in CSF from a reference population.*** Correlation of CSF AA and age (r=-0.043, p=0.67, *n*=99). Samples were prepared in air saturated conditions at ambient temperature. Correlation determined by the Pearson test.

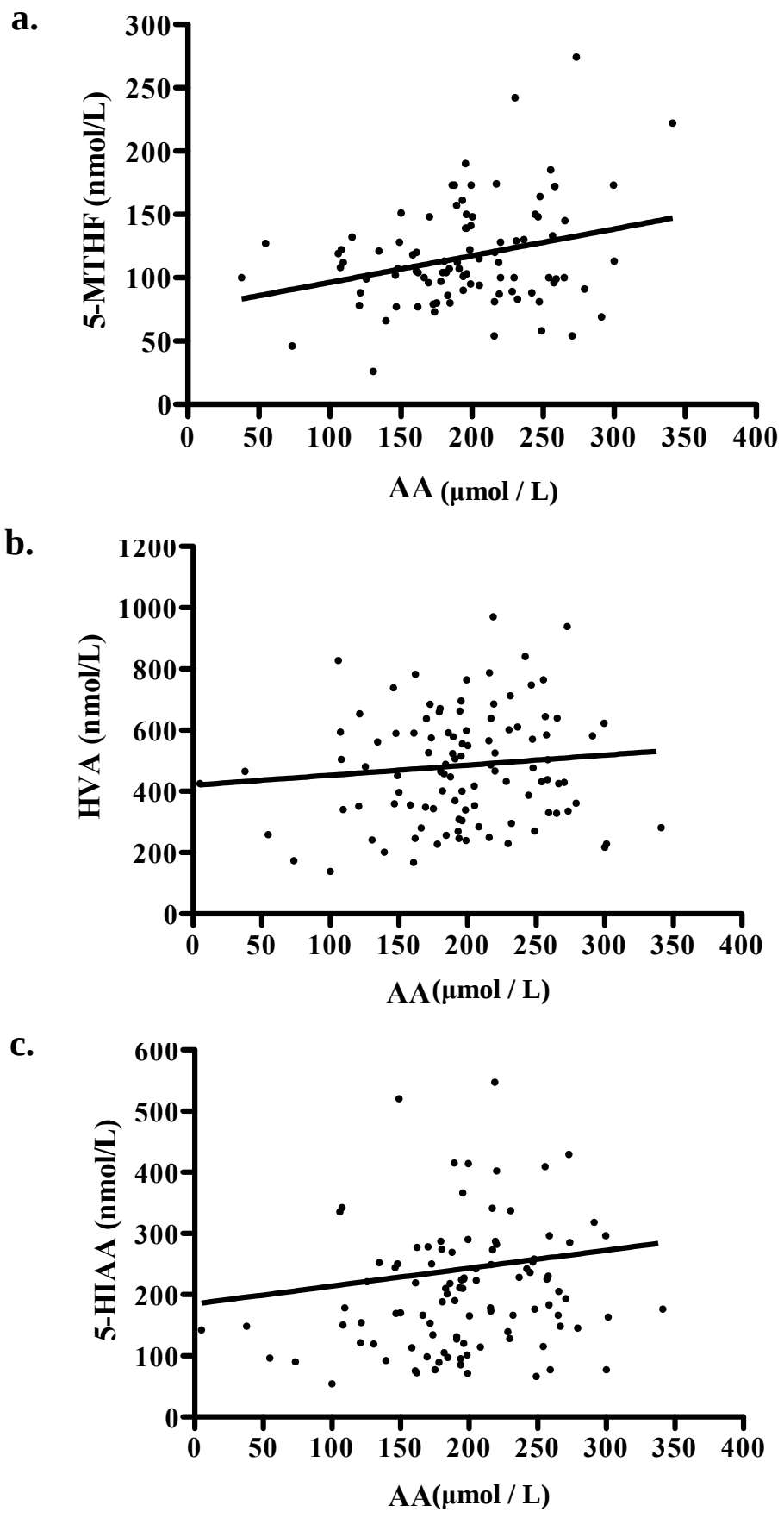


***Figure 51 Correlation of AA with 5-MTHF, HVA and 5-HIAA in CSF*. a.** Correlation of AA and 5-MTHF (r=0.284; p=0.002, *n*=96) **b.** Correlation of AA and HVA in CSF (r=0.111, p=0.27, *n*=97) **c.** Correlation of AA and 5-HIAA in CSF (r=0.173, p=0.08, *n*=98). Samples were prepared in air saturated conditions at ambient temperature. Correlations determined by the Pearson test.

(r=0.111, p=0.27, *n*=97) (Figure 51b), and AA and 5-HIAA (r=0.173, p=0.08, *n*=98) (Figure 51c).

### 5.5.4 Correlation between 5-MTHF and 5-HIAA in CSF, but not with 5-MTHF and HVA

5-MTHF, HVA and 5-HIAA concentrations were determined in the same CSF samples utilised to determine the reference range for AA in CSF (*n*=105). The data were analysed and outliers for both HVA and 5-HIAA tested (*n*=5, *n*=4, for HVA and 5-HIAA correlations with 5-MTHF, respectively) were excluded. Since 5-MTHF, HVA and 5-HIAA concentrations in CSF are age dependent, multivariate analysis of the data was performed, which removes the effect of age on the parameters when testing for correlations (see section 2.9). A non-significant correlation was observed between 5-MTHF and HVA (r=0.187, p=0.11, *n*=100) (Figure 52a). However, a significant positive correlation was observed between 5-MTHF and 5-HIAA (r=0.234, p=0.03, *n*=101) (Figure 52b).

### 5.5.5 CSF AA concentration is low in a proportion of patients with low CSF 5-MTHF

To further evaluate the relationship between AA and 5-MTHF in CSF, CSF AA concentration was measured in CSF of patients with low CSF 5-MTHF (*n*=21) (Table 12). Using the in-house CSF AA reference range established in this Chapter, 8 individuals (38%, Patients 1-8 inclusive) with low CSF 5-MTHF, also had evidence of a CSF AA deficiency (Figure 53; Table 13).

**a.**

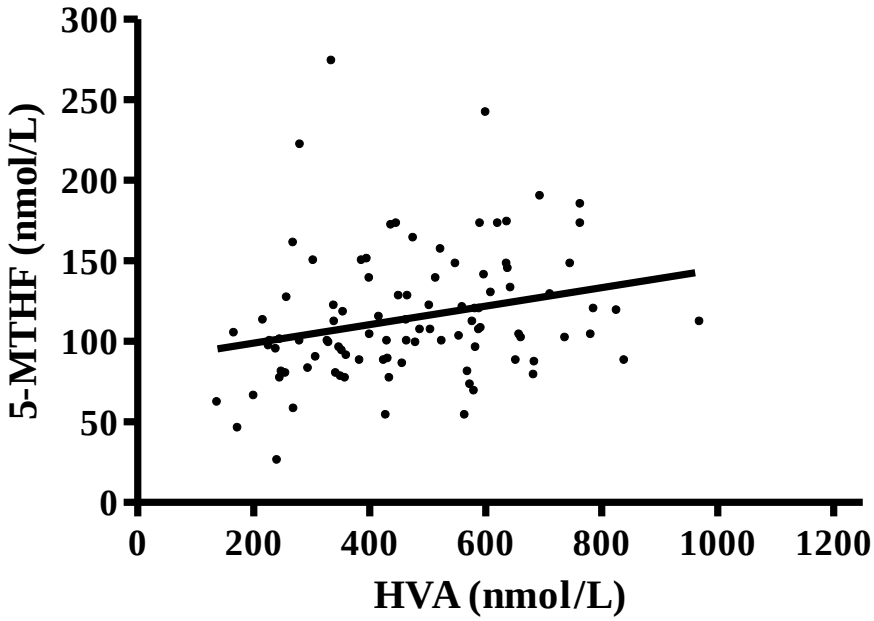


**b.**

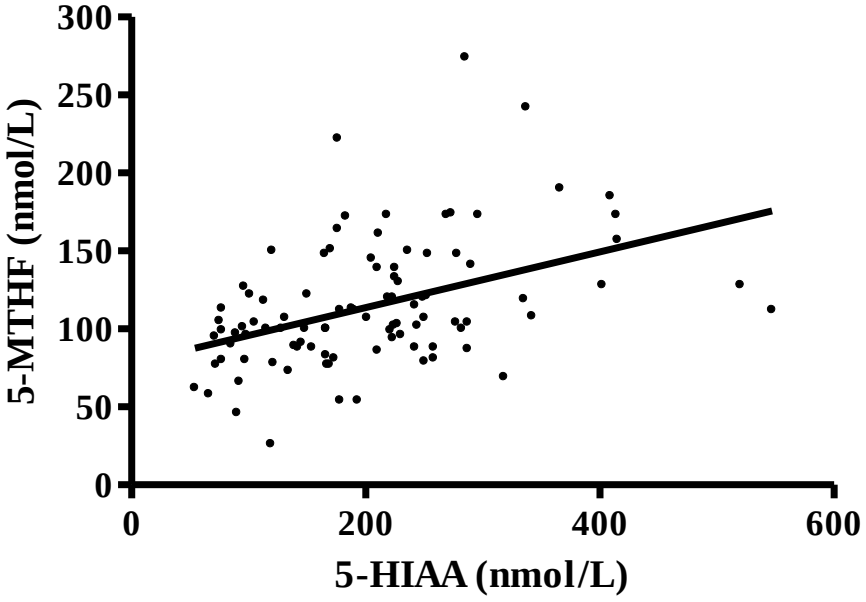


***Figure 52 Correlation of 5-MTHF with HVA and 5-HIAA in CSF*. a.** Correlation of 5-MTHF and HVA (r=0.187, p=0.11, *n*=100) **b.** Correlation of 5-MTHF and 5-HIAA in CSF (r=0.234, p=0.03, *n*=101). Samples were prepared in air saturated conditions at ambient temperature. Correlations determined by multivariate analysis.

***Table 12 CSF AA analysis in patients with low CSF 5-MTHF.*** Data relating to the determination of CSF AA and 5-MTHF in patients with low CSF 5-MTHF.

| CSF AA measurement in patients with a documented CSF 5-MTHF deficiency | | |
|---|---|---|
| **Sample parameters** | AA (µmol/L) | 5-MTHF (nmol/L) |
| **Minimum value** | 13 | 8 |
| **Median** | 131 | 43 |
| **Maximum value** | 300 | 67 |
| **Mean ± SD** | 134 ± 84 | 41 ± 4 |

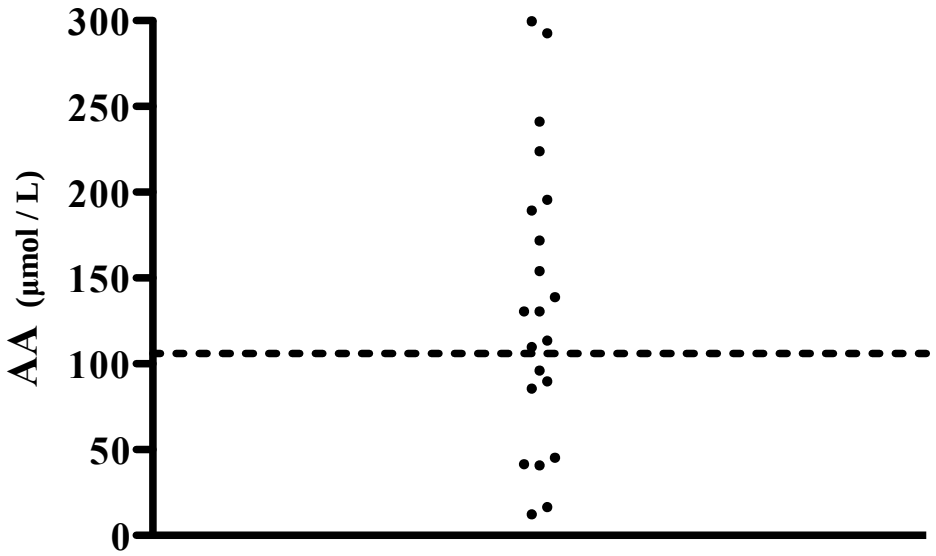


***Figure 53 Distribution of CSF AA concentrations in 21 patients with low CSF 5-MTHF*.** The age-independent AA reference range utilised was 103 – 303 µmol/L. The dotted line represents the lower CSF AA reference range value of 103 µmol/L.

***Table 13 Patients with low CSF 5-MTHF and corresponding CSF AA status.*** CSF 5-MTHF reference ranges are dependent on age and the reference range used are according to the reference ranges used in the Neurometabolic Unit at the National Hospital for Neurology and Neurosurgery, London, UK (see Table 5). The age-independent AA reference range utilised was 103-303 µmol/L, as described in this Chapter. Concentrations of CSF 5-MTHF or AA below the lower reference range limit are highlighted in bold.

| **Patient** | **Age at CSF sampling (years)** | **Sex** | **Major clinical features** | **CSF 5-MTHF nmol/L (reference range)** | **CSF AA(µmol/L)** |
|---|---|---|---|---|---|
| 1 | 41.5 | M | Generalised muscle twitches | **22** (46-160) | **96** |
| 2 | 9.7 | F | Chorea and involuntary movements, myopathic | **62** (72-172) | **90** |
| 3 | 2.6 | F | Movement disorder, seizures | **48** (52-178) | **45** |
| 4 | 53.8 | M | Seizures, progressive dystonia, ataxia | **35** (46-160) | **17** |
| 5 | 3.7 | M | Developmental delay, impaired vision | **44** (52-178) | **12** |
| 6 | 1.5 | M | Developmental delay, seizures, folate malabsorption | **<10** (72-305) | **40** |
| 7 | 1.7 | F | Neuroregression | **52** (72-305) | **42** |

| | | | | | |
|---|---|---|---|---|---|
| 8 | 0.7 | F | Seizures, developmental delay | **63** (72-172) | **86** |
| 9 | 14.6 | F | Paroxysmal dystonia (exercise-induced) | **26** (46-160) | 131 |
| 10 | 2.9 | M | Dihydropteridine reductase deficiency | **8** (52-178) | 131 |
| 11 | 6.4 | M | Ptosis, loss of motor skills | **43** (72-172) | 293 |
| 12 | 15.8 | M | Muscle wasting | **24** (46-160) | 139 |
| 13 | 1.8 | M | Developmental delay, visual impairment, seizures | **67** (72-305) | 172 |
| 14 | 15.9 | M | Dystonia, myoclonic jerks | **39** (46-160) | 224 |
| 15 | 11.9 | F | Developmental delay | **42** (46-160) | 196 |
| 16 | 6.7 | F | Previous low CSF 5-MTHF deficiency – now on treatment | **26** (72-172) | 241 |
| 17 | 6.8 | F | Developmental delay, seizures, choreo-athetosis, Missense *FOLR1* mutation in exon 5 [c.335A>T; p.N112I] (Patient 4 in Chapter 3) | **<10** (72-172) | 189 |

| | | | | | |
|---|---|---|---|---|---|
| 18 | 41.6 | M | Progressive generalised dystonia, tremor | **45** (46-160) | 154 |
| 19 | 5.2 | F | Encephalitis | **66** (72-172) | 108 |
| 20 | 9.7 | M | Seizures, severe behavioural problems, psychosis | **58** (72-172) | 114 |
| 21 | 9.8 | M | Spastic diplegia | **61** (72-172) | 300 |

## 5.6 Discussion

In Chapter 4, AA was shown to confer protection of 5-MTHF and as a consequence of the relative stability of 5-MTHF in CSF, AA was implicated as a biologically relevant protective factor of 5-MTHF in the CNS. In view of these observations and since CFD is diagnosed in the absence of a peripheral folate deficiency in the CSF compartment of the CNS (Ramaekers and Blau, 2004), the relationship between AA and 5-MTHF in CSF was examined in this Chapter. In order to facilitate this investigation, development and utilisation of a reliable HPLC-ECD method for analysis of AA concentration in CSF was carried out (Nagy and Degrell, 1989). Optimisation, linearity, recovery, stability and reproducibility of the method were demonstrated. An in-house, age independent reference range for AA in CSF was also determined.

A significant positive correlation was demonstrated between AA and 5-MTHF in CSF. Since AA, like 5-MTHF, is an essential water-soluble vitamin that is actively transported into the CNS from the periphery (Harrison and May, 2009; Hyland et al., 2010; Rice, 1999), such a correlation may be a reflection that both AA and 5-MTHF status is dependent upon dietary intake and active transport into the CSF compartment (Grapp et al., 2013; Liang et al., 2001). However, this correlation could also indicate an antioxidant protective role of AA towards 5-MTHF. This suggestion is supported by the observation of enhanced serum 5-MTHF in individuals also taking AA (Verlinde et al., 2008). The significant positive correlation between these two water-soluble vitamins also adds credence to the hypothesis that AA may be one of a number of biologically relevant factors needed to conserve 5-MTHF concentrations within the normal physiological range in CSF. There were no clear correlations observed between AA and HVA or 5-HIAA suggesting that AA concentration may not directly impact upon the availability of these neurotransmitter metabolites in CSF.

The relationships between 5-MTHF and HVA or 5-HIAA were also examined. A significant positive correlation was observed between 5-MTHF and 5-HIAA. However, a non-significant correlation was observed between 5-MTHF and HVA, which suggests that 5-MTHF may not affect HVA concentration in CSF. These data are in accordance with a previous study (Verbeek et al., 2008), and partly in accordance with another study which concluded that children with decreased CSF 5-

MTHF concentrations also had concomitant decreased concentrations of 5-HIAA and HVA (Surtees et al., 1994). Non-significant correlations between CSF 5-MTHF and 5-HIAA and HVA have also been reported, which similarly, are partly in accordance with the data described here (Ormazabal et al., 2006). The correlation between 5-MTHF and 5-HIAA observed here cannot readily be explained. It has been suggested that 5-MTHF may regenerate tetrahydrobiopterin from quinoid dihydrobiopterin through 5,10-methylenetetrahydrofolate reductase (MTHFR) (Kaufman, 1991; Matthews and Kaufman, 1980). Since tetrahydrobiopterin is a cofactor for tryptophan hydroxylase, regeneration of tetrahydrobiopterin by 5-MTHF would link 5-MTHF to serotonin synthesis, and in turn, production of the metabolite 5-HIAA (Figure 54) (Clot et al., 2009). Another possible explanation for this correlation could be through neurotransmitter synaptic vesicle loading or release (Serrano et al., 2010; Surtees et al., 1994). Vesicular loading or release of neurotransmitters depends upon energy metabolism and ATP production (Bai et al., 2001). Since 5-MTHF is involved in *de novo* purine and thymidylate synthesis (MacFarlane et al., 2011; Samsonoff et al., 1997), decreased levels of 5-MTHF may disturb mtDNA synthesis and subsequently lead to mitochondrial dysfunction.

When considering the cohort of 21 patients with a CSF 5-MTHF deficiency in this Chapter, 38% were shown to also have evidence of an AA deficiency (Patients 1-8). However, there was no obvious link between AA concentration and the degree of CSF 5-MTHF deficiency observed in these patients. Although this was not a clinical evaluation study and only minimal clinical details were available, the clinical data reflect the known heterogeneity of patients presenting with a CSF 5-MTHF deficiency. It is of interest to note that AA deficiency could be demonstrated in a patient with folate malabsoption (Patient 6) but not in Patient 17 (Patient 4 in Chapter 3) who had a novel missense *FOLR1* mutation in exon 5 [c.335A>T; p.N112I]. Whilst AA deficiency was not universal amongst the cohort of patients described, this finding may indicate that for a significant subset of individuals with a CSF 5-MTHF deficiency, the biochemical interaction between these two water-soluble vitamins deserves further evaluation. In view of the positive correlation between CSF AA and 5-MTHF demonstrated in this Chapter, it could be hypothesised that the deficiency of CSF AA documented in Patients 1-8 may be a factor determining CSF 5-MTHF availability.

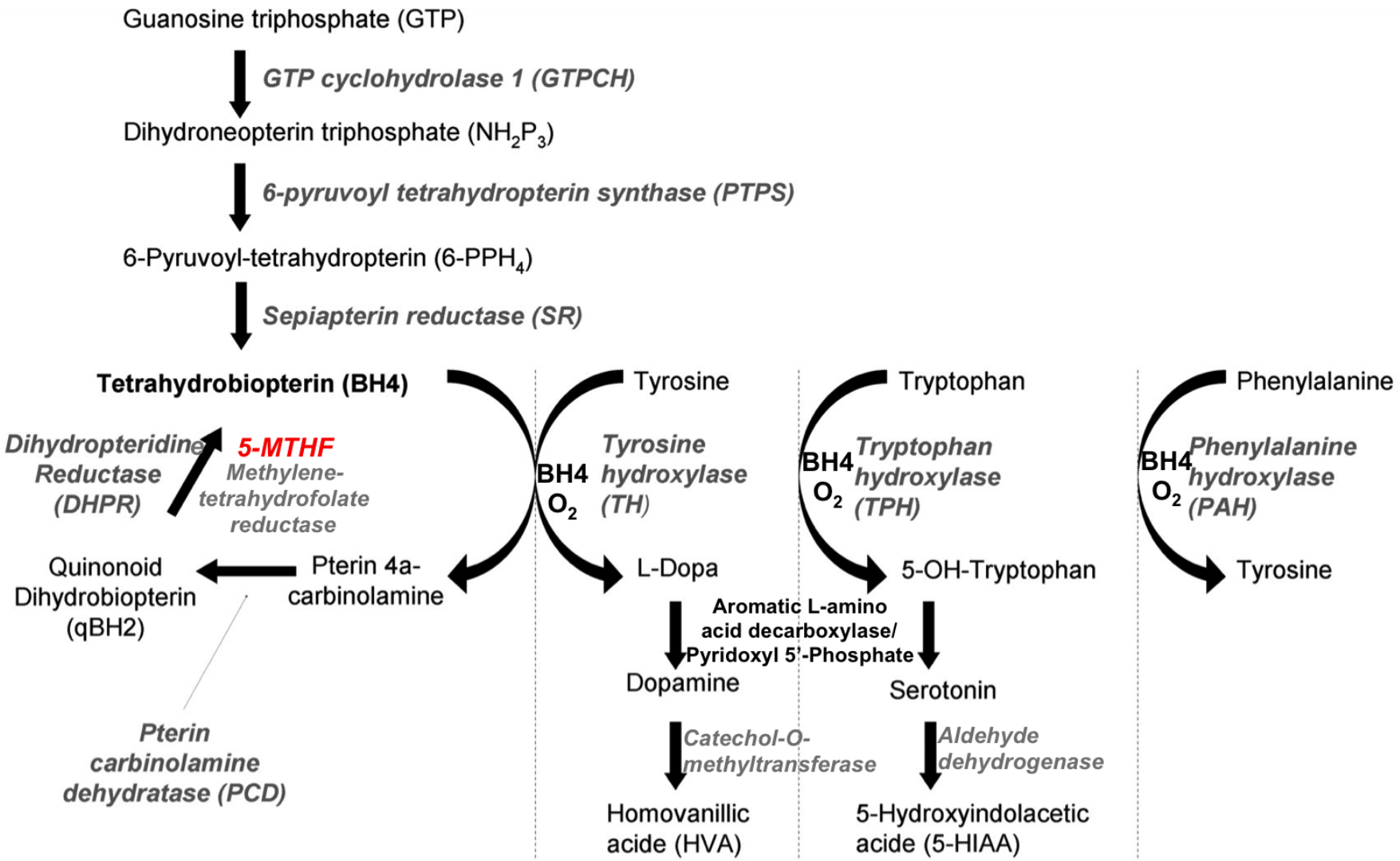


***Figure 54 Synthesis and catabolism of dopamine and serotonin.*** Dopamine and serotonin are formed from the amino acids tyrosine and tryptophan, respectively. Tetrahydrobiopterin (BH4) is formed in a three-step pathway from GTP and is regenerated from quinoid dihydrobiopterin by dihydropteridine reductase with 5-MTHF as a cofactor. Tetrahydrobiopterin is the cofactor for tyrosine hydroxylase, tryptophan hydroxylase and phenylalanine hydroxylase, together with oxygen. Aromatic L-amino acid decarboxylase and pyridoxal 5′-phosphate are required for the conversion of L-Dopa to dopamine and 5-hydroxytryptophan to serotonin. Dopamine and serotonin are rapidly metabolised to form HVA and 5-HIAA, respectively, and these metabolites are measured in CSF to provide an indication of the overall turnover of these neurotransmitters. Noradrenaline may be formed from dopamine via the activity of dopamine-β-hydroxylase. Figure adapted from Clot et al. (2009).

Interestingly, a CSF 5-MTHF deficiency was observed in one patient with dihydropteridine reductase deficiency (Patient 10). Previous studies have also reported similar findings (Irons et al., 1987; Kaufman, 1991; Smith et al., 1985). The deficiency in CSF 5-MTHF in this patient may be attributed to quinoid dihydrobiopterin interfering with folate metabolism. Dihydropteridine reductase and 5,10-methylenetetrahydrofolate reductase catalyse the production of tetrahydrobiopterin from quinoid dihydrobioptein (Matthews and Kaufman, 1980). 5,10-Methylenetetrahydrofolate reductase uses 5-MTHF as a coenzyme for the reaction, which results in the production of 5,10-methylenetetrahydrofolate (Bailey, 2010). In the absence of dihydropteridine reductase, quinoid dihydrobiopterin accumulates and 5-MTHF levels may be depleted owing the activity of 5,10-methylenetetrahydrofolate reductase (Kaufman, 1991). Alternatively or in addition, dihydrofolate reductase may also catalyse the production of tetrahydrobiopterin from quinoid dihydrobiopterin (Crabtree and Channon, 2011). In this reaction, dihydrofolate reductase uses tetrahydrofolate as a coenzyme, which results in the production of dihydrofolate. Similarly, in the absence of dihydropteridine reductase, quinoid dihydrobiopterin accumulates and tetrahydrofolate levels may be depleted owing the activity of dihydrofolate reductase, which in turn, impedes one-carbon metabolism (Stahl, 2007). In general, the role of 5-MTHF in regenerating tetrahydrobiopterin from quinoid dihydrobiopterin, catalysed by 5,10-methylenetetrahydrofolate reductase, provides an escape from the “methyl trap” (see section 1.4.4.1) (Kaufman, 1991).

## 5.7 Conclusion

In conclusion, AA may be a significant antioxidant protective factor that determines the availability of 5-MTHF in CSF. AA deficiency was not universal among the CFD patients studied, but it was only possible to examine a relatively small number of patients during this study. This finding may suggest that for a significant subset of individuals with CFD, the biochemical interaction between these two vitamins deserves further evaluation. CSF AA deficiency may be a factor governing 5-MTHF availability in those patients with a documented CSF 5-MTHF deficiency.

# Chapter 6
# The impact of mitochondrial respiratory chain enzyme inhibition in SH-SY5Y cells or selenite treatment of SH-SY5Y cells on the stability of 5-MTHF in extracellular minimal medium

# 6. The impact of mitochondrial respiratory chain enzyme inhibition in SH-SY5Y cells or selenite treatment of SH-SY5Y cells on the stability of 5-MTHF in extracellular minimal medium

## 6.1 Introduction

As shown in Chapter 3, low CSF 5-MTHF is associated in a number of patients with mitochondrial RCE defects. Complex I and complex IV deficiency were the most frequently observed skeletal muscle mitochondrial RCE defects in this Chapter. The mitochondrial RC is considered to be a major quantitative source of intracellular ROS production (see section 1.1.3) (Boveris and Chance, 1973; Boveris et al., 1972; Loschen and Azzi, 1975). In conditions associated with mitochondrial dysfunction, including mitochondrial RCE defects, an increase in electron leakage from the mitochondrial RC and ROS generation may be plausible. Previous studies have demonstrated that partial inhibition of the mitochondrial RC, to a degree insufficient to perturb oxidative phosphorylation, can lead to an increase in ROS production (Jacobson et al., 2005; Sipos et al., 2003). Studies documented in Chapter 4 demonstrated the susceptibility of 5-MTHF to oxidative catabolism in the presence of hydroxyl radicals. Therefore, increased ROS production as a consequence of mitochondrial RC dysfunction could provide a mechanistic link between mitochondrial disorders and CFD.

Additionally in Chapter 4, the effect of selenite, GSH and selenite, and GSH and selenite at a ratio of 40:1 on the stability of endogenous 5-MTHF in CSF was examined. As discussed in section 1.6.2.1, elevated CSF selenium concentrations have been documented in six patients with KSS (Tondo et al., 2011) but selenium was not implicated as a factor responsible for CFD in these patients and the data were not correlated to 5-MTHF availability. Metabolism of selenium may result in increased ROS production as a consequence of selenide redox cycling with reduced thiols, for example GSH (Chen et al., 2007a; Tarze et al., 2007; Yan and Spallholz, 1993). In Chapter 4 the stability of 5-MTHF in CSF was unaffected following the addition of selenite, GSH plus selenite and GSH plus selenite at a ratio of 40:1. Since CSF contains endogenous antioxidants (Alho et al., 1998; Kolmakova et al., 2010), this system may not have represented an effective model to study the potential impact of selenite on the stability of 5-MTHF. It was suggested in section

4.7 that the presence of a cellular environment may facilitate selenium metabolism and redox cycling with reduce thiols in order to propagate ROS (Yan and Spallholz, 1993).

In this Chapter, the effect of partial inhibition of mitochondrial complex I or complex IV, or selenite treatment of SH-SY5Y cells (see section 2.4.1) on extracellular 5-MTHF stability was determined. In view of the ability of AA to confer protection of 5-MTHF, as demonstrated in Chapters 4 and 5, co-incubation of AA with 5-MTHF was carried out in studies where loss of 5-MTHF was observed.

## 6.2 Aims

1. To examine the effect of partial inhibition of the mitochondrial RC at the level of complex I or complex IV on the stability of 5-MTHF in the extracellular minimal medium.

2. To examine the effect of selenite treatment of SH-SY5Y cells on the stability of 5-MTHF in the extracellular minimal medium.

3. To examine the ability of AA to confer protection of 5-MTHF.

## 6.3 Acknowledgement

Part of the work presented in this Chapter has been published (Aylett et al., 2013). I can confirm that all of the work documented was my own.

## 6.4 Materials and Methods

### 6.4.1 Materials

Purchasing details of all materials used throughout this Chapter are described in section 2.1, unless otherwise stated.

### 6.4.2 Treatment solutions and cell culture medium

*5-MTHF*

5-MTHF stock solutions as indicated in section 6.5 were prepared fresh for each experiment in minimal medium (pH 7.4).

*Rotenone*

Rotenone stock solutions as indicated in section 6.5 were prepared fresh for each experiment in HPLC grade ethanol. Rotenone is commonly used in studies to inhibit mitochondrial complex I activity (Shaikh and Nicholson, 2009). It is an irreversible, competitive inhibitor that binds to the ubiquinone binding site of complex I (Adam-Vizi, 2005).

*AA*

An AA stock solution as indicated in section 6.5 was prepared fresh for each experiment in minimal medium (pH 7.4).

*MitoSOX™ Red*

MitoSOX™ Red was prepared according to the manufacturer's instructions (Invitrogen Ltd). Briefly, 50 µg of reagent was dissolved in 13 µL of DMSO to make a stock solution of 5 mmol/L as indicated in section 6.5.

*Potassium cyanide*

Potassium cyanide (KCN) stock solutions as indicated in section 6.5 were prepared fresh for each experiment in HPLC grade water. KCN is commonly used in studies to inhibit mitochondrial complex IV activity. It is an irreversible inhibitor that binds to the $Haem_{a3}$-$Cu_B$ binuclear centre of complex IV (Way, 1984).

*Sodium selenite*

Selenite stock solutions as indicated in section 6.5 were prepared fresh for each experiment in HPLC grade water.

*Minimal medium*

Minimal medium was prepared fresh every 4 weeks and consisted of 44 mmol/L sodium bicarbonate, 110 mmol/L sodium chloride, 1.8 mmol/L calcium chloride, 5.4 mmol/L magnesium sulphate, 0.92 mmol/L sodium phosphate monobasic and 5 mmol/L D-glucose prepared in sterile cell culture grade water adjusted to pH 7.4 with $CO_2$. Minimal medium was stored at +4°C when not in use and warmed to +37°C prior to cell culture. The pH was checked and, if necessary, re-adjusted to pH 7.4 with $CO_2$ with every use. Minimal medium was used to culture cells during experiments detailed in section 6.5. Minimal medium was used as a maintenance medium to keep the cells alive by providing essential components including glucose, and to reduce cell proliferation.

### 6.4.3 Measurement of 5-MTHF

5-MTHF was measured by HPLC as described in section 2.3.

### 6.4.4 SH-SY5Y cell culture

SH-SY5Y cells were cultured according to the protocols described in section 2.4. SH-SY5Y cells were used because this model system has been extensively used for neurological research. Undifferentiated cells were used owing to their ability to proliferate for long periods of time and are a good model for studying toxicity and oxidative stress (Cheung et al., 2009; Schneider et al., 2011).

### 6.4.5 Measurement of mitochondrial respiratory chain enzyme activity in SH-SY5Y cells

Mitochondrial RCE assays were performed as described in section 2.5. Mitochondrial RCE activities were calculated as a ratio to citrate synthase, a mitochondrial marker enzyme, to compensate for mitochondrial enrichment of the muscle samples, and as expressed as nmol/min/mg of protein, to compensate for changes in cell number.

### 6.4.6 Total protein assay

Total protein was measured as described in section 2.6.

### 6.4.7 Flow cytometry

Flow cytometric analysis was carried out as described in section 2.7.

### 6.4.8 Data analysis

Data analyses were carried out as described in section 2.9 and section 4.4.5.

## 6.5 Experimental protocol

### 6.5.1 5-MTHF stability in extracellular minimal medium

Cells were cultured as described in section 2.4. After a period of 24 hours of cell stabilisation and attachment, growth medium (DMEM/F-12 + 100 ml/L FBS + 5 mmol/L L-glutamine) was removed and replaced with minimal medium containing 5-MTHF. Minimal medium containing 5-MTHF was prepared by adding 100 µL or 30 µL of 50 µmol/L 5-MTHF (final concentrations: 500 nmol/L or 150 nmol/L) made up in minimal medium (pH 7.4), to 9,900 µL or 9,970 µL of minimal medium (total volume: 10 ml). The minimal medium was mixed thoroughly. Control flasks were prepared in the absence of cells. Cell containing flasks and control flasks were incubated at +37°C in 5% $CO_2$ for 30 minute timed intervals, from 0-150 minutes. At each 30 minute time interval, minimal media samples (120 µL) were immediately snap frozen in liquid nitrogen and stored at -80°C until analysis of 5-MTHF by HPLC as described in section 2.3. All subsequent experiments were compared to the stability of 5-MTHF in minimal medium in the presence of SH-SY5Y cells used as a control as described in section 6.6.1.

### 6.5.2 5-MTHF stability in extracellular minimal medium of complex I inhibited SH-SY5Y cells in the absence and presence of AA

Initially, complex I activity in rotenone treated cells was determined. Cells were cultured as described in section 2.4. After a period of 24 hours of cell stabilisation and attachment, growth medium was removed and replaced with rotenone containing growth medium. Rotenone containing growth medium was prepared by adding 5 µL or 10 µL of 100 µmol/L rotenone (final concentrations: 50 nmol/L or 100 nmol/L) made up in ethanol and 0.2 µm sterile filtered, to 9,995 µL or 9,990 µL of growth medium (total volume: 10 ml). An equivalent volume of 0.2 µm sterile filtered ethanol was added to an equivalent volume of growth medium (control). The growth media preparations were thoroughly mixed. Cells were left to incubate at +37°C in 5% $CO_2$ for 24 hours. Following incubation, cells were harvested as described in section 2.4. Complex I and citrate synthase activity were measured as described in section 2.5. Total protein was measured as described in section 2.6. A rotenone concentration of 100 nmol/L and cell incubation period of 24 hours were used for all subsequent experiments (see section 6.6.2).

Rotenone (100 nmol/L) containing growth medium was prepared and cells cultured and incubated as described in section 6.5.2 (above). After 24 hours cell incubation, rotenone containing growth medium or control growth medium was removed and replaced with either minimal medium containing 5-MTHF (as described in section 6.5.1) or minimal medium containing 5-MTHF and AA. Minimal medium containing 5-MTHF and AA was prepared by adding 100 µL or 30 µL of 50 µmol/L 5-MTHF (final concentrations: 500 nmol/L or 150 nmol/L) and 100 µL of 15 mmol/L AA (final concentration: 150 µmol/L), made up in minimal medium (pH 7.4), to 9,800 µL or 9,870 µL of minimal medium (total volume: 10 ml). The minimal medium was mixed thoroughly. Cells were incubated at +37°C in 5% $CO_2$ for 150 minutes (the conditions 5-MTHF is known to be stable for in CSF as determined by experiment 4.5.1). Following incubation, minimal media samples (120 µL) were immediately snap frozen in liquid nitrogen and stored at -80°C until analysis of 5-MTHF by HPLC as described in section 2.3.

### 6.5.3 Measurement of mitochondrial superoxide generation in complex I inhibited SH-SY5Y cells

Rotenone (100 nmol/L) containing growth medium was prepared, and cells cultured and incubated as described in section 6.5.2. After 24 hours cell incubation, rotenone containing growth medium and control growth medium were removed and replaced with minimal medium containing MitoSOX$^{TM}$ Red or control minimal medium. Protected from light, minimal medium containing MitoSOX$^{TM}$ Red was prepared by adding 10 µL of 5 mmol/L MitoSOX$^{TM}$ Red (final concentration: 5 µmol/L) made up in DMSO, to 9990 µL of minimal medium (total volume: 10 ml). An equivalent volume of DMSO was added to an equivalent volume of control minimal medium. The minimal media preparations were thoroughly mixed. Cells were incubated in the dark, owing to the light sensitivity of the MitoSOX$^{TM}$ Red stain, at +37°C in 5% $CO_2$ for 30 minutes. Following incubation, cells were harvested as described in section 2.4 and immediately analysed by flow cytometry as described in section 2.7.

### 6.5.4 5-MTHF stability in extracellular minimal medium of complex IV inhibited SH-SY5Y cells

Initially, complex IV activity in KCN treated cells was determined. Cells were cultured as described in section 2.4. After a period of 24 hours of cell stabilisation and attachment, growth medium was removed and replaced with KCN containing

growth medium. KCN containing growth medium was prepared by adding 100 µL of 100 mmol/L KCN (final concentration: 1 mmol/L) made up in ultrapure water and 0.2 µm sterile filtered, to 9,900 µL of growth medium (total volume: 10 ml). An equivalent volume of 0.2 µm sterile filtered ultrapure water was added to an equivalent volume of growth medium (control). The minimal media preparations were thoroughly mixed. Cells were left to incubate at +37°C in 5% $CO_2$ for 24 hours. Following incubation, cells were harvested as described in section 2.4. Complex IV and citrate synthase were measured as described in section 2.5. Total protein was measured as described in section 2.6. A KCN concentration of 1 mmol/L and cell incubation period of 24 hours were used for all subsequent experiments (see section 6.6.4).

KCN (1 mmol/L) containing growth medium was prepared, and cells cultured and incubated as described in section 6.5.4 (above). After 24 hours incubation, KCN containing growth medium and control growth medium were removed and replaced with minimal medium containing 5-MTHF as described in section 6.5.1. Cells were incubated at +37°C in 5% $CO_2$ for 150 minutes (the conditions 5-MTHF is known to be stable for in CSF as determined by experiment 4.5.1). Following incubation, minimal media samples (120 µL) were immediately snap frozen in liquid nitrogen and stored at -80°C until analysis of 5-MTHF by HPLC as described in section 2.3.

### 6.5.5 Measurment of mitochondrial superoxide generation in complex IV inhibited SH-SY5Y cells

KCN (1 mmol/L) containing growth medium was prepared and cells cultured and incubated as described in section 6.5.4. After 24 hours cell incubation, KCN containing growth medium and control growth medium were removed and replaced with either minimal medium containing MitoSOX$^{TM}$ Red or control minimal medium. Protected from light, minimal medium containing MitoSOX$^{TM}$ Red and control minimal medium was prepared as described in section 6.5.3. Cells were incubated in the dark, owing to the light sensitivity of the MitoSOX$^{TM}$ Red stain, at +37°C in 5% $CO_2$ for 30 minutes. Following incubation, cells were harvested as described in section 2.4 and immediately analysed by flow cytometry as described in section 2.7.

### 6.5.6 5-MTHF stability in extracellular minimal medium of selenite treated SH-SY5Y cells in the absence and presence of AA

Cells were cultured as described in section 2.4. After a period of 24 hours of cell stabilisation and attachment, growth medium was removed and replaced with selenite containing growth medium. Selenite containing growth medium was prepared by adding 20 µL, 100µL or 200 µL of 1 mg/L selenite (final concentrations: 2 µg/L, 10 µg/L or 20 µg/L) made up in ultrapure water and 0.2 µm sterile filtered, to 9,980 µL, 9,900 µL or 9,800 µL of growth medium (total volume: 10 ml). An equivalent volume of 0.2 µm sterile filtered ultrapure water was added to an equivalent volume of growth medium (control). The minimal media preparations were thoroughly mixed. Cells were left to incubate at +37°C in 5% $CO_2$ for 1 hour. Following incubation, selenite containing growth medium and control growth medium were removed and replaced with either minimal medium containing 5-MTHF or minimal medium containing 5-MTHF and AA as described in sections 6.5.1 and 6.5.2, respectively. Cells were incubated at +37°C in 5% $CO_2$ for 150 minutes (the conditions 5-MTHF is known to be stable for in CSF as determined by experiment 4.5.1). Following incubation, minimal media samples (120 µL) were immediately snap frozen in liquid nitrogen and stored at -80°C until analysis of 5-MTHF by HPLC as described in section 2.3.

### 6.5.7 Complex I activity in selenite treated SH-SY5Y cells

Selenite (2 µg/L, 10 µg/L and 20 µg/L) containing growth media was prepared and cells cultured and incubated as described in section 6.5.6. Following incubation, cells were harvested as described in section 2.4. Complex I and citrate synthase were measured as described in section 2.5. Total protein was measured as described in section 2.6.

### 6.5.8 Mitochondrial superoxide generation in selenite treated SH-SY5Y cells

Selenite (10 µg/L and 20 µg/L) containing growth media was prepared, and cells cultured and incubated as described in section 6.5.6. After 1 hour cell incubation, selenite containing growth medium and control growth medium were removed and replaced with either minimal medium containing MitoSOX$^{TM}$ Red or control minimal medium. Protected from light, minimal medium containing MitoSOX$^{TM}$ Red and control minimal medium was prepared as described in section 6.5.3. Cells were incubated in the dark, owing to the light sensitivity of the MitoSOX$^{TM}$ Red

stain, at +37°C in 5% $CO_2$ for 30 minutes. Following incubation, cells were harvested as described in section 2.4 and immediately analysed by flow cytometry as described in section 2.7.

## 6.6 Results

### 6.6.1 5-MTHF is more stable in extracellular minimal medium than in minimal medium alone

In view of the labile nature of 5-MTHF, as previously demonstrated in Chapter 4, the stability of 5-MTHF in minimal medium in the presence and absence of SH-SY5Y cells was initially determined. Stability was first determined in the presence of cells at an initial 5-MTHF concentration of 500 nmol/L, a concentration within the linearity of the 5-MTHF assay as shown in section 2.3 and comparable to concentrations used in previous studies (Opladen et al., 2006; Ormazabal et al., 2006). A 5-MTHF concentration of 284.3 ± 2.1 nmol/L was recorded at 0 minute. Over time, 5-MTHF progressively decreased in concentration (Figure 55a). An overall significant loss of 21% was observed at 150 minutes, compared to 0 minute ($p<0.05$). The stability of 5-MTHF at an initial concentration of 500 nmol/L was also determined in the absence of cells. A 5-MTHF concentration of 285.3 ± 1.7 nmol/L 5-MTHF was recorded at 0 minute. Over time, 5-MTHF progressively decreased in concentration (Figure 55a). An overall significant loss of 38% was observed at 150 minutes, compared to 0 minute ($p<0.001$). The decay of 5-MTHF in minimal medium was found to obey first order kinetics over the 150 minute time period analysed (Table 14). 5-MTHF (500 nmol/L) degraded at a faster rate in the absence of cells than in the presence of cells (Table 14).

Similar findings were observed when the stability of 5-MTHF in the presence of cells was determined at a more physiological CSF concentration of 150 nmol/L. This 5-MTHF concentration is within the CSF reference range across all ages (72-305 nmol/L [0-2 years], 52-178 nmol/L [2-5 years], 72-172 nmol/L [5-10 years], 46-160 nmol/L [10 years-adult]). A 5-MTHF concentration of 63.3 ± 3.7 nmol/L was recorded at 0 minute. Over time, 5-MTHF progressively decreased in concentration (Figure 55b). At 150 minutes, an overall loss of 24% was observed, compared to 0 minute. The stability of 5-MTHF at an initial concentration of 150 nmol/L was also determined in the absence of cells. A 5-MTHF concentration of 64.0 ± 4.5 nmol/L 5-MTHF was recorded at 0 minute. Over time, 5-MTHF progressively decreased in concentration (Figure 55b). An overall significant loss of

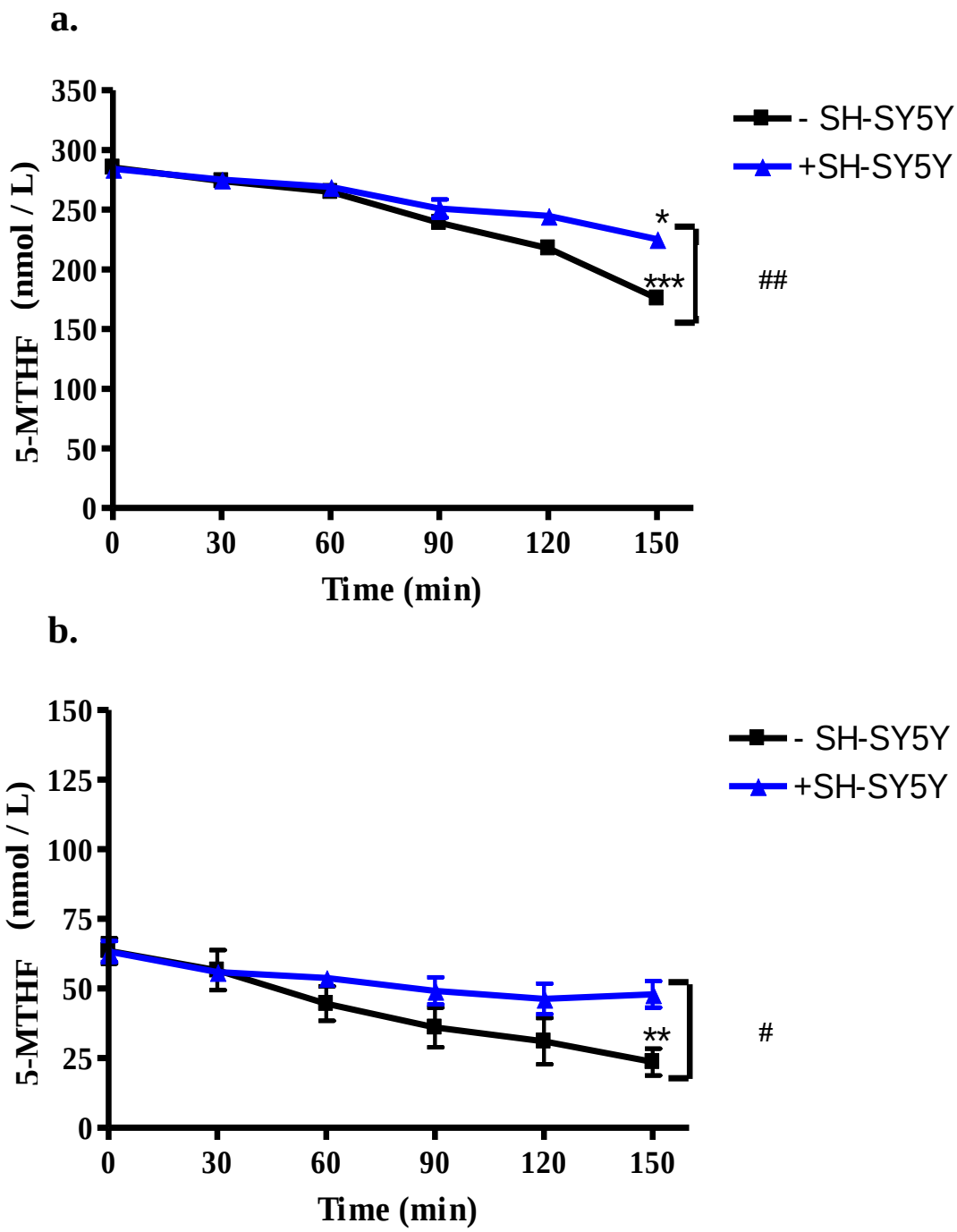


***Figure 55 5-MTHF stability in minimal medium in the absence and presence of SH-SY5Y cells.*** **a.** 5-MTHF stability at an initial concentration of 500 nmol/L and **b.** at an initial concentration 150 nmol/L. Samples were incubated in air saturated conditions at 37˚C. All values are mean ± SEM of 4 independent experiments. *p<0.05, **p<0.01, ***p<0.001 difference in comparison to 0 minute determined by one-way ANOVA followed by Bonferroni's multiple comparison test. #p<0.05, ##p<0.01 difference in comparison to absence of cells at 150 minutes (in brackets) determined by Student's t-test.

***Table 14 Calculated first order rate constant for 5-MTHF degradation in minimal medium in the absence and presence of SH-SY5Y cells.*** All values are mean ± SEM of 4 independent experiments.

| Conditions | Rate (k/min) |
|---|---|
| **+ SH-SY5Y (5-MTHF 500 nmol/L)** | 0.002 ± 0.0001 |
| **- SH-SY5Y (5-MTHF 500 nmol/L)** | 0.004 ± 0.0004 |
| **+ SH-SY5Y (5-MTHF 150 nmol/L)** | 0.006 ± 0.0001 |
| **- SH-SY5Y (5-MTHF 150 nmol/L)** | 0.009 ± 0.0002 |

63% was observed at 150 minutes, compared to 0 minute ($p<0.01$). The decay of 5-MTHF in minimal medium was found to obey first order kinetics over the 150 minute time period analysed (Table 14). 5-MTHF (150 nmol/L) degraded at a faster rate in the absence of cells than in the presence of cells (Table 14).

The differences between the concentration of 5-MTHF remaining at 150 minutes in the presence and absence of cells at both initial concentrations of 500 nmol/L and 150 nmol/L were statistically significant, ($p<0.001$, $p<0.05$) respectively (Figures 55a and 55b).

All subsequent experiments were compared to the stability of 5-MTHF in extracellular minimal medium in the presence of SH-SY5Y cells, used as a control.

### 6.6.2 Rotenone mediated mitochondrial complex I inhibition in SH-SY5Y cells causes a significant loss of 5-MTHF from extracellular minimal medium which is prevented by AA

As previously described in section 6.1, partial inhibition, to a degree insufficient to perturb oxidative phosphorylation, has been shown to increase ROS production (Jacobson et al., 2005). Threshold levels of complex I before major changes in rate of ATP synthesis or oxygen consumption, vary according to the *in vitro* model used. For example, *in situ* non-synaptic mitochondria have a complex I threshold of approximately 72% (Davey and Clark, 1996), whilst synaptic isolated nerve terminals have a complex I threshold of between 16% and 25% (Davey et al., 1998; Sipos et al., 2003). A rotenone concentration range of 50-100 nmol/L has previously been shown to inhibit complex I by approximately 50-60% in SH-SY5Y cells (Sherer et al., 2001). In addition, incubation of SH-SY5Y cells with 100 nmol/L rotenone for 24 hours, has previously been shown to increase ROS production (Xiong et al., 2013). Therefore, SH-SY5Y cells were incubated with 50 nmol/L or 100 nmol/L rotenone for 24 hours and mitochondrial complex I activity measured. A decrease in complex I activity of 40% was observed in cells treated with 50 nmol/L rotenone which was not significant when compared to control. Whereas, a significant decrease in complex I activity of 58% ($p<0.05$) was observed following 100 nmol/L rotenone treatment compared to control (Figure 56, Table 15). These effects were apparent when complex I activity was expressed as either a ratio to

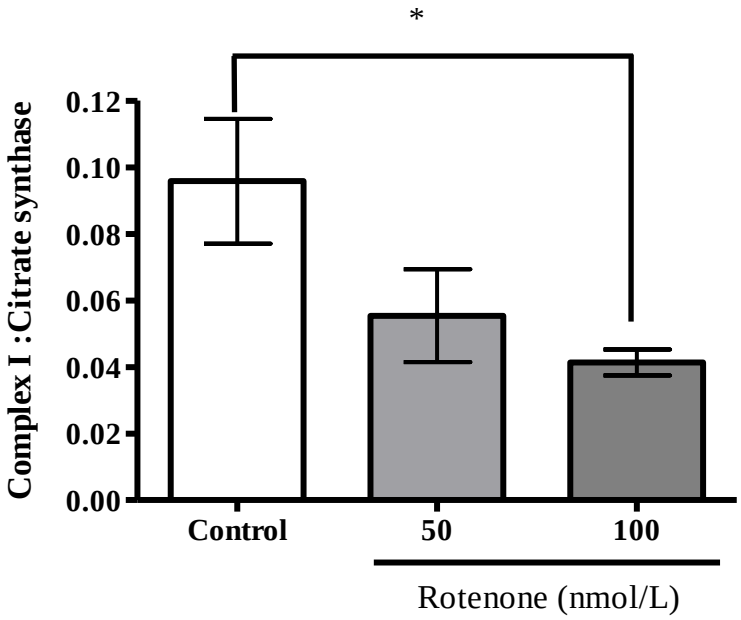


***Figure 56 Complex I activity in rotenone treated SH-SY5Y cells for 24 hours.*** Complex I activity is expressed as a ratio to citrate synthase. Rotenone treatment (50 nmol/L and 100 nmol/L) led to a 40% and 58% reduction in complex I activity, respectively. All values are mean ± SEM of 4 independent experiments. *$p<0.05$ determined by one-way ANOVA followed by Bonferroni's multiple comparison test.

***Table 15 Mitochondrial RCE activity in SH-SY5Y cells following rotenone or KCN treatment.*** Complex I activity (nmol/min/mg of protein), complex IV activity (nmol/min/mg of protein) and citrate synthase activity (nmol/min/mg of protein). Complex I % inhibition following rotenone treatment for 24 hours. Complex IV % inhibition following KCN treatment for 24 hours. All values are mean ± SEM of 4 independent experiments. *p<0.05 compared to control determined by one-way ANOVA followed by Bonferroni's multiple comparison test. ***p<0.001 compared to control determined by Student's t-test.

| Conditions | Complex I (nmol/min/mg of protein) | | Complex IV (nmol/min/mg of protein) | | Citrate Synthase (nmol/min/mg of protein) |
|---|---|---|---|---|---|
| | Activity | % inhibition | Activity | % inhibition | |
| **Control (no rotenone)** | 11.8 ± 2.1 | - | - | - | 125.0 ± 8.5 |
| **Rotenone 50 nmol/L** | 7.1 ± 2.4 | 40 | - | - | 125.0 ± 17.0 |
| **Rotenone 100 nmol/L** | * 4.9 ± 0.3 | 58 | - | - | 120.1 ± 4.9 |
| **Control (no KCN)** | - | - | 0.7 ± 0.05 | - | 123.2 ± 1.6 |
| **KCN 1 mmol/L** | - | - | *** 0.1 ± 0.03 | 86 | 122.2 ± 1.9 |

citrate synthase or as nmol/min/mg of protein (Figure 56; Table 15). This level of complex I inhibition did not appear to cause cell morbidity under a light microscope. In view of the data documented in the literature regarding increased ROS generation following partial inhibition of complex I (Davey and Clark, 1996; Jacobson et al., 2005) and statistical significance, a rotenone concentration of 100 nmol/L and cell incubation period of 24 hours were used for all subsequent experiments.

Using these culture conditions, the stability of 5-MTHF in extracellular minimal medium of rotenone (100 nmol/L) treated cells for 150 minutes was evaluated. Stability was first determined at an initial 5-MTHF concentration of 500 nmol/L. A 5-MTHF concentration of 257.6 ±9.3 nmol/L was recorded at 0 minute. A significant 5-MTHF loss of 25% from the extracellular minimal medium of rotenone treated cells was observed at 150 minutes, compared to control ($p<0.001$) (Figure 57a). A similar finding was observed when the experiment was carried out at an initial 5-MTHF concentration of 150 nmol/L. A 5-MTHF concentration of 64.0 ± 5.2 nmol/L was recorded at 0 minute. A significant 5-MTHF loss of 40% from the extracellular minimal medium of rotenone treated cells was observed at 150 minutes, compared to control ($p<0.01$) (Figure 57b).

Since rotenone (100 nmol/L) treatment of cells led to a statistically significant reduction in 5-MTHF remaining in the extracellular minimal medium compared to control, the ability of AA to counteract 5-MTHF decay in this system was evaluated. At an initial 5-MTHF concentration of 500 nmol/L, co-incubation of 5-MTHF with a physiological CSF concentration of AA of 150 µmol/L (Brau et al., 1984) in minimal medium in the presence of rotenone (100 nmol/L) treated cells, led to a significantly greater amount of 5-MTHF remaining in the minimal medium at 150 minutes of 18% ($p<0.01$) and 57% ($p<0.001$), when compared to control and 5-MTHF incubated with rotenone treated cells only, respectively (Figure 57a). Similarly, at the 5-MTHF initial concentration 150 nmol/L, co-incubation of 5-MTHF with AA (150 µmol/L) in minimal medium in the presence of rotenone treated cells, led to a significantly greater amount of 5-MTHF remaining in the minimal medium at 150 minutes of 30% ($p<0.05$) and 115% ($p<0.001$), when compared to control and 5-MTHF incubated with rotenone treated cells only (Figure 57b).

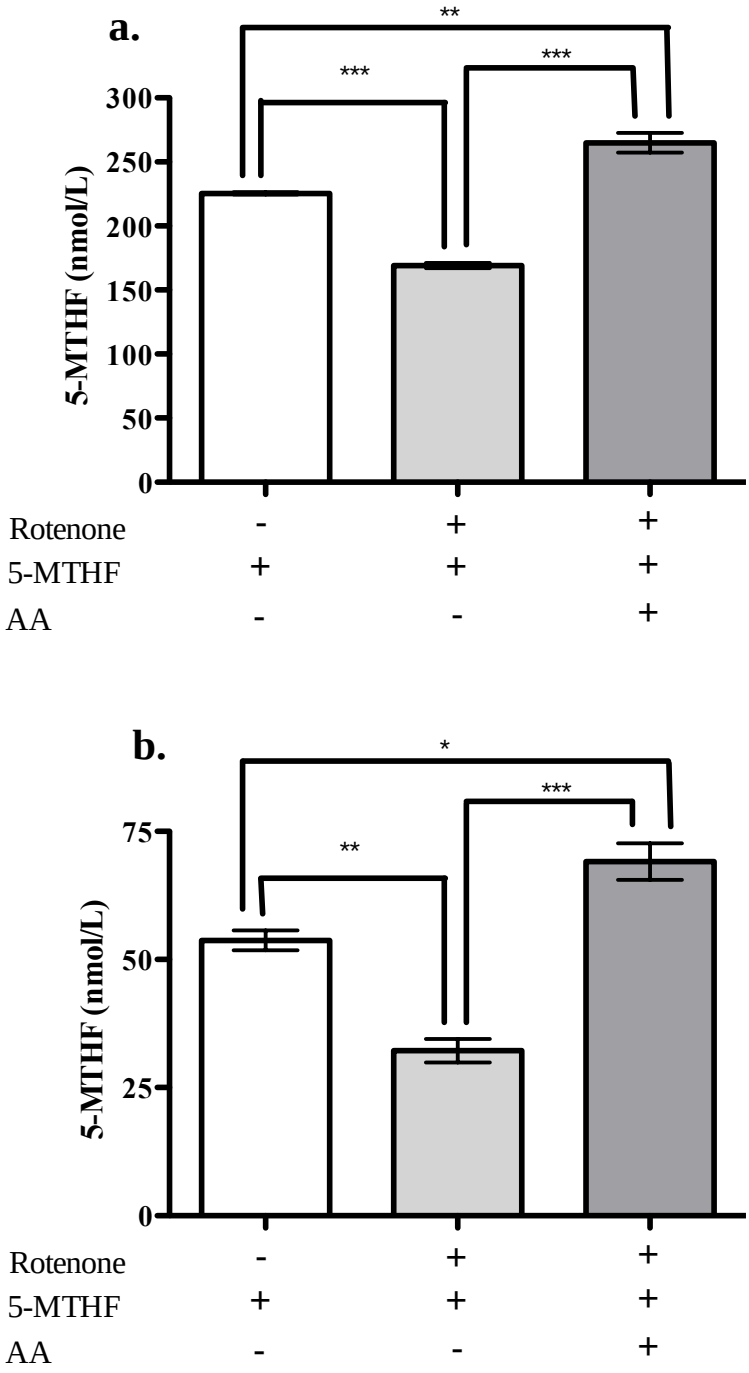


***Figure 57 5-MTHF stability in the extracellular minimal medium of SH-SY5Y cells pre-treated in the absence and presence of rotenone (100 nmol/L) for 24 hours, following a 150 minute incubation with or without AA (150 µmol/L).*** **a.** 5-MTHF stability at an initial concentration of 500 nmol/L and **b.** at an initial concentration 150 nmol/L. All values are mean ± SEM of 4 independent experiments. *p<0.05, **p<0.01, ***p<0.001 determined by one-way ANOVA followed by Bonferroni's Multiple comparison test.

### 6.6.3 Mitochondrial superoxide generation is significantly increased in rotenone treated SH-SY5Y cells

To elucidate whether rotenone (100 nmol/L) treatment of SH-SY5Y cells led to an increase in mitochondrial superoxide production, the MitoSOX$^{TM}$ Red assay system was utilised. A significant increase above basal levels in mitochondrial superoxide production of 23% was observed in rotenone (100 nmol/L) treated cells, compared to matched controls ($p<0.05$) (Figure 58).

### 6.6.4 KCN mediated complex IV inhibition in SH-SY5Y cells has no effect on 5-MTHF stability in extracellular minimal medium

As previously described in section 6.1, partial inhibition, to a degree insufficient to perturb oxidative phosphorylation, has been shown to increase ROS production (Jacobson et al., 2005). Threshold levels of complex IV before major changes in rate of ATP synthesis or oxygen consumption, vary according to the *in vitro* model used. For example, *in situ* non-synaptic mitochondria have a complex IV threshold of approximately 60% (Davey and Clark, 1996), whilst synaptic isolated nerve terminals have a complex IV threshold of >70% (Davey et al., 1998; Sipos et al., 2003). KCN at a concentration of 10 mmol/L for 24 hours has been shown to induce apoptosis in SH-SY5Y cells (Watabe and Nakaki, 2007). Therefore, a x10 lower concentration of KCN (1 mmol/L) was used to inhibit complex IV activity in SH-SY5Y cells and cells were incubated for 24 hours. This concentration and incubation time has previously been shown to induce a sustained 50% inhibition of complex IV in astrocytes (Hargreaves et al., 2007). A significant decrease in complex IV activity of 86% was observed following KCN treatment, compared to control ($p<0.001$). This effect was apparent when complex IV activity was expressed as either a ratio to citrate synthase or as nmol/min/mg of protein (Figure 59; Table 15). This level of complex IV inhibition did not appear to cause cell morbidity under a light microscope. In view of the complex IV respiratory thresholds (Davey and Clark, 1996; Davey et al., 1998; Sipos et al., 2003) and statistical significance, a KCN concentration of 1 mmol/L and cell incubation period of 24 hours were used for all subsequent experiments.

Using these culture conditions, the stability of 5-MTHF in the presence of KCN treated cells for 150 minutes was evaluated. Stability was first determined at an

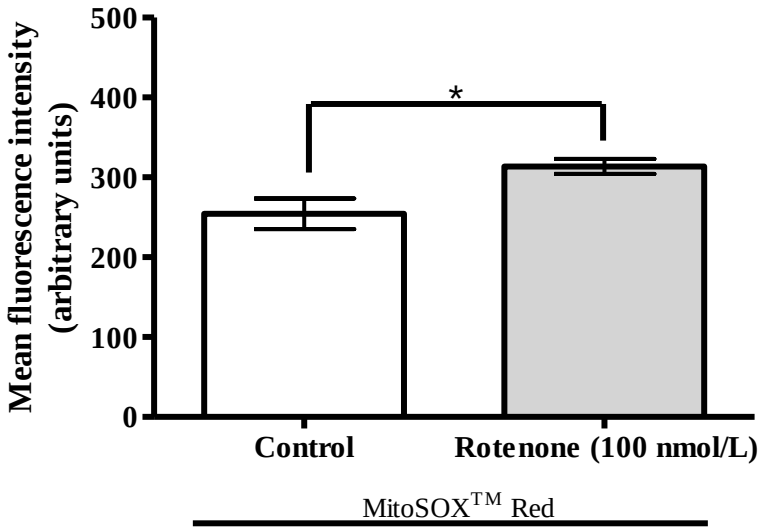


***Figure 58 Mitochondrial superoxide production in rotenone pre-treated SH-SY5Y cells for 24 hours, following a 30 minute incubation with MitoSOX™ Red.*** All values are mean ± SEM of 3 independent experiments. *p<0.05 determined by Student's t-test.

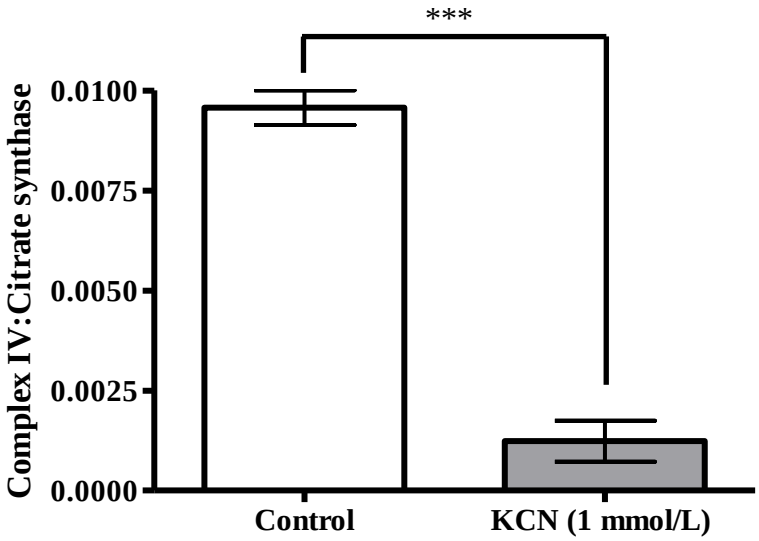


***Figure 59 Complex IV activity in KCN treated SH-SY5Y cells for 24 hours.*** Complex IV activity is expressed as a ratio to citrate synthase. All values are mean ± SEM of 4 independent experiments. *** $p<0.001$ determined by Student's t-test.

initial 5-MTHF concentration of 500 nmol/L. A 5-MTHF concentration of 282.7 ± 7.9 nmol/L was recorded at 0 minute. No significant loss of 5-MTHF from the minimal medium in the presence of KCN treated cells was observed at 150 minutes, compared to control (Figure 60a). A similar finding was observed when the experiment was carried out at an initial 5-MTHF concentration of 150 nmol/L. A 5-MTHF concentration of 63.0 ± 2.7 nmol/L 5-MTHF was recorded at 0 minute. No significant loss of 5-MTHF from the minimal medium in the presence of KCN treated cells was observed at 150 minutes, compared to control (Figure 60b).

### 6.6.5 KCN treatment of SH-SY5Y cells has no effect on mitochondrial superoxide generation

To elucidate whether KCN treatment of SH-SY5Y cells led to an increase in mitochondrial superoxide production, the MitoSOX$^{TM}$ Red assay system was utilised. There was no significant increase in mitochondrial superoxide production above basal levels observed in KCN treated cells compared to matched controls (Figure 61).

### 6.6.6 Selenite treatment of SH-SY5Y cells causes a significant loss of 5-MTHF from extracellular minimal medium which is prevented by AA

The stability of 5-MTHF in minimal medium in the presence of SH-SY5Y cells treated with various concentrations of selenite, was further determined. Similarly to SH-SY5Y cells, the neuroblastoma cell line SK-N-BE cells originated from a bone marrow biopsy in 1972 (Biedler et al., 1978). A previous study showed that treatment of SK-N-BE cells, with selenite concentrations >100 nmol/L (7.9 µg/L) for 1 hour, led to an increase in ROS generation (Maraldi et al., 2011). Moreover, selenite has been shown to induce ROS production at very low concentrations, in the order of 8-80 µg/L (Vinceti et al., 2009). Therefore, cells were treated with either 2 µg/L [a selenium concentration within the CSF reference range across all ages (1.8-4.7 µg/L (1–30 days), 0.68-3.00 µg/L (1 month – 3 years) 0.73-2.13 µg/L (4 – 18 years) (Tondo et al., 2010)], 10 µg/L or 20 µg/L selenite and incubated for 1 hour (Maraldi et al., 2011; Vinceti et al., 2009).

Using these culture conditions, the stability of 5-MTHF in the extracellular minimal medium of selenite treated cells for 150 minutes was evaluated. Stability was first

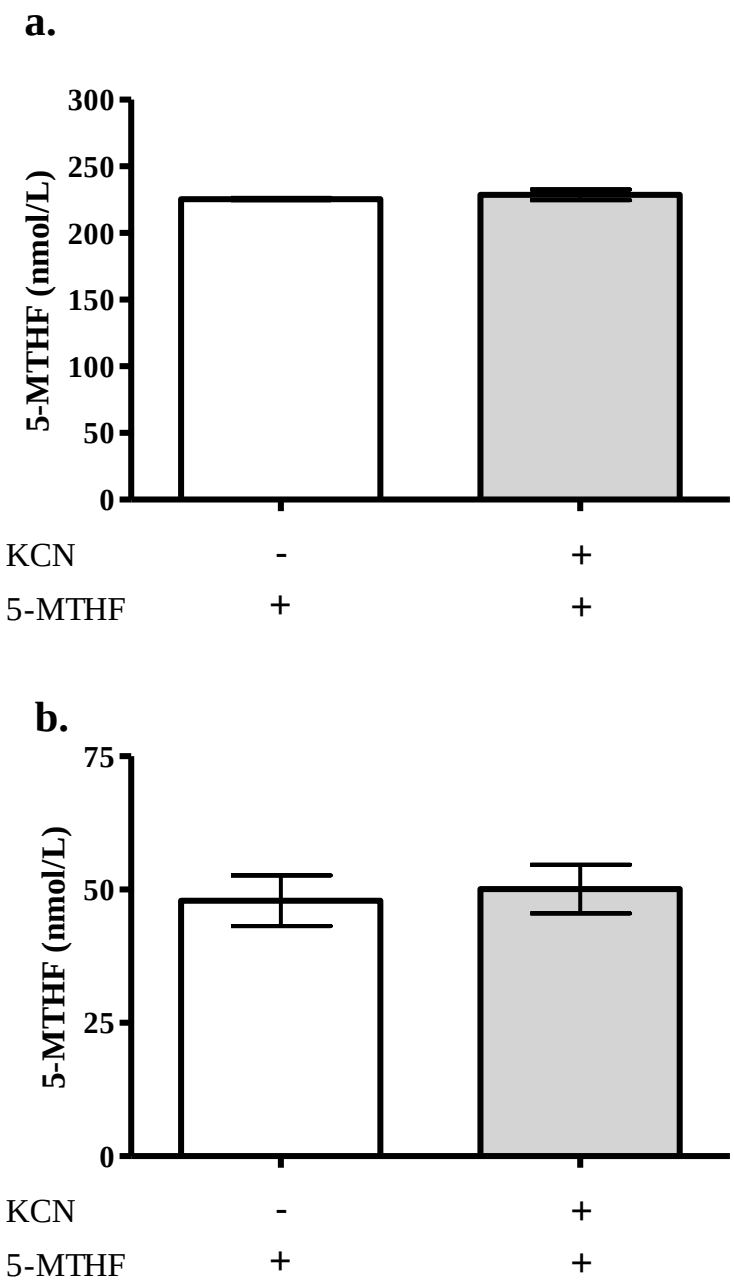


***Figure 60 5-MTHF stability in the extracellular minimal medium of SH-SY5Y cells pre-treated in the absence and presence of KCN (1 mmol/L), following a 150 minute incubation.*** **a.** 5-MTHF stability at an initial concentration of 500 nmol/L and **b.** at an initial concentration 150 nmol/L. All values are mean ± SEM of 4 independent experiments. In some cases the error bars were small owing to the tightness of the data.

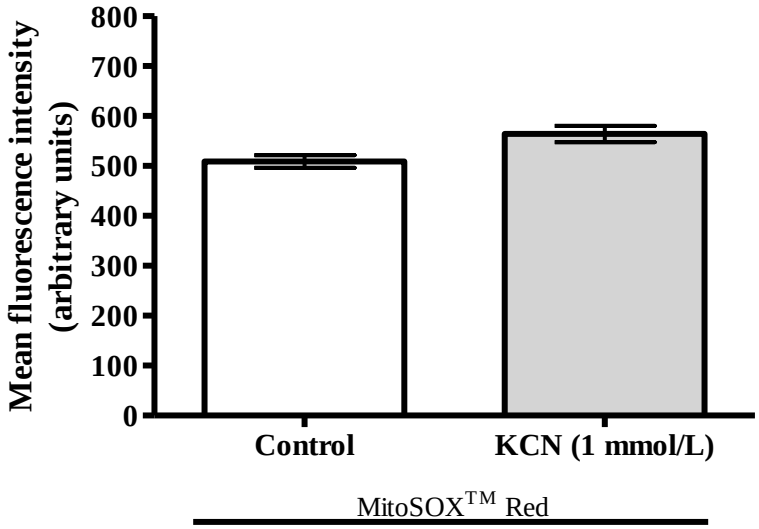


***Figure 61 Mitochondrial superoxide production in KCN pre-treated SH-SY5Y cells for 24 hours following a 30 minute incubation with MitoSOX™ Red.*** All values are mean ± SEM of 3 independent experiments.

determined at an initial 5-MTHF concentration of 500 nmol/L. A 5-MTHF concentration of 267.9 ± 3.1 nmol/L was recorded at 0 minute. There was no significant difference in 5-MTHF concentration remaining in the minimal medium of 2 µg/L selenite treated cells, compared to control (Figure 62a). In contrast, a significant 5-MTHF loss of 15% ($p<0.01$) and 18% ($p<0.01$) from the extracellular minimal medium of cells treated with 10 µg/L or 20 µg/L selenite at 150 minutes was observed, compared to control respectively (Figure 62b, Figure 62c). A similar finding was observed when the experiment was carried out at an initial 5-MTHF concentration of 150 nmol/L. A 5-MTHF concentration of 67.1 ± 1.3 nmol/L was recorded at 0 minute. There was no significant difference in 5-MTHF concentration remaining in the minimal medium of 2 µg/L selenite treated cells, compared to control (Figure 63a). In contrast, a significant 5-MTHF loss of 17% ($p<0.05$) and 28% ($p<0.01$) from the extracellular minimal medium of cells treated with 10 µg/L or 20 µg/L selenite at 150 minutes was observed, compared to control respectively (Figure 63b, Figure 63c).

Since treatment of cells with selenite (10 µg/L and 20 µg/L) led to a statistically significant reduction in 5-MTHF concentration remaining in the extracellular minimal medium compared to control at 150 minutes, the ability of AA to prevent 5-MTHF decay in this system was evaluated. At an initial 5-MTHF concentration of 500 nmol/L, co-incubation of 5-MTHF with AA (150 µmol/L), led to a significantly greater amount of 5-MTHF remaining in the extracellular minimal medium of 10 µg/L selenite treated cells at 150 minutes of 26% ($p<0.001$), when compared to 5-MTHF incubated with 10 µg/L selenite treated cells only (Figure 62b). Similarly, co-incubation of 5-MTHF with AA (150 µmol/L), led to a significantly greater amount of 5-MTHF remaining in the extracellular minimal medium of 20 µg/L selenite treated cells at 150 minutes of 33% ($p<0.001$), when compared to 5-MTHF incubated with 20 µg/L selenite treated cells only (Figure 62c). At a 5-MTHF initial concentration 150 nmol/L, co-incubation of 5-MTHF with AA (150 µmol/L) led to a significantly greater amount of 5-MTHF remaining in the minimal medium at 150 minutes of 24% ($p<0.01$), when compared to 5-MTHF incubated with 10 µg/L selenite treated cells only (Figure 63b). Similarly, a significant increase in 5-MTHF remaining in the minimal medium at 150 minutes following co-incubation

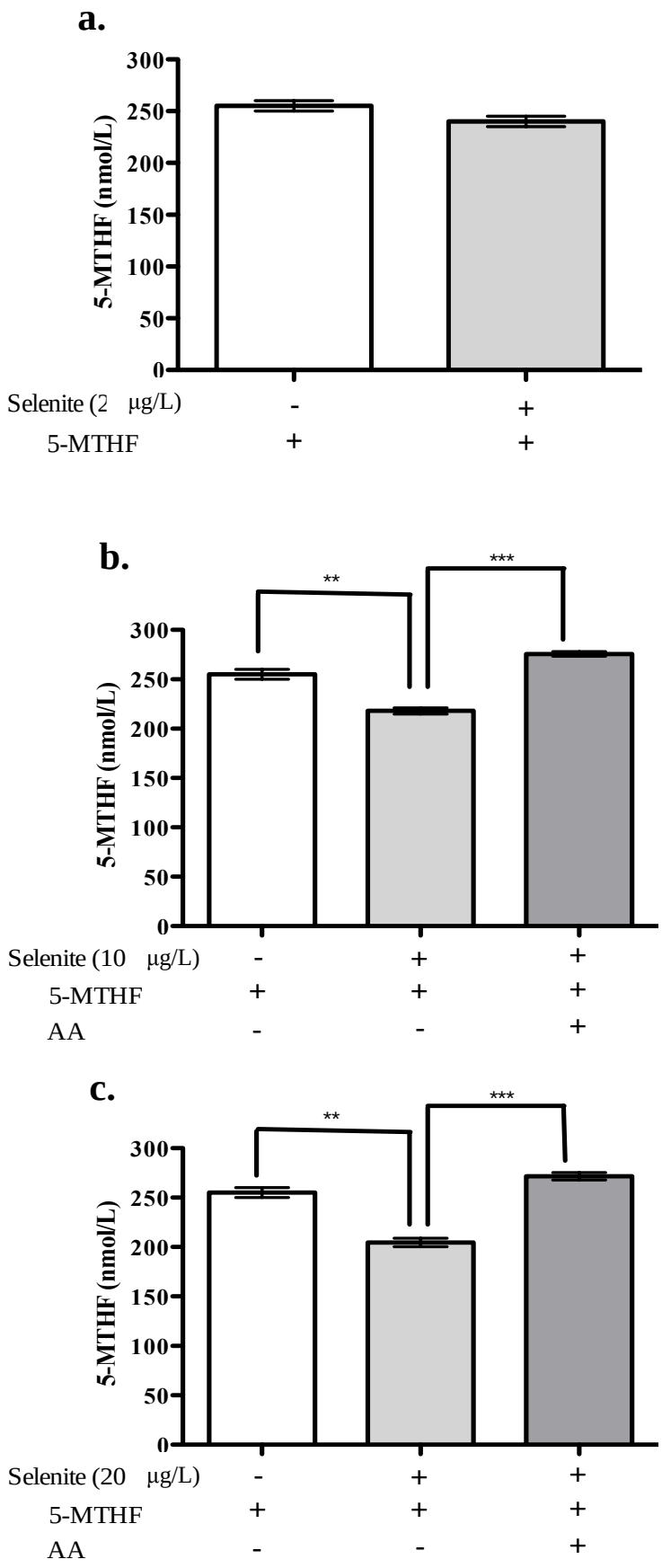


***Figure 62 5-MTHF stability at an initial concentration of 500 nmol/L in the extracellular minimal medium of SH-SY5Y cells pre-treated in the absence and presence of selenite for 1 hour, following a 150 minute incubation with or without AA (150 µmol/L).*** **a.** SH-SY5Y cells treated with 2 µg/L, **b.** 10 µg/L or **c.** 20 µg/L selenite. All values are mean ± SEM of 4 independent experiments. **p<0.01, ***p<0.001 determined by one-way ANOVA followed by Bonferroni's Multiple comparison test.

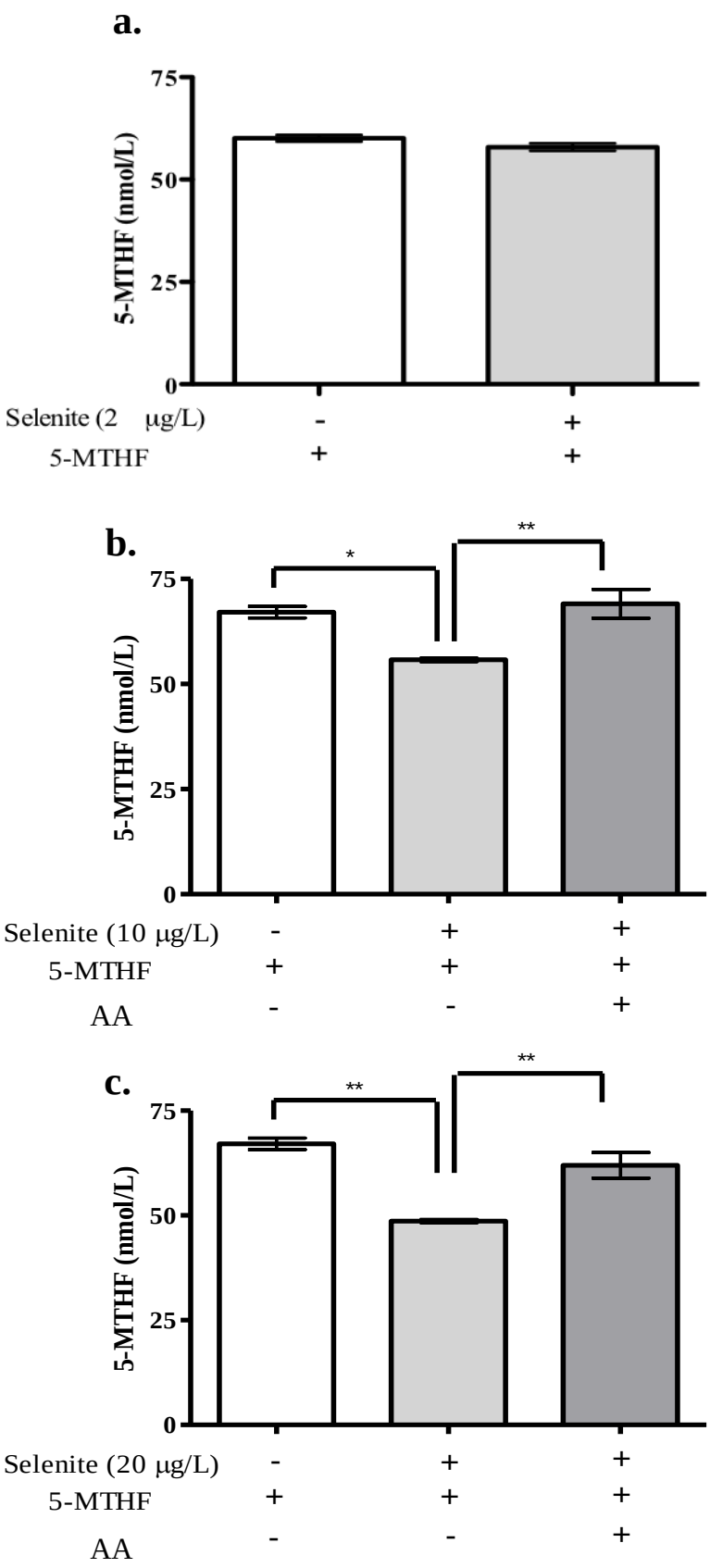


***Figure 63 5-MTHF stability at an initial concentration of 150 nmol/L in the extracellular minimal medium of SH-SY5Y cells pre-treated in the absence and presence of selenite for 1 hour, following a 150 minute incubation with or without AA (150 µmol/L).*** **a.** SH-SY5Y cells treated with 2 µg/L, **b.** 10 µg/L or **c.** 20 µg/L selenite. All values are mean ± SEM of 4 independent experiments. *p<0.01, **p<0.001 determined by one-way ANOVA followed by Bonferroni's Multiple comparison test.

with AA (150 µmol/L) of 27% ($p<0.01$), was observed when compared to 5-MTHF incubated with 20 µg/L selenite treated cells only (Figure 63c).

### 6.6.7 Selenite treatment of SH-SY5Y cells has no effect on complex I activity

Since mitochondrial superoxide generation was associated with rotenone treatment of SH-SY5Y cells potentially as a consequence of complex I inhibition (section 6.6.3), elucidation of whether selenite treatment had any effect on mitochondrial complex I activity was determined. Complex I activity was measured in cells treated with either 2 µg/L, 10 µg/L or 20 µg/L selenite. There was no significant difference in complex I activity observed between selenite (2 µg/L, 10 µg/L or 20 µg/L) treated cells compared to control (Figure 64). This effect was apparent when complex I activity was expressed as either a ratio to citrate synthase or as nmol/min/mg of protein (Figure 64, Table 16).

### 6.6.8 Selenite treatment has no effect on mitochondrial superoxide generation

To elucidate whether treatment of cells with selenite (10 µg/L or 20 µg/L) led to an increase in mitochondrial superoxide production, the MitoSOX$^{TM}$ Red assay system was utilised. There was no significant increase in mitochondrial superoxide production above basal levels observed in selenite (10 µg/L or 20 µg/L) treated cells compared to matched controls (Figure 65).

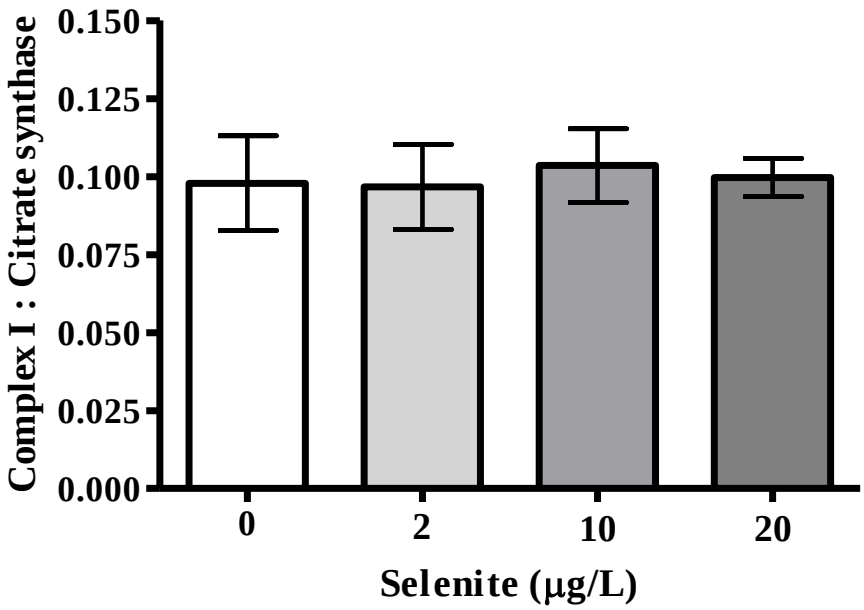


***Figure 64 Complex I activity in selenite treated SH-SY5Y cells for 1 hour.*** Complex I activity is expressed as a ratio to citrate synthase. All values are mean ± SEM of 4 independent experiments.

***Table 16 Mitochondrial RCE activity in SH-SY5Y cells following selenite treatment for 1 hour.*** Complex I activity (nmol/min/mg of protein) and citrate synthase activity (nmol/min/mg of protein). Complex I % inhibition following selenite treatment for 1 hour. All values are mean ± SEM of 4 independent experiments. ND=not detectable.

| Conditions | Complex I (nmol/min/mg of protein) | | Citrate Synthase (nmol/min/mg of protein) |
|---|---|---|---|
| | Activity | % inhibition | |
| **Control (selenite)** | 12.5 ± 1.7 | - | 128.3 ± 5.8 |
| **Selenite 2 µg/L** | 13.6 ± 1.8 | ND | 121.7 ± 8.5 |
| **Selenite 10 µg/L** | 12.8 ± 1.4 | ND | 123.4 ± 1.6 |
| **Selenite 20 µg/L** | 12.4 ± 0.5 | ND | 122.2 ± 4.2 |

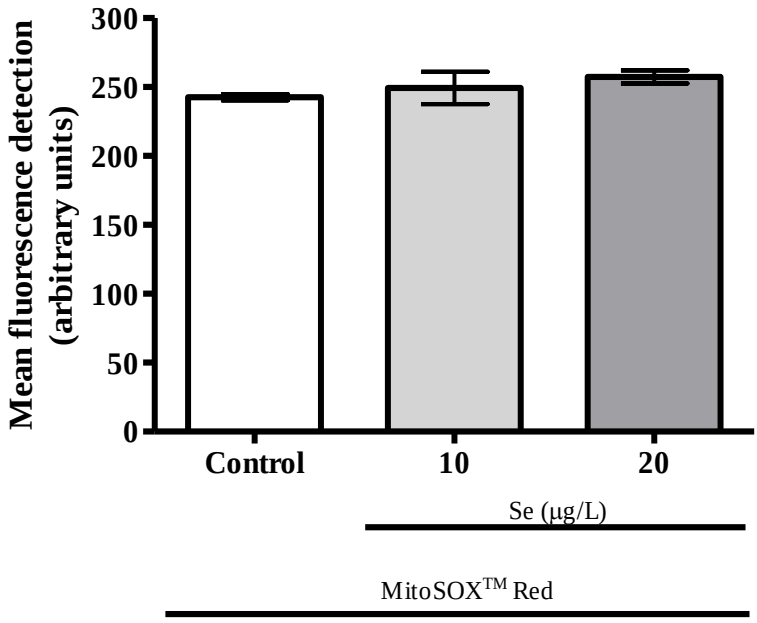


***Figure 65 Mitochondrial superoxide production in selenite pre-treated SH-SY5Y cells for 1 hour, following a 30 minute incubation with MitoSOX™ Red.*** All values are mean ± SEM of 3 independent experiments. Se = selenite

## 6.7 Discussion

An initial loss of 5-MTHF from the minimal medium was observed between sample preparation and 0 minute (see section 6.6.1) and in control samples (see sections 6.6.2, 6.6.4, 6.6.6), owing to the susceptibility of 5-MTHF to autoxidation in the presence of molecular oxygen and the lack of antioxidants present. In addition, glucose, which is present in minimal medium, is susceptible to autoxidation yielding superoxide (Stewart et al., 2002; Wolff and Dean, 1987). Thus, the minimal medium may be a potential source of oxidising species, which additionally could contribute to the loss of 5-MTHF observed. The loss of 5-MTHF from the minimal medium between sample preparation and 0 minute observed is similar to that seen in potassium phosphate buffer in Chapter 4 (see section 4.7 for detailed discussion), and would be expected to occur prior to quantification of 5-MTHF at the initial time point, for the reasons dicussed above and in section 4.7. The degree of loss of 5-MTHF from the minimal medium in the experiments described in this Chapter appears to be comparable and so 5-MTHF stability in the various experimental systems investigated is being tested against a relatively consistent background.

5-MTHF decay in minimal medium at both initial 5-MTHF concentrations followed first order kinetics, as previously described in section 4.7. However, there was a greater concentration of 5-MTHF remaining in minimal medium in the presence of SH-SY5Y cells and the rate of 5-MTHF decay in this model was slower, compared with minimal medium alone. These results suggest that SH-SY5Y cells may secrete protective factors counteracting 5-MTHF decay. Neurones, astrocytes and glia have been shown to release factors into the extracellular space including antioxidants, and anti-inflammatory and trophic factors. For example, in co-cultures astrocytes facilitate glutathione trafficking and provide a source of cysteine in order to maintain neuronal glutathione content (Dringen et al., 1999; Sagara et al., 1993). Moreover, astrocytes and neurones additionally release ecSOD to prevent oxidation of extracellular glutathione, whilst the latter have also been shown to release GSH (Hirrlinger et al., 2002; Pope et al., 2008; Stewart et al., 2002; Stone et al., 1999; Strand and Marklund, 1992). Therefore, the increased preservation of 5-MTHF in minimal medium observed here in the presence of SH-SY5Y cells may indicate a similar phenomenon, demonstrating the potential neuroprotective capabilities of SH-SY5Y cells. Further studies are required in order to fully elucidate this neurone-

derived protective factor(s). All subsequent experiments were compared to the stability of 5-MTHF in extracellular minimal medium in the presence of SH-SY5Y cells, used as a control.

The mitochondrial RC is considered to be an important source of ROS production and partial inhibition of the mitochondrial RC has been shown to lead to an increase in ROS production in the absence of ATP perturbation (Jacobson et al., 2005; Sipos et al., 2003). In view of this and the link between CFD and mitochondrial RCE defects as demonstrated in Chapter 3 and in the literature (Garcia-Cazorla et al., 2008), complex I or complex IV was inhibited using either rotenone or KCN in SH-SY5Y cells in order to ascertain whether a mechanistic link between compromised mitochondrial RCE activity and loss of 5-MTHF could be demonstrated. Complex I or complex IV inhibition were selected as model systems because these were the most frequently observed mitochondrial RCE defects in skeletal muscle of children with mitochondrial disease studied in Chapter 3. The effect of complex I inhibition on extracellular 5-MTHF stability in minimal medium was initially determined. Rotenone treatment (50 nmol/L) did not cause a significant decrease in complex I activity when expressed as a ratio to citrate synthase activity and as a proportion to cellular protein. However, following 100 nmol/L rotenone treatment, a significant decrease in complex I activity was observed when expressed both as a ratio to citrate synthase activity and as a proportion to cellular protein. Citrate synthase is commonly used as a mitochondrial marker and as a measure of mitochondrial enrichment (Almeida and Medina, 1998; Hargreaves et al., 1999). Citrate synthase activity was unaffected following cellular treatment with rotenone. This suggests that any change in complex I activity may not be the result of a change in mitochondrial number. Similarly, total protein was unaffected following cellular treatment with rotenone. This suggests that any change in complex I activity is not an artefact of change in cell number.

Interestingly, following cellular rotenone treatment (100 nmol/L), a significantly greater loss of 5-MTHF was observed from the extracellular minimal medium compared to control at both initial 5-MTHF concentrations studied. However, co-incubation of AA with 5-MTHF at both initial concentrations led to a significantly greater amount of 5-MTHF remaining in extracellular minimal medium compared to control and rotenone treated cells only. In view of the antioxidant role of AA

(Arrigoni and De Tullio, 2002; Regoli and Winston, 1999; Rice, 1999), this observation may indicate a role for an oxidative process whereby the significantly greater loss of 5-MTHF from the extracellular minimal medium of rotenone treated cells may be attributed to an increase in cellular production and release of ROS, which may outweigh the antioxidant capacity of the cells. This suggestion is supported by the significant increase in mitochondrial superoxide production above basal levels following inhibition of mitochondrial complex I with rotenone. The latter finding is also consistent with previous studies demonstrating increased ROS production in rotenone treated SH-SY5Y cells (Xiong et al., 2013).

However, it is important to consider that other ROS may also be responsible for the observed loss of 5-MTHF from the extracellular minimal medium in these studies. It has been postulated that rotenone induced neurotoxicity in the extracellular environment may be a result of the conversion of superoxide into membrane permeable hydrogen peroxide by ecSOD and other ROS, including the hydroxyl radical, produced as a result of the Fenton reaction (Bienert et al., 2007; Okado-Matsumoto and Fridovich, 2001). Furthermore, other factors, in addition to ROS generation, may contribute to the loss of 5-MTHF from extracellular medium of complex I inhibited SH-SY5Y cells, for example, alterations in cellular uptake of 5-MTHF. Loss of mitochondrial RC activity per se does not appear to influence this process as evidenced by the lack of significant effect observed with the complex IV inhibited cells, as discussed below. Regarding AA, whilst its antioxidant ability may neutralise mitochondrial derived ROS, AA may also neutralise ROS produced by 5-MTHF autoxidation and glucose autoxidation.

The effect of complex IV inhibition on the stability of 5-MTHF in the extracellular minimal medium of KCN treated cells was also assessed. In cells treated with KCN, complex IV activity was significantly decreased when expressed as a ratio to citrate synthase activity and as a proportion to cellular protein. Citrate synthase activity and total protein were unaffected following KCN treatment, suggesting that the change in complex IV activity is not the result of a change in mitochondrial number or an artefact of change in cell number (Almeida and Medina, 1998; Hargreaves et al., 1999). In contrast to complex I inhibited cells, inhibition of complex IV with KCN in cells did not affect 5-MTHF stability in extracellular minimal medium at both initial 5-MTHF concentrations. In addition, inhibition of complex IV was not

associated with an increase in mitochondrial superoxide formation above basal levels in KCN treated SH-SY5Y cells. These findings suggest that oxidative stress may not be induced in this system. This may be attributed to the undifferentiated neuronal cell type used in these studies. For example, complex IV subunits are increased in differentiated SH-SY5Y cells compared to undifferentiated cells (Schneider et al., 2011) and increased ROS production has been observed in other cell types following complex IV inhibition including cultured astrocytes (Jacobson et al., 2005). Additionally, there is on-going debate in the literature regarding the role of complex IV in ROS production. Complex IV has been implicated as a major source of mitochondrial ROS production in some studies (Jacobson et al., 2005; Zhao et al., 2003), whilst in other studies mitochondrial ROS production at the level of complex IV has been reported to be negligible (Babcock and Wikström, 1992; Chen et al., 2003; Wikström, 2004).

Expanding upon the studies in Chapter 4, as detailed in section 6.1 of this Chapter, the effect of selenite treatment of SH-SY5Y cells on 5-MTHF stability in extracellular minimal medium was determined. Interestingly, a significantly greater loss of 5-MTHF at both initial concentrations was observed in cultures treated with selenite concentrations (10 µg/L and 20 µg/L) previously associated with induction of ROS production in the literature, compared to control (Maraldi et al., 2011). Co-incubation of AA with 5-MTHF at both initial concentrations led to a significant increase in 5-MTHF concentration remaining in the extracellular minimal medium of selenite treated cells compared to selenite treated cells only. This observation may indicate a role for an oxidative process whereby the significantly greater loss of 5-MTHF from the extracellular minimal medium of selenite treated cells may be attributed to an increase in cellular production and release of ROS, overwhelming the antioxidant capacity of the cells. This may occur via redox cycling of selenite with reduce thiols propagating ROS (Chen et al., 2007b; Tarze et al., 2007; Yan and Spallholz, 1993). The observed susceptibility of 5-MTHF to decay observed in this Chapter, in contrast to studies in CSF in Chapter 4, could be attributed to the presence of a cellular system facilitating the formation of selenium metabolites that more easily oxidise with intracellular and extracellular antioxidant systems (Yan and Spallholz, 1993).

Since the mitochondrial RC is considered to be a major site of ROS production (Boveris and Chance, 1973; Boveris et al., 1972; Loschen and Azzi, 1975), it was of interest to determine whether selenite treatment had any effect on mitochondrial function and mitochondrial-derived superoxide production. Regarding the former, in view of the observed mitochondrial superoxide generation following inhibition of mitochondrial complex I with rotenone, mitochondrial complex I activity was determined in selenite treated cells. There was no significant change in complex I activity in selenite treated cells when complex I activity was expressed as a ratio to citrate synthase activity and as a proportion to cellular protein. Citrate synthase activity and total protein were also unaffected following selenite treatment, suggesting that the unchanged complex I activity is not the result of a change in mitochondrial number or an artefact of change in cell number (Almeida and Medina, 1998; Hargreaves et al., 1999). This, in turn, suggests that selenite treatment may not lead to inhibition of the mitochondrial RC at the level of complex I. In addition, selenite treatment in cells was not associated with an increase in mitochondrial superoxide formation above basal levels compared to control. However, this does not exclude the possibility that ROS may be produced at a cellular location other than the mitochondria. Measurement of cytoplasmic ROS to associate ROS production as a potential cause of 5-MTHF degradation observed in this system is required.

## 6.8 Conclusion

In conclusion, inhibition of the mitochondrial RC at the level of complex I led to significantly greater loss of 5-MTHF from the extracellular minimal medium which was counteracted following the addition of AA. This suggests a role for an oxidative process, which is supported by the observed increase in mitochondrial superoxide production in SH-SY5Y cell following rotenone treatment. In contrast, the stability of 5-MTHF was unaffected in the extracellular minimal medium of cells treated with KCN leading to complex IV inhibition. Mitochondrial superoxide production was not increased in this system. This may be attributed to the undifferentiated neuronal cell line used in these studies and the controversial role inhibition of complex IV plays in generating ROS (Babcock and Wikström, 1992; Jacobson et al., 2005; Schneider et al., 2011; Zhao et al., 2003). Selenite treatment of cells with concentrations known to be associated with increases in ROS production, led to a

significantly greater loss of 5-MTHF from the extracellular minimal medium, which was counteracted following the addition of AA. An oxidative process may occur in this system, however, selenite treatment of SH-SY5Y cell was not associated with abnormal mitochondrial complex I activity or an increase in mitochondrial superoxide generation. Cytoplasmic ROS may be propagated in this system via redox cycling of selenite with reduce thiols propagating ROS (Lu et al., 2009).

# Chapter 7
# General discussion, conclusion and further work

# 7. General discussion, conclusion and further work

## 7.1 General discussion

Decreased levels of 5-MTHF in the CSF compartment of the CNS is increasingly recognised to be associated with heterogeneous neurological disorders, including mitochondrial disorders (Garcia-Cazorla et al., 2008; Hyland et al., 2010; Ormazábal et al., 2011; Pérez-Dueñas et al., 2011; Pineda et al., 2006; Ramaekers et al., 2007c; Serrano et al., 2010). Whilst decreased CSF 5-MTHF concentration in patients with mitochondrial disease has previously been documented, from the available literature and current knowledge, no large-scale systematic analysis of CFD in this patient group has been performed. Additionally, whilst *FOLR1* gene mutations and generation of auto-antibodies directed against the FRα can explain some causes of CFD (Cario et al., 2009; Frye et al., 2013; Pérez-Dueñas et al., 2010; Ramaekers et al., 2007a, 2005; Ramaekers et al., 2013b; Steinfeld et al., 2009), other mechanisms need to be identified to explain the low CSF 5-MTHF concentration that occurs in conditions such as mitochondrial disorders. Therefore, the main aims of this thesis were to evaluate the prevalence and significance of CFD in patients with a suspected or proven mitochondrial disease and to consider the potential role oxidative stress may play with regard to the development of a CSF deficiency of 5-MTHF.

CFD and mitochondrial disease phenotypes have substantially overlapping clinical heterogeneity (Chi et al., 2010; Jackson et al., 1995; Nissenkorn et al., 1999; Ramaekers et al., 2002). Therefore, CFD may represent an under-recognised condition in patients with mitochondrial disease. Consequently, patients may be excluded from comprehensive diagnosis, and since CFD is a potentially treatable aspect of mitochondrial disease (Hansen and Blau, 2005; Moretti et al., 2005; Pérez-Dueñas et al., 2011), patients may also be excluded from receiving effective treatment. The prevalence and significance of CFD in patients with a suspected or proven mitochondrial disease were evaluated in Chapter 3 of this thesis, and a number of key and novel findings addressing the above hypotheses were documented, as summarised in Table 17.

***Table 17 Summary of the key findings and interpretation/recommendations discussed in Chapter 3.***

| | Key findings | Interpretation/recommendations |
|---|---|---|
| **1.** | The prevalence of CSF 5-MTHF deficiency in suspected mitochondrial disease patients and in those patients who had a biochemically confirmed skeletal muscle RCE defect, were both 15%, and the minimum population prevalence of mitochondrial disease with CFD is approximately one in 30,000. | CSF 5-MTHF deficiency is more common in patients with mitochondrial disease than is currently recognised. |
| **2.** | Patients with CSF 5-MTHF deficiency, including those with proven mitochondrial diseases share a heterogeneous clinical presentation and normal or non-specific MRI data. | CSF 5-MTHF analysis should be carried out in all patients at risk of CFD, rather than relying on clinical manifestations. |
| **3.** | Severe CSF 5-MTHF (<10 nmol/L) deficiencies were seen in patients with KSS and *FOLR1* or *PCFT1* mutations. A novel homozygous missense *FOLR1* mutation in exon 5 (c.335A>T; p.N112I) was identified. | In the absence of a clinical diagnosis, *FOLR1* sequence analysis should be performed in all patients with CSF 5-MTHF values <10 nmol/L in the absence of peripheral folate deficiency. In the presence of a peripheral folate deficiency, *PCFT1* sequence analysis should be performed. |
| **4.** | Complex IV deficiency was the most common RCE defect in patients with CSF 5-MTHF deficiency in the cohort. One complex IV deficient patient had a severe CSF 5-MTHF (<10 nmol/L) deficiency and a homozygous *FOLR1* mutation in exon 7 (c.610C>T; p.R204X). | RCE defects in patients with low CSF 5-MTHF cannot be predicted from CSF 5-MTHF data and vice versa, highlighting the importance of performing both a skeletal muscle biopsy and lumbar puncture in patients with suspected mitochondrial disease. This may be especially appropriate in patients with CSF 5-MTHF <10 nmol/L who have suspected or confirmed *FOLR1* mutations. |
| **5.** | A lack of correlation between CSF 5-MTHF values and the degree of RCE deficiency measured in skeletal muscle was documented. | Other mechanisms arising from loss of mitochondrial function may need to be considered, e.g oxidative stress leading to increased 5-MTHF catabolism. |
| **6.** | Genetically confirmed mitochondrial disease was associated with CSF 5-MTHF deficiency and normal RCE activities in two patients, one with KSS and one with *POLG* mutations. | The former may be explained by the mtDNA deletion being heteroplasmic and there was enough wild type mtDNA to compensate. The latter had *POLG* mutations with a predominantly CNS phenotype and very low levels of multiple mtDNA deletions in skeletal muscle. |
| **7.** | No difference in CSF 5-MTHF concentration was observed between patients receiving and not receiving AEDs. | Opladen et al. (2010) demonstrated decreased cellular 5-MTHF uptake owing to ROS generation with the use of AEDs. The data from the cohort reported in Chapter 3 do not necessarily support this work. The impact of specific AEDs on CSF 5-MTHF availability was not determined owing to small sample size. |
| **8.** | Positive biochemical response to folinic acid treatment was documented in patients with KSS and *FOLR1* mutations. The onset of CSF 5-MTHF deficiency may be associated with disease progression from Pearson syndrome to KSS. | Specifically for KSS, empirical treatment with folinic acid to all paediatric patients with single large scale mtDNA deletions may be beneficial. Folinic acid treatment should be commenced in all other patients, including those with *FOLR1* mutations, as soon as low 5-MTHF levels have been documented in CSF. |

5-MTHF, together with other reduced pterins, is a labile molecule and is known to be prone to oxidative catabolism (Blair et al., 1975; Heales et al., 1988; Lam and Heales, 2007). Consequently, increased generation of ROS and/or loss of antioxidants could have a deleterious effect upon 5-MTHF availability. As discussed in Chapter 1, high levels of selenium in CSF (Lu et al., 2009; Wallenberg et al., 2010), low CSF AA concentration (Buettner and Jurkiewicz, 2010; Fisher and Naughton, 2003) and inhibition of mitochondrial RCE(s) may induce oxidative stress (Chen et al., 2007b; Jacobson et al., 2005; Liu et al., 2002), represented by an imbalance between ROS generation and antioxidant availability. With regard to mitochondrial disease, elevated CSF selenium concentrations have been reported in six patients with KSS and secondary CFD (Tondo et al., 2011), and low CSF AA concentration has been predicted in patients such as these (Spector and Johanson, 2010). Furthermore, mitochondrial dysfunction and impaired RCE activity is associated with an increase in ROS production in the absence of ATP perturbation (Jacobson et al., 2005). As such, oxidative stress, induced under the aforementioned conditions, may represent a putative mechanism responsible for the development of a CSF deficiency of 5-MTHF, including in mitochondrial diseases. Studies were designed to evaluate this hypothesis in Chapters 4, 5 and 6 of this thesis and a summary diagram of the data documented in these Chapters is shown in Figure 66.

In Chapter 4, the relative stability of 5-MTHF in CSF, in contrast to potassium phosphate buffer, suggests the presence of antioxidant molecules in CSF counteracting 5-MTHF degradation. AA is one of a number of antioxidants present in CSF (Barabás et al., 1995; Brau et al., 1984; Mandl et al., 2009) and as discussed above, has been purported to be low in patients with KSS and secondary CFD (Spector and Johanson, 2010). The potential importance of AA to convey protection towards 5-MTHF was illustrated in this Chapter by retardation of 5-MTHF catabolism observed in potassium phosphate buffer incubations carried out in the presence of AA at a concentration comparable to that seen in CSF. Introduction of a hydroxyl radical generating system to the CSF overcame the ability of AA to prevent 5-MTHF catabolism. Comparable observations were documented in potassium phosphate buffer incubations. This observation implies that the antioxidant systems present in CSF can be overwhelmed by ROS generation leading to loss of 5-MTHF from the CSF.

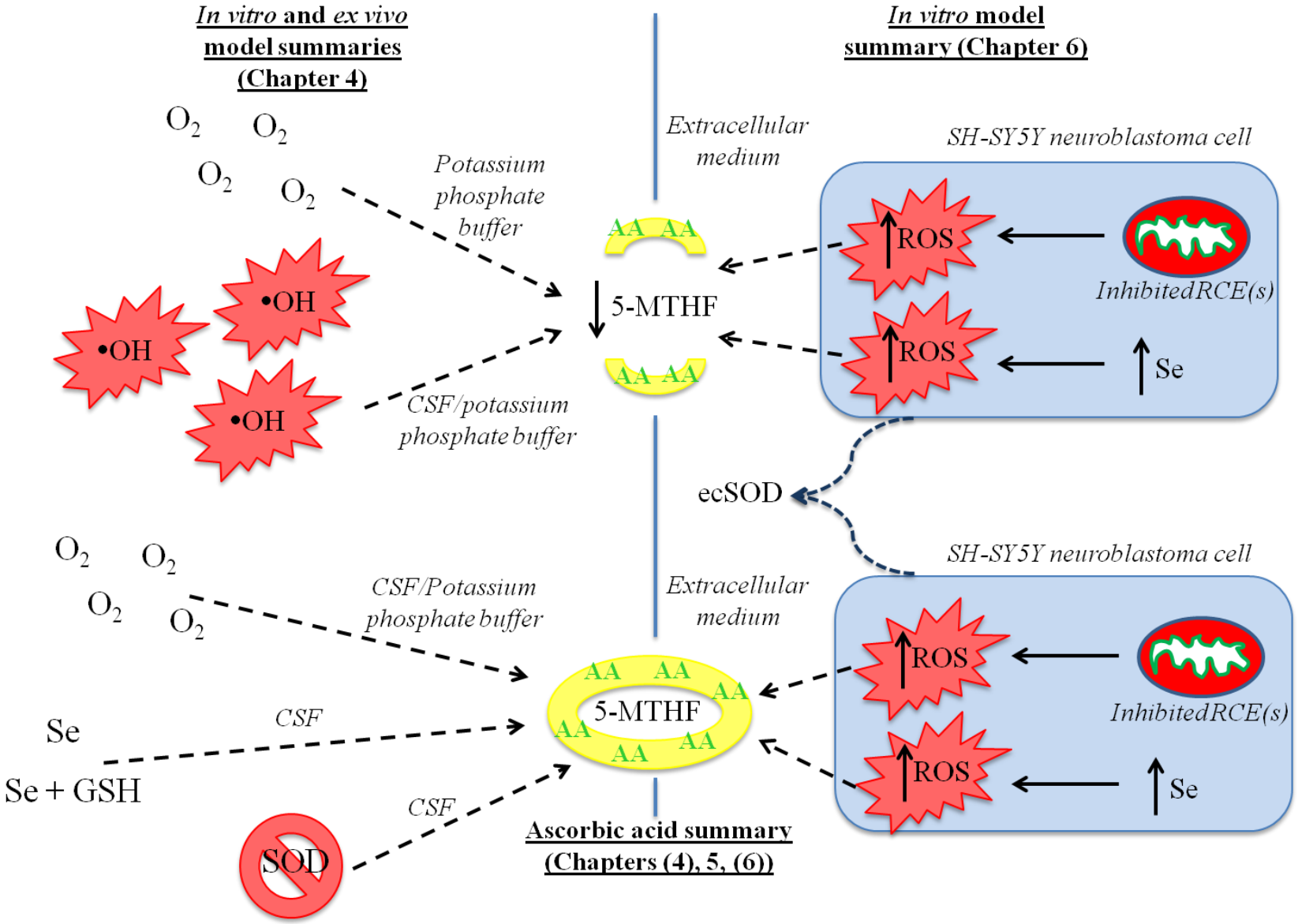


***Figure 66 Summary of results in Chapters 4, 5 and 6.*** 5-MTHF is susceptible to oxidative catabolism. However, the relative stability of CSF 5-MTHF may indicate the presence of antioxidants, for example AA. Such antioxidants may account for the stability of 5-MTHF in CSF only, following the addition of Se or Se+GSH and the removal of antioxidants >10 kDa, for example ecSOD. Release of ecSOD and/or GSH may account for the relative stability of 5-MTHF in extracellular medium of cultured SH-SY5Y cells. Inhibition of the mitochondrial RC, specifically complex I, leads to an increase in mitochondrial superoxide production which may degrade 5-MTHF in the extracellular medium. High selenium (Se) concentration leads to 5-MTHF degradation from the extracellular medium owing possibly to increased cytoplasmic ROS generation. AA protects against 5-MTHF degradation in the extracellular medium. Oxidative stress may represent a putative mechanism for secondary CFD observed in mitochondrial disease. $O_2$ = oxygen, •OH = hydroxyl radical, CSF = cerebrospinal fluid, Se = selenium, GSH = glutathione (reduced), ecSOD = extracellular Cu/Zn superoxide dismutase, 5-MTHF = 5-methyltetrahydrofolate, AA = ascorbic acid, ROS = reactive oxygen species, RCE(s) = (mitochondrial) respiratory chain enzyme(s).

The apparent stability of 5-MTHF in CSF following the addition of selenite alone, selenite plus GSH and selenite plus GSH at a ratio of 40:1, could be attributed to the presence of AA, in addition to other antioxidant systems likely to be present in CSF that could also convey protection towards 5-MTHF (although other explanations may also be possible (see section 4.7)) (Alho et al., 1998; Kolmakova et al., 2010). These could include enzymes such as the extracellular form of superoxide dismutase (ecSOD) (Stewart et al., 2002; Strand and Marklund, 1992), as well as other antioxidant molecules with a molecular mass >10 kDa (see section 4.7) (Montecinos et al., 2007). However, CSF filtration through 10 kDa pore size filters still conveyed 5-MTHF protection indicating a possible protective role for smaller antioxidant molecules with regard to 5-MTHF (see section 4.7). AA is present in filtered CSF, as shown in Chapter 5 (see section 5.4.3.9), which adds further credence to this suggestion.

CSF AA availability has previously been proposed, but not evaluated, to play a role in the development of CFD (Spector and Johanson, 2010). In Chapter 5, a method for the determination of CSF AA was developed (see section 5.4.3), an age-independent CSF AA reference range was established (see sections 5.5.1 and 5.5.2) and a significant positive correlation between AA and 5-MTHF in CSF was demonstrated. Such a correlation may be a reflection that both AA and 5-MTHF status are dependent upon dietary intake and active transport into the CSF compartment (Grapp et al., 2013; Liang et al., 2001; Verlinde et al., 2008). However, this correlation could also indicate an antioxidant protective role of AA towards 5-MTHF. This suggestion is supported by the observation of enhanced serum 5-MTHF in individuals also taking AA (Verlinde et al., 2008).

Whilst a significant positive correlation, when looking at all the data, could be demonstrated between CSF 5-MTHF and AA in Chapter 5, closer inspection revealed 38% of individuals with a demonstrable deficiency of CSF 5-MTHF had CSF AA deficiency. Although this was not a clinical evaluation study and only minimal clinical details were available, the clinical data reflect the known diversity of patients presenting with a CSF 5-MTHF deficiency. It is also of interest to note that the patient with a *FOLR1* mutation (patient 17) did not have an associated AA deficiency. This is in contrast to the finding for the patient with reported folate malabsorption (patient 6) where both CSF AA and 5-MTHF deficiency could be

demonstrated. Whilst AA deficiency was not universal amongst the 5-MTHF deficient patients studied, this finding may indicate that for a significant sub-set of individuals with a CSF 5-MTHF deficiency, the biochemical interaction between these two vitamins deserves further evaluation.

In accordance with previous studies (Surtees et al., 1994; Verbeek et al., 2008), a positive correlation between CSF 5-MTHF and CSF 5-HIAA was also documented in Chapter 5. Whilst this relationship could not readily be explained, possible hypotheses have been suggested. For example, the role of 5-MTHF in tetrahydrobiopterin regeneration may link 5-MTHF to serotonin synthesis and subsequently 5-HIAA metabolite production (Kaufman, 1991; Matthews and Kaufman, 1980). Conversely, decreased 5-MTHF levels may disturb *de novo* purine and thymidylate synthesis, which may lead to mitochondrial dysfunction. Subsequently, decreased ATP production could impair neurotransmitter vesicular loading and release (Serrano et al., 2010; Surtees et al., 1994).

The mitochondrial RC is considered to be an important source of ROS production (Jacobson et al., 2005). In view of this and the link between CFD and mitochondrial RCE defects as demonstrated in Chapter 3 and in the literature (Garcia-Cazorla et al., 2008; Serrano et al., 2010), a neuronal cell line model of complex I or IV inhibition was utilised in Chapter 6 in order to ascertain whether a mechanistic link between compromised mitochondrial RCE activity and loss of 5-MTHF could be demonstrated. Complex I or complex IV inhibition were selected as model systems because these are the most frequently observed mitochondrial RCE defects in skeletal muscle of children with mitochondrial disease identified in Chapter 3 and at Great Ormond Street Hospital, London, UK. Loss of 5-MTHF from the minimal medium utilised was expected to occur in all cases owing to the lack of antioxidants. However, the presence of cells slowed this loss of 5-MTHF from the extracellular medium, suggesting cellular release of protective factors. Such protective factors could include ecSOD and GSH, which have previously been demonstrated to be released into the medium of cultured primary rat neurons (Hirrlinger et al., 2002; Stewart et al., 2002; Strand and Marklund, 1992; Tulpule et al., 2013), although further work would need to be carried out in order to confirm this.

For complex I inhibited cells, a significantly greater loss of 5-MTHF from the

extracellular medium was noted. The finding that AA could significantly limit this loss may indicate a role for an oxidative process in the development of CFD, a suggestion supported by the finding that superoxide generation is significantly increased in rotenone treated cells. This latter finding is also consistent with previous observations relating to ROS production following complex I inhibition in these cells (Xiong et al., 2013). Inhibition of complex IV was not associated with an increase in superoxide formation and it is of note that, under the conditions employed, there was no significant increase in the disappearance of 5-MTHF from the extracellular medium. Interestingly, in Chapter 3 all patients with a confirmed mitochondrial RCE defects and low CSF 5-MTHF were complex IV deficient. However, as discussed above, a significant loss of 5-MTHF from the extracellular medium was associated with inhibition of complex I, but not complex IV. This may be attributed to the neuronal cell type (SH-SY5Y neuroblastoma cells) used in the studies of Chapter 6, since complex IV inhibition has previously been associated with an increase in ROS production in cultured astrocytes (see section 6.7) (Hargreaves et al., 2007; Jacobson et al., 2005). Further work could be directed towards determining the stability of 5-MTHF in the extracellular medium of complex IV inhibited astrocytes in culture, for example using the 1321N1 astrocytoma cell line.

Similarly to pharmacological inhibition of complex I in neuronal cells, treatment of cells with selenite led to a significantly greater loss of 5-MTHF from the extracellular medium which was counteracted following the addition of AA. These findings may indicate an oxidative process in the development of CFD where selenium levels are elevated. However, selenite treatment was not associated with abnormal complex I activity or increased mitochondrial superoxide formation, suggesting that any oxidative process taking place may be independent of the mitochondrial RC within the cell. For example, intracellular and extracellular redox cycling of selenite with reduced thiols, including GSH, which is present in CSF, has been shown to generate ROS (Lu et al., 2009; Wallenberg et al., 2010; Yan and Spallholz, 1993).

It is important to consider that a number of factors, in addition to ROS generation, may contribute to the degradation/disappearance of 5-MTHF from extracellular medium, for example, alterations in cellular uptake of 5-MTHF. Loss of mitochondrial RCE activity per se does not appear to influence this process as

evidenced by the lack of significant effect observed with the KCN treated complex IV inhibited cells. However, further work is required to measure cytosolic ROS in order to associate ROS as potential cause of 5-MTHF degradation from the extracellular minimal medium of selenite treated cells.

## 7.2 Conclusion

In conclusion, the data presented in this thesis indicate that 5-MTHF is susceptible to oxidative catabolism. The extracellular environment, including CSF, may convey protection to 5-MTHF owing to the presence of antioxidants such as AA. However, under conditions of increased ROS generation and/or loss of antioxidants, for example, high selenium concentration, low AA concentration and mitochondrial RCE inhibition, which may occur in some mitochondrial disorders, this protective capacity could be exceeded leading to CFD. The data presented here further raise the possibility that co-supplementation of AA together with appropriate folate replacement therapy may be beneficial for all patients in order to increase 5-MTHF bioavailability.

## 7.3 Further work

The data presented in Chapter 3 suggest it may be plausible that CFD could also complicate more common neurodegenerative disorders known to be associated with secondary mitochondrial dysfunction, including Parkinson's disease and Alzheimer's disease (dos Santos et al., 2009; Duan et al., 2002; Shea, 2006). A decrease in neuronal function owing to mitochondrial dysfunction could, theoretically at least, lead to concomitant deficiency of CSF 5-MTHF, which in turn could exacerbate the clinical phenotype. Initiation of folinic acid supplementation in those presenting with CFD, could result in significant biochemical improvements and represent a wider therapeutic application of folinic acid supplementation in the clinic. Additionally, the potential antioxidant role of AA to convey protection towards 5-MTHF may also complicate the biochemical presentation of these patients and AA supplementation may also be a therapeutic benefit. Further work to initially address this hypothesis could be carried out by:

- Combined determination of CSF 5-MTHF and AA values in patients with Parkinson's disease and Alzheimer's disease.

In this thesis, HPLC coupled to a fluorescence detector was used to quantify 5-MTHF in human CSF samples for both diagnostic and research purposes. However, the concentration of other folate species could be of diagnostic use and pose additional research questions. This work could be extended by:

- Developing and utilising a method of measuring all the folate species comprising the one-carbon metabolism pathway using a mass spectrometry method (Hannisdal et al., 2009) and generating metabolic profiles.
- Developing and utilising a method of measuring the 5-MTHF oxidation products 5-methyl-5,6-dihydrofolate and 4a-hydroxy-5-methyltetrahydrofolate in the extracellular medium (Blair et al., 1975), using a mass spectrometry method (Hannisdal et al., 2009).

CSF AA was shown to be positively correlated with CSF 5-MTHF. This could indicate an antioxidant protective role of AA towards 5-MTHF. Further evaluation of this relationship could be investigated by:

- Measuring CSF AA and 5-MTHF, and peripheral AA and 5-MTHF, in paired CSF and serum samples.
- Monitoring CSF AA status in patients with low CSF 5-MTHF to determine whether CSF AA levels may be of concern with regard to CSF 5-MTHF bioavailability. The method to quantify CSF AA developed in Chapter 5 is now established in the Neurometabolic Unit at the National Hospital for Neurology and Neurosurgery, London, UK.

CSF 5-MTHF, AA and HVA were measured in individual patient samples in Chapter 5. Whilst no correlation was observed between CSF 5-MTHF and HVA in this thesis, increased HVA has previously been reported in patients with low CSF 5-MTHF (Tondo et al., 2011). Based on the findings presented in Chapter 5 and of Tondo et al. (2011), the following testable hypothesis could be formulated. AA is a cofactor required for the enzymatic conversion of noradrenaline to dopamine catalysed by dopamine-β-hydroxylase (Menniti et al., 1986; Rebouche, 1991). It could be hypothesised that in patients with CFD associated with AA deficiency,

dopamine conversion could be impaired. This could lead to increased dopamine turnover, providing a putative explanation for the elevated HVA levels observed in these patients. Further work measuring CSF AA and HVA in patients with low CSF 5-MTHF concentration and carrying out statistical analyses on the data, could be performed to evaluate this hypothesis.

The SH-SY5Y cell line was used as a neuronal model to investigate mitochondrial RCE inhibition and the effect of high physiological selenite concentrations on 5-MTHF stability in the extracellular medium, since RCE inhibition and high selenite concentrations are associated with ROS generation. This work could be extended by:

- Repeating these experiments in other cell models for example, keratin forming Henrietta Lacks (HeLa) cells (KB cells), which express the FRα (Sadasivan and Rothenberg, 1989) and which could be used as a model of the choroid plexus (Opladen et al., 2010), and primary neurons.
- Investigating the effect of inducing oxidative stress on intracellular 5-MTHF levels.

Selenium has previously been reported to be elevated in CSF of patients with KSS (Tondo et al., 2011). In this thesis, to investigate the effect of selenium on 5-MTHF stability, the selenium compound selenite was used, since selenite is routinely used throughout the literature to study thiol-mediated redox cycling of selenium (Selenius et al., 2008; Wallenberg et al., 2010). This work could be extended by:

- Developing and utilising an inductively coupled plasma mass spectrometry (ICP-MS) method to measure selenium species and other trace elements in human CSF (Mandal et al., 2012).
- Utilising the above developed method to measure intracellular selenium species in selenite treated cells in order to generate metabolic profiles.

# Published Journal Article Related to this Thesis

Published in the peer-reviewed journal, Neurochemistry International. A full text copy of the publication is at the back of this thesis.

Aylett, S.-B., Neergheen, V., Hargreaves, I.P., Eaton, S., Land, J.M., Rahman, S., Heales, S.J.R., 2013. Levels of 5-Methyltetrahydrofolate and Ascorbic Acid in Cerebrospinal Fluid are Correlated: Implications for the Accelerated Degradation of Folate by Reactive Oxygen Species. Neurochem. Int. 63 (8) 750-755.

# List of Published Conference Abstracts Related to this Thesis

Presented at the 5th Conference on Advances in Molecular Mechanisms Underlying Neurological Disorders in Bath, UK, June 2013.

Sophie-Beth Aylett, Viruna Neergheen, Simon Eaton, John Land, Shamima Rahman and Simon Heales, 2013. Impaired Complex I Activity Accelerates 5-Methyltetrahydrofolate Degradation which is Prevented by Ascorbate; Implications for Inherited and Acquired Mitochondrial Disorders. Biochem. Soc. Trans. P021.

Presented at the Society for the Study of Inborn Errors of Metabolism Conference in Birmingham, UK, September 2012.

Aylett S.-B., Neergheen V., Eaton S., Land JM., Rahman S., Heales SJ., 2012. Factors Affecting 5-Methyltetrahydrofolate (5MTHF) Stability: Implications for Cerebral 5MTHF Deficiency. J. Inherit. Metab. Dis. 35, S141.

Presented at the Society for the Study of Inborn Errors of Metabolism Conference in Birmingham, UK, September 2012.

Aylett S.-B., Varadkar S., Fassone E., Pope S., Neergheen V., Hargreaves I.P., Land J.M., Heales S.J., Rahman S., 2012. Cerebral Folate Deficiency Associated with a Homozygous Nonsense Mutation in *FOLR1*. J. Inherit. Metab. Dis. 35, S138.

Presented at the Advances and Controversies in B-Vitamins and Choline Conference in Leipzig, Germany, March 2012.

S.-B. Aylett, V. Neergheen, S. Eaton, J. Land, S. Rahman, S. Heales, 2012. Factors Affecting 5-Methyltetrahydrofolate (5MTHF) Stability: Implications for 5MTHF Deficiency Observed in Inherited Metabolic Disorders. Advances and Controversies in B-Vitamins and Choline, A35, WS10 04.

# References


Abali, E.E., Skacel, N.E., Celikkaya, H., Hsieh, Y.-C., 2008. Regulation of human dihydrofolate reductase activity and expression. Vitam. Horm. 79, 267–292.

Adachi, S., Cross, A.R., Babior, B.M., Gottlieb, R.A., 1997. Bcl-2 and the outer mitochondrial membrane in the inactivation of cytochrome c during Fas-mediated apoptosis. J. Biol. Chem. 272, 21878–21882.

Adachi, T., Yamamoto, M., Hara, H., Masuda, K., Mitsui, N., Oh-ishi, T., Okazaki, M., 2001. Extracellular-superoxide dismutase in cerebrospinal fluid from infants/children. Clin. Chim. Acta Int. J. Clin. Chem. 308, 191–193.

Adam-Vizi, V., 2005. Production of reactive oxygen species in brain mitochondria: contribution by electron transport chain and non-electron transport chain sources. Antioxid. Redox Signal. 7, 1140–1149.

Alho, H., Leinonen, J.S., Erhola, M., Lönnrot, K., Aejmelaeus, R., 1998. Assay of antioxidant capacity of human plasma and CSF in aging and disease. Restor. Neurol. Neurosci. 12, 159–165.

Allegra, C.J., Fine, R.L., Drake, J.C., Chabner, B.A., 1986. The effect of methotrexate on intracellular folate pools in human MCF-7 breast cancer cells. Evidence for direct inhibition of purine synthesis. J. Biol. Chem. 261, 6478–6485.

Allen, R.J., DiMauro, S., Coulter, D.L., Papadimitriou, A., Rothenberg, S.P., 1983. Kearns-Sayre syndrome with reduced plasma and cerebrospinal fluid folate. Ann. Neurol. 13, 679–682.

Almeida, A., Medina, J.M., 1998. A rapid method for the isolation of metabolically active mitochondria from rat neurons and astrocytes in primary culture. Brain Res. Brain Res. Protoc. 2, 209–214.

Altmann, R., 1890. Die Elementarorganismen und ihre Beziehungen zu den Zellen. Leipzig, Germany.

Alvira-Botero, X., Pérez-Gonzalez, R., Spuch, C., Vargas, T., Antequera, D., Garzón, M., Bermejo-Pareja, F., Carro, E., 2010. Megalin interacts with APP and the intracellular adapter protein FE65 in neurons. Mol. Cell. Neurosci. 45, 306–315.

Amorim, M.R., Lima, M.A.C., Castilla, E.E., Orioli, I.M., 2007. Non-Latin European descent could be a requirement for association of NTDs and MTHFR variant 677C > T: a meta-analysis. Am. J. Med. Genet. A. 143A, 1726–1732.

Anderson, D.D., Woeller, C.F., Chiang, E.-P., Shane, B., Stover, P.J., 2012. Serine hydroxymethyltransferase anchors de novo thymidylate synthesis pathway to nuclear lamina for DNA synthesis. J. Biol. Chem. 287, 7051–7062.

Angelini, C., Bello, L., Spinazzi, M., Ferrati, C., 2009. Mitochondrial disorders of the nuclear genome. Acta Myol. Myopathies Cardiomyopathies Off. J. Mediterr. Soc. Myol. Ed. Gaetano Conte Acad. Study Striated Muscle Dis. 28, 16–23.

Anguera, M.C., Field, M.S., Perry, C., Ghandour, H., Chiang, E.-P., Selhub, J., Shane, B., Stover, P.J., 2006. Regulation of folate-mediated one-carbon metabolism by 10-formyltetrahydrofolate dehydrogenase. J. Biol. Chem. 281, 18335–18342.

Aon, M.A., Stanley, B.A., Sivakumaran, V., Kembro, J.M., O'Rourke, B., Paolocci, N., Cortassa, S., 2012. Glutathione/thioredoxin systems modulate

mitochondrial H2O2 emission: an experimental-computational study. J. Gen. Physiol. 139, 479–491.
Araújo, J.R., Gonçalves, P., Martel, F., 2010. Characterization of uptake of folates by rat and human blood-brain barrier endothelial cells. BioFactors Oxf. Engl. 36, 201–209.
Arrigoni, O., De Tullio, M.C., 2002. Ascorbic acid: much more than just an antioxidant. Biochim. Biophys. Acta BBA - Gen. Subj. 1569, 1–9.
Arthur, J.R., Beckett, G.J., Mitchell, J.H., 1999. The interactions between selenium and iodine deficiencies in man and animals. Nutr. Res. Rev. 12, 55–73.
Aust, S.D., Morehouse, L.A., Thomas, C.E., 1985. Role of metals in oxygen radical reactions. J. Free Radic. Biol. Med. 1, 3–25.
Aylett, S.-B., Neergheen, V., Hargreaves, I.P., Eaton, S., Land, J.M., Rahman, S., Heales, S.J.R., 2013. Levels of 5-Methyltetrahydrofolate and Ascorbic Acid in Cerebrospinal Fluid are Correlated: Implications for the Accelerated Degradation of Folate by Reactive Oxygen Species. Neurochem. Int. 63, 8, 750-755
Babcock, G.T., Wikström, M., 1992. Oxygen activation and the conservation of energy in cell respiration. Nature 356, 301–309.
Baggott, J.E., Morgan, S.L., Vaughn, W.H., 1994. Differences in methotrexate and 7-hydroxymethotrexate inhibition of folate-dependent enzymes of purine nucleotide biosynthesis. Biochem. J. 300 ( Pt 3), 627–629.
Baggott, J.E., Vaughn, W.H., Hudson, B.B., 1986. Inhibition of 5-aminoimidazole-4-carboxamide ribotide transformylase, adenosine deaminase and 5'-adenylate deaminase by polyglutamates of methotrexate and oxidized folates and by 5-aminoimidazole-4-carboxamide riboside and ribotide. Biochem. J. 236, 193–200.
Bai, L., Xu, H., Collins, J.F., Ghishan, F.K., 2001. Molecular and Functional Analysis of a Novel Neuronal Vesicular Glutamate Transporter. J. Biol. Chem. 276, 36764–36769.
Bailey, L.B., 2010. Folate in Health and Disease, Second Edition. CRC Press.
Balsa, E., Marco, R., Perales-Clemente, E., Szklarczyk, R., Calvo, E., Landázuri, M.O., Enríquez, J.A., 2012. NDUFA4 is a subunit of complex IV of the mammalian electron transport chain. Cell Metab. 16, 378–386.
Banerjee, R.V., Matthews, R.G., 1990. Cobalamin-dependent methionine synthase. FASEB J. 4, 1450–1459.
Banka, S., Blom, H.J., Walter, J., Aziz, M., Urquhart, J., Clouthier, C.M., Rice, G.I., de Brouwer, A.P.M., Hilton, E., Vassallo, G., Will, A., Smith, D.E.C., Smulders, Y.M., Wevers, R.A., Steinfeld, R., Heales, S., Crow, Y.J., Pelletier, J.N., Jones, S., Newman, W.G., 2011. Identification and characterization of an inborn error of metabolism caused by dihydrofolate reductase deficiency. Am. J. Hum. Genet. 88, 216–225.
Barabás, J., Nagy, E., Degrell, I., 1995. Ascorbic acid in cerebrospinal fluid - a possible protection against free radicals in the brain. Arch. Gerontol. Geriatr. 21, 43–48.
Barja, G., 1999. Mitochondrial oxygen radical generation and leak: sites of production in states 4 and 3, organ specificity, and relation to aging and longevity. J. Bioenerg. Biomembr. 31, 347–366.
Barja, G., Herrero, A., 1998. Localization at complex I and mechanism of the higher free radical production of brain nonsynaptic mitochondria in the short-lived rat than in the longevous pigeon. J. Bioenerg. Biomembr. 30, 235–243.

Barkovich, A.J., Good, W.V., Koch, T.K., Berg, B.O., 1993. Mitochondrial disorders: analysis of their clinical and imaging characteristics. AJNR Am. J. Neuroradiol. 14, 1119–1137.

Barnes, A.E., 1947. A case of scurvy. Br. Med. J. 1, 338.

Benda, C., 1898. Über die Spermatogenese der Vertebraten und höheren Evertebraten, II Theil: die Histiogenese der Spermien. Arch Anat Physiol 73, 393–398.

Bendich, A., Deckelbaum, R.J., 2010. Preventive Nutrition: The Comprehensive Guide for Health Professionals. Springer.

Berg, J.M., Tymoczko, J.L., Stryer, L., 2002. Purine Bases Can Be Synthesized de Novo or Recycled by Salvage Pathways. Biochemistry 5th Edition, New York.

Bering, E.A., Jr, 1955. Choroid plexus and arterial pulsation of cerebrospinal fluid; demonstration of the choroid plexuses as a cerebrospinal fluid pump. AMA Arch. Neurol. Psychiatry 73, 165–172.

Biedler, J.L., Helson, L., Spengler, B.A., 1973. Morphology and growth, tumorigenicity, and cytogenetics of human neuroblastoma cells in continuous culture. Cancer Res. 33, 2643–2652.

Bienert, G.P., Møller, A.L.B., Kristiansen, K.A., Schulz, A., Møller, I.M., Schjoerring, J.K., Jahn, T.P., 2007. Specific aquaporins facilitate the diffusion of hydrogen peroxide across membranes. J. Biol. Chem. 282, 1183–1192.

Bird, A., 2008. The methyl-CpG-binding protein MeCP2 and neurological disease. Biochem. Soc. Trans. 36, 575–583.

Bittles, A.H., Mason, W.M., Greene, J., Rao, N.A., 1991. Reproductive behavior and health in consanguineous marriages. Science 252, 789–794.

Björnstedt, M., Kumar, S., Björkhem, L., Spyrou, G., Holmgren, A., 1997. Selenium and the thioredoxin and glutaredoxin systems. Biomed. Environ. Sci. BES 10, 271–279.

Blair, J.A., Pearson, A.J., 1974. Kinetics and mechanism of the autoxidation of the 2-amino-4-hydroxy-5,6,7,8-tetrahydropteridines. J. Chem. Soc. Perkin Trans. 2 80–88.

Blair, J.A., Pearson, A.J., Robb, A.J., 1975. Autoxidation of 5-methyl-5,6,7,8-tetrahydrofolic acid. J. Chem. Soc. Perkin Trans. 2 18–21.

Blau, N., Bonafé, L., Krägeloh-Mann, I., Thöny, B., Kierat, L., Häusler, M., Ramaekers, V., 2003. Cerebrospinal fluid pterins and folates in Aicardi-Goutières syndrome: a new phenotype. Neurology 61, 642–647.

Bleijenberg, B.G., Van Eijk, H.G., Leijnse, B., 1971. The determination of non-heme iron and transferrin in cerebrospinal fluid. Clin. Chim. Acta 31, 277–281.

Blount, B.C., Mack, M.M., Wehr, C.M., MacGregor, J.T., Hiatt, R.A., Wang, G., Wickramasinghe, S.N., Everson, R.B., Ames, B.N., 1997. Folate deficiency causes uracil misincorporation into human DNA and chromosome breakage: implications for cancer and neuronal damage. Proc. Natl. Acad. Sci. U. S. A. 94, 3290–3295.

Borle, A.B., 1975. Regulation of cellular calcium metabolism and calcium transport by calcitonin. J. Membr. Biol. 21, 125–146.

Boveris, A., Cadenas, E., Stoppani, A.O., 1976. Role of ubiquinone in the mitochondrial generation of hydrogen peroxide. Biochem. J. 156, 435–444.

Boveris, A., Chance, B., 1973. The mitochondrial generation of hydrogen peroxide. General properties and effect of hyperbaric oxygen. Biochem. J. 134, 707–716.

Boveris, A., Oshino, N., Chance, B., 1972. The cellular production of hydrogen peroxide. Biochem. J. 128, 617–630.

Boyer, R.F., J. McCleary, C., 1987. Superoxide ion as a primary reductant in ascorbate-mediated ferretin iron release. Free Radic. Biol. Med. 3, 389–395.

Brackmann, F., Abicht, A., Ahting, U., Schröder, R., Trollmann, R., 2012. Classical MERRF phenotype associated with mitochondrial tRNALeu (m. 3243A> G) mutation. Eur. J. Pediatr. 171, 859–862.

Bradbury, M.W.B., 1997. Transport of Iron in the Blood-Brain-Cerebrospinal Fluid System. J. Neurochem. 69, 443–454.

Brau, R.H., García-Castiñeiras, S., Rifkinson, N., 1984. Cerebrospinal fluid ascorbic acid levels in neurological disorders. Neurosurgery 14, 142–146.

Brodbelt, A., Stoodley, M., 2007. CSF pathways: a review. Br. J. Neurosurg. 21, 510–520.

Brody, T., Watson, J.E., Stokstad, E.L., 1982. Folate pentaglutamate and folate hexaglutamate mediated one-carbon metabolism. Biochemistry (Mosc.) 21, 276–282.

Brown, P.D., Davies, S.L., Speake, T., Millar, I.D., 2004. Molecular mechanisms of cerebrospinal fluid production. Neuroscience 129, 957–970.

Brzezinski, P., Gennis, R.B., 2008. Cytochrome c oxidase: exciting progress and remaining mysteries. J. Bioenerg. Biomembr. 40, 521–531.

Buettner, G.R., Jurkiewicz, B.A., 2010. Catalytic Metals, Ascorbate and Free Radicals: Combinations to Avoid. Radiat. Res. 145(5):532-41

Burk, R.F., Hill, K.E., Olson, G.E., Weeber, E.J., Motley, A.K., Winfrey, V.P., Austin, L.M., 2007. Deletion of apolipoprotein E receptor-2 in mice lowers brain selenium and causes severe neurological dysfunction and death when a low-selenium diet is fed. J. Neurosci. Off. J. Soc. Neurosci. 27, 6207–6211.

Cadenas, E., Boveris, A., Ragan, C.I., Stoppani, A.O., 1977. Production of superoxide radicals and hydrogen peroxide by NADH-ubiquinone reductase and ubiquinol-cytochrome c reductase from beef-heart mitochondria. Arch. Biochem. Biophys. 180, 248–257.

Caprile, T., Salazar, K., Astuya, A., Cisternas, P., Silva-Alvarez, C., Montecinos, H., Millán, C., de Los Angeles García, M., Nualart, F., 2009. The Na+-dependent L-ascorbic acid transporter SVCT2 expressed in brainstem cells, neurons, and neuroblastoma cells is inhibited by flavonoids. J. Neurochem. 108, 563–577.

Carbajo, R.J., Kellas, F.A., Runswick, M.J., Montgomery, M.G., Walker, J.E., Neuhaus, D., 2005. Structure of the F1-binding domain of the stator of bovine F1Fo-ATPase and how it binds an alpha-subunit. J. Mol. Biol. 351, 824–838.

Carbajo, R.J., Kellas, F.A., Yang, J.-C., Runswick, M.J., Montgomery, M.G., Walker, J.E., Neuhaus, D., 2007. How the N-terminal domain of the OSCP subunit of bovine F1Fo-ATP synthase interacts with the N-terminal region of an alpha subunit. J. Mol. Biol. 368, 310–318.

Cario, H., Bode, H., Debatin, K.-M., Opladen, T., Schwarz, K., 2009. Congenital null mutations of the FOLR1 gene: a progressive neurologic disease and its treatment. Neurology 73, 2127–2129.

Cario, H., Smith, D.E.C., Blom, H., Blau, N., Bode, H., Holzmann, K., Pannicke, U., Hopfner, K.-P., Rump, E.-M., Ayric, Z., Kohne, E., Debatin, K.-M., Smulders, Y., Schwarz, K., 2011. Dihydrofolate reductase deficiency due to a homozygous DHFR mutation causes megaloblastic anemia and cerebral folate deficiency leading to severe neurologic disease. Am. J. Hum. Genet. 88, 226–231.

Carl, G.F., Hudson, F.Z., McGuire, B.S., Jr, 1997. Phenytoin-induced depletion of folate in rats originates in liver and involves a mechanism that does not discriminate folate form. J. Nutr. 127, 2231–2238.

Carpenter, K.J., 2012. The discovery of vitamin C. Ann. Nutr. Metab. 61, 259–264.

Catania, C., Spitaleri, G., Delmonte, A., Giovannini, M., Toffalorio, F., Noberasco, C., Bresolin, N., Comi, G., Pas, T.D., 2012. Safety of Systemic Chemotherapy in a Patient With Mitochondrial Myopathy and Non–Small-Cell Lung Cancer. J. Clin. Oncol. 30, e226–e228.

Cecchini, G., 2003. Function and structure of complex II of the respiratory chain. Annu. Rev. Biochem. 72, 77–109.

Chacinska, A., van der Laan, M., Mehnert, C.S., Guiard, B., Mick, D.U., Hutu, D.P., Truscott, K.N., Wiedemann, N., Meisinger, C., Pfanner, N., Rehling, P., 2010. Distinct forms of mitochondrial TOM-TIM supercomplexes define signal-dependent states of preprotein sorting. Mol. Cell. Biol. 30, 307–318.

Chan, S.S.L., Longley, M.J., Naviaux, R.K., Copeland, W.C., 2005. Mono-allelic POLG expression resulting from nonsense-mediated decay and alternative splicing in a patient with Alpers syndrome. DNA Repair 4, 1381–1389.

Chen, C., Ke, J., Zhou, X.E., Yi, W., Brunzelle, J.S., Li, J., Yong, E.-L., Xu, H.E., Melcher, K., 2013. Structural basis for molecular recognition of folic acid by folate receptors. Nature 500, 486–489.

Chen, J.-J., Boylan, L.M., Wu, C.-K., Spallholz, J.E., 2007a. Oxidation of glutathione and superoxide generation by inorganic and organic selenium compounds. BioFactors Oxf. Engl. 31, 55–66.

Chen, Q., Lesnefsky, E.J., 2006. Depletion of cardiolipin and cytochrome c during ischemia increases hydrogen peroxide production from the electron transport chain. Free Radic. Biol. Med. 40, 976–982.

Chen, Q., Vazquez, E.J., Moghaddas, S., Hoppel, C.L., Lesnefsky, E.J., 2003. Production of Reactive Oxygen Species by Mitochondria CENTRAL ROLE OF COMPLEX III. J. Biol. Chem. 278, 36027–36031.

Chen, Q.P., Li, Q.T., 2001. Effect of cardiolipin on proton permeability of phospholipid liposomes: the role of hydration at the lipid-water interface. Arch. Biochem. Biophys. 389, 201–206.

Chen, Y., McMillan-Ward, E., Kong, J., Israels, S.J., Gibson, S.B., 2007b. Mitochondrial electron-transport-chain inhibitors of complexes I and II induce autophagic cell death mediated by reactive oxygen species. J. Cell Sci. 120, 4155–4166.

Chen, Z.-S., Lee, K., Walther, S., Raftogianis, R.B., Kuwano, M., Zeng, H., Kruh, G.D., 2002. Analysis of methotrexate and folate transport by multidrug resistance protein 4 (ABCC4): MRP4 is a component of the methotrexate efflux system. Cancer Res. 62, 3144–3150.

Cheung, E., D'Ari, L., Rabinowitz, J.C., Dyer, D.H., Huang, J.Y., Stoddard, B.L., 1997. Purification, crystallization, and preliminary x-ray studies of a bifunctional 5,10-methenyl/methylene-tetrahydrofolate cyclohydrolase/dehydrogenase from Escherichia coli. Proteins 27, 322–324.

Cheung, Y.-T., Lau, W.K.-W., Yu, M.-S., Lai, C.S.-W., Yeung, S.-C., So, K.-F., Chang, R.C.-C., 2009. Effects of all-trans-retinoic acid on human SH-SY5Y neuroblastoma as in vitro model in neurotoxicity research. Neurotoxicology 30, 127–135.

Chi, C.-S., Lee, H.-F., Tsai, C.-R., Chen, C.C.-C., Tung, J.-N., 2011. Cranial magnetic resonance imaging findings in children with nonsyndromic mitochondrial diseases. Pediatr. Neurol. 44, 171–176.

Chi, C.-S., Lee, H.-F., Tsai, C.-R., Lee, H.-J., Chen, L.-H., 2010. Clinical manifestations in children with mitochondrial diseases. Pediatr. Neurol. 43, 183–189.

Chinnery, P.F., Howell, N., Lightowlers, R.N., Turnbull, D.M., 1997. Molecular pathology of MELAS and MERRF. The relationship between mutation load and clinical phenotypes. Brain J. Neurol. 120 ( Pt 10), 1713–1721.

Chinnery, P.F., Hudson, G., 2013. Mitochondrial genetics. Br. Med. Bull. 106, 135–159.

Choumenkovitch, S.F., Jacques, P.F., Nadeau, M.R., Wilson, P.W., Rosenberg, I.H., Selhub, J., 2001. Folic acid fortification increases red blood cell folate concentrations in the Framingham study. J. Nutr. 131, 3277–3280.

Christensen, K.E., Deng, L., Leung, K.Y., Arning, E., Bottiglieri, T., Malysheva, O.V., Caudill, M.A., Krupenko, N.I., Greene, N.D., Jerome-Majewska, L., Mackenzie, R.E., Rozen, R., 2013. A novel mouse model for genetic variation in 10-formyltetrahydrofolate synthetase exhibits disturbed purine synthesis with impacts on pregnancy and embryonic development. Hum. Mol. Genet. 22, 3705–3719.

Clifford, A.J., Noceti, E.M., Block-Joy, A., Block, T., Block, G., 2005. Erythrocyte folate and its response to folic acid supplementation is assay dependent in women. J. Nutr. 135, 137–143.

Clot, F., Grabli, D., Cazeneuve, C., Roze, E., Castelnau, P., Chabrol, B., Landrieu, P., Nguyen, K., Ponsot, G., Abada, M., Doummar, D., Damier, P., Gil, R., Thobois, S., Ward, A.J., Hutchinson, M., Toutain, A., Picard, F., Camuzat, A., Fedirko, E., Sân, C., Bouteiller, D., LeGuern, E., Durr, A., Vidailhet, M., Brice, A., French Dystonia Network, 2009. Exhaustive analysis of BH4 and dopamine biosynthesis genes in patients with Dopa-responsive dystonia. Brain J. Neurol. 132, 1753–1763.

Cole, P.D., Kamen, B.A., Gorlick, R., Banerjee, D., Smith, A.K., Magill, E., Bertino, J.R., 2001. Effects of overexpression of gamma-Glutamyl hydrolase on methotrexate metabolism and resistance. Cancer Res. 61, 4599–4604.

Collinson, I.R., Runswick, M.J., Buchanan, S.K., Fearnley, I.M., Skehel, J.M., van Raaij, M.J., Griffiths, D.E., Walker, J.E., 1994. Fo membrane domain of ATP synthase from bovine heart mitochondria: purification, subunit composition, and reconstitution with F1-ATPase. Biochemistry (Mosc.) 33, 7971–7978.

Connors, K.A., 1990. Chemical kinetics: the study of reaction rates in solution. VCH, New York, N.Y.

Cooper, C.E., Davies, N.A., 2000. Effects of nitric oxide and peroxynitrite on the cytochrome oxidase K(m) for oxygen: implications for mitochondrial pathology. Biochim. Biophys. Acta 1459, 390–396.

Copp, A.J., Greene, N.D., 2000. Neural tube defects: prevention by folic acid and other vitamins. Indian J. Pediatr. 67, 915–921.

Copp, A.J., Greene, N.D.E., 2010. Genetics and development of neural tube defects. J. Pathol. 220, 217–230.

Copp, A.J., Stanier, P., Greene, N.D.E., 2013. Neural tube defects: recent advances, unsolved questions, and controversies. Lancet Neurol. 12, 799–810.

Corti, A., Casini, A.F., Pompella, A., 2010. Cellular pathways for transport and efflux of ascorbate and dehydroascorbate. Arch. Biochem. Biophys. 500, 107–115.

Crabtree, M.J., Channon, K.M., 2011. Synthesis and recycling of tetrahydrobiopterin in endothelial function and vascular disease. Nitric Oxide Biol. Chem. Off. J. Nitric Oxide Soc. 25, 81–88.

Craven, L., Tuppen, H.A., Greggains, G.D., Harbottle, S.J., Murphy, J.L., Cree, L.M., Murdoch, A.P., Chinnery, P.F., Taylor, R.W., Lightowlers, R.N., Herbert, M., Turnbull, D.M., 2010. Pronuclear transfer in human embryos to prevent transmission of mitochondrial DNA disease. Nature 465, 82–85.

Cree, L.M., Samuels, D.C., de Sousa Lopes, S.C., Rajasimha, H.K., Wonnapinij, P., Mann, J.R., Dahl, H.-H.M., Chinnery, P.F., 2008. A reduction of mitochondrial DNA molecules during embryogenesis explains the rapid segregation of genotypes. Nat. Genet. 40, 249–254.

Crofts, A.R., 2004. Proton-coupled electron transfer at the Qo-site of the bc1 complex controls the rate of ubihydroquinone oxidation. Biochim. Biophys. Acta 1655, 77–92.

Crossgrove, J.S., Li, G.J., Zheng, W., 2005. The choroid plexus removes beta-amyloid from brain cerebrospinal fluid. Exp. Biol. Med. Maywood NJ 230, 771–776.

Cuddihy, S.L., Parker, A., Harwood, D.T., Vissers, M.C.M., Winterbourn, C.C., 2008. Ascorbate interacts with reduced glutathione to scavenge phenoxyl radicals in HL60 cells. Free Radic. Biol. Med. 44, 1637–1644.

Cui, S.-Y., Jin, H., Kim, S.-J., Kumar, A.P., Lee, Y.-I., 2008. Interaction of glutathione and sodium selenite in vitro investigated by electrospray ionization tandem mass spectrometry. J. Biochem. (Tokyo) 143, 685–693.

Cupello, A., Rapallino, M.V., Tabaton, M., Lunardi, G.L., 2002. A simple, inexpensive, and precise spectrophotometric method for evaluating the concentration of ascorbic acid in CSF samples: data from different neurological pathologies. Int. J. Neurosci. 112, 1337–1345.

Czech, M.P., Lawrence, J.C., Jr, Lynn, W.S., 1974. Evidence for the involvement of sulfhydryl oxidation in the regulation of fat cell hexose transport by insulin. Proc. Natl. Acad. Sci. U. S. A. 71, 4173–4177.

Daly, S., Mills, J., Molloy, A., Kirke, P., Scott, J., 1998. Folic acid food fortification to prevent neural tube defects. The Lancet 351, 834–835.

Das, K.C., Das, C.K., 2000. Thioredoxin, a singlet oxygen quencher and hydroxyl radical scavenger: redox independent functions. Biochem. Biophys. Res. Commun. 277, 443–447.

Davey, G.P., Clark, J.B., 1996. Threshold effects and control of oxidative phosphorylation in nonsynaptic rat brain mitochondria. J. Neurochem. 66, 1617–1624.

Davey, G.P., Peuchen, S., Clark, J.B., 1998. Energy thresholds in brain mitochondria. Potential involvement in neurodegeneration. J. Biol. Chem. 273, 12753–12757.

Dawson, T.L., Gores, G.J., Nieminen, A.L., Herman, B., Lemasters, J.J., 1993. Mitochondria as a source of reactive oxygen species during reductive stress in rat hepatocytes. Am. J. Physiol. 264, C961–967.

De Vries, S., Albracht, S.P., Berden, J.A., Slater, E.C., 1982. The pathway of electrons through OH2:cytochrome c oxidoreductase studied by pre-steady - state kinetics. Biochim. Biophys. Acta 681, 41–53.

DelVecchio, B., Dancea, S., 2011. Clinical Images: Scurvy in the modern era. Arthritis Rheum. 63, 310.

Depeint, F., Bruce, W.R., Shangari, N., Mehta, R., O'Brien, P.J., 2006. Mitochondrial function and toxicity: role of B vitamins on the one-carbon transfer pathways. Chem. Biol. Interact. 163, 113–132.

Di Pietro, E., Sirois, J., Tremblay, M.L., MacKenzie, R.E., 2002. Mitochondrial NAD-dependent methylenetetrahydrofolate dehydrogenase-methenyltetrahydrofolate cyclohydrolase is essential for embryonic development. Mol. Cell. Biol. 22, 4158–4166.

Dill, P., Schneider, J., Weber, P., Trachsel, D., Tekin, M., Jakobs, C., Thöny, B., Blau, N., 2011. Pyridoxal phosphate-responsive seizures in a patient with cerebral folate deficiency (CFD) and congenital deafness with labyrinthine aplasia, microtia and microdontia (LAMM). Mol. Genet. Metab. 104, 362–368.

Dimauro, S., Davidzon, G., 2005. Mitochondrial DNA and disease. Ann. Med. 37, 222–232.

DiMauro, S., Hirano, M., 1993. Mitochondrial DNA Deletion Syndromes, in: Pagon, R.A., Adam, M.P., Bird, T.D., Dolan, C.R., Fong, C.-T., Stephens, K. (Eds.), GeneReviews$^{TM}$. University of Washington, Seattle, Seattle (WA).

DiMauro, S., Schon, E.A., 2003. Mitochondrial respiratory-chain diseases. N. Engl. J. Med. 348, 2656–2668.

Ding, Y., Leng, J., Fan, F., Xia, B., Xu, P., 2013. The Role of Mitochondrial DNA Mutations in Hearing Loss. Biochem. Genet. 1–15.

Dixon, M.M., Huang, S., Matthews, R.G., Ludwig, M., 1996. The structure of the C-terminal domain of methionine synthase: presenting S-adenosylmethionine for reductive methylation of B12. Struct. Lond. Engl. 1993 4, 1263–1275.

Djukic, A., 2007. Folate-responsive neurologic diseases. Pediatr. Neurol. 37, 387–397.

Dos Santos, E.F., Busanello, E.N.B., Miglioranza, A., Zanatta, A., Barchak, A.G., Vargas, C.R., Saute, J., Rosa, C., Carrion, M.J., Camargo, D., Dalbem, A., da Costa, J.C., de Sousa Miguel, S.R.P., de Mello Rieder, C.R., Wajner, M., 2009. Evidence that folic acid deficiency is a major determinant of hyperhomocysteinemia in Parkinson's disease. Metab. Brain Dis. 24, 257–269.

Doudney, K., Grinham, J., Whittaker, J., Lynch, S.A., Thompson, D., Moore, G.E., Copp, A.J., Greene, N.D.E., Stanier, P., 2009. Evaluation of folate metabolism gene polymorphisms as risk factors for open and closed neural tube defects. Am. J. Med. Genet. A. 149A, 1585–1589.

Dringen, R., Kussmaul, L., Gutterer, J.M., Hirrlinger, J., Hamprecht, B., 1999. The glutathione system of peroxide detoxification is less efficient in neurons than in astroglial cells. J. Neurochem. 72, 2523–2530.

Dropp, J.J., 1976. Mast cells in mammalian brain. Acta Anat. (Basel) 94, 1–21.

Du, J., Cullen, J.J., Buettner, G.R., 2012. Ascorbic acid: chemistry, biology and the treatment of cancer. Biochim. Biophys. Acta 1826, 443–457.

Duan, W., Ladenheim, B., Cutler, R.G., Kruman, I.I., Cadet, J.L., Mattson, M.P., 2002. Dietary folate deficiency and elevated homocysteine levels endanger

dopaminergic neurons in models of Parkinson's disease. J. Neurochem. 80, 101–110.
Duchen, M.R., 2000. Mitochondria and calcium: from cell signalling to cell death. J. Physiol. 529, 57–68.
Dudeja, P.K., Kode, A., Alnounou, M., Tyagi, S., Torania, S., Subramanian, V.S., Said, H.M., 2001. Mechanism of folate transport across the human colonic basolateral membrane. Am. J. Physiol. Gastrointest. Liver Physiol. 281, G54–60.
Dunlevy, L.P.E., Chitty, L.S., Burren, K.A., Doudney, K., Stojilkovic-Mikic, T., Stanier, P., Scott, R., Copp, A.J., Greene, N.D.E., 2007. Abnormal folate metabolism in foetuses affected by neural tube defects. Brain J. Neurol. 130, 1043–1049.
Duno, M., Wibrand, F., Baggesen, K., Rosenberg, T., Kjaer, N., Frederiksen, A.L., 2012. A novel mitochondrial mutation m. 8989G> C associated with neuropathy, ataxia, retinitis pigmentosa-The NARP syndrome. Gene. 515, 372-375.
Enright, H.U., Miller, W.J., Hebbel, R.P., 1992. Nucleosomal histone protein protects DNA from iron-mediated damage. Nucleic Acids Res 20, 3341–3346.
Ernster, L., Ikkos, D., Luft, R., 1959. Enzymic activities of human skeletal muscle mitochondria: a tool in clinical metabolic research. Nature 184, 1851–1854.
Esterházy, D., King, M.S., Yakovlev, G., Hirst, J., 2008. Production of reactive oxygen species by complex I (NADH:ubiquinone oxidoreductase) from Escherichia coli and comparison to the enzyme from mitochondria. Biochemistry (Mosc.) 47, 3964–3971.
Fairweather-Tait, S.J., Bao, Y., Broadley, M.R., Collings, R., Ford, D., Hesketh, J.E., Hurst, R., 2011. Selenium in human health and disease. Antioxid. Redox Signal. 14, 1337–1383.
Farrell, C.L., Yang, J., Pardridge, W.M., 1992. GLUT-1 glucose transporter is present within apical and basolateral membranes of brain epithelial interfaces and in microvascular endothelia with and without tight junctions. J. Histochem. Cytochem. Off. J. Histochem. Soc. 40, 193–199.
Fell, D., Steele, R.D., 1982. Enhancement of histidine and one-carbon metabolism in rats fed high levels of retinol. J. Nutr. 112, 474–479.
Fenton, H.J.H., 1894. LXXIII.—Oxidation of tartaric acid in presence of iron. J. Chem. Soc. Trans. 65, 899–910.
Fernandes, A.P., Wallenberg, M., Gandin, V., Misra, S., Tisato, F., Marzano, C., Rigobello, M.P., Kumar, S., Björnstedt, M., 2012. Methylselenol formed by spontaneous methylation of selenide is a superior selenium substrate to the thioredoxin and glutaredoxin systems. PloS One 7, e. 50727.
Fernández, O., Carreras, O., Murillo, M.L., 1998. Intestinal absorption and enterohepatic circulation of folic acid: effect of ethanol. Digestion 59, 130–133.
Field, M.S., Szebenyi, D.M.E., Stover, P.J., 2006. Regulation of de novo purine biosynthesis by methenyltetrahydrofolate synthetase in neuroblastoma. J. Biol. Chem. 281, 4215–4221.
Filosto, M., Scarpelli, M., Tonin, P., Lucchini, G., Pavan, F., Santus, F., Parini, R., Donati, M.A., Cotelli, M.S., Vielmi, V., Todeschini, A., Canonico, F., Tomelleri, G., Padovani, A., Rovelli, A., 2012. Course and management of

allogeneic stem cell transplantation in patients with mitochondrial neurogastrointestinal encephalomyopathy. J. Neurol. 259, 2699–2706.
Fisher, A.E.O., Naughton, D.P., 2003. Vitamin C contributes to inflammation via radical generating mechanisms: a cautionary note. Med. Hypotheses 61, 657–660.
Flanagan, R.J., Perrett, D., Whelpton, R., 2005. Electrochemical Detection in Hplc: Analysis of Drugs And Poisons. Royal Society of Chemistry.
Fleischer, S., Rouser, G., Fleischer, B., Casu, A., Kritchevsky, G., 1967. Lipid composition of mitochondria from bovine heart, liver, and kidney. J. Lipid Res. 8, 170–180.
Forner, F., Foster, L.J., Campanaro, S., Valle, G., Mann, M., 2006. Quantitative proteomic comparison of rat mitochondria from muscle, heart, and liver. Mol. Cell. Proteomics MCP 5, 608–619.
Fox, J.T., Stover, P.J., 2008. Folate-mediated one-carbon metabolism. Vitam. Horm. 79, 1–44.
Fox, T.D., 2012. Mitochondrial Protein Synthesis, Import, and Assembly. Genetics 192, 1203–1234.
Friedrich, T., Böttcher, B., 2004. The gross structure of the respiratory complex I: a Lego System. Biochim. Biophys. Acta 1608, 1–9.
Frye, R.E., Sequeira, J.M., Quadros, E.V., James, S.J., Rossignol, D.A., 2013. Cerebral folate receptor autoantibodies in autism spectrum disorder. Mol. Psychiatry 18, 369–381.
Fujii, K., Nagasaki, T., Huennekens, F.M., 1982. Accumulation of 5-methyltetrahydrofolate in cobalamin-deficient L1210 mouse leukemia cells. J. Biol. Chem. 257, 2144–2146.
Gabel-Jensen, C., Lunøe, K., Gammelgaard, B., 2010. Formation of methylselenol, dimethylselenide and dimethyldiselenide in in vitro metabolism models determined by headspace GC-MS. Met. Integr. Biometal Sci. 2, 167–173.
Galluzzi, L., Kepp, O., Trojel-Hansen, C., Kroemer, G., 2012. Non-apoptotic functions of apoptosis-regulatory proteins. EMBO Rep. 13, 322–330.
Ganichkin, O.M., Xu, X.-M., Carlson, B.A., Mix, H., Hatfield, D.L., Gladyshev, V.N., Wahl, M.C., 2008. Structure and catalytic mechanism of eukaryotic selenocysteine synthase. J. Biol. Chem. 283, 5849–5865.
Garcia-Cazorla, A., Quadros, E.V., Nascimento, A., Garcia-Silva, M.T., Briones, P., Montoya, J., Ormazábal, A., Artuch, R., Sequeira, J.M., Blau, N., Arenas, J., Pineda, M., Ramaekers, V.T., 2008. Mitochondrial diseases associated with cerebral folate deficiency. Neurology 70, 1360–1362.
Girgis, S., Suh, J.R., Jolivet, J., Stover, P.J., 1997. 5-Formyltetrahydrofolate regulates homocysteine remethylation in human neuroblastoma. J. Biol. Chem. 272, 4729–4734.
Golbahar, J., Aminzadeh, M.A., Hamidi, S.A., Omrani, G.R., 2005. Association of red blood cell 5-methyltetrahydrofolate folate with bone mineral density in postmenopausal Iranian women. Osteoporos. Int. J. Establ. Result Coop. Eur. Found. Osteoporos. Natl. Osteoporos. Found. USA 16, 1894–1898.
Gomez-Fernandez, J.C., Villalain, J., Aranda, F.J., Ortiz, A., Micol, V., Coutinho, A., Berberan-Santos, M.N., Prieto, M.J., 1989. Localization of alpha-tocopherol in membranes. Ann. N. Y. Acad. Sci. 570, 109–120.
Grapp, M., Just, I.A., Linnankivi, T., Wolf, P., Lucke, T., Hausler, M., Gartner, J., Steinfeld, R., 2012. Molecular characterization of folate receptor 1 mutations delineates cerebral folate transport deficiency. Brain 135, 2022–2031.

Grapp, M., Wrede, A., Schweizer, M., Hüwel, S., Galla, H.-J., Snaidero, N., Simons, M., Bückers, J., Low, P.S., Urlaub, H., Gärtner, J., Steinfeld, R., 2013. Choroid plexus transcytosis and exosome shuttling deliver folate into brain parenchyma. Nat. Commun. 4, 2123.

Gray, M.W., Burger, G., Lang, B.F., 1999. Mitochondrial evolution. Science 283, 1476–1481.

Green, D.E., Blondin, G.A., 1978. Molecular mechanism of mitochondrial energy coupling. Bioscience 28, 18–24.

Green, D.E., Zande, H.V., 1982. On the enzymic mechanism of oxidative phosphorylation. Proc. Natl. Acad. Sci. 79, 1064–1068.

Grönlund, M.A., Honarvar, A.K.S., Andersson, S., Moslemi, A.R., Oldfors, A., Holme, E., Tulinius, M., Darin, N., 2010. Ophthalmological findings in children and young adults with genetically verified mitochondrial disease. Br. J. Ophthalmol. 94, 121–127.

Gropman, A., Chen, T.-J., Perng, C.-L., Krasnewich, D., Chernoff, E., Tifft, C., Wong, L.-J.C., 2004. Variable clinical manifestation of homoplasmic G14459A mitochondrial DNA mutation. Am. J. Med. Genet. A. 124A, 377–382.

Guillausseau, P.J., Massin, P., Dubois-LaForgue, D., Timsit, J., Virally, M., Gin, H., Bertin, E., Blickle, J.F., Bouhanick, B., Cahen, J., Caillat-Zucman, S., Charpentier, G., Chedin, P., Derrien, C., Ducluzeau, P.H., Grimaldi, A., Guerci, B., Kaloustian, E., Murat, A., Olivier, F., Paques, M., Paquis-Flucklinger, V., Porokhov, B., Samuel-Lajeunesse, J., Vialettes, B., 2001. Maternally inherited diabetes and deafness: a multicenter study. Ann. Intern. Med. 134, 721–728.

Guo, J., Lemire, B.D., 2003. The ubiquinone-binding site of the Saccharomyces cerevisiae succinate-ubiquinone oxidoreductase is a source of superoxide. J. Biol. Chem. 278, 47629–47635.

Ha, H., Hajek, P., Bedwell, D.M., Burrows, P.D., 1993. A mitochondrial porin cDNA predicts the existence of multiple human porins. J. Biol. Chem. 268, 12143–12149.

Halliwell, B., 1992. Reactive oxygen species and the central nervous system. J. Neurochem. 59, 1609–1623.

Halliwell, B., 1996. Antioxidants in human health and disease. Annu. Rev. Nutr. 16, 33–50.

Halliwell, B., Gutteridge, J.M., 1990. Role of free radicals and catalytic metal ions in human disease: an overview. Methods Enzymol. 186, 1–85.

Halliwell, B., Whiteman, M., 2004. Measuring reactive species and oxidative damage in vivo and in cell culture: how should you do it and what do the results mean? Br. J. Pharmacol. 142, 231–255.

Halpner, A.D., Handelman, G.J., Harris, J.M., Belmont, C.A., Blumberg, J.B., 1998. Protection by vitamin C of loss of vitamin E in cultured rat hepatocytes. Arch. Biochem. Biophys. 359, 305–309.

Hamamy, H., 2012. Consanguineous marriages. J. Community Genet. 3, 185–192.

Hamilton, G.A., Workman, R.J., Woo, L., 1964. Oxidation by Molecular Oxygen. I. Reactions of a Possible Model System for Mixed-Function Oxidases. J. Am. Chem. Soc. 86, 3390–3391.

Hannisdal, R., Ueland, P.M., Svardal, A., 2009. Liquid chromatography-tandem mass spectrometry analysis of folate and folate catabolites in human serum. Clin. Chem. 55, 1147–1154.

Hansen, F.J., Blau, N., 2005. Cerebral folate deficiency: life-changing supplementation with folinic acid. Mol. Genet. Metab. 84, 371–373.
Hara, K., Sata, T., Shigematsu, A., 2004. Anesthetic management for cardioverter-defibrillator implantation in a patient with Kearns-Sayre syndrome. J. Clin. Anesth. 16, 539–541.
Hargreaves, I.P., Duncan, A.J., Wu, L., Agrawal, A., Land, J.M., Heales, S.J.R., 2007. Inhibition of mitochondrial complex IV leads to secondary loss complex II-III activity: implications for the pathogenesis and treatment of mitochondrial encephalomyopathies. Mitochondrion 7, 284–287.
Hargreaves, I.P., Heales, S.J., Land, J.M., 1999. Mitochondrial respiratory chain defects are not accompanied by an increase in the activities of lactate dehydrogenase or manganese superoxide dismutase in paediatric skeletal muscle biopsies. J. Inherit. Metab. Dis. 22, 925–931.
Harrison, F.E., May, J.M., 2009. Vitamin C function in the brain: vital role of the ascorbate transporter SVCT2. Free Radic. Biol. Med. 46, 719–730.
Harrison, W.W., Netsky, M.G., Brown, M.D., 1968. Trace elements in human brain: Copper, zinc, iron, and magnesium. Clin. Chim. Acta 21, 55–60.
Hashmi, M.H., Shahid, M.A., Akhtar, M.A., Chughtai, N.A., 1973. Colorimetric determination of ascorbic acid. Microchim. Acta 61, 901–906.
Hasselmann, O., Blau, N., Ramaekers, V.T., Quadros, E.V., Sequeira, J.M., Weissert, M., 2010. Cerebral folate deficiency and CNS inflammatory markers in Alpers disease. Mol. Genet. Metab. 99, 58–61.
Heales, S.J., Blair, J.A., Meinschad, C., Ziegler, I., 1988. Inhibition of monocyte luminol-dependent chemiluminescence by tetrahydrobiopterin, and the free radical oxidation of tetrahydrobiopterin, dihydrobiopterin and dihydroneopterin. Cell Biochem. Funct. 6, 191–195.
Heales, S.J.R., Gegg, M.E., Clark, J.B., 2002. Oxidative phosphorylation: structure, function, and intermediary metabolism. Int. Rev. Neurobiol. 53, 25–56.
Herbig, K., Chiang, E.-P., Lee, L.-R., Hills, J., Shane, B., Stover, P.J., 2002. Cytoplasmic serine hydroxymethyltransferase mediates competition between folate-dependent deoxyribonucleotide and S-adenosylmethionine biosyntheses. J. Biol. Chem. 277, 38381–38389.
Hernández-Díaz, S., Werler, M.M., Walker, A.M., Mitchell, A.A., 2001. Neural tube defects in relation to use of folic acid antagonists during pregnancy. Am. J. Epidemiol. 153, 961–968.
Hinken, M., Halwachs, S., Kneuer, C., Honscha, W., 2011. Subcellular localization and distribution of the reduced folate carrier in normal rat tissues. Eur. J. Histochem. EJH 55, e3.
Hinterberger, M., Fischer, P., 2013. Folate and Alzheimer: when time matters. J. Neural Transm. Vienna Austria 1996 120, 211–224.
Hirrlinger, J., Schulz, J.B., Dringen, R., 2002. Glutathione release from cultured brain cells: multidrug resistance protein 1 mediates the release of GSH from rat astroglial cells. J. Neurosci. Res. 69, 318–326.
Hirst, J., 2010. Towards the molecular mechanism of respiratory complex I. Biochem. J. 425, 327–339.
Hirst, J., King, M.S., Pryde, K.R., 2008. The production of reactive oxygen species by complex I. Biochem. Soc. Trans. 36, 976–980.
Ho, A., Michelson, D., Aaen, G., Ashwal, S., 2010. Cerebral folate deficiency presenting as adolescent catatonic schizophrenia: a case report. J. Child Neurol. 25, 898–900.

Honein, M.A., Paulozzi, L.J., Mathews, T.J., Erickson, J.D., Wong, L.Y., 2001. Impact of folic acid fortification of the US food supply on the occurrence of neural tube defects. JAMA J. Am. Med. Assoc. 285, 2981–2986.

Hooijberg, J.H., Peters, G.J., Assaraf, Y.G., Kathmann, I., Priest, D.G., Bunni, M.A., Veerman, A.J.P., Scheffer, G.L., Kaspers, G.J.L., Jansen, G., 2003. The role of multidrug resistance proteins MRP1, MRP2 and MRP3 in cellular folate homeostasis. Biochem. Pharmacol. 65, 765–771.

Hori, T., Ayusawa, D., Shimizu, K., Koyama, H., Seno, T., 1984. Chromosome breakage induced by thymidylate stress in thymidylate synthase-negative mutants of mouse FM3A cells. Cancer Res. 44, 703–709.

Horsefield, R., Iwata, S., Byrne, B., 2004. Complex II from a structural perspective. Curr. Protein Pept. Sci. 5, 107–118.

Horváth, R., Bender, A., Abicht, A., Holinski-Feder, E., Czermin, B., Trips, T., Schneiderat, P., Lochmüller, H., Klopstock, T., 2009. Heteroplasmic mutation in the anticodon-stem of mitochondrial tRNA(Val) causing MNGIE-like gastrointestinal dysmotility and cachexia. J. Neurol. 256, 810–815.

Hosoya, K., Nakamura, G., Akanuma, S., Tomi, M., Tachikawa, M., 2008. Dehydroascorbic acid uptake and intracellular ascorbic acid accumulation in cultured Müller glial cells (TR-MUL). Neurochem. Int. 52, 1351–1357.

Huang, C.-C., Chen, R.-S., Chu, N.-S., Pang, C.-Y., Wei, Y.-H., 1996. Random mitotic segregation of mitochondrial DNA in MELAS syndrome. Acta Neurol. Scand. 93, 198–202.

Huang, C.-C., Kuo, H.-C., Chu, C.-C., Liou, C.-W., Ma, Y.-S., Wei, Y.-H., 2002. Clinical phenotype, prognosis and mitochondrial DNA mutation load in mitochondrial encephalomyopathies. J. Biomed. Sci. 9, 527–533.

Hussein, E., 2013. Non-myeloablative bone marrow transplant and platelet infusion can transiently improve the clinical outcome of mitochondrial neurogastrointestinal encephalopathy: a case report. Transfus. Apher. Sci. Off. J. World Apher. Assoc. Off. J. Eur. Soc. Haemapheresis 49, 208–211.

Hyland, K., 1993. Abnormalities of biogenic amine metabolism. J. Inherit. Metab. Dis. 16, 676–690.

Hyland, K., Bottiglieri, T., 1992. Measurement of total plasma and cerebrospinal fluid homocysteine by fluorescence following high-performance liquid chromatography and precolumn derivatization with o-phthaldialdehyde. J. Chromatogr. 579, 55–62.

Hyland, K., Shoffner, J., Heales, S.J., 2010. Cerebral folate deficiency. J. Inherit. Metab. Dis. 33, 563–570.

Hyland, K., Smith, I., Bottiglieri, T., Perry, J., Wendel, U., Clayton, P.T., Leonard, J.V., 1988. Demyelination and decreased S-adenosylmethionine in 5,10-methylenetetrahydrofolate reductase deficiency. Neurology 38, 459–462.

Hyland, K., Surtees, R., 1992. Measurement of 5-methyltetrahydrofolate in cerebrospinal fluid using HPLC with coulometric electrochemical detection. Pteridines 3, 149–150.

Hyland, K., Surtees, R.A., Heales, S.J., Bowron, A., Howells, D.W., Smith, I., 1993. Cerebrospinal fluid concentrations of pterins and metabolites of serotonin and dopamine in a pediatric reference population. Pediatr. Res. 34, 10–14.

Imbard, A., Smulders, Y.M., Barto, R., Smith, D.E.C., Kok, R.M., Jakobs, C., Blom, H.J., 2013. Plasma choline and betaine correlate with serum folate, plasma S-

adenosyl-methionine and S-adenosyl-homocysteine in healthy volunteers. Clin. Chem. Lab. Med. CCLM FESCC 51, 683–692.

Irons, M., Levy, H.L., O'Flynn, M.E., Stack, C.V., Langlais, P.J., Butler, I.J., Milstien, S., Kaufman, S., 1987. Folinic acid therapy in treatment of dihydropteridine reductase deficiency. J. Pediatr. 110, 61–67.

Ito, A., Hayashi, S., Yoshida, T., 1981. Participation of a cytochrome b5-like hemoprotein of outer mitochondrial membrane (OM cytochrome b) in NADH-semidehydroascorbic acid reductase activity of rat liver. Biochem. Biophys. Res. Commun. 101, 591–598.

Jackson, M.J., Schaefer, J.A., Johnson, M.A., Morris, A.A., Turnbull, D.M., Bindoff, L.A., 1995. Presentation and clinical investigation of mitochondrial respiratory chain disease. A study of 51 patients. Brain J. Neurol. 118 ( Pt 2), 339–357.

Jacobson, J., Duchen, M.R., Hothersall, J., Clark, J.B., Heales, S.J.R., 2005. Induction of mitochondrial oxidative stress in astrocytes by nitric oxide precedes disruption of energy metabolism. J. Neurochem. 95, 388–395.

Jägerstad, M., Jastrebova, J., 2013. Occurrence, Stability, and Determination of Formyl Folates in Foods. J. Agric. Food Chem. 61, 9758-68

Jencks, D.A., Mathews, R.G., 1987. Allosteric inhibition of methylenetetrahydrofolate reductase by adenosylmethionine. Effects of adenosylmethionine and NADPH on the equilibrium between active and inactive forms of the enzyme and on the kinetics of approach to equilibrium. J. Biol. Chem. 262, 2485–2493.

Johanson, C., McMillan, P., Tavares, R., Spangenberger, A., Duncan, J., Silverberg, G., Stopa, E., 2004. Homeostatic capabilities of the choroid plexus epithelium in Alzheimer's disease. Cerebrospinal Fluid Res. 1, 3.

Kaufman, S., 1991. Some metabolic relationships between biopterin and folate: Implications for the "methyl trap hypothesis". Neurochem. Res. 16, 1031–1036.

Khan, A., Khan, M.I., Iqbal, Z., Shah, Y., Ahmad, L., Nazir, S., Watson, D.G., Khan, J.A., Nasir, F., Khan, A., Ismail, 2011. A new HPLC method for the simultaneous determination of ascorbic acid and aminothiols in human plasma and erythrocytes using electrochemical detection. Talanta 84, 789–801.

Khatami, M., Stramm, L.E., Rockey, J.H., 1986. Ascorbate transport in cultured cat retinal pigment epithelial cells. Exp. Eye Res. 43, 607–615.

Kholodenko, B., Zilinskiene, V., Borutaite, V., Ivanoviene, L., Toleikis, A., Praskevicius, A., 1987. The role of adenine nucleotide translocators in regulation of oxidative phosphorylation in heart mitochondria. FEBS Lett. 223, 247–250.

Khurana, D., Salganicoff, L., Melvin, J., Hobdell, E., Valencia, I., Hardison, H., Marks, H., Grover, W., Legido, A., 2008. Epilepsy and respiratory chain defects in children with mitochondrial encephalopathies. Epilepsia 49, 1972–1972.

Kierdaszuk, B., Jamrozik, Z., Tońska, K., Bartnik, E., Kaliszewska, M., Kamińska, A., Kwieciński, H., 2009. Mitochondrial cytopathies: clinical, morphological and genetic characteristics. Neurol. Neurochir. Pol. 43, 216–227.

Kim, E.H., Sohn, S., Kwon, H.J., Kim, S.U., Kim, M.-J., Lee, S.-J., Choi, K.S., 2007. Sodium selenite induces superoxide-mediated mitochondrial damage

and subsequent autophagic cell death in malignant glioma cells. Cancer Res. 67, 6314–6324.
King, T.E., 1967. Preparation of succinate cytochrome c reductase and cytochrome b-cl particle and reconstitution of succinate cytochrome c reductase. Methods Enzymol. 10, 217–235.
Kirsch, M., Korth, H.-G., Stenert, V., Sustmann, R., de Groot, H., 2003. The autoxidation of tetrahydrobiopterin revisited. Proof of superoxide formation from reaction of tetrahydrobiopterin with molecular oxygen. J. Biol. Chem. 278, 24481–24490.
Kluck, R.M., Bossy-Wetzel, E., Green, D.R., Newmeyer, D.D., 1997. The release of cytochrome c from mitochondria: a primary site for Bcl-2 regulation of apoptosis. Science 275, 1132–1136.
Koga, Y., Akita, Y., Nishioka, J., Yatsuga, S., Povalko, N., Tanabe, Y., Fujimoto, S., Matsuishi, T., 2005. L-arginine improves the symptoms of strokelike episodes in MELAS. Neurology 64, 710–712.
Kolmakova, T.S., Smirnova, O.B., Belyakova, E.I., 2010. Antioxidant properties of the cerebrospinal fluid in neurodegenerative diseases. Neurochem. J. 4, 41–45.
Koury, M.J., Ponka, P., 2004. New insights into erythropoiesis: the roles of folate, vitamin B12, and iron. Annu. Rev. Nutr. 24, 105–131.
Kowaltowski, A.J., de Souza-Pinto, N.C., Castilho, R.F., Vercesi, A.E., 2009. Mitochondria and reactive oxygen species. Free Radic. Biol. Med. 47, 333–343.
Kratzer, I., Vasiljevic, A., Rey, C., Fevre-Montange, M., Saunders, N., Strazielle, N., Ghersi-Egea, J.-F., 2012. Complexity and developmental changes in the expression pattern of claudins at the blood-CSF barrier. Histochem. Cell Biol. 138, 861–879.
Kronenberg, G., Gertz, K., Overall, R.W., Harms, C., Klein, J., Page, M.M., Stuart, J.A., Endres, M., 2011. Folate deficiency increases mtDNA and D-1 mtDNA deletion in aged brain of mice lacking uracil-DNA glycosylase. Exp. Neurol. 228, 253–258.
Kushnareva, Y., Murphy, A.N., Andreyev, A., 2002. Complex I-mediated reactive oxygen species generation: modulation by cytochrome c and NAD(P)+ oxidation-reduction state. Biochem. J. 368, 545–553.
Kussmaul, L., Hirst, J., 2006. The mechanism of superoxide production by NADH:ubiquinone oxidoreductase (complex I) from bovine heart mitochondria. Proc. Natl. Acad. Sci. U. S. A. 103, 7607–7612.
Kwong, L.K., Sohal, R.S., 2000. Age-related changes in activities of mitochondrial electron transport complexes in various tissues of the mouse. Arch. Biochem. Biophys. 373, 16–22.
Lam, A.A.J., Heales, S.J.R., 2007. Nitric oxide accelerates the degradation of tetrahydrobiopterin but not total neopterin in cerebrospinal fluid; potential implications for the assessment of tetrahydrobiopterin metabolism. Ann. Clin. Biochem. 44, 394–396.
Lamarre, S.G., Molloy, A.M., Reinke, S.N., Sykes, B.D., Brosnan, M.E., Brosnan, J.T., 2012. Formate can differentiate between hyperhomocysteinemia due to impaired remethylation and impaired transsulfuration. Am. J. Physiol. Endocrinol. Metab. 302, E61–67.

Lambert, A.J., Brand, M.D., 2004. Inhibitors of the quinone-binding site allow rapid superoxide production from mitochondrial NADH:ubiquinone oxidoreductase (complex I). J. Biol. Chem. 279, 39414–39420.

Lammer, E.J., Sever, L.E., Oakley, G.P., Jr, 1987. Teratogen update: valproic acid. Teratology 35, 465–473.

Larsson, N.-G., 2010. Somatic mitochondrial DNA mutations in mammalian aging. Annu. Rev. Biochem. 79, 683–706.

Lebovitz, R.M., Zhang, H., Vogel, H., Cartwright, J., Jr, Dionne, L., Lu, N., Huang, S., Matzuk, M.M., 1996. Neurodegeneration, myocardial injury, and perinatal death in mitochondrial superoxide dismutase-deficient mice. Proc. Natl. Acad. Sci. U. S. A. 93, 9782–9787.

Leclerc, D., Odièvre, M.-H., Wu, Q., Wilson, A., Huizenga, J.J., Rozen, R., Scherer, S.W., Gravel, R.A., 1999. Molecular cloning, expression and physical mapping of the human methionine synthase reductase gene. Gene 240, 75–88.

Lee, H.-F., Chi, C.-S., Tsai, C.-R., Chen, C.-H., 2011. Epileptic seizures in infants and children with mitochondrial diseases. Pediatr. Neurol. 45, 169–174.

Lee, P.Y., Costumbrado, J., Hsu, C.-Y., Kim, Y.H., 2012. Agarose gel electrophoresis for the separation of DNA fragments. J. Vis. Exp. JoVE. 62, 3923.

Lee, W.-K., Thévenod, F., 2006. A role for mitochondrial aquaporins in cellular life-and-death decisions? Am. J. Physiol. Cell Physiol. 291, C195–202.

Leggas, M., Adachi, M., Scheffer, G.L., Sun, D., Wielinga, P., Du, G., Mercer, K.E., Zhuang, Y., Panetta, J.C., Johnston, B., Scheper, R.J., Stewart, C.F., Schuetz, J.D., 2004. Mrp4 confers resistance to topotecan and protects the brain from chemotherapy. Mol. Cell. Biol. 24, 7612–7621.

Leigh-Brown, S., Enriquez, J.A., Odom, D.T., 2010. Nuclear transcription factors in mammalian mitochondria. Genome Biol. 11, 215.

Leuzzi, V., Mastrangelo, M., Celato, A., Carducci, C., Carducci, C., 2012. A new form of cerebral folate deficiency with severe self-injurious behaviour. Acta Paediatr. Oslo Nor. 1992 101, e482–483.

Lev, D., Nissenkorn, A., Leshinsky-Silver, E., Sadeh, M., Zeharia, A., Garty, B.-Z., Blieden, L., Barash, V., Lerman-Sagie, T., 2004. Clinical presentations of mitochondrial cardiomyopathies. Pediatr. Cardiol. 25, 443–450.

Li, Q., Liu, M., Hou, J., Jiang, C., Li, S., Wang, T., 2012. The prevalence of Keshan disease in China. Int. J. Cardiol. 168, 1121-1126.

Li, X., Franke, A.A., 2009. Fast HPLC-ECD analysis of ascorbic acid, dehydroascorbic acid and uric acid. J. Chromatogr. B Analyt. Technol. Biomed. Life. Sci. 877, 853–856.

Li, Y., Huang, T.T., Carlson, E.J., Melov, S., Ursell, P.C., Olson, J.L., Noble, L.J., Yoshimura, M.P., Berger, C., Chan, P.H., Wallace, D.C., Epstein, C.J., 1995. Dilated cardiomyopathy and neonatal lethality in mutant mice lacking manganese superoxide dismutase. Nat. Genet. 11, 376–381.

Liang, W.J., Johnson, D., Jarvis, S.M., 2001. Vitamin C transport systems of mammalian cells. Mol. Membr. Biol. 18, 87–95.

Lim, B.C., Park, J.D., Hwang, H., Kim, K.J., Hwang, Y.S., Chae, J.-H., Cheon, J.-E., Kim, I.O., Lee, R., Moon, H.K., 2009. Mutations in ND subunits of complex I are an important genetic cause of childhood mitochondrial encephalopathies. J. Child Neurol. 24, 828–832.

Lindner, A., Hofmann, E., Naumann, M., Becker, G., Reichmann, H., 1997. Clinical, morphological, biochemical, and neuroradiological features of mitochondrial encephalomyopathies. Presentation of 19 patients. Mol. Cell. Biochem. 174, 297–303.

Liu, K., Zhao, H., Ji, K., Yan, C., 2013a. MERRF/MELAS overlap syndrome due to the m. 3291T> C mutation. Metab. Brain Dis. 1–6.

Liu, Y., Barber, D.S., Zhang, P., Liu, B., 2013b. Complex II of the Mitochondrial Respiratory Chain Is the Key Mediator of Divalent Manganese-Induced Hydrogen Peroxide Production in Microglia. Toxicol. Sci. 132, 298-306.

Liu, Y., Fiskum, G., Schubert, D., 2002. Generation of reactive oxygen species by the mitochondrial electron transport chain. J. Neurochem. 80, 780–787.

Lloyd, J.V., Davis, P.S., Emery, H., Lander, H., 1972. Platelet ascorbic acid levels in normal subjects and in disease. J. Clin. Pathol. 25, 478–483.

Loschen, G., Azzi, A., 1975. On the formation of hydrogen peroxide and oxygen radicals in heart mitochondria. Recent Adv. Stud. Cardiac Struct. Metab. 7, 3–12.

Lough, W.J., Wainer, I.W., 1996. High performance liquid chromatography: fundamental principles and practice. Blackie Academic & Professional, London; New York.

Lowry, O.H., Rosenbrough, N.J., Farr, A.L., Randall, R.J., 1951. Protein measurement with the Folin phenol reagent. J. Biol. Chem. 193, 265–275.

Lu, J., Berndt, C., Holmgren, A., 2009. Metabolism of selenium compounds catalyzed by the mammalian selenoprotein thioredoxin reductase. Biochim. Biophys. Acta 1790, 1513–1519.

Lu, J., Holmgren, A., 2009. Selenoproteins. J. Biol. Chem. 284, 723–727.

Lucock, M.D., Priestnall, M., Daskalakis, I., Schorah, C.J., Wild, J., Levene, M.I., 1995. Nonenzymatic degradation and salvage of dietary folate: physicochemical factors likely to influence bioavailability. Biochem. Mol. Med. 55, 43–53.

Luka, Z., 2008. Methyltetrahydrofolate in folate-binding protein glycine N-methyltransferase. Vitam. Horm. 79, 325–345.

Luka, Z., Pakhomova, S., Loukachevitch, L.V., Egli, M., Newcomer, M.E., Wagner, C., 2007. 5-methyltetrahydrofolate is bound in intersubunit areas of rat liver folate-binding protein glycine N-methyltransferase. J. Biol. Chem. 282, 4069–4075.

Lyman, C.M., Schultze, M.O., King, C.G., 1937. The Effect of Metaphosphoric Acid and Some Other Inorganic Acids on the Catalytic Oxidation of Ascorbic Acid. J. Biol. Chem. 118, 757–764.

Ma, Y.-S., Wu, S.-B., Lee, W.-Y., Cheng, J.-S., Wei, Y.-H., 2009. Response to the increase of oxidative stress and mutation of mitochondrial DNA in aging. Biochim. Biophys. Acta 1790, 1021–1029.

MacFarlane, A.J., Anderson, D.D., Flodby, P., Perry, C.A., Allen, R.H., Stabler, S.P., Stover, P.J., 2011. Nuclear localization of de novo thymidylate biosynthesis pathway is required to prevent uracil accumulation in DNA. J. Biol. Chem. 286, 44015–44022.

MacFarlane, A.J., Liu, X., Perry, C.A., Flodby, P., Allen, R.H., Stabler, S.P., Stover, P.J., 2008. Cytoplasmic serine hydroxymethyltransferase regulates the metabolic partitioning of methylenetetrahydrofolate but is not essential in mice. J. Biol. Chem. 283, 25846–25853.

MacKenzie, R.E., 1997. Mitochondrial NAD-dependent methylenetetrahydrofolate dehydrogenase-methenyltetrahydrofolate cyclohydrolase. Methods Enzymol. 281, 171–177.
Macron, J.M., Mizon, J.P., Rosa, A., 1983. Disorders of folate metabolism in the Kearns-Sayre syndrome. Rev. Neurol. (Paris) 139, 673–677.
Mandal, R., Guo, A.C., Chaudhary, K.K., Liu, P., Yallou, F.S., Dong, E., Aziat, F., Wishart, D.S., 2012. Multi-platform characterization of the human cerebrospinal fluid metabolome: a comprehensive and quantitative update. Genome Med. 4, 38.
Mandl, J., Szarka, A., Bánhegyi, G., 2009. Vitamin C: update on physiology and pharmacology. Br. J. Pharmacol. 157, 1097–1110.
Mangold, S., Blau, N., Opladen, T., Steinfeld, R., Wessling, B., Zerres, K., Häusler, M., 2011. Cerebral folate deficiency: a neurometabolic syndrome? Mol. Genet. Metab. 104, 369–372.
Mansergh, F.C., Millington-Ward, S., Kennan, A., Kiang, A.-S., Humphries, M., Farrar, G.J., Humphries, P., Kenna, P.F., 1999. Retinitis pigmentosa and progressive sensorineural hearing loss caused by a C12258A mutation in the mitochondrial MTTS2 gene. Am. J. Hum. Genet. 64, 971–985.
Maraldi, T., Riccio, M., Zambonin, L., Vinceti, M., De Pol, A., Hakim, G., 2011. Low levels of selenium compounds are selectively toxic for a human neuron cell line through ROS/RNS increase and apoptotic process activation. Neurotoxicology 32, 180–187.
Margulis, L., 1975. Symbiotic theory of the origin of eukaryotic organelles; criteria for proof. Symp. Soc. Exp. Biol. 21–38.
Markkanen, T., Pajula, R.L., Himanen, P., Virtanen, S., 1973. Serum folic acid activity (L. casei) in Sephadex gel chromatography. J. Clin. Pathol. 26, 486–493.
Markkanen, T., Peltola, O., 1971. Carrier proteins of folic acid activity in human serum. Acta Haematol. 45, 106–111.
Markkanen, T., Virtanen, S., Himanen, P., Pajula, R.L., 1972. Transferrin, the third carrier protein of folic acid activity in human serum. Acta Haematol. 48, 213–217.
Marquardt, D., Williams, J.A., Kučerka, N., Atkinson, J., Wassall, S.R., Katsaras, J., Harroun, T.A., 2013. Tocopherol activity correlates with its location in a membrane: a new perspective on the antioxidant vitamin E. J. Am. Chem. Soc. 135, 7523–7533.
Marshall, W.J., Bangert, S.K., 2008. Clinical Biochemistry: Metabolic and Clinical Aspects. Elsevier Health Sciences.
Massie, R., Wong, L.-J.C., Milone, M., 2010. Exercise intolerance due to cytochrome b mutation. Muscle Nerve 42, 136–140.
Matherly, L.H., Goldman, D.I., 2003. Membrane transport of folates. Vitam. Horm. 66, 403–456.
Matthews, R.G., Daubner, S.C., 1982. Modulation of methylenetetrahydrofolate reductase activity by S-adenosylmethionine and by dihydrofolate and its polyglutamate analogues. Adv. Enzyme Regul. 20, 123–131.
Matthews, R.G., Kaufman, S., 1980. Characterization of the dihydropterin reductase activity of pig liver methylenetetrahydrofolate reductase. J. Biol. Chem. 255, 6014–6017.

Mattman, A., Sirrs, S., Mezei, M., Salvarinova-Zivkovic, R., Alfadhel, M., Lillquist, Y., 2011. Mitochondrial disease clinical manifestations: An overview. BC Med. J. 53, 183–187.

Mattson, M.P., 2003. Methylation and acetylation in nervous system development and neurodegenerative disorders. Ageing Res. Rev. 2, 329–342.

Matyszak, M.K., Lawson, L.J., Perry, V.H., Gordon, S., 1992. Stromal macrophages of the choroid plexus situated at an interface between the brain and peripheral immune system constitutively express major histocompatibility class II antigens. J. Neuroimmunol. 40, 173–181.

May, J.M., 1998. Ascorbate function and metabolism in the human erythrocyte. Front. Biosci. J. Virtual Libr. 3, d1–10.

May, J.M., Mendiratta, S., Hill, K.E., Burk, R.F., 1997. Reduction of dehydroascorbate to ascorbate by the selenoenzyme thioredoxin reductase. J. Biol. Chem. 272, 22607–22610.

May, J.M., Qu, Z., Cobb, C.E., 2001a. Recycling of the ascorbate free radical by human erythrocyte membranes. Free Radic. Biol. Med. 31, 117–124.

May, J.M., Qu, Z., Li, X., 2001b. Requirement for GSH in recycling of ascorbic acid in endothelial cells. Biochem. Pharmacol. 62, 873–881.

May, J.M., Qu, Z., Neel, D.R., Li, X., 2003. Recycling of vitamin C from its oxidized forms by human endothelial cells. Biochim. Biophys. Acta 1640, 153–161.

McFarland, R., Chinnery, P.F., Blakely, E.L., Schaefer, A.M., Morris, A.A.M., Foster, S.M., Tuppen, H.A.L., Ramesh, V., Dorman, P.J., Turnbull, D.M., Taylor, R.W., 2007. Homoplasmy, heteroplasmy, and mitochondrial dystonia. Neurology 69, 911–916.

McShane, M.A., Hammans, S.R., Sweeney, M., Holt, I.J., Beattie, T.J., Brett, E.M., Harding, A.E., 1991. Pearson syndrome and mitochondrial encephalomyopathy in a patient with a deletion of mtDNA. Am. J. Hum. Genet. 48, 39–42.

Melov, S., Doctrow, S.R., Schneider, J.A., Haberson, J., Patel, M., Coskun, P.E., Huffman, K., Wallace, D.C., Malfroy, B., 2001. Lifespan extension and rescue of spongiform encephalopathy in superoxide dismutase 2 nullizygous mice treated with superoxide dismutase-catalase mimetics. J. Neurosci. Off. J. Soc. Neurosci. 21, 8348–8353.

Mendiratta, S., Qu, Z.C., May, J.M., 1998. Enzyme-dependent ascorbate recycling in human erythrocytes: role of thioredoxin reductase. Free Radic. Biol. Med. 25, 221–228.

Menniti, F.S., Knoth, J., Diliberto, E.J., Jr, 1986. Role of ascorbic acid in dopamine beta-hydroxylation. The endogenous enzyme cofactor and putative electron donor for cofactor regeneration. J. Biol. Chem. 261, 16901–16908.

Mezghani, N., Mnif, M., Mkaouar-Rebai, E., Kallel, N., Charfi, N., Abid, M., Fakhfakh, F., 2013. A maternally inherited diabetes and deafness patient with the 12S rRNA m.1555A>G and the ND1 m.3308T>C mutations associated with multiple mitochondrial deletions. Biochem. Biophys. Res. Commun. 431, 670–674.

Milhorat, T.H., 1969. Choroid plexus and cerebrospinal fluid production. Science 166, 1514–1516.

Minagawa, H., Watanabe, A., Akatsu, H., Adachi, K., Ohtsuka, C., Terayama, Y., Hosono, T., Takahashi, S., Wakita, H., Jung, C.-G., Komano, H., Michikawa,

M., 2010. Homocysteine, another risk factor for Alzheimer disease, impairs apolipoprotein E3 function. J. Biol. Chem. 285, 38382–38388.
Miró, O., Laguno, M., Masanés, F., Perea, M., Urbano-Márquez, A., Grau, J.M., 2000. Congenital and metabolic myopathies of childhood or adult onset. Semin. Arthritis Rheum. 29, 335–347.
Mitchell, P., 1961. Coupling of phosphorylation to electron and hydrogen transfer by a chemi-osmotic type of mechanism. Nature 191, 144–148.
Mitchell, P., Moyle, J., 1965. Stoichiometry of proton translocation through the respiratory chain and adenosine triphosphatase systems of rat liver mitochondria. Nature 208, 147–151.
Miyazono, F., Schneider, P.M., Metzger, R., Warnecke-Eberz, U., Baldus, S.E., Dienes, H.P., Aikou, T., Hoelscher, A.H., 2002. Mutations in the mitochondrial DNA D-Loop region occur frequently in adenocarcinoma in Barrett's esophagus. Oncogene 21, 3780–3783.
Moghadaszadeh, B., Beggs, A.H., 2006. Selenoproteins and their impact on human health through diverse physiological pathways. Physiol. Bethesda Md 21, 307–315.
Montecinos, V., Guzmán, P., Barra, V., Villagrán, M., Muñoz-Montesino, C., Sotomayor, K., Escobar, E., Godoy, A., Mardones, L., Sotomayor, P., Guzmán, C., Vásquez, O., Gallardo, V., van Zundert, B., Bono, M.R., Oñate, S.A., Bustamante, M., Cárcamo, J.G., Rivas, C.I., Vera, J.C., 2007. Vitamin C is an essential antioxidant that enhances survival of oxidatively stressed human vascular endothelial cells in the presence of a vast molar excess of glutathione. J. Biol. Chem. 282, 15506–15515.
Montero, R., Grazina, M., López-Gallardo, E., Montoya, J., Briones, P., Navarro-Sastre, A., Land, J.M., Hargreaves, I.P., Artuch, R., Coenzyme $Q_{10}$ Deficiency Study Group, 2013. Coenzyme $Q_{10}$ deficiency in mitochondrial DNA depletion syndromes. Mitochondrion 13, 337–341.
Moran, N.F., Bain, M.D., Muqit, M.M.K., Bax, B.E., 2008. Carrier erythrocyte entrapped thymidine phosphorylase therapy for MNGIE. Neurology 71, 686–688.
Moran, R.G., Colman, P.D., 1984. Mammalian folyl polyglutamate synthetase: partial purification and properties of the mouse liver enzyme. Biochemistry (Mosc.) 23, 4580–4589.
Moreno-Sánchez, R., Hernández-Esquivel, L., Rivero-Segura, N.A., Marín-Hernández, A., Neuzil, J., Ralph, S.J., Rodríguez-Enríquez, S., 2013. Reactive oxygen species are generated by the respiratory complex II--evidence for lack of contribution of the reverse electron flow in complex I. FEBS J. 280, 927–938.
Moretti, P., Peters, S.U., Del Gaudio, D., Sahoo, T., Hyland, K., Bottiglieri, T., Hopkin, R.J., Peach, E., Min, S.H., Goldman, D., Roa, B., Bacino, C.A., Scaglia, F., 2008. Brief report: autistic symptoms, developmental regression, mental retardation, epilepsy, and dyskinesias in CNS folate deficiency. J. Autism Dev. Disord. 38, 1170–1177.
Moretti, P., Sahoo, T., Hyland, K., Bottiglieri, T., Peters, S., del Gaudio, D., Roa, B., Curry, S., Zhu, H., Finnell, R.H., Neul, J.L., Ramaekers, V.T., Blau, N., Bacino, C.A., Miller, G., Scaglia, F., 2005. Cerebral folate deficiency with developmental delay, autism, and response to folinic acid. Neurology 64, 1088–1090.

Moriarty-Craige, S.E., Jones, D.P., 2004. Extracellular Thiols and Thiol/Disulfide Redox in Metabolism. Annu. Rev. Nutr. 24, 481–509.

Moslemi, A.-R., Oldfors, A., Melberg, A., Holme, E., 1996. Clonal expansion of mitochondrial DNA with multiple deletions in autosomal dominant progressive external ophthalmoplegia. Ann. Neurol. 40, 707–713.

Mühlenbein, N., Hofmann, S., Rothbauer, U., Bauer, M.F., 2004. Organization and Function of the Small Tim Complexes Acting along the Import Pathway of Metabolite Carriers into Mammalian Mitochondria. J. Biol. Chem. 279, 13540–13546.

Mullis, K., Faloona, F., Scharf, S., Saiki, R., Horn, G., Erlich, H., 1986. Specific enzymatic amplification of DNA in vitro: the polymerase chain reaction. Cold Spring Harb. Symp. Quant. Biol. 51 Pt 1, 263–273.

Mun, G.H., Kim, M.J., Lee, J.H., Kim, H.J., Chung, Y.H., Chung, Y.B., Kang, J.S., Hwang, Y.I., Oh, S.H., Kim, J.-G., Hwang, D.H., Shin, D.H., Lee, W.J., 2006. Immunohistochemical study of the distribution of sodium-dependent vitamin C transporters in adult rat brain. J. Neurosci. Res. 83, 919–928.

Munnich, A., Rötig, A., Chretien, D., Saudubray, J.M., Cormier, V., Rustin, P., 1996. Clinical presentations and laboratory investigations in respiratory chain deficiency. Eur. J. Pediatr. 155, 262–274.

Murad, S., Tajima, S., Johnson, G.R., Sivarajah, S., Pinnell, S.R., 1983. Collagen synthesis in cultured human skin fibroblasts: effect of ascorbic acid and its analogs. J. Invest. Dermatol. 81, 158–162.

Murphy, J.L., Blakely, E.L., Schaefer, A.M., He, L., Wyrick, P., Haller, R.G., Taylor, R.W., Turnbull, D.M., Taivassalo, T., 2008. Resistance training in patients with single, large-scale deletions of mitochondrial DNA. Brain 131, 2832–2840.

Murphy, M.P., 2009. How mitochondria produce reactive oxygen species. Biochem. J. 417, 1–13.

Murta, S.M.F., Vickers, T.J., Scott, D.A., Beverley, S.M., 2009. Methylene tetrahydrofolate dehydrogenase/cyclohydrolase and the synthesis of 10-CHO-THF are essential in Leishmania major. Mol. Microbiol. 71, 1386–1401.

Musatov, A., Robinson, N.C., 2012. Susceptibility of mitochondrial electron-transport complexes to oxidative damage. Focus on cytochrome c oxidase. Free Radic. Res. 46, 1313–1326.

Nagy, E., Degrell, I., 1989. Determination of ascorbic acid and dehydroascorbic acid in plasma and cerebrospinal fluid by liquid chromatography with electrochemical detection. J. Chromatogr. 497, 276–281.

Nakagawa, Y., Cotgreave, I.A., Moldéus, P., 1991. Relationships between ascorbic acid and alpha-tocopherol during diquat-induced redox cycling in isolated rat hepatocytes. Biochem. Pharmacol. 42, 883–888.

Narisawa, A., Komatsuzaki, S., Kikuchi, A., Niihori, T., Aoki, Y., Fujiwara, K., Tanemura, M., Hata, A., Suzuki, Y., Relton, C.L., Grinham, J., Leung, K.-Y., Partridge, D., Robinson, A., Stone, V., Gustavsson, P., Stanier, P., Copp, A.J., Greene, N.D.E., Tominaga, T., Matsubara, Y., Kure, S., 2012. Mutations in genes encoding the glycine cleavage system predispose to neural tube defects in mice and humans. Hum. Mol. Genet. 21, 1496–1503.

Naviaux, R.K., 2004. Developing a systematic approach to the diagnosis and classification of mitochondrial disease. Mitochondrion 4, 351–361.

Netsky, M.G., Shuangshoti, S., 1975. The choroid plexus in health and disease. J. Wright, Bristol.

Neul, J.L., Maricich, S.M., Islam, M., Barrish, J., Smith, E.O., Bottiglieri, T., Hyland, K., Humphreys, P., Percy, A., Glaze, D., 2005. Spinal fluid 5-methyltetrahydrofolate levels are normal in Rett syndrome. Neurology 64, 2151–2152.

Ng, C.F., Schafer, F.Q., Buettner, G.R., Rodgers, V.G.J., 2007. The rate of cellular hydrogen peroxide removal shows dependency on GSH: mathematical insight into in vivo H2O2 and GPx concentrations. Free Radic. Res. 41, 1201–1211.

Nguyen, M.V.C., Du, F., Felice, C.A., Shan, X., Nigam, A., Mandel, G., Robinson, J.K., Ballas, N., 2012. MeCP2 is critical for maintaining mature neuronal networks and global brain anatomy during late stages of postnatal brain development and in the mature adult brain. J. Neurosci. Off. J. Soc. Neurosci. 32, 10021–10034.

Nickel, A., Kottra, G., Schmidt, G., Danier, J., Hofmann, T., Daniel, H., 2009. Characteristics of transport of selenoamino acids by epithelial amino acid transporters. Chem. Biol. Interact. 177, 234–241.

Nilsson, C., Lindvall-Axelsson, M., Owman, C., 1992. Neuroendocrine regulatory mechanisms in the choroid plexus-cerebrospinal fluid system. Brain Res. Brain Res. Rev. 17, 109–138.

Ning, Y.J., Wang, X., Ren, L., Guo, X., 2013. Effects of dietary factors on selenium levels of children to prevent Kashin-Beck disease during a high-prevalence period in an endemic area: a cohort study. Biol. Trace Elem. Res. 153, 58–68.

Nishikimi, M., Fukuyama, R., Minoshima, S., Shimizu, N., Yagi, K., 1994. Cloning and chromosomal mapping of the human nonfunctional gene for L-gulono-gamma-lactone oxidase, the enzyme for L-ascorbic acid biosynthesis missing in man. J. Biol. Chem. 269, 13685–13688.

Nissenkorn, A., Zeharia, A., Lev, D., Fatal-Valevski, A., Barash, V., Gutman, A., Harel, S., Lerman-Sagie, T., 1999. Multiple presentation of mitochondrial disorders. Arch. Dis. Child. 81, 209–214.

Nogueira, V., Rigoulet, M., Piquet, M.A., Devin, A., Fontaine, E., Leverve, X.M., 2001. Mitochondrial respiratory chain adjustment to cellular energy demand. J. Biol. Chem. 276, 46104–46110.

Nualart, F., Castro, T., Low, M., Henríquez, J.P., Oyarce, K., Cisternas, P., García, A., Yáñez, A.J., Bertinat, R., Montecinos, V.P., García-Robles, M.A., 2013. Dynamic expression of the sodium-vitamin C co-transporters, SVCT1 and SVCT2, during perinatal kidney development. Histochem. Cell Biol. 139, 233–247.

Obara-Moszynska, M., Maceluch, J., Bobkowski, W., Baszko, A., Jaremba, O., Krawczynski, M.R., Niedziela, M., 2013. A novel mitochondrial DNA deletion in a patient with Kearns-Sayre syndrome: a late-onset of the fatal cardiac conduction deficit and cardiomyopathy accompanying long-term rGH treatment. BMC Pediatr. 13, 27.

Ogasahara, S., Engel, A.G., Frens, D., Mack, D., 1989. Muscle coenzyme Q deficiency in familial mitochondrial encephalomyopathy. Proc. Natl. Acad. Sci. U. S. A. 86, 2379–2382.

Ohta, Y., Suzuki, K.T., 2008. Methylation and demethylation of intermediates selenide and methylselenol in the metabolism of selenium. Toxicol. Appl. Pharmacol. 226, 169–177.

Okado-Matsumoto, A., Fridovich, I., 2001. Subcellular distribution of superoxide dismutases (SOD) in rat liver: Cu,Zn-SOD in mitochondria. J. Biol. Chem. 276, 38388–38393.

Okamura-Ikeda, K., Hosaka, H., Yoshimura, M., Yamashita, E., Toma, S., Nakagawa, A., Fujiwara, K., Motokawa, Y., Taniguchi, H., 2005. Crystal structure of human T-protein of glycine cleavage system at 2.0 Å resolution and its implication for understanding non-ketotic hyperglycinemia. J. Mol. Biol. 351, 1146–1159.

Oldfors, A., Fyhr, I.M., Holme, E., Larsson, N.G., Tulinius, M., 1990. Neuropathology in Kearns-Sayre syndrome. Acta Neuropathol. (Berl.) 80, 541–546.

Olmedo, J.M., Yiannias, J.A., Windgassen, E.B., Gornet, M.K., 2006. Scurvy: a disease almost forgotten. Int. J. Dermatol. 45, 909–913.

Opladen, T., Blau, N., Ramaekers, V.T., 2010. Effect of antiepileptic drugs and reactive oxygen species on folate receptor 1 (FOLR1)-dependent 5-methyltetrahydrofolate transport. Mol. Genet. Metab. 101, 48–54.

Opladen, T., Ramaekers, V.T., Heimann, G., Blau, N., 2006. Analysis of 5-methyltetrahydrofolate in serum of healthy children. Mol. Genet. Metab. 87, 61–65.

Ormazabal, A., Artuch, R., Vilaseca, M.A., Aracil, A., Pineda, M., 2005. Cerebrospinal fluid concentrations of folate, biogenic amines and pterins in Rett syndrome: treatment with folinic acid. Neuropediatrics 36, 380–385.

Ormazabal, A., García-Cazorla, A., Pérez-Dueñas, B., Gonzalez, V., Fernández-Alvarez, E., Pineda, M., Campistol, J., Artuch, R., 2006. Determination of 5-methyltetrahydrofolate in cerebrospinal fluid of paediatric patients: reference values for a paediatric population. Clin. Chim. Acta Int. J. Clin. Chem. 371, 159–162.

Ormazábal, A., Perez-Dueñas, B., Sierra, C., Urreitzi, R., Montoya, J., Serrano, M., Campistol, J., García-Cazorla, A., Pineda, M., Artuch, R., 2011. Folate analysis for the differential diagnosis of profound cerebrospinal fluid folate deficiency. Clin. Biochem. 44, 719–721.

Ormerod, M.G., 2000. Flow Cytometry: A Practical Approach. Oxford University Press.

Padayatty, S.J., Sun, H., Wang, Y., Riordan, H.D., Hewitt, S.M., Katz, A., Wesley, R.A., Levine, M., 2004. Vitamin C pharmacokinetics: implications for oral and intravenous use. Ann. Intern. Med. 140, 533–537.

Palade, G.E., 1956. Enzymes: Units of Biological Structure and Function. New York: Academic.

Paradies, G., Petrosillo, G., Pistolese, M., Ruggiero, F.M., 2000. The effect of reactive oxygen species generated from the mitochondrial electron transport chain on the cytochrome c oxidase activity and on the cardiolipin content in bovine heart submitochondrial particles. FEBS Lett. 466, 323–326.

Pasternack, L.B., Laude, D.A., Jr, Appling, D.R., 1992. 13C NMR detection of folate-mediated serine and glycine synthesis in vivo in Saccharomyces cerevisiae. Biochemistry (Mosc.) 31, 8713–8719.

Pasternack, L.B., Laude, D.A., Jr, Appling, D.R., 1994. 13C NMR analysis of intercompartmental flow of one-carbon units into choline and purines in Saccharomyces cerevisiae. Biochemistry (Mosc.) 33, 74–82.

Pasternak, J.J., 2005. An Introduction to Human Molecular Genetics: Mechanisms of Inherited Diseases. John Wiley & Sons.

Patterson, D., Graham, C., Cherian, C., Matherly, L.H., 2008. A humanized mouse model for the reduced folate carrier. Mol. Genet. Metab. 93, 95–103.

Paul, S.P., Candy, D.C., Clayton, P., Chong, W., Wallace, A., 2011. Hereditary Folate Malabsorption: Effect of systemic folate supplements on myelination. Infant 7, 158–61.

Pawelek, P.D., MacKenzie, R.E., 1998. Methenyltetrahydrofolate cyclohydrolase is rate limiting for the enzymatic conversion of 10-formyltetrahydrofolate to 5,10-methylenetetrahydrofolate in bifunctional dehydrogenase-cyclohydrolase enzymes. Biochemistry (Mosc.) 37, 1109–1115.

Pérez-Dueñas, B., Ormazábal, A., Toma, C., Torrico, B., Cormand, B., Serrano, M., Sierra, C., De Grandis, E., Marfa, M.P., García-Cazorla, A., Campistol, J., Pascual, J.M., Artuch, R., 2011. Cerebral folate deficiency syndromes in childhood: clinical, analytical, and etiologic aspects. Arch. Neurol. 68, 615–621.

Pérez-Dueñas, B., Toma, C., Ormazábal, A., Muchart, J., Sanmartí, F., Bombau, G., Serrano, M., García-Cazorla, A., Cormand, B., Artuch, R., 2010. Progressive ataxia and myoclonic epilepsy in a patient with a homozygous mutation in the FOLR1 gene. J. Inherit. Metab. Dis. 33, 795–802.

Perry, J., Chanarin, I., 1972. Observations on folate absorption with particular reference to folate polyglutamate and possible inhibitors to its absorption. Gut 13, 544–550.

Peterson, G.L., 1977. A simplification of the protein assay method of Lowry et al. which is more generally applicable. Anal. Biochem. 83, 346–356.

Pfeffer, G., Majamaa, K., Turnbull, D.M., Thorburn, D., Chinnery, P.F., 2012. Treatment for mitochondrial disorders. Cochrane Database Syst. Rev. 4, CD004426.

Piedrahita, J.A., Oetama, B., Bennett, G.D., van Waes, J., Kamen, B.A., Richardson, J., Lacey, S.W., Anderson, R.G., Finnell, R.H., 1999. Mice lacking the folic acid-binding protein Folbp1 are defective in early embryonic development. Nat. Genet. 23, 228–232.

Pineda, M., Ormazabal, A., López-Gallardo, E., Nascimento, A., Solano, A., Herrero, M.D., Vilaseca, M.A., Briones, P., Ibáñez, L., Montoya, J., Artuch, R., 2006. Cerebral folate deficiency and leukoencephalopathy caused by a mitochondrial DNA deletion. Ann. Neurol. 59, 394–398.

Pitceathly, R.D., Rahman, S., Wedatilake, Y., Polke, J.M., Cirak, S., Foley, A.R., Sailer, A., Hurles, M.E., Stalker, J., Hargreaves, I., 2013. NDUFA4 Mutations Underlie Dysfunction of a Cytochrome c Oxidase Subunit Linked to Human Neurological Disease. Cell Rep. 3, 1795-805.

Pogozelski, W.K., McNeese, T.J., Tullius, T.D., 1995. What Species Is Responsible for Strand Scission in the Reaction of [FeIIEDTA]2- and H2O2 with DNA? J. Am. Chem. Soc. 117, 6428–6433.

Pope, S., Land, J.M., Heales, S.J.R., 2008. Oxidative stress and mitochondrial dysfunction in neurodegeneration; cardiolipin a critical target? Biochim. Biophys. Acta 1777, 794–799.

Porter, D.H., Cook, R.J., Wagner, C., 1985. Enzymatic properties of dimethylglycine dehydrogenase and sarcosine dehydrogenase from rat liver. Arch. Biochem. Biophys. 243, 396–407.

Presgraves, S.P., Ahmed, T., Borwege, S., Joyce, J.N., 2004. Terminally differentiated SH-SY5Y cells provide a model system for studying neuroprotective effects of dopamine agonists. Neurotox. Res. 5, 579–598.

Quinlan, C.L., Orr, A.L., Perevoshchikova, I.V., Treberg, J.R., Ackrell, B.A., Brand, M.D., 2012. Mitochondrial complex II can generate reactive oxygen species at high rates in both the forward and reverse reactions. J. Biol. Chem. 287, 27255–27264.

Radi, R., Turrens, J.F., Chang, L.Y., Bush, K.M., Crapo, J.D., Freeman, B.A., 1991. Detection of catalase in rat heart mitochondria. J. Biol. Chem. 266, 22028–22034.

Ragan, C.I., Wilson, M.T., Darley-Usmar, V.M., Lowe, P.N., 1987. Subfractionation of mitochondria and isolation of proteins of oxidative phosphorylation, Darley-Usmar V M, Rickwood D and Wilson M T. ed. IRL Press, Oxford.

Rahman, S., 2012. Mitochondrial disease and epilepsy. Dev. Med. Child Neurol. 54, 397–406.

Rahman, S., 2013. Gastrointestinal and hepatic manifestations of mitochondrial disorders. J. Inherit. Metab. Dis. 36, 659–673.

Rahman, S., Hanna, M.G., 2009. Diagnosis and therapy in neuromuscular disorders: diagnosis and new treatments in mitochondrial diseases. J. Neurol. Neurosurg. Psychiatry 80, 943–953.

Rahman, S., Hargreaves, I., Clayton, P., Heales, S., 2001. Neonatal presentation of coenzyme Q10 deficiency. J. Pediatr. 139, 456–458.

Rahman, S., Poulton, J., Marchington, D., Suomalainen, A., 2001. Decrease of 3243 A-->G mtDNA mutation from blood in MELAS syndrome: a longitudinal study. Am J Hum Genet. 68, 238-240.

Ramaekers, V., Sequeira, J.M., Quadros, E.V., 2013a. Clinical recognition and aspects of the cerebral folate deficiency syndromes. Clin. Chem. Lab. Med. CCLM FESCC 51, 497–511.

Ramaekers, V.T., Blau, N., 2004. Cerebral folate deficiency. Dev. Med. Child Neurol. 46, 843–851.

Ramaekers, V.T., Blau, N., Sequeira, J.M., Nassogne, M.-C., Quadros, E.V., 2007a. Folate receptor autoimmunity and cerebral folate deficiency in low-functioning autism with neurological deficits. Neuropediatrics 38, 276–281.

Ramaekers, V.T., Hansen, S.I., Holm, J., Opladen, T., Senderek, J., Häusler, M., Heimann, G., Fowler, B., Maiwald, R., Blau, N., 2003. Reduced folate transport to the CNS in female Rett patients. Neurology 61, 506–515.

Ramaekers, V.T., Häusler, M., Opladen, T., Heimann, G., Blau, N., 2002. Psychomotor retardation, spastic paraplegia, cerebellar ataxia and dyskinesia associated with low 5-methyltetrahydrofolate in cerebrospinal fluid: a novel neurometabolic condition responding to folinic acid substitution. Neuropediatrics 33, 301–308.

Ramaekers, V.T., Quadros, E.V., Sequeira, J.M., 2013b. Role of folate receptor autoantibodies in infantile autism. Mol. Psychiatry 18, 270–271.

Ramaekers, V.T., Rothenberg, S.P., Sequeira, J.M., Opladen, T., Blau, N., Quadros, E.V., Selhub, J., 2005. Autoantibodies to folate receptors in the cerebral folate deficiency syndrome. N. Engl. J. Med. 352, 1985–1991.

Ramaekers, V.T., Sequeira, J.M., Artuch, R., Blau, N., Temudo, T., Ormazabal, A., Pineda, M., Aracil, A., Roelens, F., Laccone, F., Quadros, E.V., 2007b. Folate receptor autoantibodies and spinal fluid 5-methyltetrahydrofolate deficiency in Rett syndrome. Neuropediatrics 38, 179–183.

Ramaekers, V.T., Sequeira, J.M., Blau, N., Quadros, E.V., 2008. A milk-free diet downregulates folate receptor autoimmunity in cerebral folate deficiency syndrome. Dev. Med. Child Neurol. 50, 346–352.

Ramaekers, V.T., Weis, J., Sequeira, J.M., Quadros, E.V., Blau, N., 2007c. Mitochondrial complex I encephalomyopathy and cerebral 5-methyltetrahydrofolate deficiency. Neuropediatrics 38, 184–187.

Rao, V.V., Dahlheimer, J.L., Bardgett, M.E., Snyder, A.Z., Finch, R.A., Sartorelli, A.C., Piwnica-Worms, D., 1999. Choroid plexus epithelial expression of MDR1 P glycoprotein and multidrug resistance-associated protein contribute to the blood-cerebrospinal-fluid drug-permeability barrier. Proc. Natl. Acad. Sci. U. S. A. 96, 3900–3905.

Ray, P.D., Huang, B.-W., Tsuji, Y., 2012. Reactive oxygen species (ROS) homeostasis and redox regulation in cellular signaling. Cell. Signal. 24, 981–990.

Rebouche, C.J., 1991. Ascorbic acid and carnitine biosynthesis. Am. J. Clin. Nutr. 54, 1147S–1152S.

Regoli, F., Winston, G.W., 1999. Quantification of total oxidant scavenging capacity of antioxidants for peroxynitrite, peroxyl radicals, and hydroxyl radicals. Toxicol. Appl. Pharmacol. 156, 96–105.

Reisenauer, A.M., Chandler, C.J., Halsted, C.H., 1986. Folate binding and hydrolysis by pig intestinal brush-border membranes. Am. J. Physiol. 251, G481–486.

Revel, H.R.B., Magasanik, B., 1958. The enzymatic degradation of urocanic acid. J. Biol. Chem. 233, 930–935.

Rice, G.I., Forte, G.M.A., Szynkiewicz, M., Chase, D.S., Aeby, A., Abdel-Hamid, M.S., Ackroyd, S., Allcock, R., Bailey, K.M., Balottin, U., Barnerias, C., Bernard, G., Bodemer, C., Botella, M.P., Cereda, C., Chandler, K.E., Dabydeen, L., Dale, R.C., De Laet, C., De Goede, C.G.E.L., Del Toro, M., Effat, L., Enamorado, N.N., Fazzi, E., Gener, B., Haldre, M., Lin, J.-P.S.-M., Livingston, J.H., Lourenco, C.M., Marques, W., Jr, Oades, P., Peterson, P., Rasmussen, M., Roubertie, A., Schmidt, J.L., Shalev, S.A., Simon, R., Spiegel, R., Swoboda, K.J., Temtamy, S.A., Vassallo, G., Vilain, C.N., Vogt, J., Wermenbol, V., Whitehouse, W.P., Soler, D., Olivieri, I., Orcesi, S., Aglan, M.S., Zaki, M.S., Abdel-Salam, G.M.H., Vanderver, A., Kisand, K., Rozenberg, F., Lebon, P., Crow, Y.J., 2013. Assessment of interferon-related biomarkers in Aicardi-Goutières syndrome associated with mutations in TREX1, RNASEH2A, RNASEH2B, RNASEH2C, SAMHD1, and ADAR: a case-control study. Lancet Neurol. 12, 1159–1169.

Rice, M.E., 1999. Ascorbate compartmentalization in the CNS. Neurotox. Res. 1, 81–90.

Richardson, D.R., 2005. More roles for selenoprotein P: local selenium storage and recycling protein in the brain. Biochem. J. 386, e5–7.

Roberts, L.M., Black, D.S., Raman, C., Woodford, K., Zhou, M., Haggerty, J.E., Yan, A.T., Cwirla, S.E., Grindstaff, K.K., 2008. Subcellular localization of transporters along the rat blood-brain barrier and blood-cerebral-spinal fluid barrier by in vivo biotinylation. Neuroscience 155, 423–438.

Rosenquist, T.H., Ratashak, S.A., Selhub, J., 1996. Homocysteine induces congenital defects of the heart and neural tube: Effect of folic acid. Proc. Natl. Acad. Sci. 93, 15227–15232.

Rossignol, R., Faustin, B., Rocher, C., Malgat, M., Mazat, J.-P., Letellier, T., 2003. Mitochondrial threshold effects. Biochem. J. 370, 751–762.

Rossignol, R., Malgat, M., Mazat, J.-P., Letellier, T., 1999. Threshold effect and tissue specificity implication for mitochondrial cytopathies. J. Biol. Chem. 274, 33426–33432.

Rubartelli, A., Bajetto, A., Allavena, G., Wollman, E., Sitia, R., 1992. Secretion of thioredoxin by normal and neoplastic cells through a leaderless secretory pathway. J. Biol. Chem. 267, 24161–24164.
Rubenstein, E., 1998. Relationship of senescence of cerebrospinal fluid circulatory system to dementias of the aged. Lancet 351, 283–285.
Rustin, P., von Kleist-Retzow, J.-C., Rötig, A., Munnich, A., 1998. Iron overload and mitochondrial diseases. The Lancet 351, 1286–1287.
Sadasivan, E., Rothenberg, S.P., 1989. The complete amino acid sequence of a human folate binding protein from KB cells determined from the cDNA. J. Biol. Chem. 264, 5806–5811.
Sagan, L., 1967. On the origin of mitosing cells. J. Theor. Biol. 14, 255–274.
Sagara, J.I., Miura, K., Bannai, S., 1993. Maintenance of neuronal glutathione by glial cells. J. Neurochem. 61, 1672–1676.
Salvi, M., Battaglia, V., Brunati, A.M., La Rocca, N., Tibaldi, E., Pietrangeli, P., Marcocci, L., Mondovì, B., Rossi, C.A., Toninello, A., 2007. Catalase takes part in rat liver mitochondria oxidative stress defense. J. Biol. Chem. 282, 24407–24415.
Samsonoff, W.A., Reston, J., McKee, M., O'Connor, B., Galivan, J., Maley, G., Maley, F., 1997. Intracellular location of thymidylate synthase and its state of phosphorylation. J. Biol. Chem. 272, 13281–13285.
Samuelsson, M., Vainikka, L., Öllinger, K., 2011. Glutathione in the blood and cerebrospinal fluid: A study in healthy male volunteers. Neuropeptides 45, 287–292.
Sanger, F., Coulson, A.R., 1978. The use of thin acrylamide gels for DNA sequencing. FEBS Lett. 87, 107–110.
Scaglia, F., Towbin, J.A., Craigen, W.J., Belmont, J.W., Smith, E.O., Neish, S.R., Ware, S.M., Hunter, J.V., Fernbach, S.D., Vladutiu, G.D., Wong, L.-J.C., Vogel, H., 2004. Clinical spectrum, morbidity, and mortality in 113 pediatric patients with mitochondrial disease. Pediatrics 114, 925–931.
Scarpelli, M., Ricciardi, G.K., Beltramello, A., Zocca, I., Calabria, F., Russignan, A., Zappini, F., Cotelli, M.S., Padovani, A., Tomelleri, G., Filosto, M., Tonin, P., 2013. The role of brain MRI in mitochondrial neurogastrointestinal encephalomyopathy. Neuroradiol. J. 26, 520–530.
Scarpelli, M., Zappini, F., Filosto, M., Russignan, A., Tonin, P., Tomelleri, G., 2012. Mitochondrial Sensorineural Hearing Loss: A Retrospective Study and a Description of Cochlear Implantation in a MELAS Patient. Genet. Res. Int. 2012, 287432.
Schaefer, A.M., Walker, M., Turnbull, D.M., Taylor, R.W., 2013. Endocrine disorders in mitochondrial disease. Mol. Cell. Endocrinol. 379, 2–11.
Schalinske, K.L., Steele, R.D., 1996. Quantification of the carbon flow through the folate-dependent one-carbon pool using radiolabeled histidine: effect of altered thyroid and folate status. Arch. Biochem. Biophys. 328, 93–100.
Schapira, A., 2003. Mitochondrial Function and Dysfunction. Academic Press.
Scheffler, I.E., 2001. Mitochondria make a come back. Adv. Drug Deliv. Rev. 49, 3–26.
Schiffer, C.A., Clifton, I.J., Davisson, V.J., Santi, D.V., Stroud, R.M., 1995. Crystal structure of human thymidylate synthase: a structural mechanism for guiding substrates into the active site. Biochemistry (Mosc.) 34, 16279–16287.
Schirch, V., Strong, W.B., 1989. Interaction of folylpolyglutamates with enzymes in one-carbon metabolism. Arch. Biochem. Biophys. 269, 371–380.

Schneider, L., Giordano, S., Zelickson, B.R., S Johnson, M., A Benavides, G., Ouyang, X., Fineberg, N., Darley-Usmar, V.M., Zhang, J., 2011. Differentiation of SH-SY5Y cells to a neuronal phenotype changes cellular bioenergetics and the response to oxidative stress. Free Radic. Biol. Med. 51, 2007–2017.

Schomburg, L., Köhrle, J., 2008. On the importance of selenium and iodine metabolism for thyroid hormone biosynthesis and human health. Mol. Nutr. Food Res. 52, 1235–1246.

Schon, E.A., DiMauro, S., Hirano, M., 2012. Human mitochondrial DNA: roles of inherited and somatic mutations. Nat. Rev. Genet. 13, 878–890.

Schon, E.A., DiMauro, S., Hirano, M., Gilkerson, R.W., 2010. Therapeutic prospects for mitochondrial disease. Trends Mol. Med. 16, 268–276.

Schreuder, L., Peters, G., Nijhuis-van der Sanden, R., Morava, E., 2010. Aerobic exercise in children with oxidative phosphorylation defects. Neurol. Int. 2, e4.

Sciacco, M., Prelle, A., Comi, G.P., Napoli, L., Battistel, A., Bresolin, N., Tancredi, L., Lamperti, C., Bordoni, A., Fagiolari, G., Ciscato, P., Chiveri, L., Perini, M.P., Fortunato, F., Adobbati, L., Messina, S., Toscano, A., Martinelli-Boneschi, F., Papadimitriou, A., Scarlato, G., Moggio, M., 2001. Retrospective study of a large population of patients affected with mitochondrial disorders: clinical, morphological and molecular genetic evaluation. J. Neurol. 248, 778–788.

Scott, J.M., Weir, D.G., 1998. Folic acid, homocysteine and one-carbon metabolism: a review of the essential biochemistry. J. Cardiovasc. Risk 5, 223–227.

Selenius, M., Fernandes, A.P., Brodin, O., Björnstedt, M., Rundlöf, A.-K., 2008. Treatment of lung cancer cells with cytotoxic levels of sodium selenite: effects on the thioredoxin system. Biochem. Pharmacol. 75, 2092–2099.

Selivanov, V.A., Votyakova, T.V., Pivtoraiko, V.N., Zeak, J., Sukhomlin, T., Trucco, M., Roca, J., Cascante, M., 2011. Reactive oxygen species production by forward and reverse electron fluxes in the mitochondrial respiratory chain. PLoS Comput. Biol. 7, e. 1001115.

Serot, J.M., Bene, M.C., Faure, G.C., 1994. Comparative immunohistochemical characteristics of human choroid plexus in vascular and Alzheimer's dementia. Hum. Pathol. 25, 1185–1190.

Serot, J.M., Christmann, D., Dubost, T., Béne, M.C., Faure, G.C., 2001. CSF-folate levels are decreased in late-onset AD patients. J. Neural Transm. Vienna Austria 1996 108, 93–99.

Serrano, M., García-Silva, M.T., Martin-Hernandez, E., O'Callaghan, M. del M., Quijada, P., Martinez-Aragón, A., Ormazábal, A., Blázquez, A., Martín, M.A., Briones, P., López-Gallardo, E., Ruiz-Pesini, E., Montoya, J., Artuch, R., Pineda, M., 2010. Kearns-Sayre syndrome: cerebral folate deficiency, MRI findings and new cerebrospinal fluid biochemical features. Mitochondrion 10, 429–432.

Serrano, M., Pérez-Dueñas, B., Montoya, J., Ormazabal, A., Artuch, R., 2012. Genetic causes of cerebral folate deficiency: clinical, biochemical and therapeutic aspects. Drug Discov. Today 17, 1299–1306.

Shaikh, S.B., Nicholson, L.F., 2009. Effects of chronic low dose rotenone treatment on human microglial cells. Mol. Neurodegener. 4, 55.

Shane, B., 1989. Folylpolyglutamate synthesis and role in the regulation of one-carbon metabolism. Vitam. Horm. 45, 263–335.

Shea, T.B., 2006. Folate, the methionine cycle, and Alzheimer's disease. J. Alzheimers Dis. JAD 9, 359–360.
Shennan, D.B., 1988. Selenium (selenate) transport by human placental brush border membrane vesicles. Br. J. Nutr. 59, 13–19.
Shepherd, D., Garland, P.B., 1969. The kinetic properties of citrate synthase from rat liver mitochondria. Biochem. J. 114, 597–610.
Sherer, T.B., Trimmer, P.A., Borland, K., Parks, J.K., Bennett Jr., J.P., Tuttle, J.B., 2001. Chronic reduction in complex I function alters calcium signaling in SH-SY5Y neuroblastoma cells. Brain Res. 891, 94–105.
Sherratt, H.S., 1991. Mitochondria: structure and function. Rev. Neurol. (Paris) 147, 417–430.
Shin, D.S., Mahadeo, K., Min, S.H., Diop-Bove, N., Clayton, P., Zhao, R., Goldman, I.D., 2011. Identification of novel mutations in the proton-coupled folate transporter (PCFT-SLC46A1) associated with hereditary folate malabsorption. Mol. Genet. Metab. 103, 33–37.
Shin, H.C., Takakuwa, F., Shimoda, M., Kokue, E., 1995. Enterohepatic circulation kinetics of bile-active folate derivatives and folate homeostasis in rats. Am. J. Physiol. 269, R421–425.
Shoubridge, E.A., 2001. Nuclear genetic defects of oxidative phosphorylation. Hum. Mol. Genet. 10, 2277–2284.
Sinnathuray, A.R., Raut, V., Awa, A., Magee, A., Toner, J.G., 2003. A review of cochlear implantation in mitochondrial sensorineural hearing loss. Otol. Neurotol. Off. Publ. Am. Otol. Soc. Am. Neurotol. Soc. Eur. Acad. Otol. Neurotol. 24, 418–426.
Sipos, I., Tretter, L., Adam-Vizi, V., 2003. Quantitative relationship between inhibition of respiratory complexes and formation of reactive oxygen species in isolated nerve terminals. J. Neurochem. 84, 112–118.
Sjostrand, F.S., 1955. Fine Structure of Cells. New York.
Slow, S., Garrow, T.A., 2006. Liver choline dehydrogenase and kidney betaine-homocysteine methyltransferase expression are not affected by methionine or choline intake in growing rats. J. Nutr. 136, 2279–2283.
Smach, M.A., Jacob, N., Golmard, J.-L., Charfeddine, B., Lammouchi, T., Ben Othman, L., Dridi, H., Bennamou, S., Limem, K., 2011. Folate and homocysteine in the cerebrospinal fluid of patients with Alzheimer's disease or dementia: a case control study. Eur. Neurol. 65, 270–278.
Smeitink, J., van den Heuvel, L., DiMauro, S., 2001. The genetics and pathology of oxidative phosphorylation. Nat. Rev. Genet. 2, 342–352.
Smith, G.K., Mueller, W.T., Wasserman, G.F., Taylor, W.D., Benkovic, S.J., 1980. Characterization of the enzyme complex involving the folate-requiring enzymes of de novo purine biosynthesis. Biochemistry (Mosc.) 19, 4313–4321.
Smith, I., Hyland, K., Kendall, B., 1985. Clinical role of pteridine therapy in tetrahydrobiopterin deficiency. J. Inherit. Metab. Dis. 8 Suppl 1, 39–45.
Smithells, R.W., Sheppard, S., Schorah, C.J., 1976. Vitamin dificiencies and neural tube defects. Arch. Dis. Child. 51, 944–950.
Solanky, N., Requena Jimenez, A., D'Souza, S.W., Sibley, C.P., Glazier, J.D., 2010. Expression of folate transporters in human placenta and implications for homocysteine metabolism. Placenta 31, 134–143.
Somjai, S., Earl, F., Shigemasa, O., 1974. The release of iron from horse spleen ferritin by reduced flavins Biochem J. 143, 311–315.

Speake, T., Whitwell, C., Kajita, H., Majid, A., Brown, P.D., 2001. Mechanisms of CSF secretion by the choroid plexus. Microsc. Res. Tech. 52, 49–59.
Spector, R., 1981. Penetration of ascorbic acid from cerebrospinal fluid into brain. Exp. Neurol. 72, 645–653.
Spector, R., 2010. Nature and consequences of mammalian brain and CSF efflux transporters: four decades of progress. J. Neurochem. 112, 13–23.
Spector, R., Johanson, C.E., 2010. Choroid plexus failure in the Kearns-Sayre syndrome. Cerebrospinal Fluid Res. 7, 14.
Spector, R., Johanson, C.E., 2013. Sustained choroid plexus function in human elderly and Alzheimer's disease patients. Fluids Barriers CNS 10, 28.
Spector, R., Lorenzo, A.V., 1975. Folate transport in the central nervous system. Am. J. Physiol. 229, 777–782.
Srinivasan, S., Avadhani, N.G., 2012. Cytochrome c oxidase dysfunction in oxidative stress. Free Radic. Biol. Med. 53, 1252–1263.
Stahl, S.M., 2007. Novel therapeutics for depression: L-methylfolate as a trimonoamine modulator and antidepressant-augmenting agent. CNS Spectr. 12, 739–744.
Stam, F., Smulders, Y.M., van Guldener, C., Jakobs, C., Stehouwer, C.D.A., de Meer, K., 2005. Folic acid treatment increases homocysteine remethylation and methionine transmethylation in healthy subjects. Clin. Sci. Lond. Engl. 1979 108, 449–456.
Stankiewicz, J., Panter, S.S., Neema, M., Arora, A., Batt, C., Bakshi, R., 2007. Iron in Chronic Brain Disorders: Imaging and Neurotherapeutic Implications. Neurother. J. Am. Soc. Exp. Neurother. 4, 371–386.
Steinberg, S.E., 1984. Mechanisms of folate homeostasis. Am. J. Physiol. 246, G319–324.
Steinberg, S.E., Campbell, C.L., Hillman, R.S., 1979. Kinetics of the normal folate enterohepatic cycle. J. Clin. Invest. 64, 83–88.
Steinbrenner, H., Bilgic, E., Alili, L., Sies, H., Brenneisen, P., 2006. Selenoprotein P protects endothelial cells from oxidative damage by stimulation of glutathione peroxidase expression and activity. Free Radic. Res. 40, 936–943.
Steinfeld, R., Grapp, M., Kraetzner, R., Dreha-Kulaczewski, S., Helms, G., Dechent, P., Wevers, R., Grosso, S., Gärtner, J., 2009. Folate receptor alpha defect causes cerebral folate transport deficiency: a treatable neurodegenerative disorder associated with disturbed myelin metabolism. Am. J. Hum. Genet. 85, 354–363.
Stewart, V.C., Stone, R., Gegg, M.E., Sharpe, M.A., Hurst, R.D., Clark, J.B., Heales, S.J.R., 2002. Preservation of extracellular glutathione by an astrocyte derived factor with properties comparable to extracellular superoxide dismutase. J. Neurochem. 83, 984–991.
Stickler, D.E., Valenstein, E., Neiberger, R.E., Perkins, L.A., Carney, P.R., Shuster, J.J., Theriaque, D.W., Stacpoole, P.W., 2006. Peripheral neuropathy in genetic mitochondrial diseases. Pediatr. Neurol. 34, 127–131.
Stock, D., Gibbons, C., Arechaga, I., Leslie, A.G., Walker, J.E., 2000. The rotary mechanism of ATP synthase. Curr. Opin. Struct. Biol. 10, 672–679.
Stock, D., Leslie, A.G., Walker, J.E., 1999. Molecular architecture of the rotary motor in ATP synthase. Science 286, 1700–1705.
Stone, K.J., Townsley, B.H., 1973. The effect of L-ascorbate on catecholamine biosynthesis. Biochem. J. 131, 611–613.

Stone, R., Stewart, V.C., Hurst, R.D., Clark, J.B., Heales, S.J., 1999. Astrocyte nitric oxide causes neuronal mitochondrial damage, but antioxidant release limits neuronal cell death. Ann. N. Y. Acad. Sci. 893, 400–403.

Stover, P., Schirch, V., 1993. The metabolic role of leucovorin. Trends Biochem. Sci. 18, 102–106.

Stover, P.J., Field, M.S., 2011. Trafficking of intracellular folates. Adv. Nutr. Bethesda Md 2, 325–331.

Strachan, T., Read, A.P., Strachan, 2011. Human molecular genetics. Garland Science, New York.

Strand, T., Marklund, S.L., 1992. Release of superoxide dismutase into cerebrospinal fluid as a marker of brain lesion in acute cerebral infarction. Stroke J. Cereb. Circ. 23, 515–518.

Strazielle, N., Ghersi-Egea, J.F., 2000. Choroid plexus in the central nervous system: biology and physiopathology. J. Neuropathol. Exp. Neurol. 59, 561–574.

Sturtz, L.A., Diekert, K., Jensen, L.T., Lill, R., Culotta, V.C., 2001. A fraction of yeast Cu,Zn-superoxide dismutase and its metallochaperone, CCS, localize to the intermembrane space of mitochondria. A physiological role for SOD1 in guarding against mitochondrial oxidative damage. J. Biol. Chem. 276, 38084–38089.

Surtees, R., Heales, S., Bowron, A., 1994. Association of cerebrospinal fluid deficiency of 5-methyltetrahydrofolate, but not S-adenosylmethionine, with reduced concentrations of the acid metabolites of 5-hydroxytryptamine and dopamine. Clin. Sci. Lond. Engl. 1979 86, 697–702.

Surtees, R., Leonard, J., Austin, S., 1991. Association of demyelination with deficiency of cerebrospinal-fluid S-adenosylmethionine in inborn errors of methyl-transfer pathway. Lancet 338, 1550–1554.

Svendsen, I., Hansen, S.I., Holm, J., Lyngbye, J., 1982. Amino acid sequence homology between human and bovine low molecular weight folate binding protein isolated from milk. Carlsberg Res. Commun. 47, 371–376.

Tachikawa, M., Kasai, Y., Takahashi, M., Fujinawa, J., Kitaichi, K., Terasaki, T., Hosoya, K.-I., 2008. The blood-cerebrospinal fluid barrier is a major pathway of cerebral creatinine clearance: involvement of transporter-mediated process. J. Neurochem. 107, 432–442.

Taivassalo, T., Fu, K., Johns, T., Arnold, D., Karpati, G., Shoubridge, E.A., 1999. Gene shifting: a novel therapy for mitochondrial myopathy. Hum. Mol. Genet. 8, 1047–1052.

Tanji, K., Schon, E.A., DiMauro, S., Bonilla, E., 2000. Kearns-sayre syndrome: oncocytic transformation of choroid plexus epithelium. J. Neurol. Sci. 178, 29–36.

Tarnaris, A., Toma, A.K., Chapman, M.D., Petzold, A., Keir, G., Kitchen, N.D., Watkins, L.D., 2011. Rostrocaudal dynamics of CSF biomarkers. Neurochem. Res. 36, 528–532.

Tarze, A., Dauplais, M., Grigoras, I., Lazard, M., Ha-Duong, N.-T., Barbier, F., Blanquet, S., Plateau, P., 2007. Extracellular production of hydrogen selenide accounts for thiol-assisted toxicity of selenite against Saccharomyces cerevisiae. J. Biol. Chem. 282, 8759–8767.

Taylor, R.W., Schaefer, A.M., Barron, M.J., McFarland, R., Turnbull, D.M., 2004. The diagnosis of mitochondrial muscle disease. Neuromuscul. Disord. NMD 14, 237–245.

Taylor, R.W., Turnbull, D.M., 2005. Mitochondrial DNA mutations in human disease. Nat. Rev. Genet. 6, 389–402.

Temudo, T., Rios, M., Prior, C., Carrilho, I., Santos, M., Maciel, P., Sequeiros, J., Fonseca, M., Monteiro, J., Cabral, P., Vieira, J.P., Ormazabal, A., Artuch, R., 2009. Evaluation of CSF neurotransmitters and folate in 25 patients with Rett disorder and effects of treatment. Brain Dev. 31, 46–51.

Teng, Y.-W., Cerdena, I., Zeisel, S.H., 2012. Homocysteinemia in mice with genetic betaine homocysteine S-methyltransferase deficiency is independent of dietary folate intake. J. Nutr. 142, 1964–1967.

Thomas, C., Mackey, M.M., Diaz, A.A., Cox, D.P., 2009. Hydroxyl radical is produced via the Fenton reaction in submitochondrial particles under oxidative stress: implications for diseases associated with iron accumulation. Redox Rep. Commun. Free Radic. Res. 14, 102–108.

Thorburn, D.R., 2004. Mitochondrial disorders: prevalence, myths and advances. J. Inherit. Metab. Dis. 27, 349–362.

Tibbetts, A.S., Appling, D.R., 2010. Compartmentalization of Mammalian folate-mediated one-carbon metabolism. Annu. Rev. Nutr. 30, 57–81.

Tinggi, U., 2008. Selenium: its role as antioxidant in human health. Environ. Health Prev. Med. 13, 102–108.

Toledano, M.B., Planson, A.-G., Delaunay-Moisan, A., 2010. Reining in H(2)O(2) for safe signaling. Cell 140, 454–456.

Tondo, M., Málaga, I., O'Callaghan, M., Serrano, M., Emperador, S., Ormazabal, A., Ruiz-Pesini, E., Montoya, J., Garcia-Silva, M.T., Martin-Hernandez, E., Garcia-Cazorla, A., Pineda, M., Artuch, R., 2011. Biochemical parameters to assess choroid plexus dysfunction in Kearns-Sayre syndrome patients. Mitochondrion 11, 867–870.

Tondo, M., Moreno, J., Casado, M., Brandi, N., Sierra, C., Vilaseca, M.A., Ormazabal, A., Artuch, R., 2010. Selenium concentration in cerebrospinal fluid samples from a paediatric population. Neurochem. Res. 35, 1290–1293.

Treberg, J.R., Quinlan, C.L., Brand, M.D., 2011. Evidence for two sites of superoxide production by mitochondrial NADH-ubiquinone oxidoreductase (complex I). J. Biol. Chem. 286, 27103–27110.

Tryggvason, K., Majamaa, K., Risteli, J., Kivirikko, K.I., 1979. Partial purification and characterization of chick-embryo prolyl 3-hydroxylase. Biochem. J. 183, 303–307.

Tsuji, M., Takagi, A., Sameshima, K., Iai, M., Yamashita, S., Shinbo, H., Furuya, N., Kurosawa, K., Osaka, H., 2011. 5,10-Methylenetetrahydrofolate reductase deficiency with progressive polyneuropathy in an infant. Brain Dev. 33, 521–524.

Tsukaguchi, H., Tokui, T., Mackenzie, B., Berger, U.V., Chen, X.Z., Wang, Y., Brubaker, R.F., Hediger, M.A., 1999. A family of mammalian Na+-dependent L-ascorbic acid transporters. Nature 399, 70–75.

Tsutsui, H., Ide, T., Hayashidani, S., Suematsu, N., Shiomi, T., Wen, J., Nakamura, K., Ichikawa, K., Utsumi, H., Takeshita, A., 2001. Enhanced Generation of Reactive Oxygen Species in the Limb Skeletal Muscles From a Murine Infarct Model of Heart Failure. Circulation 104, 134–136.

Tulpule, K., Hohnholt, M.C., Dringen, R., 2013. Formaldehyde metabolism and formaldehyde-induced stimulation of lactate production and glutathione export in cultured neurons. J. Neurochem. 125, 260-272.

Turrens, J.F., 2003. Mitochondrial formation of reactive oxygen species. J. Physiol. 552, 335–344.
Turrens, J.F., Alexandre, A., Lehninger, A.L., 1985. Ubisemiquinone is the electron donor for superoxide formation by complex III of heart mitochondria. Arch. Biochem. Biophys. 237, 408–414.
Turrens, J.F., Boveris, A., 1980. Generation of superoxide anion by the NADH dehydrogenase of bovine heart mitochondria. Biochem. J. 191, 421–427.
Turrens, J.F., Freeman, B.A., Levitt, J.G., Crapo, J.D., 1982. The effect of hyperoxia on superoxide production by lung submitochondrial particles. Arch. Biochem. Biophys. 217, 401–410.
Urquhart, B.L., Gregor, J.C., Chande, N., Knauer, M.J., Tirona, R.G., Kim, R.B., 2010. The human proton-coupled folate transporter (hPCFT): modulation of intestinal expression and function by drugs. Am. J. Physiol. Gastrointest. Liver Physiol. 298, G248–254.
Vafai, S.B., Mootha, V.K., 2012. Mitochondrial disorders as windows into an ancient organelle. Nature 491, 374–383.
Van Beynum, I., Morava, E., Taher, M., Rodenburg, R.J., Karteszi, J., Toth, K., Szabados, E., 2012. Cardiac arrest in kearns-sayre syndrome. JIMD Rep. 2, 7–10.
Van Robertson, W.B., 1952. The effect of ascorbic acid deficiency on the collagen concentration of newly induced fibrous tissue. J. Biol. Chem. 196, 403–408.
Venditti, P., Di Stefano, L., Di Meo, S., 2013. Mitochondrial metabolism of reactive oxygen species. Mitochondrion 13, 71–82.
Vento, J.M., Pappa, B., 2013. Genetic counseling in mitochondrial disease. Neurother. J. Am. Soc. Exp. Neurother. 10, 243–250.
Verbeek, M.M., Blom, A.M., Wevers, R.A., Lagerwerf, A.J., van de Geer, J., Willemsen, M.A.A.P., 2008. Technical and biochemical factors affecting cerebrospinal fluid 5-MTHF, biopterin and neopterin concentrations. Mol. Genet. Metab. 95, 127–132.
Verlinde, P.H.C.J., Oey, I., Hendrickx, M.E., Van Loey, A.M., Temme, E.H.M., 2008. L-ascorbic acid improves the serum folate response to an oral dose of [6S]-5-methyltetrahydrofolic acid in healthy men. Eur. J. Clin. Nutr. 62, 1224–1230.
Vethanayagam, J.G., Green, E.H., Rose, R.C., Bode, A.M., 1999. Glutathione-dependent ascorbate recycling activity of rat serum albumin. Free Radic. Biol. Med. 26, 1591–1598.
Vinceti, M., Maraldi, T., Bergomi, M., Malagoli, C., 2009. Risk of chronic low-dose selenium overexposure in humans: insights from epidemiology and biochemistry. Rev. Environ. Health 24, 231–248.
Wagner, C., Decha-Umphai, W., Corbin, J., 1989. Phosphorylation modulates the activity of glycine N-methyltransferase, a folate binding protein. In vitro phosphorylation is inhibited by the natural folate ligand. J. Biol. Chem. 264, 9638–9642.
Wald, D.S., Law, M., Morris, J.K., 2002. Homocysteine and cardiovascular disease: evidence on causality from a meta-analysis. BMJ 325, 1202.
Walker, J.E., Collinson, I.R., Van Raaij, M.J., Runswick, M.J., 1995. Structural analysis of ATP synthase from bovine heart mitochondria. Methods Enzymol. 260, 163–190.
Wallenberg, M., Olm, E., Hebert, C., Björnstedt, M., Fernandes, A.P., 2010. Selenium compounds are substrates for glutaredoxins: a novel pathway for

selenium metabolism and a potential mechanism for selenium-mediated cytotoxicity. Biochem. J. 429, 85–93.
Wang, C.-H., Wu, S.-B., Wu, Y.-T., Wei, Y.-H., 2013. Oxidative stress response elicited by mitochondrial dysfunction: Implication in the pathophysiology of aging. Exp. Biol. Med. 238, 450–460.
Washko, P.W., Wang, Y., Levine, M., 1993. Ascorbic acid recycling in human neutrophils. J. Biol. Chem. 268, 15531–15535.
Watabe, M., Nakaki, T., 2007. ATP depletion does not account for apoptosis induced by inhibition of mitochondrial electron transport chain in human dopaminergic cells. Neuropharmacology 52, 536–541.
Wechtersbach, L., Cigić, B., 2007. Reduction of dehydroascorbic acid at low pH. J. Biochem. Biophys. Methods 70, 767–772.
Wedatilake, Y., Brown, R., McFarland, R., Yaplito-Lee, J., Morris, A.A., Champion, M., Jardine, P.E., Clarke, A., Thorburn, D.R., Taylor, R.W., Land, J.M., Forrest, K., Dobbie, A., Simmons, L., Aasheim, E.T., Ketteridge, D., Hanrahan, D., Chakrapani, A., Brown, G.K., Rahman, S., 2013. SURF1 deficiency: a multi-centre natural history study. Orphanet J. Rare Dis. 8, 96.
Weisiger, R.A., Fridovich, I., 1973. Mitochondrial superoxide simutase. Site of synthesis and intramitochondrial localization. J. Biol. Chem. 248, 4793–4796.
Weissberger, A., LuValle, J.E., Thomas, D.S., 1943. Oxidation Processes. XVI.1 The Autoxidation of Ascorbic Acid. J. Am. Chem. Soc. 65, 1934–1939.
Weng, S.-M., Bailey, M.E.S., Cobb, S.R., 2011. Rett syndrome: from bed to bench. Pediatr. Neonatol. 52, 309–316.
Wevers, R.A., Hansen, S.I., van Hellenberg Hubar, J.L., Holm, J., Høier-Madsen, M., Jongen, P.J., 1994. Folate deficiency in cerebrospinal fluid associated with a defect in folate binding protein in the central nervous system. J. Neurol. Neurosurg. Psychiatry 57, 223–226.
Wharton, D.C., Tzagoloff, A., 1967. Cytochrome oxidase from beef heart mitochondria. Methods Enzymol. 10, 245–250.
Widmaier, E.P., Raff, H., 2006. Vander's human physiology: the mechanisms of body function. McGraw-Hill, Boston.
Wikström, M., 2004. Cytochrome c oxidase: 25 years of the elusive proton pump. Biochim. Biophys. Acta 1655, 241–247.
Wilber, C.G., 1980. Toxicology of selenium: a review. Clin. Toxicol. 17, 171–230.
Williams, D., 1995. Spectroscopic Methods Organic Chemistry, Mc-Graw Hill.
Wills, L., 1931. Treatment of "Pernicious Anaemia of Pregnancy" and "Tropical Anaemia". Br. Med. J. 1, 1059–1064.
Wills, L., 1991. Treatment of "pernicious anaemia of pregnancy" and "tropical anaemia" with special reference to yeast extract as a curative agent. 1931. Nutr. Burbank Los Angel. Cty. Calif 7, 323–327; discussion 328.
Wilson, J.X., 2002. The physiological role of dehydroascorbic acid. FEBS Lett. 527, 5–9.
Wilson, S.D., Horne, D.W., 1983. Evaluation of ascorbic acid in protecting labile folic acid derivatives. Proc. Natl. Acad. Sci. U. S. A. 80, 6500–6504.
Winkler, B.S., 1992. Unequivocal evidence in support of the nonenzymatic redox coupling between glutathione/glutathione disulfide and ascorbic acid/dehydroascorbic acid. Biochim. Biophys. Acta 1117, 287–290.
Winkler, O., 1994. The redox couple between glutathione and ascorbic acid: a chemical and physiological perspective. Free Radic. Biol. Med. 17, 333–49.

Winston, G.W., Regoli, F., Dugas, A.J., Jr, Fong, J.H., Blanchard, K.A., 1998. A rapid gas chromatographic assay for determining oxyradical scavenging capacity of antioxidants and biological fluids. Free Radic. Biol. Med. 24, 480–493.

Wittwer, A.J., Wagner, C., 1980. Identification of folate binding protein of mitochondria as dimethylglycine dehydrogenase. Proc. Natl. Acad. Sci. U. S. A. 77, 4484–4488.

Woeller, C.F., Anderson, D.D., Szebenyi, D.M.E., Stover, P.J., 2007. Evidence for small ubiquitin-like modifier-dependent nuclear import of the thymidylate biosynthesis pathway. J. Biol. Chem. 282, 17623–17631.

Wolburg, H., Wolburg-Buchholz, K., Liebner, S., Engelhardt, B., 2001. Claudin-1, claudin-2 and claudin-11 are present in tight junctions of choroid plexus epithelium of the mouse. Neurosci. Lett. 307, 77–80.

Wolff, S.P., Dean, R.T., 1987. Glucose autoxidation and protein modification. The potential role of "autoxidative glycosylation" in diabetes. Biochem. J. 245, 243–250.

Wolffram, S., Ardüser, F., Scharrer, E., 1985. In vivo intestinal absorption of selenate and selenite by rats. J. Nutr. 115, 454–459.

Wollack, J.B., Makori, B., Ahlawat, S., Koneru, R., Picinich, S.C., Smith, A., Goldman, I.D., Qiu, A., Cole, P.D., Glod, J., Kamen, B., 2008. Characterization of folate uptake by choroid plexus epithelial cells in a rat primary culture model. J. Neurochem. 104, 1494–1503.

Wong, L.-J.C., 2004. Comprehensive molecular diagnosis of mitochondrial disorders: qualitative and quantitative approach. Ann. N. Y. Acad. Sci. 1011, 246–258.

Wonnapinij, P., Chinnery, P.F., Samuels, D.C., 2008. The distribution of mitochondrial DNA heteroplasmy due to random genetic drift. Am. J. Hum. Genet. 83, 582–593.

Wu, D., Pardridge, W.M., 1999. Blood-brain barrier transport of reduced folic acid. Pharm. Res. 16, 415–419.

Xiong, N., Xiong, J., Jia, M., Liu, L., Zhang, X., Chen, Z., Huang, J., Zhang, Z., Hou, L., Luo, Z., Ghoorah, D., Lin, Z., Wang, T., 2013. The role of autophagy in Parkinson's disease: rotenone-based modeling. Behav. Brain Funct. BBF 9, 13.

Yamada, K., Kawata, T., Wada, M., Isshiki, T., Onoda, J., Kawanishi, T., Kunou, A., Tadokoro, T., Tobimatsu, T., Maekawa, A., Toraya, T., 2000. Extremely low activity of methionine synthase in vitamin B-12-deficient rats may be related to effects on coenzyme stabilization rather than to changes in coenzyme induction. J. Nutr. 130, 1894–1900.

Yamada, K., Toribe, Y., Yanagihara, K., Mano, T., Akagi, M., Suzuki, Y., 2012. Diagnostic accuracy of blood and CSF lactate in identifying children with mitochondrial diseases affecting the central nervous system. Brain Dev. 34, 92–97.

Yan, L., Spallholz, J.E., 1993. Generation of reactive oxygen species from the reaction of selenium compounds with thiols and mammary tumor cells. Biochem. Pharmacol. 45, 429–437.

Zeviani, M., Di Donato, S., 2004. Mitochondrial disorders. Brain J. Neurol. 127, 2153–2172.

Zeviani, M., Moraes, C.T., DiMauro, S., Nakase, H., Bonilla, E., Schon, E.A., Rowland, L.P., 1988. Deletions of mitochondrial DNA in Kearns-Sayre syndrome. Neurology 38, 1339–1346.

Zhao, R., Diop-Bove, N., Visentin, M., Goldman, I.D., 2011. Mechanisms of membrane transport of folates into cells and across epithelia. Annu. Rev. Nutr. 31, 177–201.

Zhao, R., Matherly, L.H., Goldman, I.D., 2009a. Membrane transporters and folate homeostasis: intestinal absorption and transport into systemic compartments and tissues. Expert Rev. Mol. Med. 11, e4.

Zhao, R., Min, S.H., Wang, Y., Campanella, E., Low, P.S., Goldman, I.D., 2009b. A role for the proton-coupled folate transporter (PCFT-SLC46A1) in folate receptor-mediated endocytosis. J. Biol. Chem. 284, 4267–4274.

Zhao, Y., Wang, Z.-B., Xu, J.-X., 2003. Effect of Cytochrome c on the Generation and Elimination of O and H2O2 in Mitochondria. J. Biol. Chem. 278, 2356–2360.

Zhu, H., Wlodarczyk, B.J., Scott, M., Yu, W., Merriweather, M., Gelineau-van Waes, J., Schwartz, R.J., Finnell, R.H., 2007. Cardiovascular abnormalities in Folr1 knockout mice and folate rescue. Birt. Defects Res. A. Clin. Mol. Teratol. 79, 257–268.